OCS Study MMS 2005-055

University of Alaska Coastal Marine Institute

IN COOPERATION

Minerals Management Service

University of Alaska

State of Alaska

Annual Report No. 11

Federal Fiscal Year 2004

SUBMITTED BY

Vera Alexander
Director
University of Alaska Coastal Marine Institute

TO

U.S. Department of the Interior
Minerals Management Service
Alaska OCS Region
Anchorage, Alaska

November 2005

Contact information

email: cmi@sfos.uaf.edu
phone: 907.474.1811
fax: 907.474.1188
postal: Coastal Marine Institute
School of Fisheries and Ocean Sciences
University of Alaska Fairbanks
Fairbanks, AK 99775-7220

Table of Contents

Introduction

The University of Alaska Coastal Marine Institute (CMI) was created by a cooperative agreement between the University of Alaska and the Minerals Management Service (MMS) in June 1993, with the first full funding cycle beginning late in (federal) fiscal year 1994. CMI is pleased to present this 2004 Annual Report, our eleventh annual report and the second one under MMS Cooperative Agreement 0102CA85294. Twenty-five research projects are covered, including abstracts for nine projects in final report preparation (Kelly [TO 15162], Weingartner & Aagaard [TO 15163], Smith & Lee [15177], Wang & Jin [15178], Suydam, Lowry & Frost [TO 15179], Kelly [TO 15180], Naidu & Kelley [15181], Musgrave [74261], and Okkonen & Saupe [TO 85243]). Six of the 25 projects were funded in FY2004 and are in the New Projects section. Four additional project final reports were published in 2004 (Terschak, Henrichs & Shaw [TO 15170], Duesterloh & Shirley [TO 15171], Winker & Rocque [TO 15173], and Braddock, Gannon & Rasley [TO 15175].

The Minerals Management Service administers the outer continental shelf (OCS) natural gas, oil, and marine minerals program in which it oversees the safe and environmentally sound leasing, exploration, and production of these resources within our nation's offshore areas. The Environmental Studies Program (ESP) was formally directed in 1978, under Section 20 of the OCS Lands Act Amendments, to provide information in support of the decisions involved in the planning, leasing, and management of exploration, development, and production activities. The research agenda is driven by the identification of specific issues, concerns, or data gaps by federal decision makers and the state and local governments that participate in the process. ESP research focuses on the following broad issues associated with development of OCS gas, oil, and minerals:

- What are the fates and effects of potential OCS-related pollutants (e.g., oil, noise, drilling muds and cuttings, products of fuel combustion) in the marine and coastal environment and the atmosphere?
- What biological resources (e.g., fish populations) exist and which resources are at risk? What is the nature and extent of the risk? What measures must be taken to allow extraction to take place?
- How do OCS activities affect people in terms of jobs and the economy? What are the direct and indirect effects on local culture? What are the psychological effects of the proposed OCS activities?

Because MMS and individual states have distinct but complementary roles in the decision-making process, reliable scientific information is needed by MMS, the state, and localities potentially affected by OCS operations. In light of this, MMS has developed a locally managed CMI program. Under this program, MMS takes advantage of highly-qualified scientific expertise at local levels in order to:

1. Collect and disseminate environmental information needed for OCS oil & gas and marine minerals decisions;
2. Address local and regional OCS-related environmental and resource issues of mutual interest; and
3. Strengthen the partnership between MMS and the state in addressing OCS oil & gas and marine minerals information needs.

CMI is administered by the University of Alaska Fairbanks School of Fisheries and Ocean Sciences to address some of these mutual concerns and share the cost of research. Alaska was selected as the location for this CMI because it contains some of the major potential offshore oil and gas producing areas in the United States. The University of Alaska Fairbanks is uniquely suited to participate by virtue of its flagship status within the state and its nationally recognized marine and coastal expertise

relevant to the broad range of OCS program information needs. In addition, MMS and the University of Alaska have worked cooperatively on ESP studies for many years. Research projects funded by CMI are required to have at least one active University of Alaska investigator. Cooperative research between the University of Alaska and state agency scientists is encouraged.

Framework Issues were developed during the formation of CMI to identify and bracket the concerns to be addressed:

1. Scientific studies for better understanding marine, coastal, or human environments affected or potentially affected by offshore oil & gas or other mineral exploration and extraction on the outer continental shelf;
2. Modeling studies of environmental, social, economic, or cultural processes related to OCS oil & gas activities in order to improve scientific predictive capabilities;
3. Experimental studies for better understanding of environmental processes or the causes and effects of OCS activities;
4. Projects which design or establish mechanisms or protocols for sharing of data or scientific information regarding marine or coastal resources or human activities to support prudent management of oil & gas and marine mineral resources; and
5. Synthesis studies of scientific environmental or socioeconomic information relevant to the OCS oil & gas program.

Projects funded through CMI are directed toward providing information which can be used by MMS and the state for management decisions specifically relevant to MMS mission responsibilities. Projects must be pertinent to either the OCS oil and gas program or the marine minerals mining program. They should provide useful information for program management or for the scientific understanding of potential environmental effects of resource development activities in arctic and subarctic environments.

Initial guidelines given to prospective researchers identified Cook Inlet and Shelikof Strait, as well as the Beaufort and Chukchi seas, as areas of chief concern to MMS and the state. Primary emphasis has subsequently shifted to the Beaufort Sea, and to the Chukchi Sea as it relates to the Beaufort Sea. However, a strong interest in Cook Inlet and Shelikof Strait remains.

The proposal process is initiated each summer with a request for letters of intent to address one or more of the Framework Issues. This request is publicized and sent to researchers at the University of Alaska and to various state agencies, and to relevant profit and non-profit corporations. The CMI technical steering committee then decides which of the proposed letters of intent should be developed into proposals for more detailed evaluation and possible funding.

Successful investigators are strongly encouraged to publish their results in peer-reviewed journals as well as to present them at national meetings. In addition, investigators report their findings at the CMI's annual research review, held at UAF in February. Some investigators present information directly to the public and MMS staff in seminars.

Alaskans benefit from the examination and increased understanding of those processes unique to Alaskan OCS and coastal waters because this enhanced understanding can be applied to problems other than oil, gas, and mineral extraction, such as subsistence fisheries and northern shipping.

Many of the CMI-funded projects address some combination of issues related to fisheries, biomonitoring, physical oceanography, and the fates of oil. The ultimate intent of CMI-related research is to identify the ways in which OCS-related activities may affect our environment, and potential economic and social impacts as well.

Correction Factor for Ringed Seal Surveys in Northern Alaska

Brendan P. Kelly <brendan.kelly@uas.alaska.edu>

School of Arts and Sciences
University of Alaska Southeast
11120 Glacier Highway
Juneau, AK 99801

Task Order 15162

Abstract

The proportion of radio-tagged ringed seals visible on the ice surface from April to June in 1999 (n = 8) and 2000 (n = 10) was used to estimate correction factors for aerial surveys. Radio tracking proved effective for determining when seals were available to be counted; monitoring lair temperatures was less effective for that purpose.

The transition period, defined as the period during which the majority (75%) of the tagged seals began resting outside of lairs, was longer in 2000 (24 days) than it was in 1999 (7 days). The midpoint of the transition period, the day by which 50% of the tagged seals began resting in the open, was 31 May in both years. Only once each year was a lair used subsequent to each seal's first appearance outside of a lair. Changes in the number of seals counted during ground-based, visual surveys of seals resting on the ice corresponded to changes in the number of radio-tagged seals basking. Tagged seals spent approximately 20% of the time out of the water before appearing outside of lairs and approximately 30% of the time out of the water after they began to abandon lairs. The transition from lair use to resting in the open appeared related to measurable characteristics of the snow, and backscatter radar, sensitive to the liquid moisture content of snow, offers promise for remotely determining when seals have abandoned their subnivean lairs.

Aerial surveys underestimated actual ringed seal densities by factors ranging from 2.33 to >13 because the proportion of seals visible during the survey periods changed rapidly from day to day. Interannual comparisons of seal densities based on aerial surveys have been further compromised by a shift in survey dates from mid-June in the 1970s to late May in the 1990s. The proportion of seals visible on the ice was more stable between 12:00 and 18:00 (Alaska Daylight Saving Time [ADT]) than between 10:00 and 16:00, the current standard for aerial surveys of ringed seals in Alaska.

In April, May, and early June, most radio-tagged ringed seals remained close to their capture and release sites, with 88% of their home ranges measuring less than 500 ha in area. One seal, however, had a home range of almost 600 ha and another of almost 3,000 ha.

Circulation, Thermohaline Structure, and Cross-Shelf Transport in the Alaskan Beaufort Sea

Thomas J. Weingartner <weingart@ims.uaf.edu>

Institute of Marine Science
University of Alaska Fairbanks
Fairbanks, AK 99775-7220

Knut Aagaard <aagaard@apl.washington.edu>

Applied Physics Laboratory
University of Washington
1013 NE 40th Street
Seattle, WA 98105-6698

In collaboration with:
Taketoshi Takazawa
Japan Marine Science and Technology Center (JAMSTEC), Yokosuka, Japan

Eddy C. Carmack
Department of Fisheries and Oceans, Institute of Ocean Sciences, Sidney, British Columbia, Canada

---

The Canadian and Japanese partners are providing in-kind (matching) support to this project through ship time (Japan and Canada) and instrumented moorings (Japan).

Task Order 15163

Abstract

This program collected hourly time series of ocean velocity, temperature, and salinity properties from moored instruments deployed along the outer shelf and slope of the Alaskan Beaufort Sea for a period of one year. The goals are to: 1) quantify the vertical and cross-shore spatial and temporal scales of variability in the circulation and the density (thermohaline) field in this region and 2) estimate the transport within the eastward flowing subsurface undercurrent. The flow and the density structure on the outer shelf and slope affect the cross-shelf transfer of momentum, water properties (heat, salt, nutrients, etc.), contaminants, and pollutants. The region is also an important migratory corridor for marine mammals, particularly bowhead whales that feed here during part of the year. Previous measurements showed that the near surface flow (< ~50 m depth) here, and over the inner shelf, is westward and forced by the winds. However, flow reversals are common and often a result of upwelling of the undercurrent. Further, the pressure field responsible for the undercurrent must influence the dynamics of the inner shelf. The undercurrent originates in the eastern Arctic as a result of inflow through Fram Strait and is fed by outflows from the Eurasian shelf seas and the Chukchi Sea. Hence it is circumpolar in extent and carries with it a variety of water masses. The flow could thus transport pollutants from these regions to the Alaskan shelf. The observations will provide information crucial in guiding model development and evaluating the performance of pollution transport models. The study site is practical (from the resource manager's perspective and for logistical reasons) and optimal from a scientific perspective, for measurements here will capture the integrated effects of the circumpolar forcing which we believe force the undercurrent.

Alaska Sea Ice Atlas

Orson P. Smith <afops@uaa.alaska.edu>
William J. Lee <afwjl3@uaa.alaska.edu>

School of Engineering
University of Alaska Anchorage
3211 Providence Drive
Anchorage, AK 99508-8054

Task Order 15177

Abstract

A GIS-based atlas of sea ice conditions in the territorial waters of Alaska is in the final stages of preparation. It updates previously printed ice atlases and provides risk analysis information for engineers and resource managers. The Alaska Sea Ice Atlas includes a comprehensive collection of georeferenced digital historical data on Alaska sea ice and other environmental factors that bear directly on ice processes and conditions. Historical ice reports of the U.S. National Ice Center form the foundation of the database of ice conditions. This information is supplemented by ice and related climatological data from the U.S. National Weather Service and other archives. Areas of uniform ice concentration, stage, and form are portrayed as polygons and superimposed on a 5-km-square grid. Grid cell statistics over the period of record for each week of the calendar year include distribution parameters, reported extremes, combined probabilities of concentration and stage, and related atmospheric variables. Hindcast wind stress divergence is applied as an analog of ice compression and ridge formation. These statistics allow derivation of a navigability index for assessing difficulties in navigating ice-covered waters in various classes of vessels. The preliminary version of the Alaska Sea Ice Atlas is accessible via a customized implementation of GIS tools at the public website http://holmes-iv.engr.uaa.alaska.edu. The final version is scheduled for public access in March 2003.

A Nowcast/Forecast Model for the Beaufort Sea Ice–Ocean–Oil Spill System (NFM-BSIOS)

Jia Wang <jwang@iarc.uaf.edu>

International Arctic Research Center–Frontier Research System for Global Change
University of Alaska Fairbanks
Fairbanks, AK 99775-7340

Meibing Jin <ffjm@uaf.edu>

Institute of Marine Science
University of Alaska Fairbanks
Fairbanks, AK 99775-7220

Task Order 15178

Abstract

A nested coupled ice–ocean model was developed under the CMI/MMS project titled, "A Nowcast/ Forecast Model for the Beaufort Sea Ice–Ocean–Oil Spill System (NFM-BSIOS)." A transport-conserved scheme was used to pass information from the coarse 27.5 km resolution model to the nested fine 3.4375-km resolution model. The fine-resolution ocean model was run for a seasonal cycle, longer than would be needed for the operational purpose.

The high-resolution coupled ice–ocean model was validated using available observations. The fine structure of the ice and ocean motion was investigated to provide a precise simulation of the ice–ocean–oil spill system. The modeled circulation revealed the observed Beaufort Sea coastal current and the Beaufort Gyre. The vertical temperature and salinity profile demonstrated the observed dense water sinking process on shelf areas. The model reproduces a reasonable seasonal cycle for sea ice concentration, temperature, salinity, water masses, and other variables. The nested model reproduces mesoscale eddies, consistent with satellite images taken in the same region. Some important processes, such as winter halocline ventilation and dense water formation, are captured in the model.

The surface circulation follows the wind direction (to the west), while the slope current along the Beaufort Sea slope is reproduced below 100 m, flowing to the east, opposite to the surface current. There are some mesoscale eddies in the fine-resolution model. Neither the slope current nor the mesoscale eddies are captured in the coarse model. Thus, this fine-nested model captures some dynamic features in the Beaufort Sea and its shelves.

Using station wind data and simulated surface current, sea ice velocity and ice concentration from the coupled ice–ocean model, we conducted a series of simulations of oil spills released at different times, with and without sea ice cover. The results show significant seasonal and interannual variability of the oil spill trajectory under simulated ice conditions. Sea ice cover can affect oil spill trajectory by reducing wind effects on sea surface current, sea ice flow and oil spill velocity. Ice flows dominate oil spill movement in the winter months, and wind has a larger effect on oil spill movement during the summer.

Satellite Tracking of Eastern Chukchi Sea Beluga Whales in the Beaufort Sea and Arctic Ocean

Robert S. Suydam <robert.suydam@north-slope.org>

Department of Wildlife Management
North Slope Borough
P.O. Box 69
Barrow, AK 99723-0069

Lloyd F. Lowry <llowry@eagle.ptialaska.net>
Kathryn J. Frost <kjfrost@eagle.ptialaska.net>

Institute of Marine Science
University of Alaska Fairbanks
Fairbanks, AK 99775–7220

Task Order 15179

Abstract

*At least five stocks of beluga whales (*Delphinapterus leucas*) occur in Alaska. One of these, the eastern Chukchi Sea stock, is most commonly seen in coastal waters near Kasegaluk Lagoon in northwestern Alaska during June and July. Despite protection under the Marine Mammal Protection Act and their importance to many Alaska Native hunters for subsistence, relatively little is known about the movements and seasonal distribution of these whales during the rest of the year. In 1998–2002 we instrumented 23 belugas with satellite-linked depth recorders (SDRs), including 12 adult males, 5 immature males, 2 adult females and 4 immature females. SDRs provided location information for an average of 67 (range 5–154) days. Saddle mount tags averaged 52 days, spider mounts 68 days and side mounts 81 days, although there was no statistical difference in longevity among attachment types. Animals moved north and east into the northern Chukchi and western Beaufort seas after capture. During July–September, movement patterns differed by age and/or sex. All belugas that moved north of 75°N in the Beaufort Sea and Arctic Ocean were males. Adult males tended to use deeper water and to remain there for most of the summer. Five of nine adult males tagged from all-male groups early in their northward migration traveled through 90% pack ice cover to reach 79–80°N by late July/early August. Adult males captured from groups that included adult females also moved into deep water but apparently for shorter periods of time. In all years, adult and immature females remained at or near the shelf break throughout summer and early fall. Immature males moved farther north than immature females, but not as far north as adult males based on our small sample size. Belugas of all ages and both sexes were most often found in water deeper than 200 m along and beyond the continental shelf break. They rarely used the inshore waters within the Outer Continental Shelf lease sale area of the Beaufort Sea. Heavy ice apparently did not inhibit the movements of large adult males in summer since they traveled through and were often located in >90% ice cover. Only 3 tagged belugas transmitted data after October. Those animals migrated south through Bering Strait into the northern Bering Sea north of Saint Lawrence Island.*

Timing and Re-Interpretation of Ringed Seal Surveys

Brendan P. Kelly <brendan.kelly@uas.alaska.edu>
Oriana R. Harding
Mervi Kunnasranta
John R. Moran, Jr. <ftjrm2@uaf.edu>

University of Alaska Southeast
11120 Glacier Highway
Juneau, AK 99801

Task Order 15180

Abstract

We used radio telemetry to estimate the proportion of ringed seals (n = 61) visible resting on the ice surface during the spring months in 1999, 2000, 2001, 2002, and 2003. Changes in the number counted during ground-based, visual surveys of seals resting on the ice corresponded to changes in the number of radio-tagged seals basking. Tagged seals spent 17% (95% CL = 12–21%) of their time out of the water while using subnivean lairs and 40% (95% CL = 35–45%) of their time out of water after emerging from those lairs. Haulout bouts were more frequent (median interval = 14 hr) and longer (median duration = 9 hr) when seals were basking than when they were using subnivean lairs (median interval = 27 hr, median duration = 6 hr). Before lair abandonment was complete, the mean proportion of tagged seals basking was 0.19 (CV = 117.92). After lair abandonment was complete, the mean proportion of tagged seals basking was 0.75 (CV = 27.93).

Emergence from the lairs was related to structural failure of the snow pack, and passive microwave emissions, indicative of liquid moisture in the snow, predicted lair abandonment (r^2 = 0.982, p = 0.001). In addition, active microwave (Ku-band) backscatter detected snow melt, but also responded to an anomalous rain event.

Interannual and spatial comparisons of seal densities based on aerial surveys have not adequately accounted for the proportion of seals concealed within subnivean lairs. Previous models of the factors influencing the density of seals detected in aerial surveys have been based on densities observed during surveys conducted under limited ranges of conditions. We used the proportion of radio-tagged seals visible as our response variable to determine which environmental factors were most important in explaining the availability of seals to be counted. The most important variables were date, time of day, wind speed, and days before snow melt as determined by passive microwave emissions. A model including those terms explained 72% of the variance in the proportion of tagged seals visible. We recommend timing future surveys to take place after substantial snow melt (detected by passive microwave emissions) indicates lair abandonment is complete.

Radio-tagged ringed seals remained close to their capture and release sites in April, May, and early June. The mean home range size during the breeding season was 1.73 km^2 (SD = 4.19), and 94% of the home ranges were less than 3 km^2. Interannual fidelity to breeding sites was observed in 3 adult ringed seals (2 males and 1 female) and suggests fitness costs to displacement of seals and an unexpected level of population structuring.

Archiving of Shelikof Strait Sediment Samples at the University of Alaska Museum

A. Sathy Naidu <ffsan@uaf.edu>
John J. Kelley <ffjjk@uaf.edu>

Institute of Marine Science
University of Alaska Fairbanks
Fairbanks, AK 99775-7220

Task Order 15181

Abstract

In 1997–98, 288 surface sediment samples were collected from lower Cook Inlet and Shelikof Strait as part of a research project on trace elements and hydrocarbons by Arthur D. Little, and funded by the Minerals Management Service. After completion of the project MMS made the residual samples available for supplemental studies or archiving. These sediment samples are very valuable, as they were collected at considerable cost and effort and from an area where few sediment samples are available.

Sathy Naidu, Institute of Marine Science, University of Alaska Fairbanks, is in the process of transferring his sediment samples from marine regions of arctic and subarctic Alaska (collected over the last 33 years) to the Earth Sciences Collection at the University of Alaska Museum (UAM). The goal of the UAM repository is to be the primary marine and freshwater sediment archiving center for the arctic region. This transfer is to take place in spring–summer 2003, and archiving of the samples will be accommodated in the museum repository as part of an effort funded by the National Science Foundation to the museum. This brief proposal requests that the Cook Inlet–Shelikof Strait samples be transferred to Dr. Naidu who, in turn, will arrange for their archiving at UAM. For these samples, Dr. Naidu has been offered walk-in cooler space (maintained at 3.6°C) with a duplicate refrigeration system. The latter is wired into an alarm system that alerts the university power plant and all curators if there is a power failure. Backup electrical generators are housed next door to the refrigerator. Additionally, all samples will be maintained in a contaminant-free atmosphere. The Cook Inlet–Shelikof Strait sample suite will be integrated into Dr. Naidu's sediment collection, labeled, and arranged systematically for easy retrieval. To ensure proper use of a split of a sample, a potential user will be required to go through the protocol developed by the Museum User's Committee, of which Dr. Naidu is a member. Records (location, coordinates, water depth of collection, available analytical data and their quality) on all samples will eventually be made available on an easily accessible website.

CODAR in Alaska

Hank Statscewich <stats@ims.uaf.edu>
David L. Musgrave <musgrave@ims.uaf.edu>

Institute of Marine Science
University of Alaska Fairbanks
Fairbanks, AK 99775-7220

Task Order 74261

Abstract

Surface currents measured by High Frequency RADAR instrumentation obtained near the mouth of the Kenai River in Cook Inlet and sea level height measurements from Nikiski are analyzed for tidal constituents over a 6-month sampling interval. Harmonic analyses of sea level height records reveal a form ratio of 0.28 which classifies this region as having mixed, mainly semi-diurnal tides. A significant portion of energy is contained in the tidal currents of this region, accounting for approximately 90% of the total current variance. Currents were dominated by the M2 tidal constituents, whose magnitudes ranged from 30 to 200 cm s^{-1} and tended to be aligned with local topography. Mean subtidal currents were variable (0.5–100 cm s^{-1}) with the strongest currents occurring over the deepest sections of the channel. Particle excursions, due to tides, in this section of Cook Inlet are between 4 and 32 km and are comparable to the channel width. Predicted, barotropic tidal current ellipses agree quite well in magnitude and phase with the tidal model of Foreman et al. Computations of horizontal divergence indicate persistent regions of up and downwelling which are aligned with the edges of locally documented tidal rips.

Observations of Hydrography in Central Cook Inlet, Alaska, During Diurnal and Semidiurnal Tidal Cycles

Stephen R. Okkonen <okkonen@alaska.net>

Institute of Marine Science
University of Alaska Fairbanks
Fairbanks, AK 99775–7220

Task Order 85243

Abstract

Surface-to-bottom measurements of temperature, salinity, and transmissivity, as well as measurements of surface currents (vessel drift speeds) were acquired along an east–west section in central Cook Inlet, Alaska during a 26-hr period on 9–10 August 2003. These measurements are used to describe the evolution of frontal features (tide rips) and physical properties along this section during semidiurnal and diurnal tidal cycles. The observation that the amplitude of surface currents is a function of water depth is used to show that strong frontal features occur in association with steep bathymetry. The positions and strengths of these fronts vary with the semidiurnal tide. The presence of freshwater gradients alters the phase and duration of tidal currents across the section. Where mean density-driven flow is northward (along the eastern shore and near Kalgin Island), the onset of northward tidal flow (flood tide) occurs earlier and has longer duration than the onset and duration of northward tidal flow where mean density-driven flow is southward (in the shipping channel). Conversely, where mean density-driven flow is southward (in the shipping channel), the onset of southward tidal flow (ebb tide) occurs earlier and has longer duration than the onset and duration of southward tidal flow along the eastern shore and near Kalgin Island.

Importance of the Alaskan Beaufort Sea to King Eiders (*Somateria spectabilis*)

Abby N. Powell <ffanp@uaf.edu>
Laura M. Phillips <fslmp@uaf.edu>
Eric A. Rexstad <ffear@uaf.edu>

Institute of Arctic Biology
University of Alaska Fairbanks
Fairbanks, AK 99775-7000

Eric J. Taylor <eric_taylor@fws.gov>

U.S. Fish and Wildlife Service
101 12th Avenue
Box 19, Room 110
Fairbanks, AK 99701

Task Order 15182

Abstract

During the molt migration (early July–August) and fall migration (mid-August–October), king eiders move west along the Beaufort Sea coast to areas in the Chukchi and Bering seas, but information on distance offshore and the frequency and location of potential staging areas is lacking. This study was begun to better understand use (timing, location, duration) of nearshore (barrier island to the mainland coast) and offshore (seaward of the barrier islands) habitats of the Beaufort Sea by migrating, staging, and molting adult king eiders. We trapped 27 pre-breeding king eiders (13 females and 14 males) in 2004 using mist nets and decoys at the Kuparuk oil field on the Arctic Coastal Plain of Alaska. An experienced veterinarian surgically implanted satellite transmitters into the body cavity of each eider. The satellite platform transmitting terminal (PTT) transmitters send location information via satellites every 48 hours during late summer and fall migration. This report includes late summer location data from the 27 eiders transmittered in 2004 and molt, winter, and summer location data of 33 king eiders implanted with satellite transmitters during the 2002 and 2003 field seasons. Three of the 2003 transmittered eiders were still sending location data as of 31 July 2004. Areas the 2002 and 2003 eiders used for molting included the Chukotka Peninsula, the Kamchatka Peninsula, St. Lawrence Island, Kuskokwim Bay, the Alaska Peninsula, and the Beaufort Sea. These results are comparable to those of Dickson et al. [2000]. Winter locations were along the Kamchatka Peninsula, the Chukotka Peninsula, the Alaska Peninsula, Kvichak Bay, Chirikof Island, and the Kenai Peninsula. All 2002 and 2003 females still transmitting returned to the Kuparuk study site during the 2003 and 2004 breeding seasons. Males went to Canada, the North Slope of Alaska, and Russia during the 2003 and 2004 breeding seasons. As of 31 July 2004, most 2003 and 2004 males were heading south on molt migration, while most females remained in the Beaufort Sea.

Introduction

King eiders (*Somateria spectabilis*) migrate east along the Beaufort Sea during spring (May–June) to arctic nesting areas in Russia, Alaska and Canada. During the molt migration (early July–August) and fall migration (mid-August–October), eiders move west along the Beaufort Sea coast to areas in the Chukchi and Bering seas; however, some adult male king eiders molt in the Beaufort Sea. Although the timing and route of the offshore spring migration is likely determined by the availability of open water in the pack ice, information on distance offshore and the frequency and location of potential staging areas is lacking. Little is known about the migration corridor and staging and molting areas of non-breeders. This study was begun to better understand use (timing, location, duration) of nearshore (barrier island to the mainland coast) and offshore (seaward of the barrier islands) habitats of the Beaufort Sea by migrating, staging, and molting adult king eiders. Because eiders congregate in large, dense flocks during migration and molt, they may be particularly vulnerable to an offshore oil spill in the Beaufort Sea. An apparent decline in the western Canadian and eastern Alaskan populations of king eiders has increased concern for this species [Suydam et al. 2000]. This study will identify when, where, and how long adult king eiders use the Beaufort Sea; consequently, results may be overlapped with trajectories from modeled oil spills to better assess impacts from permitted or planned oil and gas developments.

Objectives

1. Document movements and locations of spring, summer and fall migrating adult king eiders (successful and unsuccessful breeders) marked on breeding areas in Kuparuk, Alaska;
2. Describe potential staging areas used during spring and fall migration;
3. Determine if adult female king eiders (successful and unsuccessful breeders) molt in the Beaufort Sea prior to fall migration to overwintering areas; and
4. Based on satellite imagery, describe sea ice and open water conditions of the nearshore and offshore of the Beaufort Sea relative to observed locations of satellite transmitter implanted king eiders.

Study Area

This study has two main sites on the North Slope of Alaska: Teshekpuk Lake and the Kuparuk oil fields. The Teshekpuk Lake study site was added to the project this year and is located 10 km inland from the southeast shore of the lake and has experienced very little human impact. The Kuparuk study site is an area on the Arctic Coastal Plain between the Colville and Kuparuk rivers leased by ConocoPhillips Alaska, Inc. for oil development. Both areas are characterized by numerous thaw lakes, ponds and basins. Wetland community types include wet sedge (*Carex* spp.) meadows, moist sedge–dwarf shrub (*Salix* spp.) meadows, and emergent *Carex* spp. and *Arctophila fulva* on the margins of lakes and ponds [Anderson et al. 1999]. Figure 1 shows the locations of the study areas and sites mentioned in the report.

Figure 1. Locations of study area and place names mentioned.

Methods

Transmitters were deployed at the Teshekpuk Lake field site 13 June–16 June and at the Kuparuk field site 18 June–20 June. King eiders were captured using mist net arrays set up in ponds with relatively large concentrations of eiders. Once captured, the eiders were placed in a secure, dark kennel and transported to an indoor facility or weatherport equipped for surgery. A veterinarian (Cheryl Scott, DVM) and one assistant surgically implanted a 35-g satellite platform transmitting terminal (PTT) transmitter into the abdominal cavity of each eider following the techniques described in our previous annual report [Powell et al. 2004]. We weighed each eider while in captivity, took

tarsus and culmen measurements, and fitted it with a U.S. Fish and Wildlife Service (USFWS) band. The birds were held until fully awake and recovered from anesthesia (usually about 2–3 h), and then released near the area where they were captured.

The 35-g PTTs used in this study have an expected battery life of 800 h. To obtain the greatest number of locations during periods of active migration, the transmitters were programmed to have 4 different duty cycles. They transmit for 6 h every 48 h for the first 4 months (June through September) to increase the likelihood of collecting location data in the Beaufort Sea during molt migration. The transmitters then transmit for 6 h every 84 h for 3 months (October through December), every 168 h for 3 months (January through March) and every 84 h until the end of the battery life. The battery is projected to last about 1 year.

Migration was defined as an individual remaining in an area less than 1 week, with sequential locations indicating movement in a single direction [Petersen et al. 1999]. Assuming king and spectacled eiders have a similar behavior during molt, a bird was considered molting if it remained within a restricted area and moved less than 1.5 km h^{-1}. Staging birds were identified from clusters of locations from several birds or a bird remaining in an area for at least 10 d [Petersen et al. 1999]. Location data were filtered for accuracy using PC-SAS Argos Filter V5.0 (Dave Douglas, U.S. Geological Survey/Alaska Science Center). The filtering program removes implausible locations based on location redundancy and tracking paths. Locations were then plotted using ArcView GIS.

Results

When we arrived at the Teshekpuk field site on 8 June 2004, most of the ponds in the study area were still partially frozen over and some snow remained on the ground. We trapped eiders at 2 wetland locations. Five female and seven male pre-breeding king eiders were captured and implanted with satellite transmitters between 13 and 16 June. Fifteen king eiders (8 female and 7 male) were trapped and implanted with transmitters at the Kuparuk field site between 18 and 20 June. There were no complications during the surgeries and all of the birds appeared healthy when released.

This report includes location data from 1 September 2002 through 31 July 2004 for the 33 king eiders transmittered in 2002 and 2003 and from capture date through 31 July 2004 for the 27 king eiders transmittered in 2004. Of the 33 transmitters deployed in king eiders in 2002 and 2003, all 21 from 2002 have stopped transmitting and of 12 transmitters deployed in 2003, 3 are still transmitting location information (Table 1). All 27 king eiders implanted during the 2004 field season were alive and transmitting as of 31 July 2004. The results and analysis of location data presented here are preliminary and may be subject to change at a later date based on new information received.

2002 satellite transmitter birds

Males (n = 10) staged 7–17 d (mean = 10) in the Beaufort Sea prior to fall molt migration at a mean distance from shore of 17 ± 6 km (SD) and a mean water depth of 11 ± 7 m, n = 94 location data points. Females (n = 11) staged 9–32 d (mean = 20) in the Beaufort Sea prior to molt migration at a mean distance from shore of 14 ± 3 km and a mean water depth of 8 ± 5 m, n = 174 location data points. Males reached molting areas along the Chukotka Peninsula and Kamchatka Peninsula, Russia and St. Lawrence Island and Kuskokwim Bay, Alaska from 22 July through 12 August. Females reached molting areas along the Chukotka Peninsula and Kamchatka Peninsula and St. Lawrence Island, the Arctic Coastal Plain and the Alaska Peninsula from 11 August through 18 September (Table 1, Figure 2).

Table 1. September 2002 through July 2003 molting, wintering, summering and current locations of 33 king eiders fitted with satellite transmitters at Kuparuk, Alaska.

ID	PTT #	Year Deployed	Sex	Transmitter Status	Molt Location	Wintering Location	Summer Location
KNG01	33933	2002	F	Failed	NA	NA	NA
KNG02	33934	2002	F	Indicated bird dead	Cape Chaplin, Chukotka Peninsula, Russia	NA	NA
KNG03	33935	2002	F	Failed	Alaska Peninsula	Alaska Peninsula	Kuparuk, AK
KNG04	33936	2002	M	Failed	Cape Chaplin, Chukotka Peninsula, Russia	Chukotka Peninsula, Russia	Beaufort Sea off coast of Canada
KNG05	33937	2002	F	Failed	Kvichak Bay, AK	Kenai Peninsula, AK	NA
KNG06	33938	2002	F	Failed	NA	NA	NA
KNG07	33939	2002	M	Failed	Kuskokwim Bay, AK	Kvichak Bay, AK	Banks Island, Canada
KNG08	33940	2002	M	Failed	Anadyr Bay, Chukotka Peninsula, Russia	Kvichak Bay & Alaska Peninsula	Beaufort Sea off coast of Canada
KNG09	33941	2002	F	Failed	Alaska Peninsula	Kvichak Bay & Alaska Peninsula	Kuparuk, AK
KNG10	33942	2002	M	Failed	Kamchatka Peninsula, Russia	Kamchatka Peninsula, Russia	Inland Russia
KNG11	33943	2002	M	Indicated bird dead	Karagin Bay, Kamchatka Peninsula, Russia	Kamchatka Peninsula, Russia	NA
KNG12	33944	2002	F	Failed	Karagin Bay, Kamchatka Peninsula, Russia	Karagin Bay, Kamchatka Peninsula, Russia	Kuparuk, AK
KNG13	33945	2002	F	Failed	Anadyr Bay, Chukotka Peninsula, Russia	Chirikof Island, AK	Kuparuk, AK
KNG14	33946	2002	F	Failed	Cape Nygchigen, Chukotka Peninsula, Russia	Cape Chukotka, Chukotka Peninsula, Russia	Kuparuk, AK
KNG15	33947	2002	M	Failed	St. Lawrence Island, AK	Togiak Bay, AK	Inland Russia
KNG16	33948	2002	M	Failed	Karagin Bay, Kamchatka Peninsula, Russia	Kamchatka Peninsula, Russia	South of Barrow, AK
KNG17	33949	2002	F	Failed	St. Lawrence Island, AK	Alaska Peninsula	Kuparuk, AK
KNG18	33950	2002	M	Failed	Mechigmen Bay, Chukotka Peninsula, Russia	Chirikof Island & Kvichak Bay, AK	Beaufort Sea off coast of Canada
KNG19	33952	2002	M	Failed	St. Lawrence Island, AK	Alaska Peninsula & Togiak Bay	Kuparuk, AK
KNG20	33953	2002	M	Failed	Anadyr Bay, Chukotka Peninsula, Russia	Meynypil'gyno, Russia	Cape Bathurst, Canada
KNG21	33954	2002	F	Failed	Cape Chukotka, Chukotka Peninsula, Russia	Cape Chaplin, Chukotka Peninsula, Russia	NA

Table 1. continued

ID	PTT #	Year Deployed	Sex	Transmitter Status	Molt Location	Wintering Location	Summer Location
KNG22	40898	2003	M	Failed	Russian Coast near Meynypil´gyno	Kamchatka Peninsula, Russia	NA
KNG23	40899	2003	M	Failed	Anadyr Bay, Chukotka Peninsula, Russia	Cape Chukotka, Chukotka Peninsula, Russia	NA
KNG24	40900	2003	F	Alive	Mechigmen Bay, Chukotka Peninsula, Russia	Cape Chukotka, Chukotka Peninsula, Russia	Kuparuk, AK
KNG25	40901	2003	M	Indicated bird dead	Bristol Bay, AK	Alaska Peninsula	Victoria Island, Canada
KNG26	40902	2003	M	Failed	Mechigmen Bay, Chukotka Peninsula, Russia	Chukotka Peninsula, Russia	NA
KNG27	40903	2003	F	Alive	Mechigmen Bay, Chukotka Peninsula, Russia	Alaska Peninsula	Kuparuk, AK
KNG28	40904	2003	M	Failed	Mechigmen Bay, Chukotka Peninsula, Russia	Alaska Peninsula	Inland Russia
KNG29	40905	2003	M	Failed	Mechigmen Bay, Chukotka Peninsula, Russia	Chukotka Peninsula, Russia	Beaufort Sea off coast of Canada
KNG30	40906	2003	F	Failed	Anadyr Bay, Chukotka Peninsula, Russia	Olyutor Bay, Russia	Kuparuk, AK
KNG31	40907	2003	M	Failed	Anadyr Bay, Chukotka Peninsula, Russia	Olyutor Bay, Russia	Banks Island, Canada
KNG32	40908	2003	M	Failed	Anadyr Bay, Chukotka Peninsula, Russia	Olyutor Bay, Russia	Inland Russia
KNG33	40909	2003	M	Alive	Anadyr Bay, Chukotka Peninsula, Russia	Alaska Peninsula	Beaufort Sea off coast of Canada

Wintering locations for males included areas along the Chukotka Peninsula, Kamchatka Peninsula, and Meynypil′gyno, Russia and Kvichak Bay, the Alaska Peninsula, Chirikof Island, and Togiak Bay, Alaska. Wintering locations for females included areas along Karagin Bay and the Chukotka Peninsula and the Kenai Peninsula, Kvichak Bay, Chirikof Island, and the Alaska Peninsula (Table 1, Figure 3).

The 6 females from 2002 still transmitting in June of 2003 returned to the Kuparuk study site. Of the 9 males from 2002 still transmitting into summer of 2003, 1 returned to Kuparuk, 1 spent some time south of Barrow, 3 stayed offshore of Canada near Cape Bathurst, 2 spent time onshore in Canada and 2 went onshore in Russia (Table 1, Figure 4).

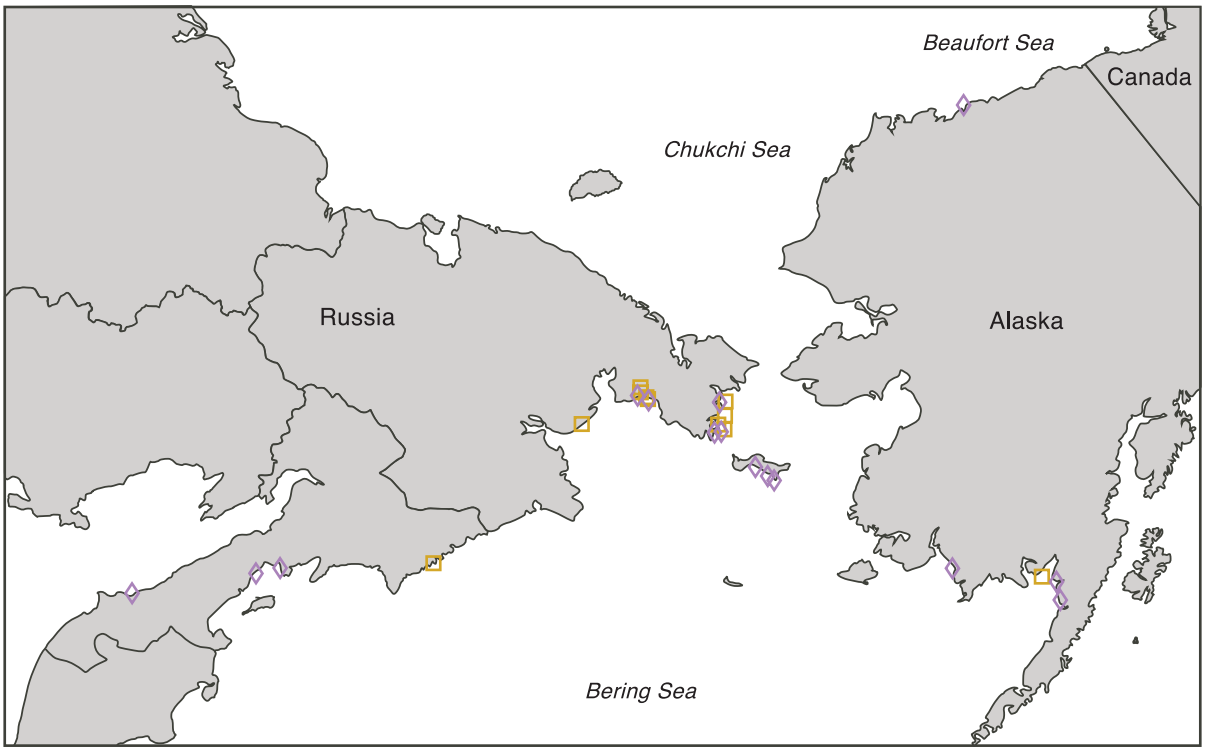

Figure 2. Molting locations of 2002 (◊) and 2003 (□) king eiders fitted with satellite transmitters at Kuparuk in 2002.

2003 satellite transmitter birds

Males (n = 9) dispersed from the breeding area 24 June through 13 July 2003 and arrived in molt areas 18 July through 17 August 2003. Females (n = 3) left the breeding area between 7 July and 30 July and arrived at molt sites 22 August through 4 September. Molt areas included the Chukotka Peninsula for both males and females and Bristol Bay and the coast of Russia for two males. (Table 1, Figure 2)

Wintering locations for males included areas along the Chukotka, Kamchatka, and Alaska peninsulas, Meynypil′gyno and Olyutor Bay, Russia. Females wintered along the Alaska and Chukotka peninsulas and in Olyutor Bay. (Table 1, Figure 3)

Nine of the twelve birds transmittered in 2003 continued to transmit into June, providing 2004 summering locations. All 3 females returned to the capture site at Kuparuk, Alaska. Males summered in Russia, Canada and the Beaufort Sea. (Table 1, Figure 4)

At the end of July 2004, only 3 of the 2003 eiders (2 females and 1 male) were still transmitting location information. Only 1 female remained at the Kuparuk study area, 1 was off the coast of Alaska in the Beaufort Sea and the male was located in the Beaufort near Banks Island, Canada. (Figure 5)

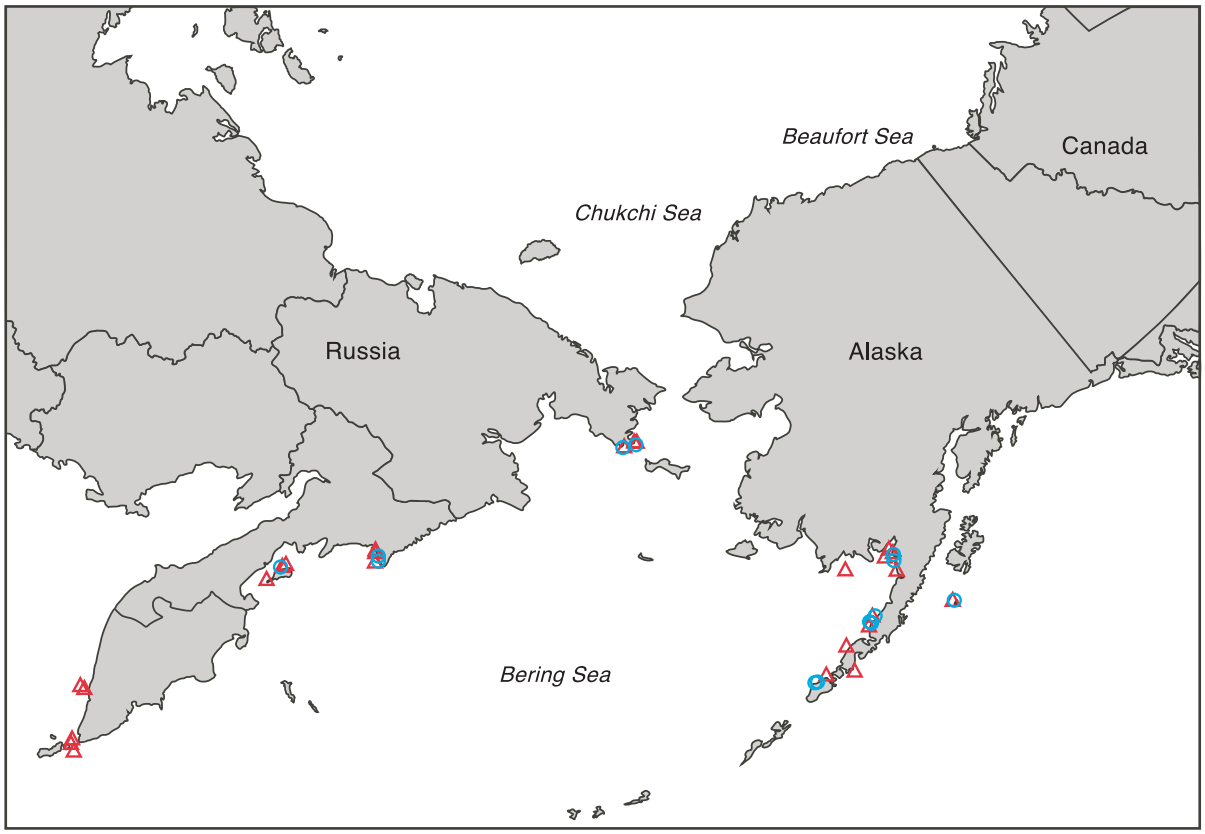

Figure 3. Wintering locations of male (△) and female (○) king eiders fitted with satellite transmitters at Kuparuk in 2002 and 2003.

2004 satellite transmitter birds

By 31 July, all 2004 transmittered male king eiders had left the study areas and moved into the Chukchi and Bering seas, with 7 males located along the Chukotka Peninsula, 4 south of St. Lawrence Island, 2 near Meynypil′gyno, Russia and 1 in the Chukchi Sea near Icy Cape. All but 2 females had left the study areas by the end of July, with 9 located in the Beaufort Sea and 2 near Icy Cape, Alaska. (Figure 5)

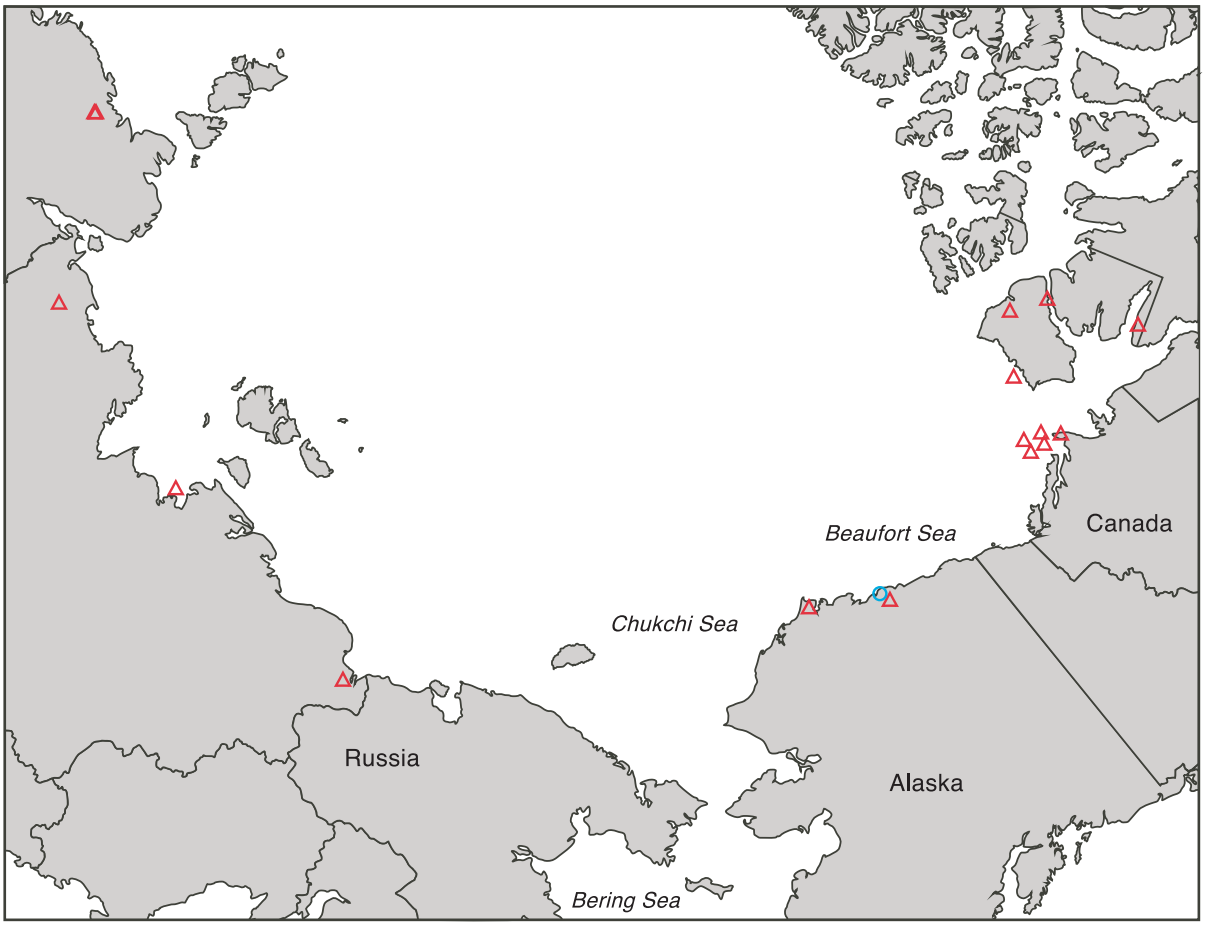

Figure 4. Summer breeding location of male (Δ) and female (○) king eiders fitted with satellite transmitters at Kuparuk in 2002. All females returned to Kuparuk and are indicated by a single marker.

Discussion

Molting areas for king eiders implanted at Kuparuk in 2002 and 2003 are similar to those found for eiders implanted at Victoria Island and Prudhoe Bay, 1997–1999 [Dickson et al. 2000]. Data on wintering locations of king eiders is limited. Dickson et al. [2000] had a small sample of king eiders (n = 9) with satellite transmitters that were transmitting location data into December. Their information suggested that similar to eiders breeding at Kuparuk, eiders breeding at Victoria Island and Prudhoe Bay wintered along the Kamchatka Peninsula, the Chukotka Peninsula, the Alaska Peninsula, and Kodiak Island. Ours is the first account of satellite transmitters in king eiders lasting into the next breeding season. Females transmittered in 2002 returning to Kuparuk for the 2003 breeding season suggests some fidelity to nesting areas.

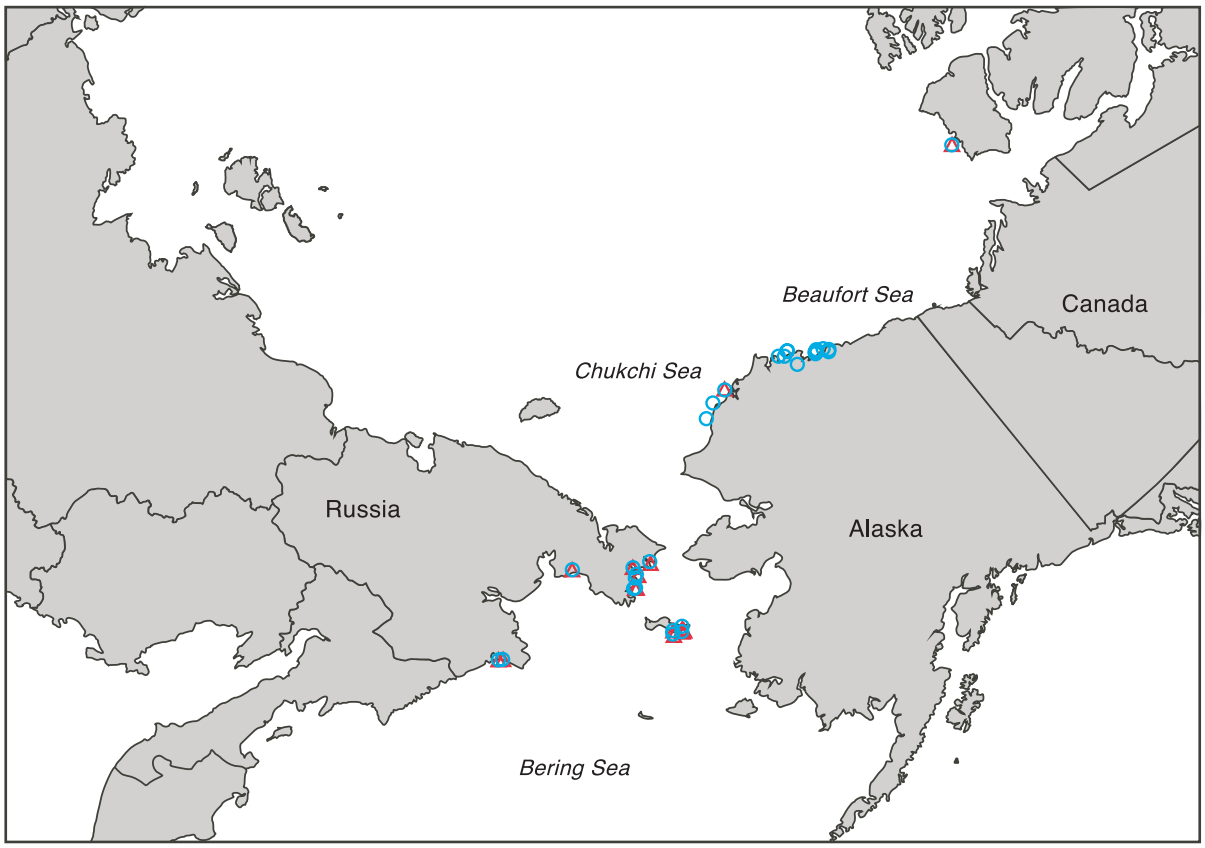

Figure 5. Location of thirty 2003/2004 male (Δ) and female (○) satellite-tagged king eiders the last week of July 2004.

Future Plans

We will continue to collect and map location information as it becomes available. Location data will be analyzed to detect staging, molting and wintering areas. We will also begin to overlay bathymetric and ice coverage maps to evaluate the impacts of these factors on migration paths.

Acknowledgements

This project would not be possible without logistic support from ConocoPhillips Alaska, Inc. and financial support from the UA Coastal Marine Institute and Minerals Management Service. Support was also provided by the North Slope Borough, the Alaska Cooperative Fish and Wildlife Research Unit, and the U.S. Fish and Wildlife Service. We would also like to thank Chuck Monnett (MMS); Declan Troy (TERA, Inc.); Betty Anderson, John Shook, and Michael Knoche (ABR, Inc.); Philip Martin and Tim Obritschkewitsch (USFWS); Caryn Rea, Anne Lazenby, Leigh McDaniel, and Justin Harth (ConocoPhillips Alaska, Inc.); Dave Douglas (U.S. Geological Survey); Robert Suydam (North Slope Borough); Paul and Chris Howey (Microwave Telemetry); our field technicians: Eric Duran, Lori Gildehaus, Amanda Prevel, Keith Roby, and Ben Soiseth; volunteers: Stacia Backensto and Corey Adler; and our veterinarian Cheryl Scott and vet technicians Kim Adams and Mindy Carlson.

References

Anderson, B.A., C.B. Johnson, B.A. Cooper, L.N. Smith and A.A. Stickney. 1999. Habitat associations of nesting spectacled eiders on the Arctic Coastal Plain of Alaska, p. 27–32. *In* R.I. Goudie, M.R. Peterson and G.J. Robertson [eds.], Behavior and Ecology of Sea Ducks. Can Wildl. Ser. Occas. Pap. 100.

Dickson, D.L., R.S. Suydam and G. Balogh. 2000. Tracking the movements of king eiders from nesting grounds at Prudhoe Bay, Alaska to their molting and wintering areas using satellite telemetry. Canadian Wildlife Service 1999/2000 Progress Report.

Petersen, M.R., W.W. Larned and D.C. Douglas. 1999. At-sea distribution of spectacled eiders: A 120-year-old mystery resolved. Auk 116:1009–1020.

Powell, A.N., L.M. Phillips, E.A. Rexstad and E.J. Taylor. 2004. Importance of the Alaskan Beaufort Sea to king eiders (*Somateria spectabilis*), p. 33–47. *In* University of Alaska Coastal Marine Institute Annual Report No. 10. OCS Study MMS 2004-002, University of Alaska Fairbanks and USDOI, MMS, Alaska OCS Region.

Suydam, R.S., D.L. Dickson, J.B. Fadely and L.T. Quakenbush. 2000. Population declines of King and Common Eiders of the Beaufort Sea. Condor 102(1):219–222.

Population Structure of Common Eiders Nesting on Coastal Barrier Islands Adjacent to Oil Facilities in the Beaufort Sea

Sarah A. Sonsthagen[1] <ftsas@uaf.edu>
Kevin G. McCracken[1] <fnkgm@uaf.edu>
Richard B. Lanctot[2] <richard_lanctot@fws.gov>
Sandra L. Talbot[3] <sandy_talbot@usgs.gov>
Kim T. Scribner[4] <scribne3@msu.edu>

[1]Institute of Arctic Biology, University of Alaska Fairbanks, Fairbanks, AK 99775-7000
[2]U.S. Fish and Wildlife Service, Migratory Bird Management,
1011 East Tudor Road, MS 201, Anchorage, AK 99503
[3]U.S. Geological Survey, Biological Resources Division, Alaska Science Center,
1011 East Tudor Road, MS 701, Anchorage, AK 99503
[4]Department of Fisheries and Wildlife, 13 Natural Sciences Building,
Michigan State University, East Lansing, MI 48824

Task Order 85239

Abstract

Common Eider populations have experienced declines through most of their range. These birds are arctic nesters, primarily on barrier islands. Females and young exhibit a high degree of nest site fidelity to island groups, which may create genetically unique groups relative to neighboring islands. Because banding and recapture data are difficult to collect in this species, we used molecular techniques to assess population structure of Common Eiders breeding in North America and Canada. Based on preliminary results of this study, there were likely two refugia during the last Pleistocene glaciation. Birds breeding on the North Slope of Alaska were probably colonized from one refugium, separate from other eider populations and therefore genetically distinct. Eiders breeding in the Yukon–Kuskokwim Delta, Canada, and Scandinavia appear to have been colonized from the other refugium. Differences in levels of population structuring among mitochondrial and nuclear DNA suggest that recent gene flow has occurred between these populations mainly through male dispersal.

Introduction

Common Eider (*Somateria mollissima*) populations have exhibited declines throughout part of their range, including Alaska, western Canada, southern Hudson Bay, and eastern Finland. Populations residing in Alaska and western Canada have declined approximately 53% since the mid-1970s [Suydam et al. 2000], while birds breeding on the Belcher Islands in southern Hudson Bay have dimished approximately 75% since the mid-1980s [Robertson and Gilchrist 1998]. Others, however, are exhibiting stable or increasing numbers, for example, some populations breeding in the Baltic Sea region and northern Hudson Bay [Tiedemann and Noer 1998; Hipfner et al. 2002]. While the reasons for the declines are unknown, factors such as increased gull and arctic fox predation, and development or other anthropogenic effects may be factors [Robertson and Gilchrist 1998; Suydam et al. 2000].

Common Eiders nest primarily on barrier islands and in coastal brackish waters [Goudie et al. 2000]. Data suggest that adult females and young exhibit a high degree of nest site fidelity to island groups, potentially creating genetically unique geographic areas relative to neighboring islands [Cooch 1965; Reed 1975]. In a sedentary population of Common Eiders breeding in the Netherlands, 641 females were studied [Swennen 1990]. Nine dispersed from their natal sites and all were found breeding in nearby colonies. Of the 17 juvenile males studied, 15 dispersed on average 1270 km from their natal site. For adult males, about 15% of those breeding dispersed each year, which was consistent with other research. Additionally, studies conducted in the Baltic Sea region concluded that Common Eiders breeding in that area are not randomly mating, i.e., that males were found to mate more often than expected with females from the same colony [Tiedemann et al. 1999]. Preferential mating among eiders of the same origin may be an artifact of colonies favoring different areas within a common winter range or early formation of pair bonds between birds that arrive early on the winter grounds from the same origin. In addition to high female philopatry exhibited in this species [Baillie and Milne 1989; Swennen 1990], non-random pair formation on the wintering grounds provides an additional avenue of limited gene flow between populations.

While some populations of Common Eiders are sedentary, birds breeding in the northern portions of their range are migratory to varying degrees: Eiders in the Beaufort Sea and western Canada have been reported to migrate 2700 km from nest sites to their winter range near the Chukotka Peninsula in Russia [Petersen and Flint 2002; Lynne Dickson, pers. comm.]. Yukon–Kuskokwim River Delta (Y–K Delta) eiders winter there or approximately 325 km south in Bristol Bay [Petersen and Flint 2002]. One population breeding on the Belcher Islands in Hudson Bay is sedentary, whereas other populations in Hudson Bay winter in ice-free waters south of their breeding sites [Robertson and Gilchrist 1998]. Scandinavian populations migrate to wintering areas in the Baltic Sea, where mixing with other European colonies likely occurs [Swennen 1990; Tiedemann and Noer 1998; Tiedemann et al. 1999]. Since pair formation takes place on the wintering grounds [Spurr and Milne 1976], populations that share winter ranges are more likely to be genetically similar, as male dispersal between those populations will have a homogenizing effect.

Objectives of this study are to assess: 1) population structure among Common Eiders breeding on the coastal barrier islands in the Beaufort Sea, 2) population structure of Common Eiders breeding at four sites in the Y–K Delta, and 3) population structure and post-glacial colonization of Common Eiders breeding throughout North America and Canada.

Methods

Sample collection

Blood, feather, or tissue samples were collected in the following localities from 17 populations that represent all five subspecies (Figure 1):

Somateria mollissima nigrum
- 2 sites in the Y–K Delta, Alaska (N = 113)
- 2 sites from the North Slope, Alaska (N = 109)
- Kent Peninsula, Canada (N = 26)

S. m. sedentaria
- Belcher Islands, Canada (N = 20)

S. m. dresseri
- New Brunswick, Canada (N = 39)
- Nova Scotia, Canada (N = 39)

S. m. borealis
- Baffin Island, Canada (N = 14)
- Hudson Strait, Canada (N = 28)
- Southampton Island, Canada (N = 52)
- Mansel Island, Canada (N = 3)

S. m. mollissima
- Svalbard, Norway (N = 37)
- Tromsø, Norway (N = 37)
- Söderskär, Finland (N = 26)

To better assess population structure among barrier islands in the Beaufort Sea, additional feather samples were extracted in an attempt to obtain approximately 30 individuals from each island for the microsatellite DNA analyses. In total, samples from 350 individuals were collected. Each of the 14 islands are represented by 10 to 38 individuals, with one sample from an additional island.

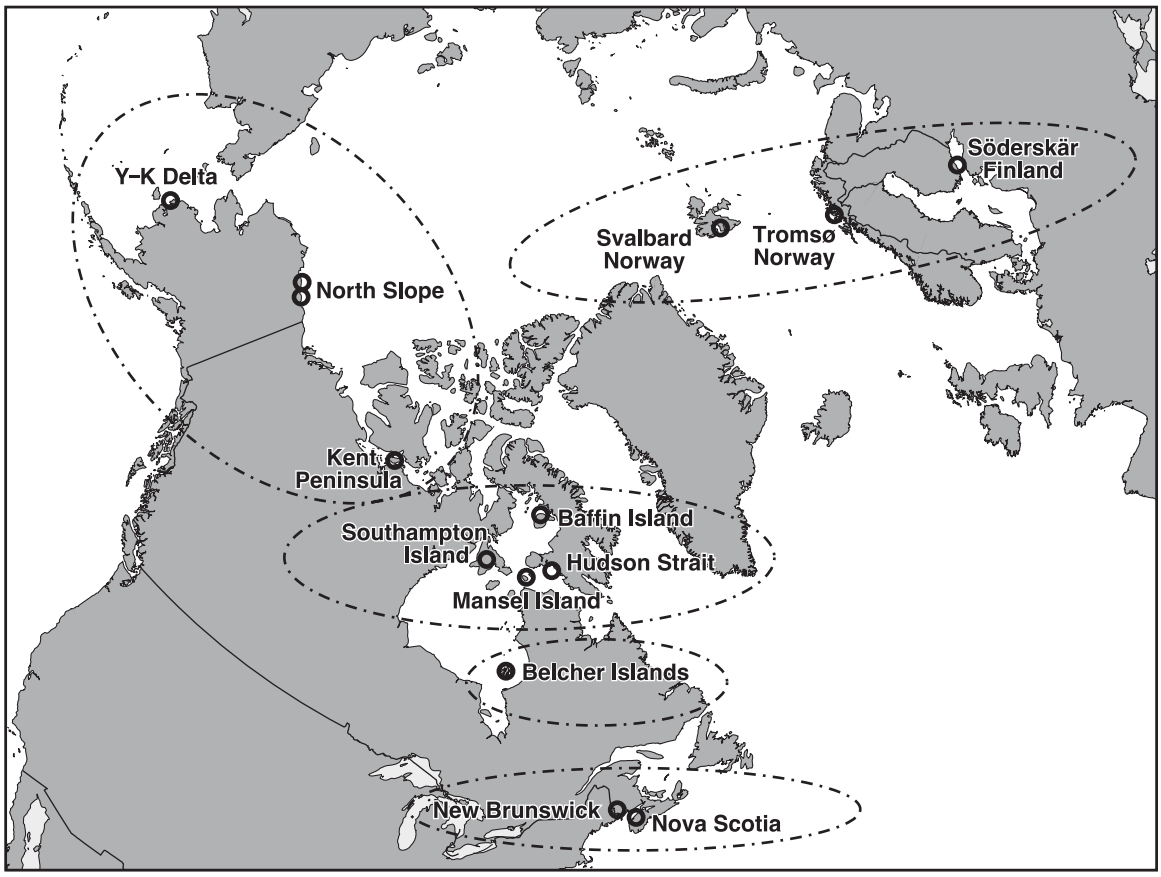

Figure 1. Sampled sites of Common Eiders used in this study. Each dashed line oval represents locations with the same subspecies: *S.m. nigrum* – Y–K Delta, North Slope and Kent Peninsula; *S.m. borealis* – Baffin Island, Southampton Island, Hudson Strait and Mansel Island; *S.m. sedentaria* – Belcher Islands; *S.m. dresseri* – New Brunswick and Nova Scotia; and *S.m. mollissima* – Svalbard, Tromsø and Söderskär.

Molecular marker data collection

Three types of molecular markers—microsatellite, mitochondrial DNA (mtDNA), and nuclear gene introns—were used to assess population differentiation. These genetic markers differ in their mode of inheritance and rate of evolution. Microsatellite alleles are inherited from both parents and have a high rate of mutation, mitochondrial DNA is maternally inherited and has a moderate rate of mutation, and nuclear gene introns are inherited from both parents with the slowest rate of mutation. Because we are using three different markers with different modes of inheritance and mutation rates, we will be able to determine if the populations are structured due to male or female breeding behavior and the relative time when these populations diverged from each other.

Microsatellites are short tandem repeats located in non-coded regions of nuclear DNA. Because these repeats are in non-coded regions and are not under selection pressures, they are highly polymorphic. Fifty-six microsatellite loci were screened for variability in Common Eiders, of which 36 were polymorphic. We have chosen 12 informative loci from autosomal regions of the genome to assess macrogeographic population structure and two additional loci for the microgeographic population structure (North Slope and Y–K Delta). Preliminary data presented will be based on genotypes of 687 individuals, with an analysis of 12–14 microsatellite loci using a LI-COR automated sequencer: Y–K Delta (N = 125), North Slope (N = 202), Kent Peninsula (N = 41), Baffin Island (N = 15), Southampton Island (N = 52), Hudson Strait (N = 28), Mansel Island (N = 3), Belcher Islands (N = 22), New Brunswick (N = 40), Nova Scotia (N = 40), Svalbard (N = 37), Tromsø (N = 38), and Söderskär (N = 27). Data were analyzed in FSTAT [Goudet 1995, 2001] and GENEPOP [Raymond and Rousset 1995] genetic data analysis programs to calculate F_{ST} values.

F_{ST} is a measure of population structure: values range from zero to one, where zero reflects panmixia and one indicates complete population isolation.

We have developed primers to sequence approximately 550 to 565 base pairs from the mitochondrial DNA control region, with preliminary data based on sequences from 423 individuals. We sequenced 250 base pairs of Lamin A intron 3 and 350 base pairs of GAPDH (glyceraldehyde-3-phosphate dehydrogenase) intron 11, and preliminary data are based on sequences from 546 individuals for Lamin A and 474 individuals for GAPDH. Sequences were collected using an ABI 3100 automated sequencer. Unique haplotypes were determined by hand and PHASE was used to reconstruct alleles for nuclear intron data [Stephens et al. 2001; Stephens and Donnelly 2003]. Data were analyzed in Arlequin 2.0 [Schneider et al. 1999] and maximum parsimony trees were constructed in PAUP* 4.0 [Swofford 1998].

Results

Microsatellite DNA analysis

Mean observed heterozygosity per locus ranged from 8.5 to 90.4%, with an overall mean of 49.3%. The overall F_{ST} (0.06) was significantly greater than zero, suggesting population subdivision. There were significant differences in pairwise F_{ST} values between North Slope, Kent Peninsula, and Y–K Delta populations and all others (F_{ST} values ranging from 0.0001 to 0.188); little significant population structuring was observed among Canadian and Scandinavian populations (Table 1).

Table 1. Pairwise F_{ST} values with significant P-values shown in bold for each population pair for 12–14 microsatellite loci.

	North Slope	Kent Peninsula	Y–K Delta	Southampton Island	Baffin Island	Hudson Strait	Belcher Islands	Nova Scotia	New Brunswick	Svalbard	Tromsø
North Slope	–										
Kent Peninsula	**0.002**	–									
Y–K Delta	**0.000**	0.001	–								
Southampton	**0.086**	**0.088**	**0.071**	–							
Baffin Island	**0.099**	**0.098**	**0.090**	0.054	–						
Hudson Strait	**0.071**	**0.077**	**0.064**	**0.033**	0.010	–					
Belcher Islands	**0.100**	**0.093**	**0.092**	0.050	0.011	0.005	–				
Nova Scotia	**0.063**	**0.075**	**0.060**	**0.042**	0.052	0.025	0.034	–			
New Brunswick	**0.066**	**0.079**	**0.061**	0.038	0.051	0.027	0.043	0.001	–		
Svalbard	**0.104**	**0.116**	**0.097**	0.054	0.031	0.006	0.021	0.030	0.040	–	
Tromsø	**0.137**	**0.160**	**0.129**	**0.079**	0.074	0.037	0.037	**0.063**	**0.076**	0.013	–
Söderskär	**0.162**	**0.188**	**0.156**	0.098	0.083	0.051	0.051	0.082	0.099	0.023	0.004

Mitochondrial DNA analysis

Two haplotype groups are present in these sequences and frequencies of individuals from each locality differ between the two groups (χ^2=127.2, df 2, P<0.0001, Figure 2). Individuals from the North Slope are predominately represented in the lower haplotype group and individuals from the Y–K Delta, Canada, and Scandinavia are predominately represented in the upper haplotype group. For pairwise population comparisons, individuals from Bodfish and Flaxman Islands (North Slope) were pooled as one population and all of the Y–K Delta sites were pooled because there were no significant differences between them. Mansel Island was removed from the analysis because of the small sample size (N = 3). There is significant population structure among all populations except between Hudson Strait and Southampton Island and Baffin Island, and between Southampton Island and Belcher Islands and Baffin Island (Table 2). High F_{ST} values are observed between North Slope populations and all other populations, with values ranging from 0.215 to 0.496, between Nova Scotia and all other populations, with values ranging from 0.361 to 0.664, and between Söderskär and all other populations, with values ranging from 0.241 to 0.664.

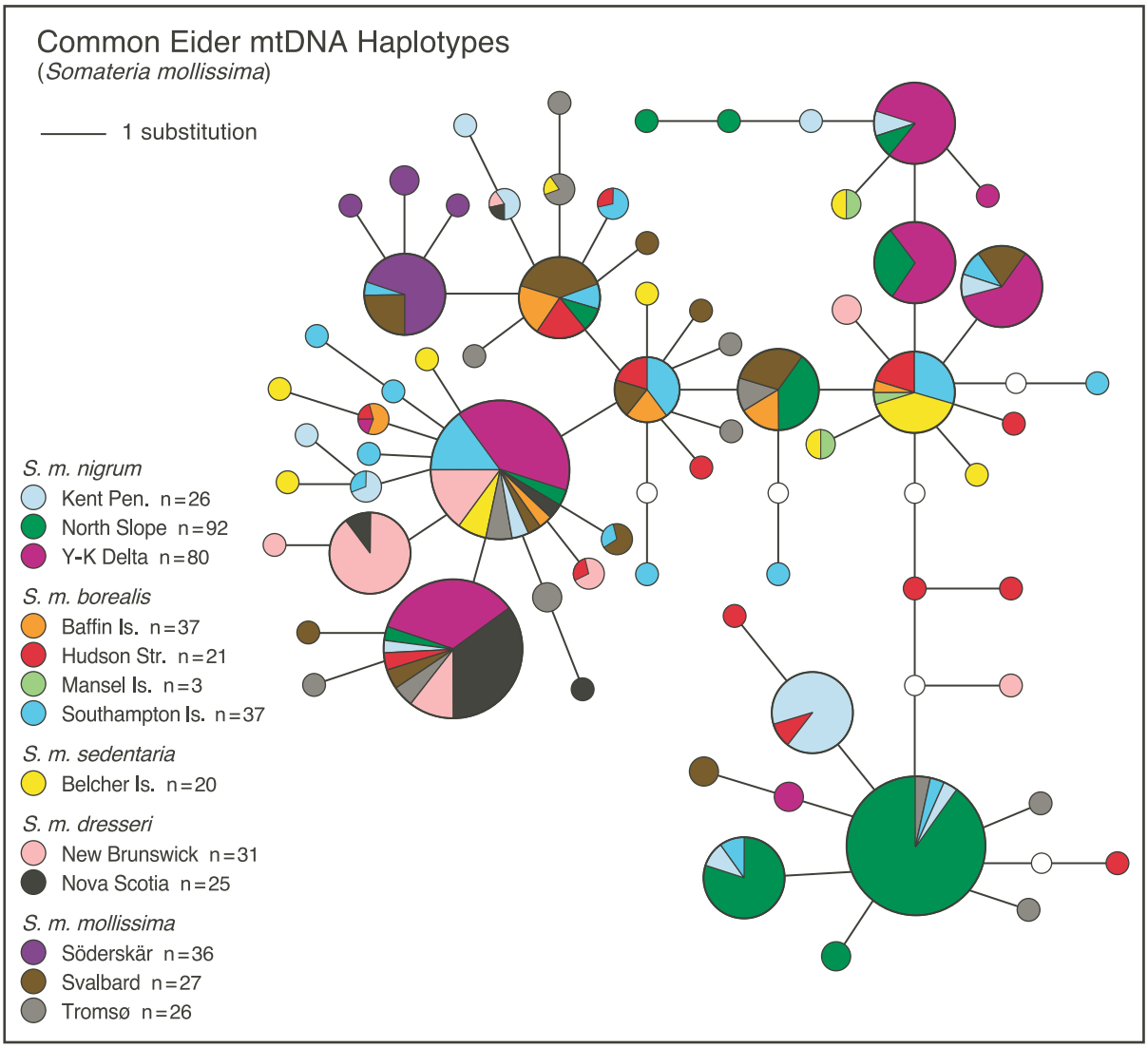

Figure 2. Mitochondrial DNA control region haplotype tree constructed from sequences collected from 17 populations. Sample size and subspecies of each population is listed on left side of tree.

Table 2. Pairwise F_{ST} values with significant P-values shown in bold for each population pair for 545–563 base pairs of mitochondrial DNA sequences.

	North Slope	Kent Peninsula	Y–K Delta	Southampton Island	Baffin Island	Hudson Strait	Belcher Islands	Nova Scotia	New Brunswick	Svalbard	Tromsø
North Slope	–										
Kent Peninsula	**0.217**	–									
Y–K Delta	**0.303**	**0.139**	–								
Southampton	**0.215**	**0.068**	**0.088**	–							
Baffin Island	**0.262**	**0.084**	**0.138**	0.018	–						
Hudson Strait	**0.253**	**0.080**	**0.169**	0.021	0.000	–					
Belcher Islands	**0.336**	**0.175**	**0.191**	0.034	**0.081**	**0.058**	–				
Nova Scotia	**0.496**	**0.402**	**0.389**	**0.366**	**0.439**	**0.370**	**0.496**	–			
New Brunswick	**0.315**	**0.126**	**0.086**	**0.081**	**0.129**	**0.144**	**0.190**	**0.407**	–		
Svalbard	**0.252**	**0.084**	**0.124**	**0.049**	**0.040**	**0.038**	**0.153**	**0.361**	**0.117**	–	
Tromsø	**0.239**	**0.082**	**0.098**	**0.049**	**0.061**	**0.076**	**0.141**	**0.367**	**0.093**	**0.062**	–
Söderskär	**0.465**	**0.353**	**0.387**	**0.310**	**0.371**	**0.337**	**0.444**	**0.664**	**0.405**	**0.241**	**0.337**

Nuclear DNA intron analysis

Like the mitochondrial DNA, two allele groups are also present within the Lamin A intron, but neither group appears to be associated with a particular locality (Figure 3). However, the two allele groups may reflect the same historical process that generated the two haplotype groups observed in mtDNA. We also pooled individuals from Bodfish and Flaxman Islands and all of the Y–K Delta sites and removed Mansel Island from the analysis. All *S.m. nigrum* populations are not significantly different from each other but are different from almost all other populations, with F_{ST} values ranging from 0.008 to 0.137 (Table 3). *S.m. borealis* populations have some structure between localities, with values ranging from 0.039 to 0.046. Belcher Islands' eiders are significantly different from all populations except Baffin Island, with F_{ST} values ranging from 0.010 to 0.151. *S.m. dresseri* populations also are not differentiated from each other but are significantly different from all other populations except for those in New Brunswick and the Y–K Delta. *S.m. mollissima* populations are showing structure between two localities, with a small F_{ST} of 0.019. Additionally, there are some insignificant F_{ST} values between the *S.m. mollissima* and *S.m. borealis* populations.

A majority of the individuals have been sequenced for nuclear intron GAPDH, which is exhibiting similar population structuring as Lamin A.

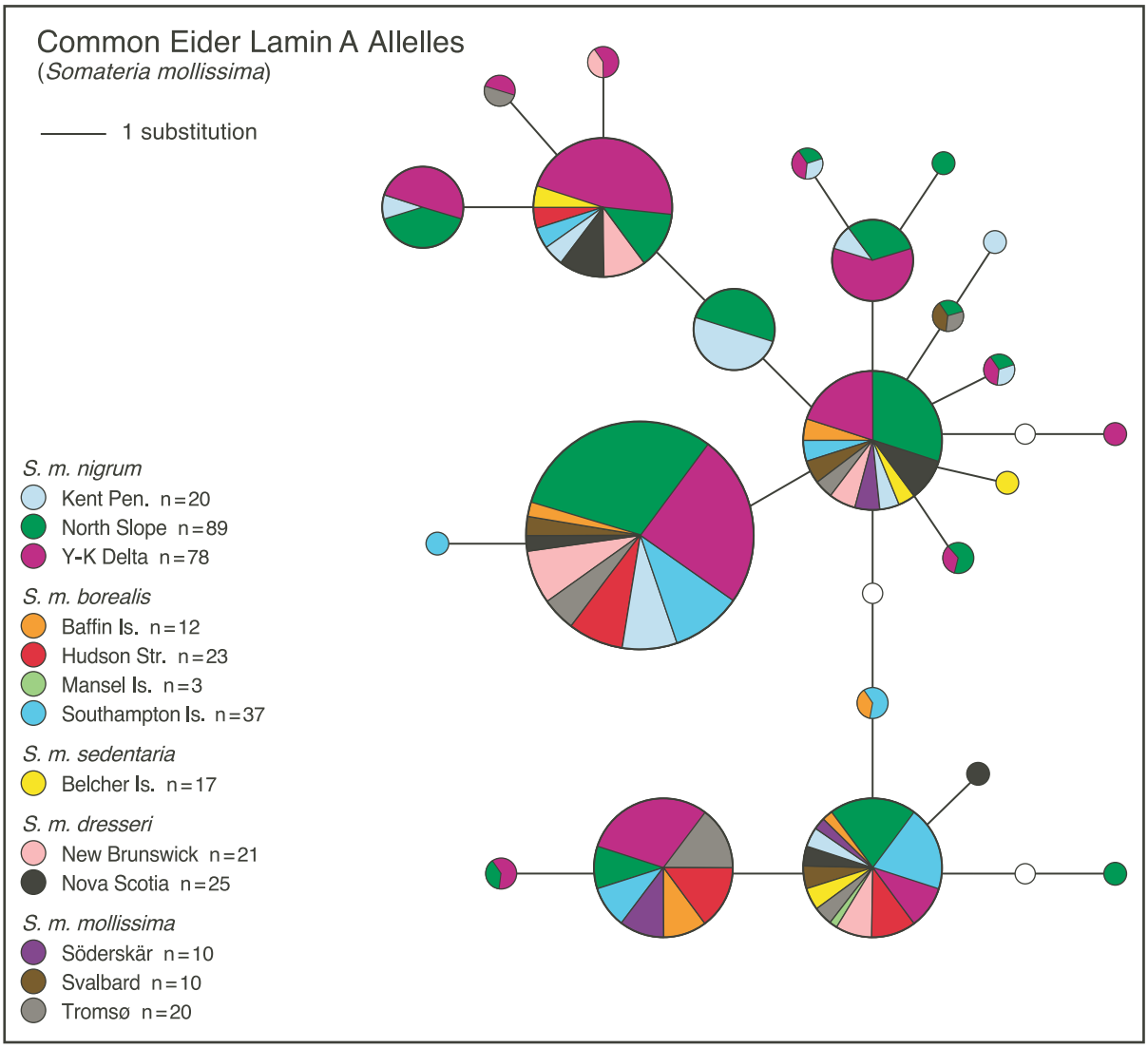

Figure 3. Nuclear intron Lamin A allele tree constructed from sequences collected from 17 populations. Sample size and subspecies of each population is listed on left side of tree.

Table 3. Pairwise F_{ST} values with significant P-values shown in bold for each population pair for nuclear intron Lamin A sequences.

	North Slope	Kent Peninsula	Y–K Delta	Southampton Island	Baffin Island	Hudson Strait	Belcher Islands	Nova Scotia	New Brunswick	Svalbard	Tromsø
North Slope	–										
Kent Peninsula	**0.002**	–									
Y–K Delta	**0.000**	0.001	–								
Southampton	**0.086**	**0.088**	**0.071**	–							
Baffin Island	**0.099**	**0.098**	**0.090**	0.054	–						
Hudson Strait	**0.071**	**0.077**	**0.064**	**0.033**	0.010	–					
Belcher Islands	**0.100**	**0.093**	**0.092**	0.050	0.011	0.005	–				
Nova Scotia	**0.063**	**0.075**	**0.060**	**0.042**	0.052	0.025	0.034	–			
New Brunswick	**0.066**	**0.079**	**0.061**	0.038	0.051	0.027	0.043	0.001	–		
Svalbard	**0.104**	**0.116**	**0.097**	0.054	0.031	0.006	0.021	0.030	0.040	–	
Tromsø	**0.137**	**0.160**	**0.129**	**0.079**	0.074	0.037	0.037	**0.063**	**0.076**	0.013	–
Söderskär	**0.162**	**0.188**	**0.156**	0.098	0.083	0.051	0.051	0.082	0.099	0.023	0.004

Conclusions

North Slope birds are genetically distinct from other eider populations as seen from the mitochondrial DNA analysis. They represent a unique haplotype group, and both allelic (for microsatellite DNA) and haplotypic (for mtDNA) frequencies are significantly different in North Slope populations relative to all other populations analyzed. The existence of two allele and haplotype groups suggests that Common Eiders were historically subdivided in two refugia during the last Pleistocene glaciation. The North Slope may have been colonized by birds expanding out of a different refugium from those that colonized the rest of North America and Scandinavia. Eiders breeding in the Y–K Delta, Southampton Island, Baffin Island, Hudson Straits, Mansel Island, Belcher Islands, New Brunswick, Nova Scotia, Svalbard, Tromsø, and Söderskär locations appear to have a ring distribution [Newton 2003; Avise 2004]; whereas those from Kent Peninsula have haplotypes from both groupings, consistent with a hypothesis that this area represents a contact zone between the two potential Pleistocene refugia [Newton 2003]. These finds are in agreement with studies conducted in Europe, which suggest that the Baltic Sea region was colonized by Common Eiders inhabiting a single Pleistocene refugium [Tiedemann and Noer 1998; Tiedemann et al. 2004]. However, shared alleles and haplotypes among localities indicate that recent gene flow via female and male dispersal has occurred. Differences in levels of population structuring between maternally and bi-parentally inherited markers suggest that gene flow in Common Eiders is most likely mediated by males.

Current Work

Data collection has been completed for the microgeographic components of this study, and the findings are now being analyzed and written up for submission to a peer-reviewed scientific journal. Additional samples have been received from Greenland (N = 20) and Gotland Island, Sweden (N = 50), and data collection has begun on these samples.

Acknowledgments

Funding sources: Alaska EPSCoR (Experimental Program to Stimulate Competitive Research) Graduate Fellowship (NSF EPS-0092040), Angus Gavin Migratory Bird Research Fund, BP Exploration Alaska Inc., UA Coastal Marine Institute, Minerals Management Service, UAF, and the U.S. Geological Survey.

Samples: Lotte Andersen, Mans Hjernquist, Bill Barrow, Fred Broerman, J.O. Bustness, Kathy Dickson, Lynne Dickson, Paul Flint, Grant Gilchrist, Martti Hario, D. Kellet, Mikael Kilpi, Lynne Noel, Kim Mawhinney, Margaret Petersen, Kim Scribner, Robert Suydam, and Pam Tuome.

References

Avise, J.C. 2004. Molecular Markers, Natural History, and Evolution, Second Edition. Sinauer Associates, Inc., Sunderland, Massachusetts.

Baillie, S.R., and H. Milne. 1989. Movements of Eiders *Somateria mollissima* on the east coast of Britain. Ibis 131:321–335.

Cooch, F.G. 1965. The breeding biology and management of the northern eider (*Somateria mollissima borealis*) in the Cape Dorset area, Northwest Territories. Can. Wildl. Serv., Wildl. Manage. Bull., Ser. 2, No. 10.

Goudet, J. 1995. FSTAT (version 1.2): A computer program to calculate F-statistics. J. Heredity 86:485–486.

Goudet, J. 2001. FSTAT, a program to estimate and test gene diversities and fixation indices (version 2.9.3). Available from http://www.unil.ch/izea/softwares/fstat.html. Updated from Goudet [1995].

Goudie, R.I., G.J. Robertson and A. Reed. 2000. Common Eider (*Somateria mollissima*), The Birds of North America, No. 546 [A. Poole and F. Gill, Eds.]. The Birds of North America, Inc., Philadelphia, 32 p.

Hipfner, J.M., H.G. Gilchrist, A.J. Gaston and D.K. Cairns. 2002. Status of Common Eiders, *Somateria mollissima*, nesting in the Digges Sound region, Nunavut. Can. Field-Nat. 116(1):22–25.

Newton, I. 2003. Speciation and Biogeography of Birds. Academic Press, 656 p.

Petersen, M.R., and P.L. Flint. 2002. Population structure of Pacific Common Eiders breeding in Alaska. Condor 104(4):780–787.

Raymond, M. and F. Rousset. 1995. GENEPOP (version 1.2): Population genetics software for exact tests and ecumenicism. J. Heredity 86:248–249.

Reed, A. 1975. Migration, homing, and mortality of breeding female eiders, *Somateria mollissima dresseri*, of the St. Lawrence Estuary, Quebec. Ornis Scand. 6:41–47.

Robertson, G. J., and H.G. Gilchrist. 1998. Evidence of population declines among Common Eiders breeding in the Belcher Islands, Northwest Territories. Arctic 51(4):378–385.

Schneider S., D. Roessli and L. Excoffier. 1999. Arlequin ver. 2.0: A software for population genetic data analysis. Genetics and Biometry Laboratory, University of Geneva, Geneva, Switzerland.

Spurr, E. and H. Milne. 1976. Adaptive significance of autumn pair formation in the Common Eider *Somateria mollissima* (L.). Ornis Scand. 7:85–89.

Stephens, M., and P. Donnelly. 2003. A comparison of Bayesian methods for haplotype reconstruction from population genotype data. Am. J. Hum. Genet. 73(5):1162–1169.

Stephens, M., N.J. Smith and P. Donnelly. 2001. A new statistical method for haplotype reconstruction from population data. Am. J. Hum. Genet. 68(4):978–989.

Suydam, R.S., D.L. Dickson, J.B. Fadely and L.T. Quakenbush. 2000. Population declines of King and Common Eiders of the Beaufort Sea. Condor, 102(1):219–222.

Swennen, C. 1990. Dispersal and migratory movements of eiders *Somateria mollissima* breeding in the Netherlands. Ornis Scand. 21(1):17–27.

Swofford, D.L. 1998. PAUP*: Phylogenetic Analysis Using Parsimony (and Other Methods), Version 4. Sinauer Associates, Inc., Sunderland, Massachusetts.

Tiedemann, R., and H. Noer. 1998. Geographic partitioning of mitochondrial DNA patterns in European Eider *Somateria mollissima*. Hereditas 128(2):159–166.

Tiedemann, R., K.B. Paulus, M. Scheer, K.G. von Kistowski, K. Skirnisson, D. Bloch and M. Dam. 2004. Mitochondrial DNA and microsatellite variation in the eider duck (*Somateria mollissima*) indicate stepwise postglacial colonization of Europe and limited current long-distance dispersal. Mol. Ecol. 13(6):1469–1480. doi: 10.111/j.1365-294X.2004.02168x

Tiedemann, R., K.G. von Kistowski and H. Noer. 1999. On sex-specific dispersal and mating tactics in the Common Eider *Somateria mollissima* as inferred from the genetic structure of breeding colonies. Behaviour 136(9):1145–1155.

Breeding Biology and Habitat Use of King Eiders on the Coastal Plain of Northern Alaska

Abby N. Powell <ffanp@uaf.edu>
Rebecca L. McGuire <ftrlm@uaf.edu>

Institute of Arctic Biology
University of Alaska Fairbanks
Fairbanks, AK 99775-7000

Robert S. Suydam <robert.suydam@north-slope.org>

Department of Wildlife Management
North Slope Borough
P.O. Box 69
Barrow, AK 99723-0069

Task Order 85240

Abstract

*Relatively little is known about the nesting ecology of king eiders (*Somateria spectabilis*). As a species that appears to be in decline, and which breeds in an area of potential oil development, it is important that we gain knowledge of their breeding ecology. During the summer of 2004 we continued the study of nesting king eiders at Teshekpuk and Kuparuk on Alaska's North Slope. This was the third year of a four-year project. We found approximately the same number of nests at both sites as we have found in previous years. Nest success didn't differ between the two sites in 2004, although Teshekpuk had slightly higher success than the previous year while Kuparuk's was somewhat lower. Both sites had lower apparent nest success than they experienced during the high in 2002.*

Introduction

Little is known about the breeding biology of king eiders (*Somateria spectabilis*), partly because they typically nest in remote areas in low densities. The western North American population of king eiders declined by more than 50% between 1976 and 1996 for unknown reasons [Suydam et al. 2000]. Additionally, the National Petroleum Reserve–Alaska (NPR-A) is being leased for oil and gas exploration and may potentially be developed. Within the northeast planning area of NPR-A is the highest known density of nesting king eiders on the North Slope of Alaska [Larned et al. 2003]. During the summers of 2002, 2003, and 2004 we studied king eiders in an area to the southeast of Teshekpuk Lake, and in the Kuparuk oil fields on the North Slope to evaluate the potential impacts of development and to provide information on their basic breeding biology and habitat use. We will examine and compare timing of nesting, clutch size, reproductive success, and habitat use between a relatively undisturbed site at Teshekpuk Lake and the active oil field at Kuparuk. This report summarizes the results of the third field season of data collection.

Objectives

1. Document the timing of nest initiation of king eiders.
2. Document nest success and apparent causes of failure.
3. Document nest site characteristics.
4. Compare data collected from above objectives between Teshekpuk Lake and the Kuparuk oil fields.

Study Areas

This study has two main sites on the North Slope of Alaska—Teshekpuk Lake and the Kuparuk oil fields. The Teshekpuk Lake study site is 10 km inland from the southeast shore of the lake and has experienced very little human impact: There is no sign of anthropogenic disturbance and no people other than those connected with this project have been observed over the past four summers. The Kuparuk study site, located on the Arctic Coastal Plain between the Colville and Kuparuk rivers, is leased by ConocoPhillips Alaska, Inc. and actively being developed for oil production. Both areas are characterized by numerous thaw lakes, ponds and basins. Wetland community types include wet sedge (*Carex* spp.) meadows, moist sedge–dwarf shrub (*Salix* spp.) meadows, and emergent *Carex* spp. and *Arctophila fulva* on the margins of the lakes and ponds [Anderson et al. 1999]. Some wetlands at Kuparuk are intersected by roads and/or created with the closure and rehabilitation of gravel pits.

Methods

Accessible areas around Teshekpuk Lake and Kuparuk were searched for pre-nesting and nesting king eiders during the summers of 2002, 2003, and 2004. We marked nests with a tongue depressor placed 1 m from the nest in vegetation so as to be concealed from potential predators. We measured length and width, and weighed and candled each egg to determine incubation stage. Latitude and longitude were recorded for each nest using a hand-held GPS unit. Habitat type within 50 m of each nest was classified post-hatch as to type using Bergman's classification system [1977]. Vegetation types and frequency were recorded for all nests as well as for random locations within the 2 study areas. Additionally, we recorded island size, distance to the mainland and depth of the water if the nest occurred on an island.

Data loggers (HOBO Temp) were placed in randomly selected nests at Teshekpuk (n = 10) and Kuparuk (n = 8) in both 2002 and 2003 to determine nest attendance and abandonment; they were set to record temperature every 2 min, and downloaded every 10 d. In 2004 an additional 5 loggers per site were deployed. We anchored the probe in the nest, which allowed for a quick response to any change in temperature since the probe had only an eggshell between it and the incubating female (protocol follows Quakenbush et al. [2004]).

King eiders typically incubate for 22–24 days and all nests were monitored weekly throughout this period during 2002–2004. Hatch success was determined by the presence of eggshells with detached membranes [Girard 1939] or the presence of ducklings. If there were eggshells with no membranes or if the entire egg was absent, the nest was considered depredated. Nesting success was defined as the percentage of all nests initiated in which at least one egg hatched. We attempted to determine cause of failure for nests that did not succeed.

We placed digital cameras (n = 12/site) at nests in 2004 to attempt to identify nest predators. Two camera systems were used: the Cuddeback Digital Scouting Camera by Non Typical, Inc. and the Digital Motion Detector Scouting Camera by Stealth Cam, LLC. Cameras were employed simultaneously on different nests and were moved from depredated nests to new nests as soon as possible. The cameras were either set to record 3 pictures/activation or 1 picture + a 10 sec video clip/activation. Females were not flushed during camera placement unless measurements, candling, or HOBO placement took place simultaneously. Females were not usually flushed during nest visits where camera batteries and memory cards were changed.

We also used a video system at Kuparuk through a grant from Sandpiper Technologies, Inc. The system consisted of a weatherproof miniature video camera attached via a cable to a time-lapse videocassette recorder (Panasonic AG-1070) housed in a weatherproof case powered by a 12-volt deep-cycle marine battery. The VCR and the battery were placed about 15 m from the nest. The video system was set to record 24 h of video on standard T160 VHS videotapes.

Results

Teshekpuk 2004

We found 37 active king eider nests in the study area at Teshekpuk Lake. We also found 22 nests post-depredation that were likely king eider nests. However, because spectacled eider (*Somateria fischeri*) nests look very similar they were not included in estimates of apparent nest success. Initiation of incubation ranged from 14 to 27 June (Figure 1). Apparent nest success was 24.3% in 2004 (Table 1); however, three of the hens abandoned after camera placement, probably due to the presence of a camera at the nest. Excluding these females from the analysis raised the apparent nesting success to 26.5%. King eider nests at Teshekpuk hatched between 12–20 July. Mean clutch size was 4.25 ± 0.2 (SE, n = 28). Egg length was 65.5 ± 0.21 mm (n = 121), width 43.6 ± 0.13 mm (n = 121) and mass of fresh eggs 67.6 ± 0.6 g (n = 90). In general, nests at Teshekpuk occurred in low marshy areas or on islands (n = 37) and not on the barren, dry ridges. Only 3 of the 9 successful nests occurred on islands (33.3%), although 45.9% of nests found (n = 37) occurred on islands. This pattern is the opposite of that seen in previous years (Table 1).

The digital cameras proved to be problematic. The Stealth Cam motion detector had only one sensitivity level and often did not detect events. The females on the nest did not set off the camera when moving around at the nest, and sometimes didn't even activate it when leaving the nest. This problem could be alleviated by placing the camera closer; however, 3 females abandoned after camera placement. The females that are known to have abandoned were all flushed at the time of camera placement and 2 of them never returned to the nest. Females did not abandon if cameras were placed without flushing; however, 1 female that was flushed at camera placement did not abandon. At least 1 additional female that was flushed at camera placement subsequently failed; it is unknown whether she abandoned the nest prior to depredation.

Similar low sensitivity problems plagued the Cuddeback cameras. This camera has three levels of sensitivity to events and eventually we found that a higher setting worked better. The female on the nest triggered the camera when she moved around at the higher sensitivity. However, we were expecting the cameras to be too sensitive so that by the time these problems were resolved to some extent, all the remaining females had hatched. No pictures of actual predation events were recorded with either camera system.

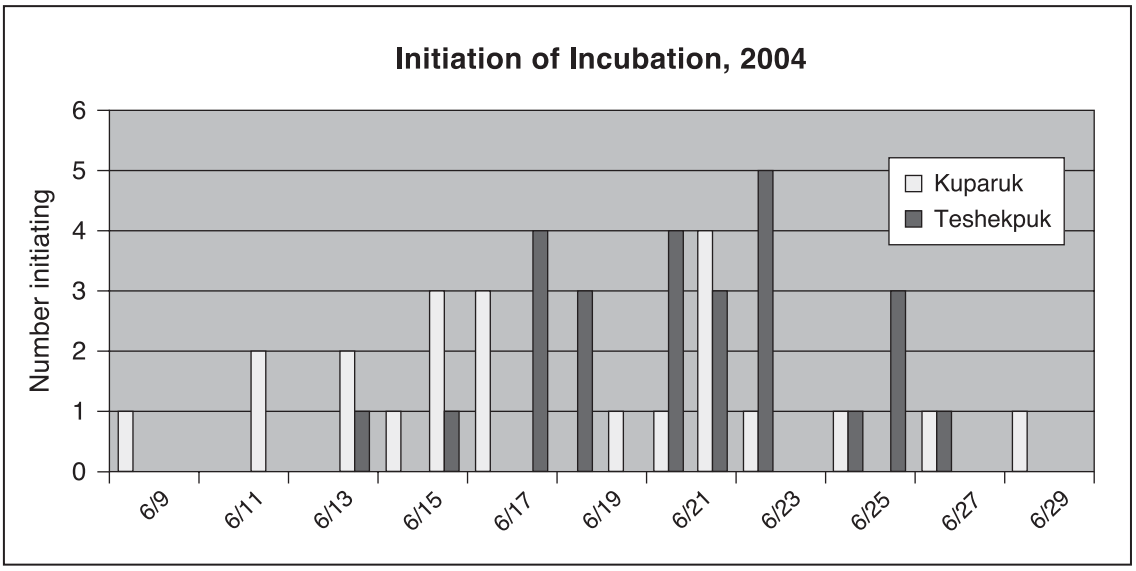

Figure 1. Initiation of incubation by king eiders at two sites on Alaska's North Slope, Kuparuk and Teshekpuk, in 2004.

Table 1. Summary of sample size, apparent nest success and percentage of total and successful nests that occurred on islands at Kuparuk and Teshekpuk from 2002 through 2004.

	Year	# Nests	Apparent Nest Success	% of All Nests on Islands	% of Successful Nests on Islands
	2002	44	33.30%	68.20%	92.90%
Teshekpuk	2003	40	17.50%	52.50%	85.70%
	2004	37	24.30%	45.90%	33.30%
	2002	42	42.90%	44.70%	72.20%
Kuparuk	2003	39	35.10%	51.30%	61.50%
	2004	31	25.80%	58.00%	62.50%

Kuparuk 2004

We found 31 active nests at Kuparuk and 23 more nests were found post-depredation. Initiation of incubation ranged from 9 to 29 June (Figure 1). The period of time in which hens began incubating was similar between Kuparuk and Teshekpuk; however the peak was a few days later at Teshekpuk. Apparent nest success was 25.8% (n =31, Table 1). King eider nests at Kuparuk hatched between 6–20 July. Mean clutch size was 4.67 ± 0.21 (SE, n = 24). Egg length was 66.3 ± 0.27 mm (n = 83) and width 44.5 ± 0.14 mm (n = 84). Fifty-eight percent of nests found (n = 31) occurred on islands (Table 1).

The digital nest cameras experienced similar problems at Kuparuk. No pictures of depredation events were recorded; however, no females are known to have abandoned there. There is always the potential that a nest was abandoned prior to predation without our detection. The HOBOs allow us to determine if the female returned to the nest after flushing, but we did not place HOBOs in every nest.

The video system was only placed on one nest at Kuparuk, because the nest did not fail until the end of incubation. This did not leave us time to move the system to another nest. We did, however, manage to record the depredation event at this nest. It was depredated by glaucous gulls (*Larus hyperboreus*), presumably the pair that was nesting about 40 m away. The video shows that the female eider fought off the gulls for at least 12 h prior to taking an incubation break during a period when the gulls had been out of the picture for 1 or 2 h. She had been on the break for about 7 min before they appeared and depredated the nest. As far as we can tell the female never came back for a close look at the nest after this happened.

Future work

Additional funding was obtained through the U.S. Geological Survey to extend this study (Ph.D. dissertation) at no cost to CMI. The work on nesting success will continue through the field season of 2005.

Program MARK will be used to estimate nest success (± SE) and to test for site-, year-, and island/mainland–specific differences in nest survival and to investigate the importance of three spatial covariates (distance to the nearest conspecific nest, distance to the nearest larid nest, and distance to the mainland) and habitat covariates on daily nest survival rates [White and Burnham 1999; Dinsmore et al. 2002]. We will investigate any effects of nesting associations between king eider and associated nesting larids, both within and between the two sites. The data from the HOBO temperature recorders will be analyzed for incubation constancy.

We intend to use landcover databases (National Petroleum Reserve–Alaska landcover inventory database of the Bureau of Land Management and Ducks Unlimited, and the Beechey Point landcover inventory database of the U.S. Army Cold Regions Engineering and Research Laboratory) and the random sites to investigate distribution and availability of habitats within the study areas and thus determine if selection of particular habitats has occurred and how the study sites compare.

Acknowledgements

This study would not be possible without the financial support of the UA Coastal Marine Institute, ConocoPhillips Alaska, Inc., and the North Slope Borough. We thank Dolores Vinas, Liza DelaRosa, April Brower, Benny Akootchook, Justin Harth, and Anne Lazenby for logistical help; and Amanda Prevel, Torsten Bentzen, Rita Frantz, Miranda Wright, and Keith Brady for their help as field technicians. We also thank ABR, Inc. for cooperation at Kuparuk.

References

Anderson B.A., C.B. Johnson, B.A. Cooper, L.N. Smith and A.A. Stickney. 1999. Habitat associations of nesting spectacled eiders on the Arctic Coastal Plain of Alaska, p. 27–32. *In* R.I. Goudie, M.R. Peterson and G.J. Robertson [eds.], Behavior and Ecology of Sea Ducks. Can Wildl. Ser. Occas. Pap. 100.

Bergman, R.D., R.L. Howard, K.F. Abraham and M.F. Weller. 1977. Water birds and their wetland resources in relation to oil development at Storkersen Point, Alaska. U.S. Fish and Wildl. Serv. Resour. Publ. 29, Washington D.C., 38 p.

Dinsmore, S.J., G.C. White and F.L. Knopf. 2002. Advanced techniques for modeling avian nest survival. Ecology 83(12):3476–3488.

Girard, G.L. 1939. Life history of the shoveler. Trans. N. Am. Wildl. Conf. 4:364–371.

Larned, W.W., R. Stehn and R. Platte. 2003. Eider breeding population survey Arctic Coastal Plain, Alaska 2002. U.S. Fish and Wildlife Service, Anchorage.

Quakenbush, L.T., R.S. Suydam, T. Obritschkewitsch and M. Deering. 2004. Breeding biology of Steller's Eiders (*Polysticta stelleri*) near Barrow, Alaska, 1991–99. Arctic 57(2):166–182.

Suydam, R.S., D.L. Dickson, J.B. Fadely and L.T. Quakenbush. 2000. Population declines of King and Common Eiders of the Beaufort Sea. Condor 102(1):219–222.

White, G.C., and K.P. Burnham. 1999. Program MARK: Survival estimation from populations of marked animals. Bird Study 46 Suppl.:120–138.

King and Common Eider Migrations Past Point Barrow

Lori T. Quakenbush <lori_quakenbush@fishgame.state.ak.us>

Institute of Marine Science
University of Alaska Fairbanks
Fairbanks, AK 99775–7220

Robert S. Suydam <robert.suydam@north-slope.org>

Department of Wildlife Management
North Slope Borough
P.O. Box 69
Barrow, AK 99723-0069

Task Order 85241

Abstract

*King (*Somateria spectabilis*) and common eiders (*S. mollissima v-nigra*) are important resources for Native people of northern Alaska and Canada. Both species pass Point Barrow, Alaska twice annually—during their northward migration in the spring and their southward migration in the fall. In 1996, we conducted spring and fall counts and compared our results with standardized data from other counts. The results indicated that both populations had declined by approximately 50% between 1976 and 1996. We have repeated the fall migration counts (July–October 2002 and 2003) and the spring counts (May 2003 and 2004) in order to update the population trends and gather information on the behavior of eiders during migration to provide a context for the behavior of individual eiders instrumented with satellite transmitters (CMI Project: Importance of the Alaskan Beaufort Sea to King Eiders [*Somateria spectabilis*]). The counts will also determine if the age composition of eiders migrating during late fall can be used as an index to annual productivity.*

Introduction

King (*Somateria spectabilis*) and common eiders (*S. mollissima v-nigra*) wintering in the Bering Sea and north Pacific Ocean migrate north to nesting areas in Russia, Alaska, and Canada. Most of the eiders nesting in Alaska and Canada pass by Point Barrow, Alaska when entering and leaving the Beaufort Sea. At Point Barrow the migration transits very close to shore and the spring passage can be spectacular. Woodby and Divoky [1982] estimated 113,000 eiders passed in 30 minutes in the spring of 1976. Murdoch [1885], Bailey [1948], Brueggeman [1980], and others have commented on the spring passage of eiders, but the magnitude of the spring migration has been estimated only on a few occasions [Woodby and Divoky 1982; Suydam et al. 1997, 2000a]. By standardizing the analysis of spring migration counts conducted at Barrow in 1953 [Thompson and Person 1963], 1970 [Johnson 1971], 1976 [Woodby and Divoky 1982], 1987, 1994 [Suydam et al. 1997], and 1996 [Suydam et al. 2000a, b] we determined that the king eider population appeared to remain stable between 1953 and 1976, but declined by 53% between 1976 and 1996 [Suydam et al. 2000a]. The common eider population declined by 56% during the same time period [Suydam et al. 2000a].

King and common eiders are an important source of fresh protein after a long winter for local residents of Alaska and Canada [Braund et al. 1993; Fabijan et al. 1997]. Residents of Barrow harvest more king and common eiders than any other species of waterfowl [Fuller and George 1997]. While the reasons for the declines are unknown they are of concern.

It appears from our previous work and the reports of others [Thompson and Person 1963; Johnson 1971; Timson 1976] that the number of eiders returning after the end of August may be indicative of the number of young produced that year. Therefore, we are investigating the age composition of the fall passage from July into October in 2002 and 2003 to explore the use of late migration numbers as an indicator of annual productivity. By collecting detailed fall migration data we will be able to address timing, behavior, molt, and weather conditions related to migration, with the result of a better understanding of the timing and use of the Beaufort Sea marine and coastal environment by king and common eiders. The data will provide information that will aid in predicting the number of eiders using the outer continental shelf area by time of year.

Methods

Summer/fall migration counts in 2002 and 2003 were conducted from land at the base of the Point Barrow spit (71° 21′N, 156° 36′W; Figure 1). In 2002, one to two observers counted eiders for up to 10 h per day from 11 July until 15 October. In 2003 counts will be conducted from 8 July to 15 October. In October the count becomes limited to 2 h per day due to decreasing day length.

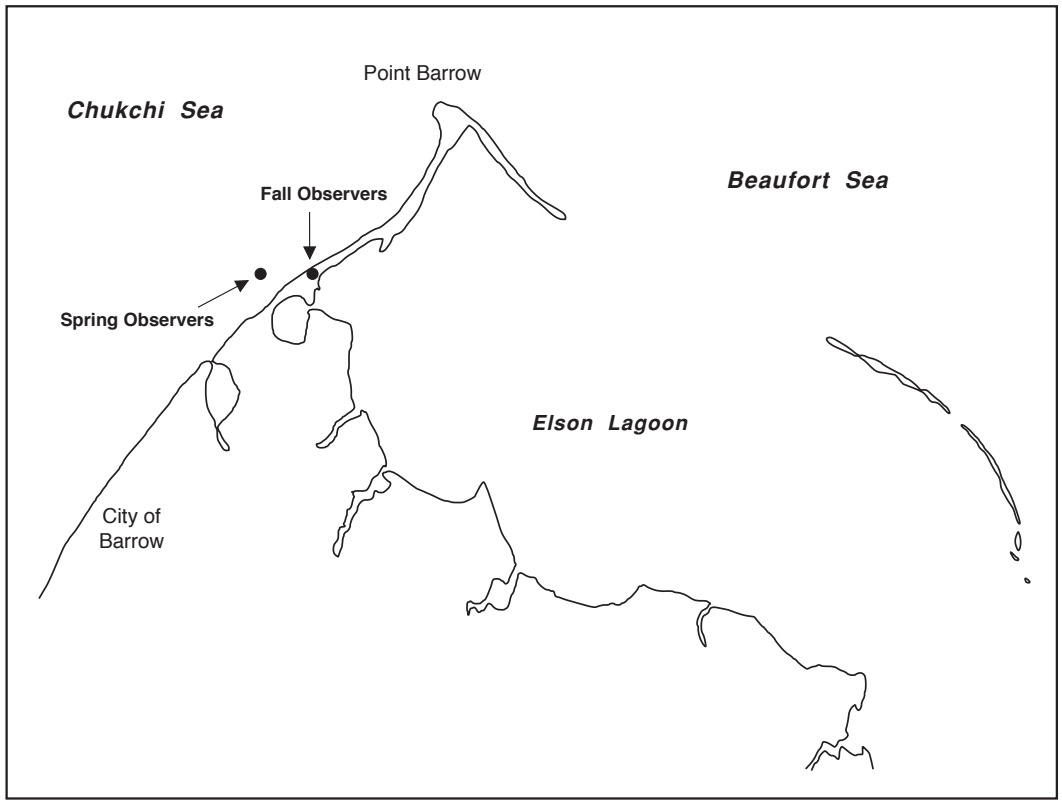

Figure 1. Fall eider migration count locations.

For the spring counts, we established an observation site on the shorefast ice southwest of Point Barrow (Figure 1). In 2003, the observation site was on a large pressure ridge approximately 20 m high (71° 21′N, 156° 43′W; Figure 1). The distance to the nearshore lead ranged from 50 to 1500 m depending upon sea ice conditions. In 2004, the observation site was on a pressure ridge approximately 10 m high (71° 23′N, 156° 41′W; Figure 1), and the distance to the nearshore lead ranged from 50 to 1000 m. Both sites allowed a view of eiders migrating along the lead as well as along the beach. Two observers conducted spring counts for 12 h each day (i.e., 2 h out of every 4) from 30 April to 2 June 2003 and 2004.

In each count period, regardless of season, data were collected on weather conditions (temperature, wind speed, wind direction, cloud cover, visibility). For each flock sighted we recorded time, direction of travel, species composition, number in flock, ratio of males to females for each species, and other comments on behavioral observations. Observers were trained on species identification and flock estimation by being paired with an experienced observer. They made independent estimates of the size of each flock. Estimates between trained observers were generally within 10% or less of each other.

We calculated daily projected passage estimates and point estimates for total passage of king and common eiders using methods similar to Suydam et al. [1997]. These estimates include eiders counted but not identified to species, which are divided between king and common eider categories in proportion to the king and common eiders that were identified that day. We assumed a constant movement throughout each 24-h period. The projected total passage was estimated by summing the daily passage estimates. We also calculated 95% confidence intervals using a procedure for stratified sampling [Thompson 1992] that treated each day as a separate stratum [Suydam et al. 2000b]. Point estimates for two time periods are presented. A point estimate for 11 July to 7 September is a standardized time period which we can compare with counts prior to 1996 [Suydam et al. 2000a]. This shorter time period represents the period prior to when young produced that year have returned. Therefore, it may be a better estimate of the adult breeding population. The 11 July to 15 October time period can be compared with our estimate in 1996 only and includes the eiders produced that year.

Results

Summer/Fall 2002

Some king eiders migrated past Point Barrow before we began counting, as indicated by the king eiders implanted with satellite transmitters in the Kuparuk oil field by Powell and Phillips (CMI project: Importance of the Alaskan Beaufort Sea to King Eiders [*Somateria spectabilis*] [hereafter Powell et al. CMI project]; Figure 2). Five of ten male king eiders with transmitters passed by Point Barrow before our count began in 2002. None of the tagged females passed prior to 29 July. The daily estimated passage of king eiders, however, shows low numbers passing until 15 July (Figure 3) and large numbers passing on 27 and 29 July, 19 and 24 August, and 12 September.

Our preliminary estimate for the passage of king eiders for the early migration period between 11 July and 7 September is 493,248 (95% CI 74,332; Table 1). For the later period (11 July–15 October) our preliminary estimate is 529,271 (95% CI 78,742). Young-of-the-year do not begin to migrate until September; therefore, fall migration counts after early September provide an index to productivity. Our estimate of passage of king eiders after 7 September was 36,023 in 2002 or 7.3% of what is estimated to be the adult projected total passage.

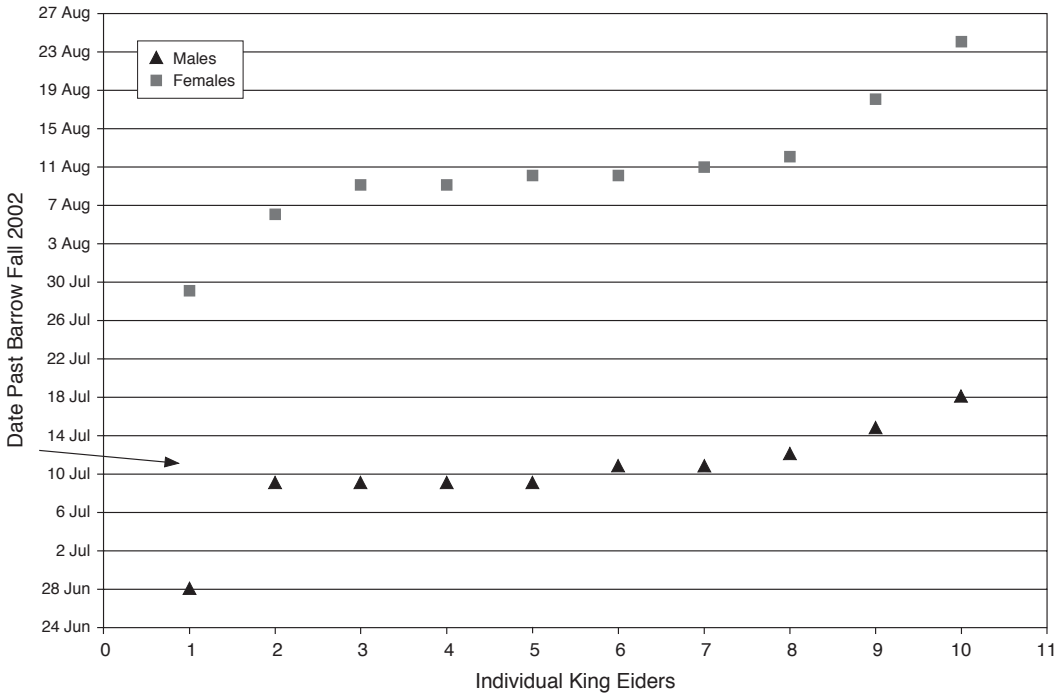

Figure 2. Dates that 10 male and 10 female king eiders with satellite transmitters passed Barrow during summer/fall 2002. Arrow denotes date migration count began (11 July). Data from A. Powell, unpublished.

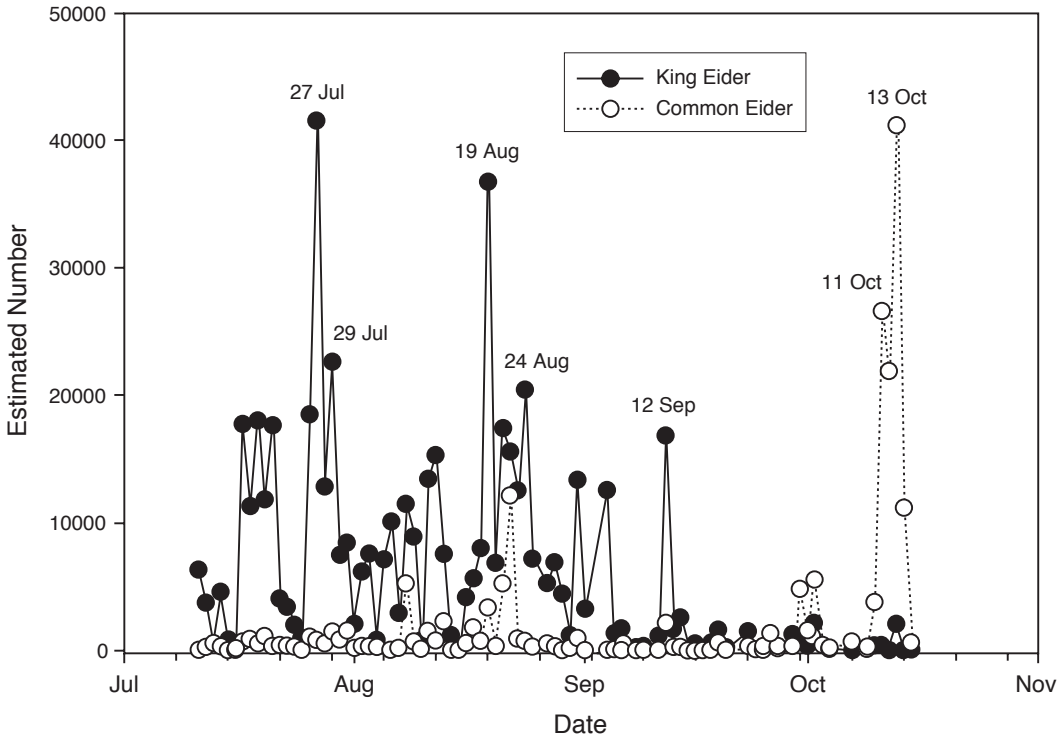

Figure 3. Projected daily passage of king and common eiders during summer/fall 2002 at Point Barrow.

Our preliminary estimate for the passage of common eiders for the early migration period was 51,622 (95% CI 21,784) and 176,109 (95% CI 42,390) for the late period. Only 29% of the estimated total of common eiders passed by before 7 September. The remaining 71% passed by in October, with the largest numbers passing on 11 and 13 October when 26,592 and 41,143 were estimated to pass, respectively (Figure 3). Because the majority of common eiders migrate later in the fall, overlapping with the migration of young-of-the-year, we do not have an index of production for this species. King eiders comprised 75% of all eiders identified and commons made up 25% (Table 1).

Table 1. Preliminary numbers, projected total passage, and 95% confidence interval of king and common eiders seen during two time periods of the summer/fall 2002 and 2003 and spring 2003 migrations, and preliminary numbers of eiders seen during the spring 2004 migration.

	King Eider	Common Eider	Eider[1]	TOTAL
Early Summer/Fall 2002 [2]				
Number seen[3]	60,177	4,810	114,164	179,151
Projected total passage[4]	493,248	51,622		544,870
95% confidence interval	74,331	21,784		
Late Summer/Fall 2002 [5]				
Number seen[3]	61,881	13,864	134,073	209,818
Projected total passage[4]	529,271	176,109		705,380
95% confidence interval	78,742	42,390		
Spring 2003 [6]				
Number seen[3]	76,420	24,091	99,902	200,413
Projected total passage[4]	362,237	119,809		482,046
95% confidence interval	88,851	26,668		
Early Summer/Fall 2003 [5]				
Number seen[3]	50,259	4,629	88,541	143,429
Projected total passage[4]	405,820	67,195		705,380
95% confidence interval	76,598	11,909		
Late Summer/Fall 2003 [5]				
Number seen[3]	50,559	10,462	94,451	155,472
Projected total passage[4]	434,057	107,770		541,827
95% confidence interval	76,781	15,222		
Spring 2004 [7]				
Number seen[3]	106,546	23,237	133,512	263,295
Projected total passage[4]				
95% confidence interval				

[1]Unidentified eiders
[2]Early period from 11 July to 7 September (458 hours counted in 2002)
[3]Net number of eiders migrating southwest (summer/fall) or northeast (spring)
[4]Sum of daily projected passage estimates
[5]Late period from 11 July to 15 October (650 hours counted in 2002)
[6]30 April–2 June (340 hours counted in 2003)
[7]30 April–1 June (280 hours counted in 2004)

Summer/Fall 2003

When we began counting on 8 July, 3 of 15 (17%) of the male king eiders with satellite transmitters had already left the Beaufort Sea (data from Powell et al. CMI project; Figure 4). The earliest female left on 2 August 2003 and the latest left on 18 September (Figure 4).

Our preliminary estimate for the passage of king eiders for the early migration period between 11 July and 7 September was 405,820 (95% CI 76,598) and 434,057 (95% CI 76,781) for the later period (11 July–15 October; Table 1). Our estimate of passage of king eiders after 7 September was 28,237 in 2003 or 7% of what is estimated to be the adult projected total passage.

Our preliminary estimate for the passage of common eiders for the early migration period was 67,195 (95% CI 11,909) and 107, 770 (95% CI 15,222) for the late period. In 2003, 62% of the estimated total number of common eiders passed by before 7 September. The remaining 38% passed by in early October (Figure 5). King eiders comprised 80% of all eiders identified and commons made up 20%.

Spring 2003 count

In spring 2003, our preliminary projected passage for king eiders was 362,237 (95% CI 88,851) and for common eiders it was 119,809 (95% CI 26,668) (Table 1). King eiders comprised 76% and commons 24% of all eiders identified. Spring appeared to be several weeks early in 2003 and eiders were seen east of Barrow prior to our start date of 30 April. None of the king eiders with satellite transmitters implanted in 2002 passed by prior to 30 April (Figure 6).

Spring 2004 count

The spring 2004 estimates are in progress. Our preliminary numbers for birds counted were 106,546 king eiders, 23,237 common eiders, and 133,512 eiders not identified to species. King eiders comprised 82% of all eiders identified and commons made up 18% (Table 1). None of the king eiders with satellite transmitters implanted in 2003 passed by prior to 30 April (Figure 7).

Carbon and nitrogen isotopes in feathers

We amended our project to incorporate a study designed by Michael Knoche, a Master's student at the University of Alaska Fairbanks. His project proposed to use carbon isotope ratios in feathers collected from king eiders passing Barrow to determine areas used by the king eiders during the fall molt when the birds are flightless. Feathers grown in one geographical region will retain the isotopic signature of the region because feathers are metabolically inert after they are grown. The objective of this amendment is to use carbon and nitrogen isotopes to investigate diet, sexual segregation, and geographical distribution during wing molt. Molt is energetically taxing, thus molting areas are important habitats for king eiders and understanding distribution during molt may provide insight into potential mortality factors.

Mr. Knoche studied feather samples from 23 captive eiders on a known diet to learn how the isotopic composition of the diet fractionated in the grown feathers and whether differences occur with sex and age. We obtained permits from the U.S. Fish and Wildlife Service and Alaska Department of Fish and Game to collect 60 king eiders during 2003, however only 17 king eiders were shot for the project. Due to the support and generosity of subsistence hunters, the majority of the primary feathers were donated from 258 king eiders taken for subsistence near Barrow. Primary feathers were also collected from 39 eiders live captured for a satellite telemetry study (Powell et al. CMI project). In addition to

primary feathers, muscle tissue was also taken from the 17 eiders collected for the study. All other samples were obtained from birds found dead.

Because the literature included several methods and chemicals for cleaning feathers prior to determining carbon isotope ratios and no data was available on whether the different cleaning methods affected the results, Mr. Knoche tested each method for differences prior to preparing his samples. Preliminary results of his study with captive eiders include no difference between sexes for how isotopes from diet are incorporated into feathers, however hatch-year eiders had lower nitrogen fractionation than adults. Results indicate that diet during molt for some female king eiders comes from both marine and freshwater habitats while male diet is marine based. Muscle tissue was not different from feathers in the spring, but muscle was different in the fall due to the incorporation of isotopes from a freshwater summer diet during the breeding season. Stable carbon isotopes were found to be highly correlated with longitude of wing molt location for male king eiders. Mr. Knoche is writing his thesis as two publishable papers. He is scheduled to defend in November 2004.

Discussion

When comparing the early summer/fall migration period (11 July–7 September) between 2002 and 1996, the total point estimate appears to be higher for king eiders in 2002 (Table 2). Comparing this early time period among years avoids comparing estimates that may include large numbers of young from highly productive years with low numbers in poorly productive years. In 1996, there were large numbers of king eiders passing in September and October; this pattern was not seen in 1994 [Suydam et al. 1997] or in 2002 or 2003 and may indicate that 1996 was a good reproductive year. Comparing the early time periods may be most appropriate and may indicate that the king eider population has increased or at least not decreased. We will use all of the spring and summer/fall estimates in our final report to better interpret this result.

Although 50% and 17% of the male king eiders fitted with satellite transmitters passed by Point Barrow prior to the beginning of our counts in fall 2002 and 2003, respectively, we do not think those percentages represent the overall timing of male king eider migration (Figures 2 and 4). The projected daily passage rates for the early season (Figure 3) did not indicate any large numbers of eiders passing until 15 July. The early departure of the male king eiders with implants may have been a reaction to surgery or it may be that males on the western portion of the breeding range, nearer to Barrow, arrive there early each year.

The bulk of the common eider summer/fall migration occurs in October; therefore, we will only compare the late time period estimates. The projected total passage of common eiders was higher in summer/fall 2002 than in 1996, but lower in 2003 (Table 2). The spring 2003 and 2004 estimates will help us evaluate this result.

Students

Michael Knoche's research activities were reported above. He was also involved in conducting the migration counts, scheduling observers, and ensuring quality counts and data collection. Rita Frantz, an undergraduate student from Ilisagvik College in Barrow has been an observer for all of the migration counts, she streamlined the data entry process, entered and proofed the data and has been assisting in data queries for analysis.

Addendum: King and Common Eider Migrations Past Point Barrow

Lori T. Quakenbush and Robert S. Suydam

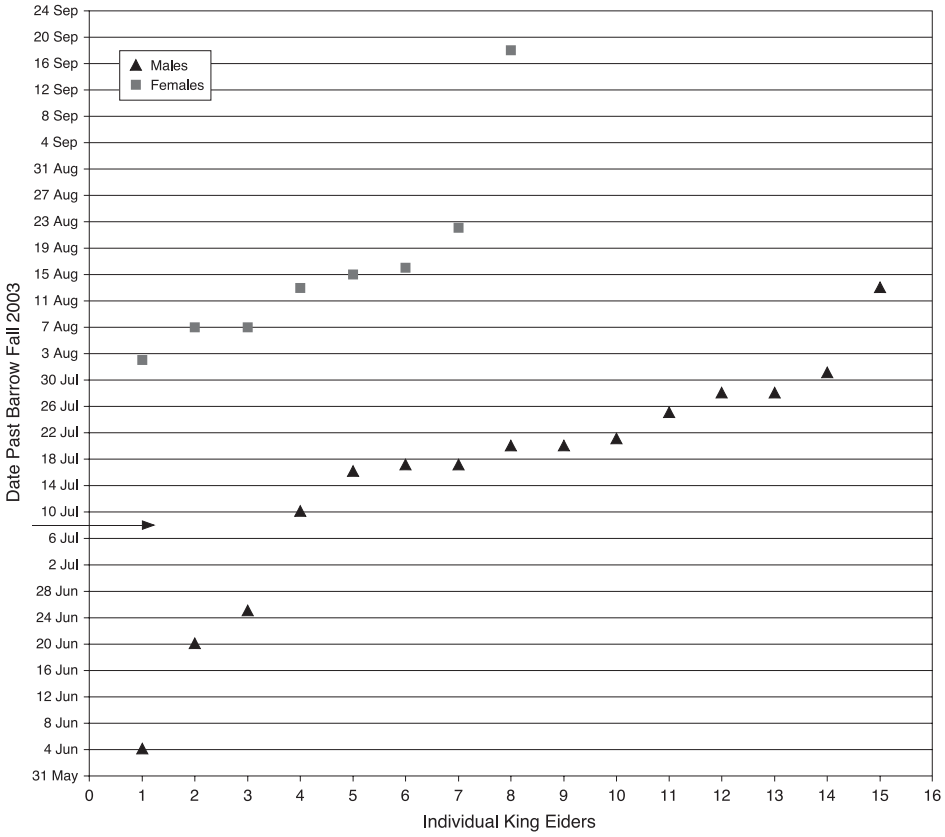

Figure 4. Dates 15 male and 8 female king eiders with satellite transmitters passed Barrow during summer/fall 2003. Arrow denotes date migration count began (8 July). Data from A. Powell.

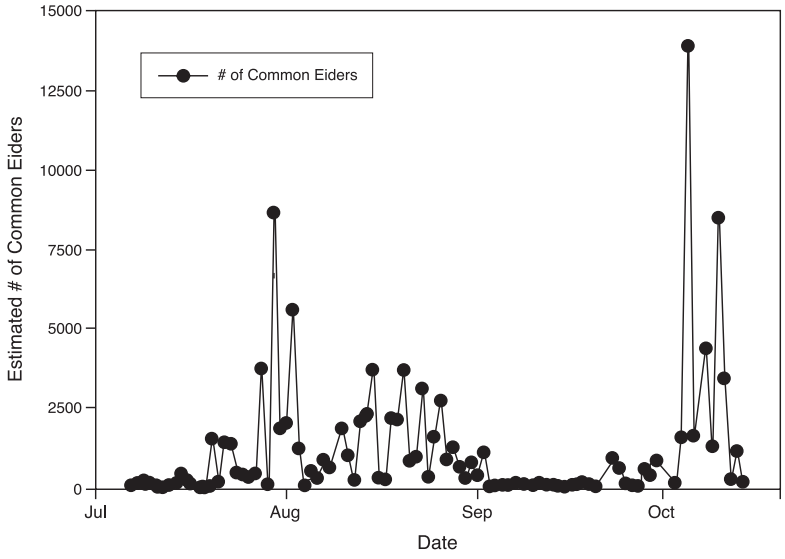

Figure 5. Daily passage of king and common eiders during summer/fall 2003 at Point Barrow.

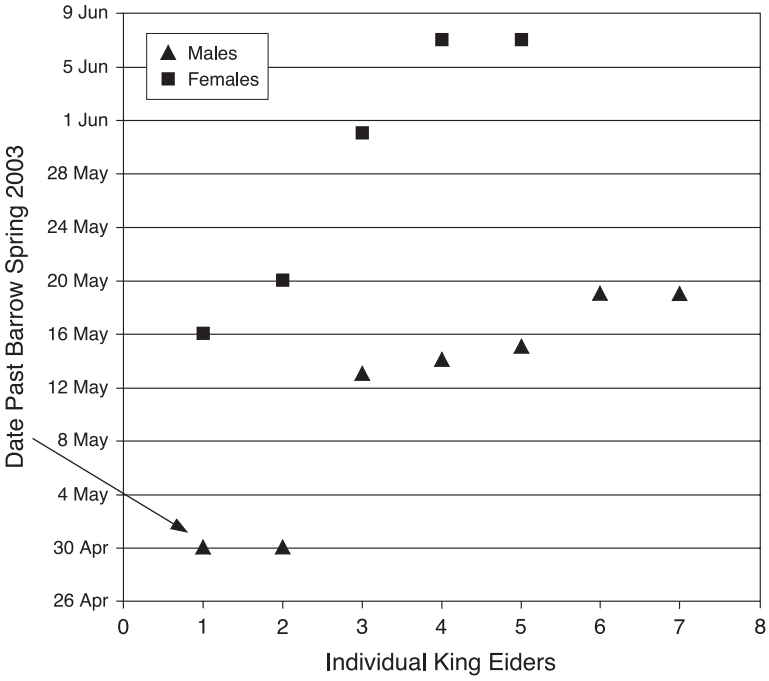

Figure 6. King eider spring 2003 migration.

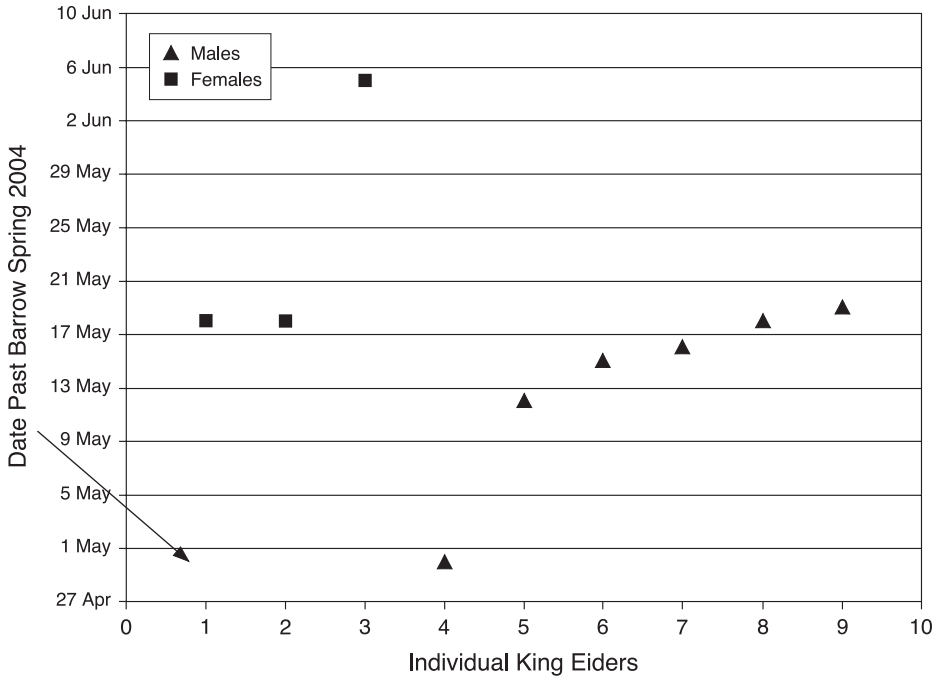

Figure 7. King eider spring 2004 migration.

Table 2. Estimated passage for king and common eiders including 95% confidence intervals for the early (11 July–7 September) and late (11 July–15 October) time periods in 1996, 2002, and 2003.

	King Eider	Common Eider
Early Summer/Fall 1996 [1]		
Projected total passage[2]	330,248	N/A
95% confidence interval	70,725	N/A
Projected total range[3]	259,493–400,943	N/A
Early Summer/Fall 2002		
Projected total passage[2]	493,248	N/A
95% confidence interval	74,332	N/A
Projected total range[3]	418,916–567,580	N/A
Early Summer/Fall 2003		
Projected total passage[2]	405,820	N/A
95% confidence interval	76,598	N/A
Projected total range[3]	329,222–482,418	N/A
Late Summer/Fall 1996 [3]		
Projected total passage[2]	507,667	111,635
95% confidence interval	84,680	42,440
Projected total range[3]	422,987–592,347	69,195–154,075
Late Summer/Fall 2002		
Projected total passage[2]	529,271	176,109
95% confidence interval	78,742	42,390
Projected total range[3]	450,667–608,013	133,719–218,499
Late Summer/Fall 2003		
Projected total passage[2]	434,057	107,770
95% confidence interval	76,781	15,222
Projected total range[3]	357,276–510,838	92,548–122,922

[1]From Suydam et al. [2000a]
[2]Sum of daily projected passage estimates
[3]Upper and lower limits of passage using confidence interval

Presentations

Lori Quakenbush made the annual CMI presentation of this study in February 2004 in Fairbanks. In addition to presenting his work at the CMI annual presentations, Michael Knoche made a presentation at the Alaska Cooperative Fish and Wildlife Research Unit review, also in February, and at the American Ornithologist Union in August 2004. Robert Suydam gave an oral presentation in Anchorage at the Alaska Bird Conference titled, “Status of King and Common Eiders Migrating Past Point Barrow, Alaska”.

Acknowledgements

This project is funded by the University of Alaska Coastal Marine Institute (Minerals Management Service) with logistic support provided by the North Slope Borough, Department of Wildlife Management. We are grateful to Lynne Dickson of the Canadian Wildlife Service for providing support and travel for Andrea Hoover and Garnet Raven to assist us with counts. The U.S. Fish and Wildlife Service was generous in allowing their employees, Dominic Bachman, Tim Obritschkewitsch, and Nate Pamperin to assist our project. Quaiyaan Aiken, Paula Earp, Quaiyaan Opie, Bruce MacTavish, Rebecca McGuire, Leslie Pierce, and Yumiko Uchiro assisted in the migration counts. In spring 2003, Michael Wald found the spring perch, made a trail to get there, and conducted counts. We thank Craig George for helping us get started in the spring and Ben Akootchook for mechanical talent. We are especially grateful to the subsistence hunters of Barrow who allowed us to look at their birds, graciously donated samples, and shared their knowledge of eiders with us. *Quyanaq*. We also appreciate the data sharing that has occurred with Abby Powell and Laura Phillips and we look forward to more in the future.

The migration portion of this project was reviewed and approved by the Institutional Animal Care and Use Committee (IACUC) of the University of Alaska Fairbanks (#02-05). The portion of this study using stable isotopes to identify molting areas of king eiders was also reviewed and approved by the IACUC (#03-15).

References

Bailey, A.M. 1948. Birds of Arctic Alaska. Colorado Museum of Natural History. Pop. Ser. No. 8. 317 p.

Braund, S.R., K. Brewster, L. Moorhead, T.P. Holmes and J.A. Kruse. 1993. North Slope Subsistence Study, Barrow, 1987, 1988, and 1989. Techn. Rep. No. 149, OCS Study, MMS 91-0086. Anchorage.

Brueggeman, J.J. 1980. Coastal occurrence of birds at Point Barrow, Alaska, in spring. Murrelet 61:31–34.

Fabijan, M., R. Brook, D. Kuptana and J.E. Hines. 1997. The subsistence harvest of King and Common eiders in the Inuvialuit Settlement Region, 1988–1994, p. 67–73. *In* D.L. Dickson [ed.], King and Common Eiders of the Western Canadian Arctic. Occ. Pap. No. 94. Can. Wildl. Ser., Ottawa.

Fuller, A.S., and J.C. George. 1997. Evaluation of Subsistence Harvest Data from the North Slope Borough 1993; Census for Eight North Slope Villages: For the Calendar Year 1992. Unpubl. report, North Slope Borough, Department of Wildlife Management, Barrow, Alaska.

Johnson, L.L. 1971. The migration, harvest and importance of waterfowl at Barrow, Alaska. M.S. thesis. University of Alaska, Fairbanks.

Murdoch, J. 1885. Birds, p. 104–128, *In* P.H. Ray [ed.], Report of the International Polar Expedition to Point Barrow, Alaska. Part 4. Government Printing Office, Washington, D.C.

Suydam, R., L. Quakenbush, M. Johnson, J.C. George and J. Young. 1997. Migration of King and Common eiders past Point Barrow, Alaska, in spring 1987, spring 1994 and fall 1994, p. 21–28. *In* D.L. Dickson [ed.], King and Common Eiders of the western Canadian Arctic. Occ. Pap. No. 94. Can. Wildl. Ser., Ottawa.

Suydam, R.S., D.L. Dickson, J.B. Fadely and L.T. Quakenbush. 2000a. Population declines of king and common eiders of the Beaufort Sea. Condor 102:219–222.

Suydam, R.S., L.T. Quakenbush, D.L. Dickson and T. Obritschkewitsch. 2000b. Migration of King, *Somateria spectabilis*, and Common, *S. mollissima v-nigra*, Eiders past Point Barrow, Alaska, during spring and summer/fall 1996. Can. Field-Naturalist 114:444–452.

Thompson, D.Q. and R.A. Person. 1963. The eider pass at Point Barrow, Alaska. J. Wildl. Mgmt. 27:348–356.

Thompson, S.K. 1992. Sampling. John Wiley & Sons, Inc., New York. 343 p.

Timson, R.S. 1976. Late summer migration at Barrow, Alaska, p. 354-400. *In* Environmental Assessment of the Alaskan Continental Shelf. Principal Investigators' Reports, April–June 1976, Vol. 1. U.S. Dept. Comm., NOAA, Boulder, Colorado.

Woodby, D.A., and G.J. Divoky. 1982. Spring migration of eiders and other waterbirds at Point Barrow, Alaska. Arctic 35:403–410.

Susceptibility of Sea Ice Biota to Disturbances in the Shallow Beaufort Sea. Phase 1: Biological Coupling of Sea Ice with the Pelagic and Benthic Realms

Rolf R. Gradinger <rgradinger@ims.uaf.edu>
Bodil A. Bluhm <bluhm@ims.uaf.edu>

Institute of Marine Science
University of Alaska Fairbanks
Fairbanks, AK 99775-7220

Task Order 85242

Abstract

The abundance, composition and isotopic signatures of biological communities in sea ice, in the water column and on the sea floor were studied in near-shore fast ice-covered waters close to Barrow, Alaska. During this project, we collected field samples in April 2002 and February, April and May/June 2003 using ice corers, water samplers, plankton nets and sediment corers at two locations which differed mainly in terms of sea ice sediment load. A strong relationship between sediment load and biological properties was observed: The spring ice algal bloom was most pronounced in the sediment-free fast ice, while it remained up to two orders of magnitude lower in the sea ice with high sediment load. The bloom in clean ice was largely produced by diatoms ≥20 μm, while these were rare in the dirty sea ice or in the plankton samples. Linked to the dissimilarity in algal abundances, low abundance of ice meiofauna was observed in sediment-loaded ice whereas abundances were high in sediment-free ice. Stable isotope analysis of ice fauna, zooplankton and ice and pelagic particulate organic matter (POM) suggests, through seasonally progressive enrichment of ice POM and ice fauna, that sea ice POM is used as a food source by ice meiofauna and ice-inhabiting benthic polychaete juveniles. Although effects were previously assumed, our study provides the first quantitative evidence that sea ice sediments play a pivotal role in structuring Arctic sea ice ecosystems. Secondly, this study showed that cryo-pelagic–benthic coupling is tight in this shallow fast ice covered area. Some of the results of our study were presented at several scientific meetings and are currently in the publication process.

Background and Scientific Goals

Sea ice is a crucial habitat for a diverse community of bacteria, protists and metazoans. While the off-shore multi-year sea ice has a high fraction of endemic species, the biology of fast ice has close links to water and benthic communities, including organism migration from the benthos into the sea ice. Specifically, benthic polychaetes spend part of their life cycle as juveniles and larvae within the sea ice, while presumably feeding on the high ice algal biomass accumulating during spring.

Light has previously been identified as the main controlling factor governing the seasonality of the ice biota. Various studies revealed that snow is the major modifying factor, other than season, for

alterations of the light availability and ultimately growth of ice algae. However, the effects of sediment load, that can be substantial in Arctic sea ice, had not been investigated so far. Our project targeted this question by comparing the seasonal development of the ice biota at two sites, which mainly differed in the amount of incorporated sea ice sediments (Figure 1). We hypothesized that increasing sediment load would cause a reduction of the biological production in the sea ice and more specifically, reduce the abundance of ice fauna including ice-associated larvae and juveniles of benthic polychaetes.

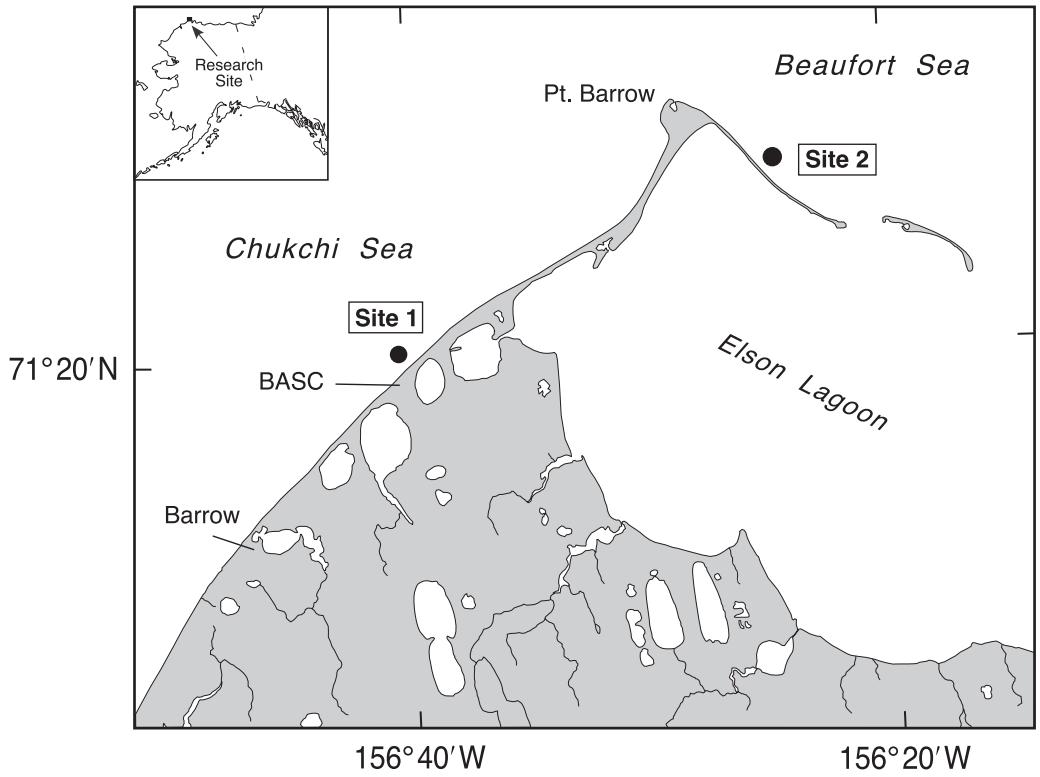

Figure 1. Location of project sampling sites. Site 1: sediment-free (clean) ice, Site 2: sediment-loaded (dirty) ice. BASC: Barrow Arctic Science Consortium facilities.

Summary of Previously Reported Results

The major part of our results was presented in detail in CMI Annual Report No. 10 [Gradinger and Bluhm 2004]. In summary, our major findings based on the field-work in Barrow were:

a) The observed sea ice sediment load in so-called “dirty sea ice” (102 mg L^{-1}) caused a reduction of available light for algal growth in the sea ice and the sea water by two orders of magnitude relative to clean ice with only a 6 mg L^{-1} particle load.

b) Within patches of dirty sea ice, the abundance of ice algae and ice meiofauna were one to two orders of magnitude below the abundances in clean sea ice during the maximum spring bloom (late May).

c) $\delta^{13}C$ stable isotope values for sea ice algae were progressively enriched with the advancing season in clean ice, which can be explained by carbon limitation of algal growth in the biomass-rich bottom layers of clean ice. Ice algal values in dirty ice remained rather constant over time.

d) Variability of ice and pelagic parameters within each sampling location and sampling period were considerably lower than variability between sites and months.

The first manuscript entitled, "The pivotal role of sea ice sediments for the seasonal development of near-shore Arctic fast ice biota off Barrow, Alaska" was submitted to Marine Ecology Progress Series (authors: Gradinger, Bluhm and Nielson) and was accepted with revisions. Referees requested the incorporation of additional data for which additional analyses are currently underway —resubmission is expected this year.

Results Previously Not Reported

Algal counts

Currently, the particle analysis is being finalized. The major tool for processing the particle samples taken from the sea ice and water column was the FlowCAM, an image analysis–based flow cytometer. Three digital pictures per second are recorded from the continuous sample stream and are simultaneously analyzed for particle abundance and size (Figure 2a–f). Absolute particle abundances were calculated based on the mean number of particles per image and a minimum count of 400 particles per size fraction and sample. The digital images of the individual particles were used to identify the particle composition within each selected size fraction (5 to <10 μm, 10 to <20 μm, and ≥20 μm). Four samples per site, realm and sampling period were analyzed.

Examples of recorded pictures in the three size classes are presented in Figure 2. Mean values (± standard deviations) for February and May 2003 are presented in Figure 3. Large single-celled diatoms dominated the size fraction ≥20 μm in May 2003 in all clean ice cores (Figure 2f), while they were nearly absent from all other samples (e.g., Figure 2c). The growth of diatoms caused the significant increase in particle numbers in this size fraction between February and May, while no such change was seen in the dirty sea ice at site 2 or in the plankton samples (Figure 3). This observation is consistent with the relative changes in chlorophyll *a* and particulate organic carbon concentrations, which we described in the previous CMI annual report [Gradinger and Bluhm 2004].

Stable isotope analysis of ice meiofauna and zooplankton

Stable isotope analysis of more than 300 samples was conducted as described in Annual Report No. 10 [Gradinger and Bluhm 2004]. For a single sample, 0.2–0.4 mg dry mass of faunal tissue are required at current equipment sensitivity. Depending on the body mass of a species/taxon, this amount required pooling up to several hundred individuals, e.g., 30–50 turbellarians, 50–80 polychaete juveniles, and 150–300 copepod nauplii or nematodes. Due to the considerable effort required to pick this amount from a sample and low faunal densities in the winter and/or at the sediment-loaded site, samples could only be obtained from taxa that were reasonably common at a site at any given time.

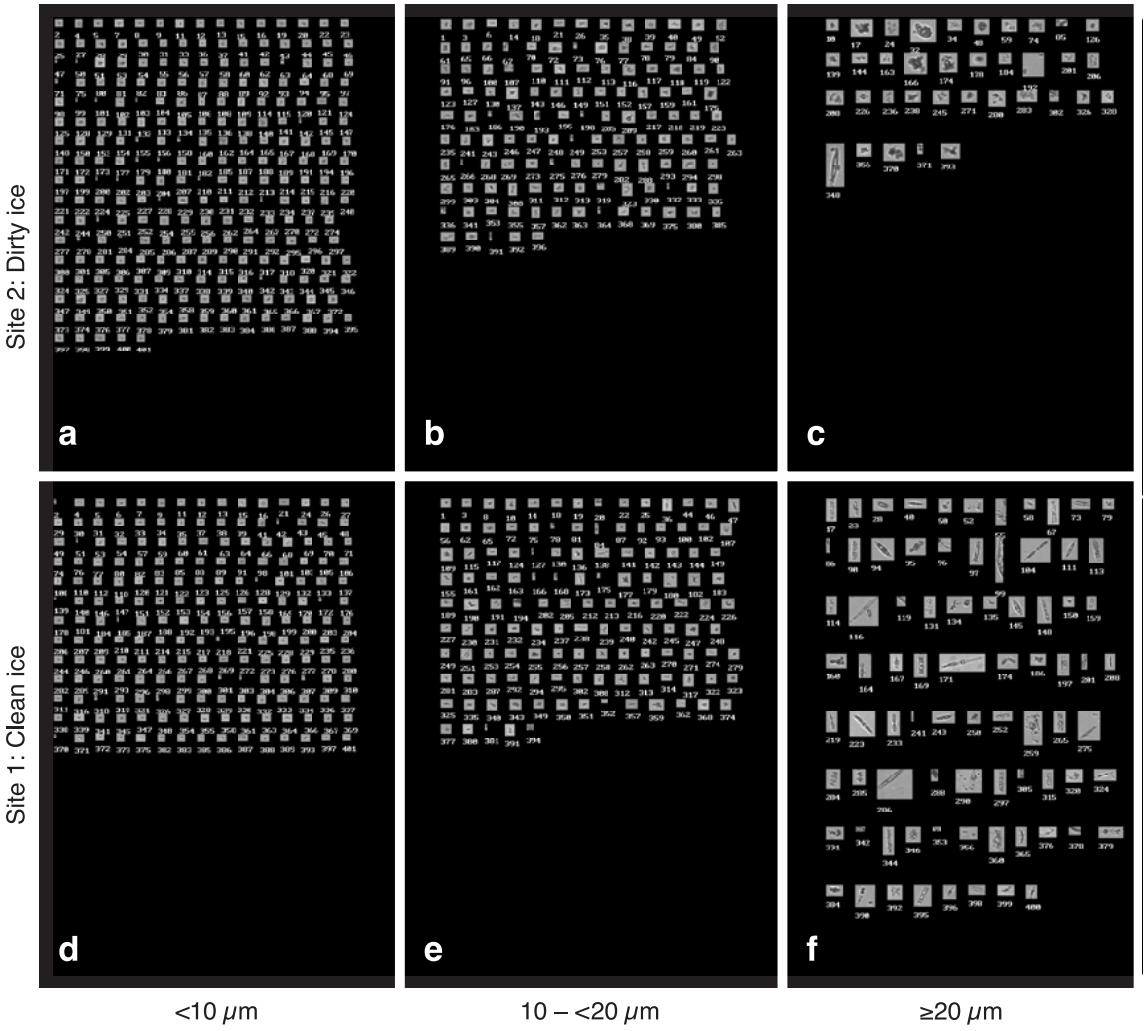

Figure 2. Examples of FlowCAM images from sea ice sites 1 and 2 collected in May 2003. Individual particles are consecutively numbered and labeled as they flow through the system (in situ, which explains the number and sequence).

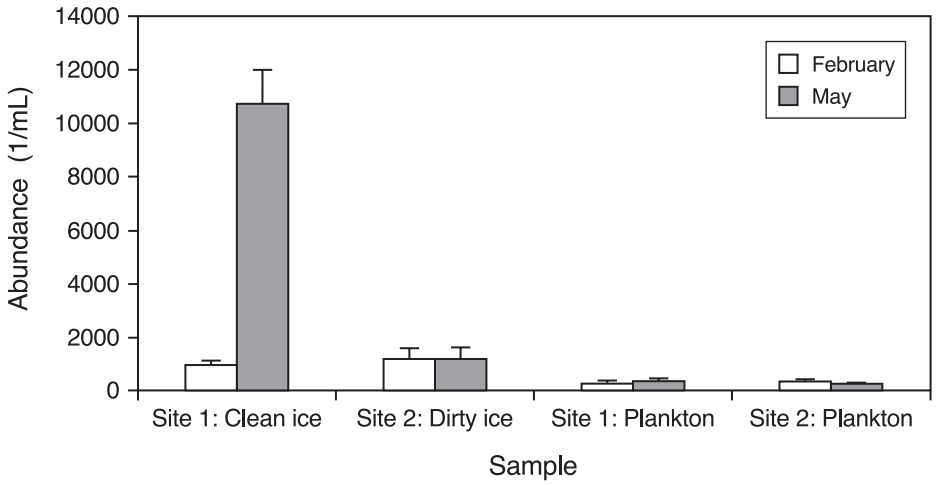

Figure 3. Abundance (n/ml) (mean ± SD) of particles larger than 20 µm in sea ice and water samples from sites 1 and 2 in 2003. The increase at site 1 is due to growth of sea ice diatoms (see Figure 2f).

Mean $\delta^{13}C$ and $\delta^{15}N$ values (± standard deviations) of all analyzed ice meiofauna and zooplankton for all sampling periods are compiled in Tables 1 and 2, respectively. Figure 4 shows the distribution of the $\delta^{13}C$ values of the more common taxa by taxonomic groups and sampling periods. At the clean ice site (Figure 4a), several ice meiofauna taxa showed progressively enriched $\delta^{13}C$ signatures with the ongoing season, e.g., by approximately 7‰ in polychaete juveniles, nematodes and turbellaria. These taxa apparently followed the ice particulate organic matter (POM) $\delta^{13}C$ signatures, suggesting that they are more tightly linked to ice algal production for food than the sympagic amphipod species *Gammaracanthus loricatus* and *Onisimus litoralis*. The lack of isotopic enrichment in these amphipods from February 2003 to April 2003, when ice algae became progressively enriched, may support Carey and Boudrias' [1987] observation from stomach content analysis that *O. litoralis* utilized ice algae when abundant while also feeding on different prey at other times. Faunal densities, and therefore the number of isotope samples, were too low to observe any trends at the dirty ice site. However, the lack of isotopic turnover rates makes solid conclusions premature.

A slight enrichment in $\delta^{13}C$ occurred in several zooplankton taxa at the clean ice site (Figures 4b and 5b), e.g., in nauplii and cyclopid copepods, while the other sampled taxa revealed no obvious trends. Partial feeding on enriched particles that were released from the sea ice during first melting processes might explain the enrichment in selected zoopankton taxa late in the sea ice season. Pelagic POM, in contrast, remained rather stable over the time sampled with respect to its carbon isotopic signature and could, therefore, not trigger any isotopic enrichment in its grazers. At site 2, pelagic POM isotope values were more variable between sampling periods while zooplankton signatures showed very little variability. The rather depleted pelagic POM signatures at both sites in April 2003 (means –27.1‰ and –28.3‰) might originate from terrestrial material that may for unknown reasons have been abundant at that time.

Table 1. $\delta^{13}C$ isotopic signatures for sea ice meiofauna and zooplankton from sampling sites 1 and 2 for 2002 and 2003. A: Mean $\delta^{13}C$ values (‰) for n = 2 to n = 9 and individual $\delta^{13}C$ values for n = 1 . B: Standard deviations (‰) for $n \geq 3$ only. The species/taxa are sorted in taxonomic order. No samples were taken at site 2 in May 2002. Note that site 2 had clean ice in 2002 and dirty ice in 2003. POM = particulate organic matter.

A

Site/Realm	**Site 1: Chukchi Sea, sea ice**					**Site 2: Beaufort Sea, sea ice**				**Site 1: Chukchi Sea, water column**					**Site 2: Beaufort Sea, water column**			
Date	Apr 02	May 02	Feb 03	Apr 03	May 03	Apr 02	Feb 03	Apr 03	May 03	Apr 02	May 02	Feb 03	Apr 03	May 03	Apr 02	Feb 03	Apr 03	May 03
POM	–20.42	–13.39	–24.92	–23.83	–15.52	–21.50	–25.54	–25.83	–24.17	–25.95	–24.24	–24.69	–27.14	–24.30	–24.53	–24.90	–28.30	–22.49
Planula											–21.82							
Ctenophora											–21.36							
Turbellaria	–19.30	–17.08		–21.40	–15.36			–20.16			–16.86			–21.52		–23.76		
Rotifers					–21.95								–22.98					
Nematoda		–16.85	–23.25		–15.63													
Polychaeta	–22.17	–16.20		–22.73			–22.31		–19.59		–18.02		–23.36			–21.42	–22.64	–19.35
Trochophora											–20.08	–21.77						
Nauplii				–25.19					–23.21	–24.05	–20.37		–25.61	–22.28		–24.60		–22.55
Calanoidea									–24.32	–22.11	–21.19	–23.57	–25.21	–21.33	–21.83	–22.81	–24.12	–22.06
Calanus glacialis										–24.71					–23.42			
Harpacticoidea	–22.58										–17.01	–20.47	–22.87		–23.20		–22.96	–22.22
Cyclopoidea				–24.15						–21.65	–19.77		–21.37			–23.62		–22.17
Onisimus litoralis			–19.34	–22.02														
Gammaracanthus loricatus			–19.24	–20.40														
Chaetognatha											–21.27							–19.70

B

Site/Realm	**Site 1: Chukchi Sea, sea ice**					**Site 2: Beaufort Sea, sea ice**				**Site 1: Chukchi Sea, water column**					**Site 2: Beaufort Sea, water column**			
Date	Apr 02	May 02	Feb 03	Apr 03	May 03	Apr 02	Feb 03	Apr 03	May 03	Apr 02	May 02	Feb 03	Apr 03	May 03	Apr 02	Feb 03	Apr 03	May 03
POM	0.20	2.15	1.64	0.95	0.76	0.11	0.44	0.19	0.15	3.79	0.17	1.85	1.24	2.72	0.15	0.27	1.73	1.15
Turbellaria				1.44	0.38													
Nematoda					0.62													
Polychaeta				0.66							0.33		1.09					
Nauplii														0.76				0.65
Calanoidea													2.88	0.46	0.13		1.22	0.45
Calanus glacialis										2.02					0.94			
Harpacticoidea											1.06		1.44				2.31	
Cyclopoidea											0.21							
Onisimus litoralis			1.78	1.42														
Gammaracanthus loricatus			0.97	0.47														

Table 2. $\delta^{15}N$ isotopic signatures for sea ice meiofauna and zooplankton from sampling sites 1 and 2 for 2002 and 2003. A: Mean $\delta^{15}N$ values (‰) for n = 2 to n = 9 and individual $\delta^{15}N$ values for n = 1. B: Standard deviations (‰) for $n \geq 3$ only. The species/taxa are sorted in taxonomic order. No samples were taken at site 2 in May 2002. Note that site 2 had clean ice in 2002 and dirty ice in 2003. POM = particulate organic matter. This table contains fewer data than Table 1 since some samples had sufficient mass for $\delta^{13}C$ measurements, but not for $\delta^{15}N$ measurements.

A

Site/Realm	**Site 1: Chukchi Sea, sea ice**					**Site 2: Beaufort Sea, sea ice**				**Site 1: Chukchi Sea, water column**					**Site 2: Beaufort Sea, water column**			
Date	Apr 02	May 02	Feb 03	Apr 03	May 03	Apr 02	Feb 03	Apr 03	May 03	Apr 02	May 02	Feb 03	Apr 03	May 03	Apr 02	Feb 03	Apr 03	May 03
POM	7.74	7.52	6.34	7.90	10.07	8.43	5.61	11.90		10.19	5.92	8.07		15.14	7.28	6.96		13.60
Planula											11.50							
Ctenophora											12.96							
Turbellaria		8.50		9.69														
Rotifers																		
Nematoda		6.00	12.00		9.13		11.66											
Polychaeta	7.74	5.71		13.89			8.24	8.49	10.27		7.44		14.63	10.44		10.37	14.68	
Trochophora											11.22	11.39						
Ostracoda													13.97					
Nauplii				10.70			9.62		14.04	10.04	10.48			15.42		8.81		14.11
Calanoidea										12.95		12.56	10.45	15.47	13.61	13.26	11.29	13.85
Calanus glacialis													11.40		11.87		10.86	
Harpacticoidea	7.60										7.39	9.95		11.85	9.50		13.67	11.81
Cyclopoidea				11.84			10.58			10.88	10.57					12.06		
Onisimus litoralis			12.90	12.73														
Gammaracanthus loricatus			12.59	11.34														
Chaetognatha											14.44							15.42
Copepoda	9.93								9.18									

B

Site/Realm	**Site 1: Chukchi Sea, sea ice**					**Site 2: Beaufort Sea, sea ice**				**Site 1: Chukchi Sea, water column**					**Site 2: Beaufort Sea, water column**			
Date	Apr 02	May 02	Feb 03	Apr 03	May 03	Apr 02	Feb 03	Apr 03	May 03	Apr 02	May 02	Feb 03	Apr 03	May 03	Apr 02	Feb 03	Apr 03	May 03
POM	0.38	1.03	1.73	0.65	0.56	0.41	0.61	1.89		0.98	0.39	1.30		0.43	0.92	0.80		0.91
Turbellaria				0.78														
Nematoda					1.54													
Polychaeta				2.03			2.03	1.92			1.14							
Trochophora											0.89							
Nauplii														1.90				0.41
Calanoidea													0.77	0.78	0.48		0.17	
Calanus glacialis													1.62		0.91		0.57	
Harpacticoidea											0.91							
Cyclopoidea											0.34							
Onisimus litoralis			1.24	0.54														
Gammaracanthus loricatus			1.73	0.95														

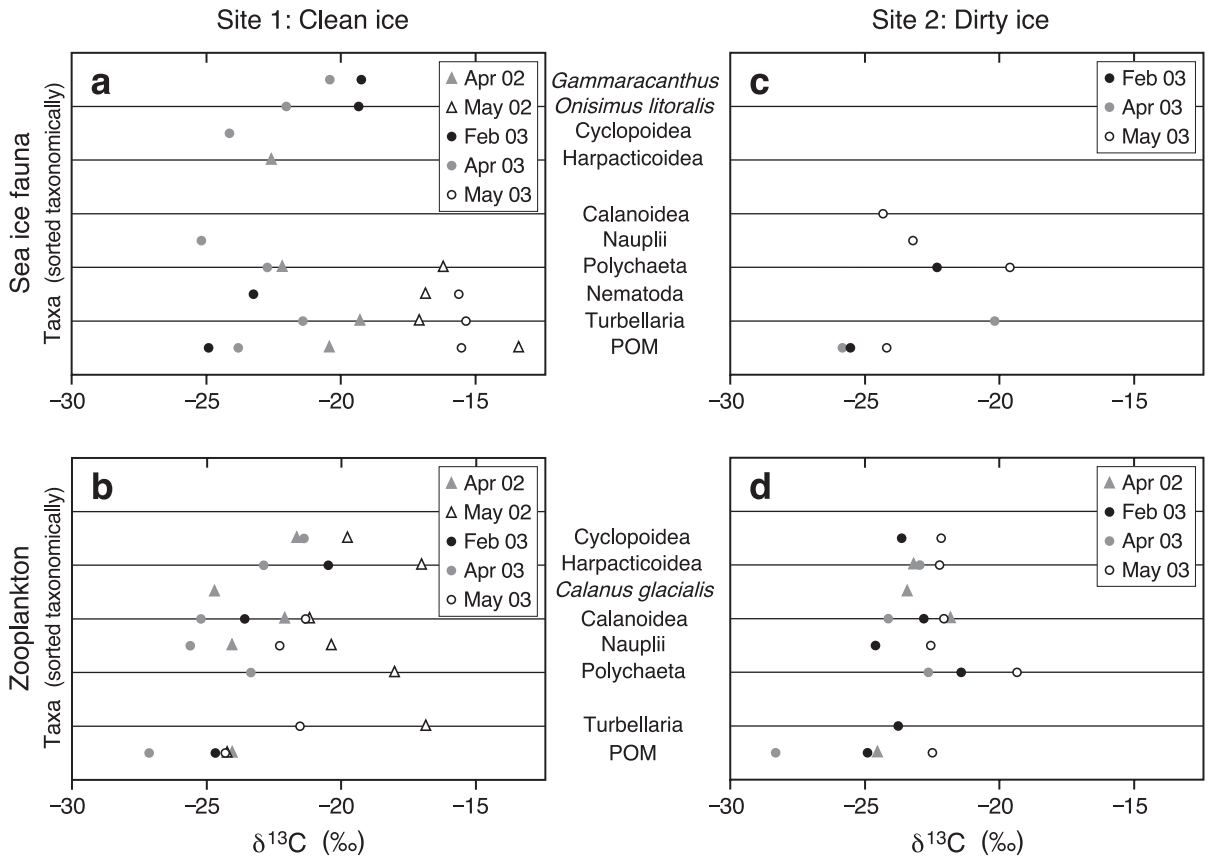

Figure 4. Distribution of $\delta^{15}C$ values of sea ice fauna and zooplankton from the Barrow area by taxonomic groups. Site 1: Clean ice – sea ice fauna (a) and zooplankton (b). Site 2: Dirty ice – sea ice fauna (c) and zooplankton (d).

Figure 5 shows the $\delta^{13}C$ isotopic signatures for sea ice meiofauna and zooplankton as dependent on the $\delta^{13}C$ values of sea ice and pelagic POM, respectively. Figure 5a demonstrates a significant positive correlation between sea ice fauna $\delta^{13}C$ signatures and ice POM $\delta^{13}C$ signatures (Kendall rank correlation test, $p = 0.04$), which, again, suggests a strong dependence of ice fauna on sea ice POM as a food source. At the dirty ice site and for the zooplankton of two sites (Figure 5), there may also be a positive correlation of faunal $\delta^{13}C$ signatures with POM $\delta^{13}C$ signatures, at least for zooplankton, but the progressive enrichment of both components with season is not obvious. The extreme enrichment in $\delta^{13}C$ in a sea ice environment has previously been documented for ice algae [Hobson et al. 1995; Schubert and Calvert 2001], but this study is the first to document isotopic signatures in general, (in sea ice meiofauna and sympagic amphipods) and their ice POM–dependent enrichment in particular. Further analysis is currently focused on quantifying the utilization of the different carbon sources 'pelagic POM' and 'sea ice POM' in the different realms and sites at different stages in phytoplankton and ice algal blooms. As yet, differences in taxon-specific turnover rates are unknown and complicate the interpretation of the data; this has led to a related thesis project for School of Fisheries and Ocean Sciences (SFOS) graduate student, Mette Nielson (see below).

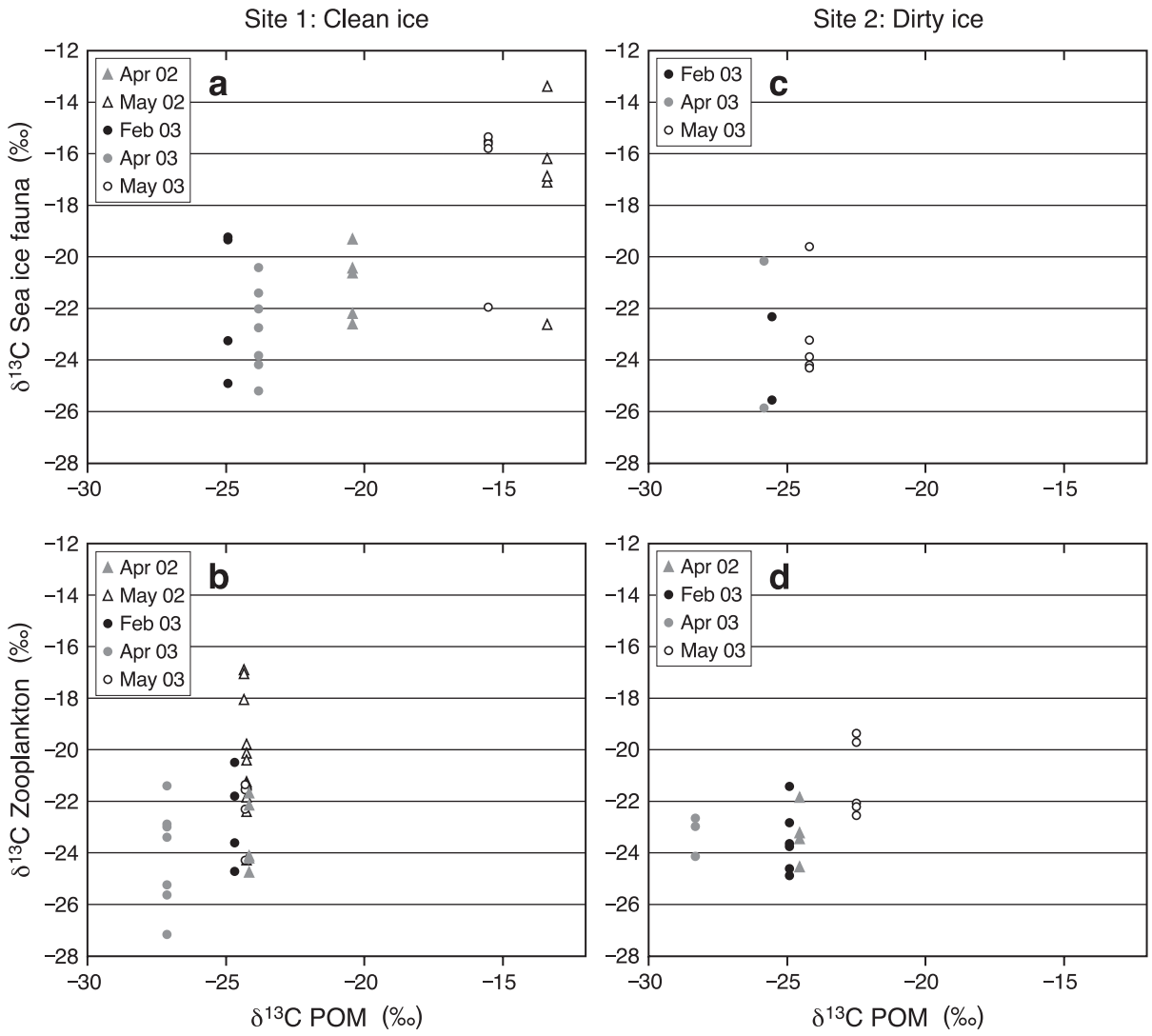

Figure 5. $\delta^{13}C$ isotopic signatures for sea ice meiofauna and zooplankton from sampling sites 1 and 2 for 2002 and 2003 as dependent on the $\delta^{13}C$ values of sea ice and pelagic POM, respectively. Site 1: Clean ice – sea ice meiofauna (a) and zooplankton (b). Site 2: Dirty ice – sea ice fauna (c) and zooplankton (d). Only the values collected in 2003 are presented in (c) as this was the time of dirty ice at this location.

A paper presenting the stable isotope results, preliminarily entitled, “Trophic dynamics and food sources in land fast ice off Barrow, Alaska: Lessons learned from stable ^{13}C and ^{15}N isotope analysis” is currently being prepared and will be submitted to the journal Marine Biology in December 2004.

Outreach and Presentations

We established a website presenting our project on the UAF School of Fisheries and Ocean Sciences server which has been accessible since January 2003. As of mid-September 2004, the site had received close to 700 hits.

Mette Nielson, an SFOS graduate student, reported on the project's progress at the CMI Annual Research Review in February 2004 in Fairbanks. Results from this study were also presented at the SEARCH (Study of Environmental Arctic Change) Open Science Meeting in Seattle (26–30 October 2003).

Mette Nielson started as a graduate student at SFOS in spring 2003. She has worked and will continue working on part of the collected material. She received CMI funding to participate in the Barrow field phase and data analysis. She is currently working on her master's thesis, which is based on data and experiences collected during this CMI project.

References

Carey, A.G., Jr., and M.A. Boudrias. 1987. Feeding ecology of *Pseudalibrotus* (=*Onisimus*) *litoralis* Kroyer (Crustacea:Amphipoda) on the Beaufort Sea inner continental shelf. Polar Biol. 8:29–33.

Gradinger, R.R., and B.A. Bluhm. 2004. Susceptibility of sea ice biota to disturbances in the shallow Beaufort Sea. Phase 1: Biological coupling of sea ice with the pelagic and benthic realms, p. 70–78. *In* University of Alaska Coastal Marine Institute Annual Report No. 10. OCS Study MMS 2004-002, University of Alaska Fairbanks and USDOI, MMS, Alaska OCS Region.

Hobson, K.A., W.G. Ambrose, Jr. and P.E. Renaud. 1995. Sources of primary production, benthic–pelagic coupling, and trophic relationships within the Northeast Water Polynya: Insights from $\delta^{13}C$ and $\delta^{15}N$ analysis. Mar. Ecol. Prog. Ser. 128:1–10.

Schubert, C.J., and S.E. Calvert. 2001. Nitrogen and carbon isotopic composition of marine and terrestrial organic matter in Arctic Ocean sediments: Implications for nutrient utilization and organic matter composition. Deep-Sea Res. I 48:789–810.

Role of Grazers on the Recolonization of Hard-Bottom Communities in the Alaska Beaufort Sea

Brenda Konar <bkonar@guru.uaf.edu>

Global Underwater Research Unit
University of Alaska Fairbanks
Fairbanks, AK 99775-7220

Task Order 85244

Abstract

This project is expanding on the recovery work completed by Dunton [1985] to determine the importance of grazing to recolonization rates of sessile organisms at the Boulder Patch. A simple manipulative study was set up in the summer of 2002 to test the suggestion that invertebrate grazing is associated with the slow recovery of Boulder Patch communities. This study was sampled in 2003 and 2004. No recruitment was seen on any of the cleared rocks and little difference was seen in the control rocks. As the experiment is still running, it would be very beneficial to resample again in 2005 to look for recruitment. This study strongly suggests that any perturbations causing scouring of hard substrate in the Beaufort Sea will result in very slow recovery of the community.

Background

Alaska's Beaufort Sea shelf is typically characterized by silty sands and mud and as having an absence of macroalgal beds and associated organisms [Barnes and Reimnitz 1974]. In 1971, a diverse kelp and invertebrate community was discovered near Prudhoe Bay in Stefansson Sound, Alaska. Since its discovery, the Boulder Patch has been subject to much biological and geological research [Dunton et al. 1982; Dunton and Schell 1987; Dunton and Jodwalis 1988; Dunton 1990; Martin and Gallaway 1994; MMS 1996, 1998; Dunton and Schonberg 2000]. This research stems from a need to protect sensitive biologically-productive regions, while allowing oil exploration in the surrounding areas [Wilson 1979].

The Boulder Patch contains large numbers of cobbles and boulders that provide a substrate for attachment for a diverse assortment of invertebrates and several species of red and brown algae. The predominant alga is the brown *Laminaria solidungula*, which constitutes 90% of the brown algal biomass [Dunton et al. 1982]. This alga is an important food source to many benthic and epibenthic organisms [Dunton and Schell 1986]. Differences in infaunal abundance and biomass between the Boulder Patch and peripheral sediment areas demonstrate the importance of this unique habitat [Dunton and Schonberg 2000]. In the Boulder Patch, algae and epilithic invertebrates cover nearly all exposed substrate, with the exception of recently upturned rocks [Dunton and Schonberg 2000].

A recolonization experiment in the Boulder Patch has shown that recovery of denuded areas is slow [Dunton et al. 1982]. In temperate systems, algal communities can recover to previous densities within one year of denuding [Foster 1975], but in the Boulder Patch 50% of the substrate was still

bare three years after an initial disturbance [Dunton et al. 1982]. One of the primary reasons suggested for the slow recolonization is grazing by invertebrates [Dunton et al. 1982]. Motile herbivorous, omnivorous, and carnivorous invertebrates such as chitons, snails, seastars and polychaetes have been frequently observed in the Boulder Patch [Dunton et al. 1982]. Many studies have shown that grazers can be very important in structuring communities [Johnson et al. 1997; Worm and Chapman 1998; Jenkins et al. 1999; Ojeda and Muñoz 1999; Morton 1999; Wilson et al. 1999; Konar 2000].

To achieve the goal of determining if grazing/predation is associated with the slow recruitment in the Boulder Patch, various comparisons were set up using exclusion cages, cage controls, and natural rock.

Objective and Hypothesis

Objective:

Determine if grazing is limiting the rate of recruitment of hard substrate communities in the Boulder Patch.

The specific hypothesis is:

H_1 There is no significant difference between recruitment of sessile organisms on bare boulders with and without cages to exclude mobile invertebrates.

Experimental Methods

This experiment was set up in summer of 2002. The boulders used in this study were collected from the Boulder Patch (DS11, Figure 1). Because of the difficulty in removing living material from rocky substrata underwater, all boulders were brought to the surface and cleared. After five days, the denuded rocks (with and without cages and cage controls) were placed back into the field.

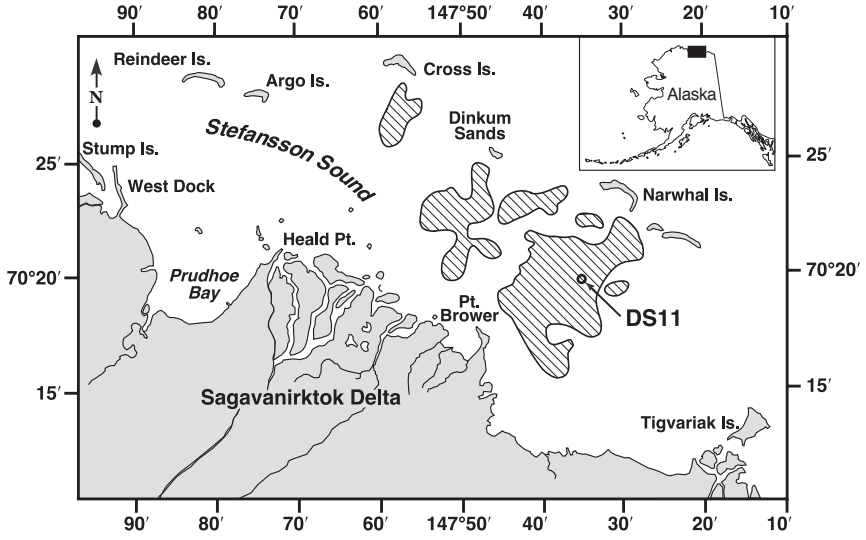

Figure 1. Chart of Boulder Patch showing Dive Site 11 (DS11). Hatched polygons are areas with high boulder/cobble density.

Six cages were deployed to exclude large mobile invertebrates at each of three locations within DS11, totaling 18 cages. The cages in this experiment were constructed of stainless steel mesh (Figure 2). All cages were coated with a non-toxic antifouling compound to inhibit growth of sessile invertebrates and algae. Eighteen cage controls were also deployed to detect any artifacts caused by the cages, such as decreased light levels or increased sedimentation. These controls were cages that had holes cut into the sides so that invertebrates could easily pass through them (Figure 3).

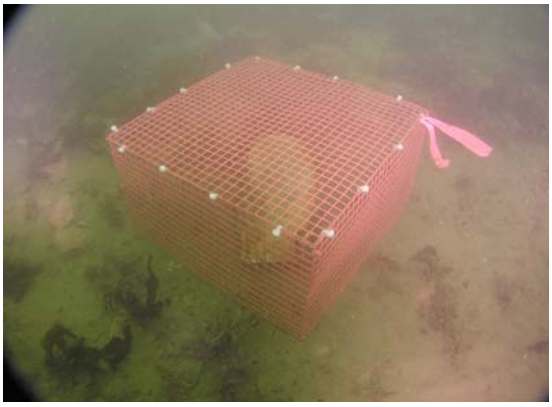

Figure 2. Cage rock in situ.

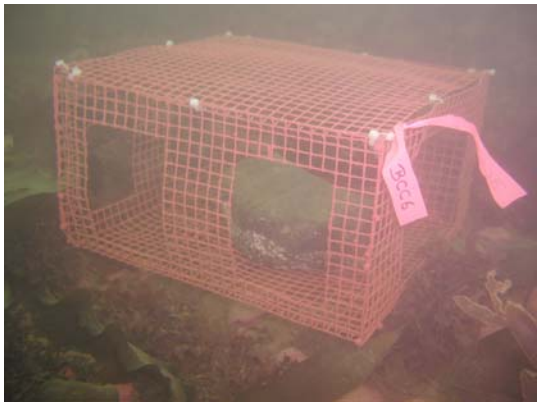

Figure 3. Cage control in situ.

For comparison, 18 cleared rocks were deployed with no cages to determine natural recruitment. As a control for natural changes in the community during the time period of this experiment, 18 non-cleared boulders were also examined.

In 2004, surveys were conducted at DS11 to determine grazer composition and abundance. For this, five random 0.25-m^2 quadrats were surveyed along three different 30-m transects. From each quadrat, all large mobile invertebrates and boulders were collected and placed in a fine mesh bag. Bags were brought to the boat and grazers were sorted and identified.

Preliminary Results

Cages

No recruitment of any sessile organisms was seen during this study on any of the cleared boulders (caged, partially caged and uncaged). Variation in the community composition of the uncleared boulders did not significantly fluctuate over time (Figure 4). The majority of uncleared boulders were covered with encrusting coralline algae and foliose algae, while very little (a mean of 2% or less) was bare. Foliose algae were primarily *Phycodrys rubens*, averaging 21% over the three year period. Other species whose overall averages ranged from 3 to 8% included *Phyllophora truncata*, *Dilsea integra* and *Odonthalia dentata.*

Grazer surveys showed that two different species of chitons (*Amicula vestita* and *Ischnochiton* spp.) and seastars were the most abundant grazers in this area (Figure 5). A few gastropods also were seen but their densities were very low.

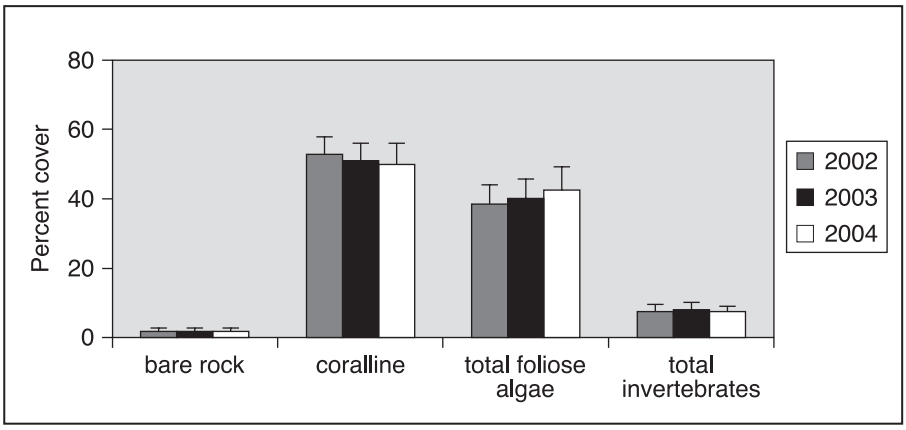

Figure 4. Mean percent cover (±1 s.e.) of bare rock, encrusting coralline algae, total foliose algae and total invertebrates on uncleared control boulders from 2002, 2003 and 2004.

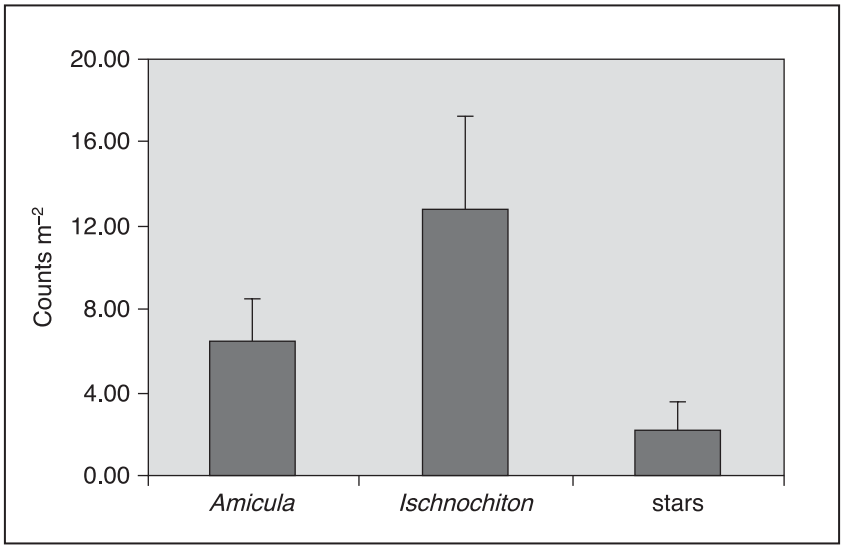

Figure 5. Mean percent cover (±1 s.e.) of various grazers on uncleared control boulders from 2004.

Light

Although light attenuation was consistently lower in 2003 than in 2004 (Figure 6), bottom irradiance was similar between years. Light readings were taken on two separate days at DS11 in 2003 and five days in 2004.

Sediments in the water column cause this lack of light. These sediments also could be seen on the encrusting organisms and rocks. Since there was no growth on the cleared rocks in this first year and sediments were found on the substrate, a pilot experiment was set up to test a method to eliminate sediments from a settling surface. In 2003, two sets of plexiglass settling plates were deployed in the middle of DS11 (Figure 7).

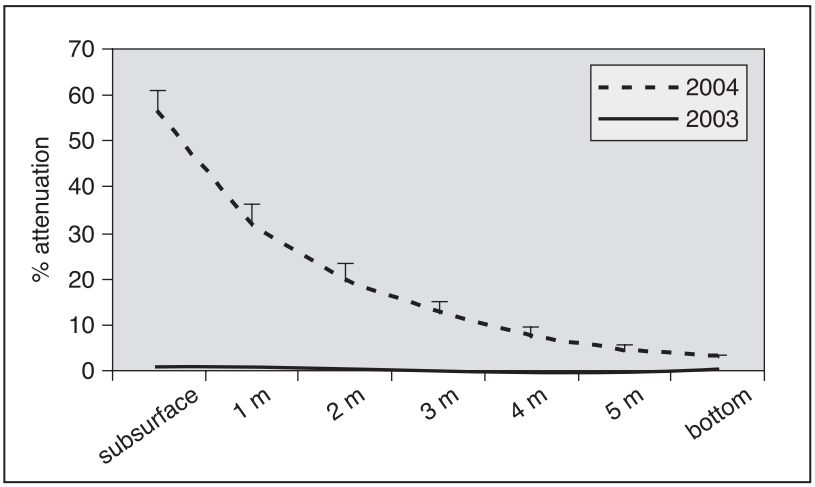

Figure 6. Mean light attenuation (±1 s.e.) at DS11 in 2003 and 2004. n=5 in 2004 and n=2 in 2003.

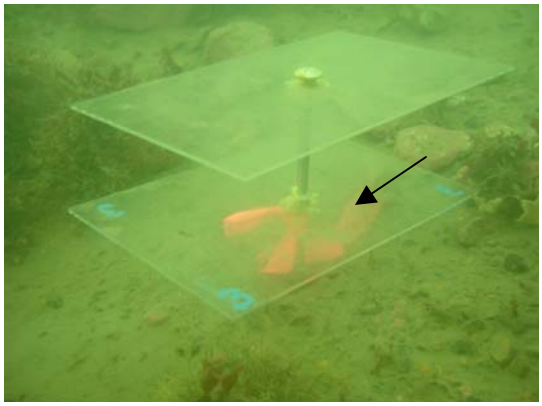

Figure 7. Plexiglas settling plates used to minimize sediments on a settling surface. Arrow points to second plate where less sedimentation will occur and settlement is more likely.

These settling plates are made of clear plexiglas so that light will penetrate through both plates and recruitment will not be hindered by sedimentation on the bottom plate because it is protected by the top plate. The plates were revisited in 2004 and were found to be relatively free of sediments but also had no growth on them. Because they appeared to minimize sedimentation on a surface, I set up two sets of plates in each of the three experimental areas in DS11, totaling six sets. It is hoped that these plates will be resampled in 2005.

Preliminary Conclusions and Recommendations

No growth occurred on any cleared substrate during the course of this experiment. This does not necessarily mean that grazing does not have any effects on recruitment of sessile organisms at the Boulder Patch but it does imply that recruitment is a slow and tenuous process. Grazers were seen at DS11 in 2004 and there was evidence of grazing on many adult *Laminaria solidungula* plants (Figure 8).

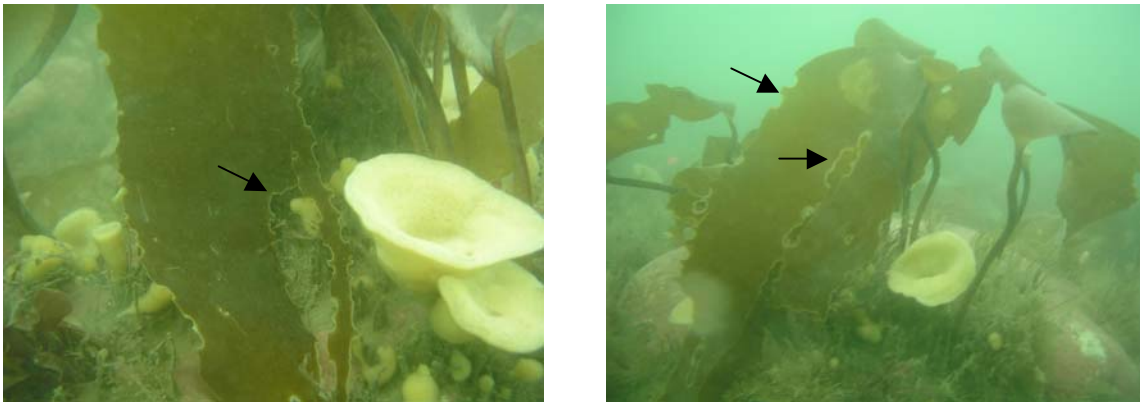

Figure 8. Grazing marks can be seen on these adult *Laminaria solidungula* plants. Arrows point to specific bite marks.

This study strongly suggests that any perturbations causing scouring of hard substrate in the Beaufort Sea will result in very slow recovery of the community. It is recommended that this caging experiment and the new settling plates be monitored for another year. This will give a full three years of recruitment data that will make comparisons to other areas very insightful.

References

Barnes, P.W., and E. Reimnitz. 1974. Sedimentary processes on arctic shelves off the northern coast of Alaska, p. 439-476. *In* J.C. Reed and J.E. Sater [eds.], The Coast and Shelf of the Beaufort Sea, Arctic Institute of North America, Arlington, VA.

Dunton, K.H. 1985. Trophic dynamics in marine nearshore systems of the Alaskan high arctic. Ph.D. dissertation. University of Alaska Fairbanks.

Dunton, K.H. 1990. Growth and production in *Laminaria solidungula*: Relation to continuous underwater light levels in the Alaskan High Arctic. Mar. Biol. 106:297–304.

Dunton, K.H., and C.M. Jodwalis. 1988. Photosynthetic performance of *Laminaria solidungula* measured *in situ* in the Alaskan High Arctic. Mar. Biol. 98:277–285.

Dunton, K.H., and D.M. Schell. 1986. A seasonal carbon budget for the kelp *Laminaria solidungula* in the Alaskan high arctic. Marine Ecology Progress Series 31:57–66.

Dunton, K.H., and S.V. Schonberg. 2000. The benthic faunal assemblage of the Boulder Patch kelp community, Chapter 18. *In* The Natural History of an Arctic Oil Field. Academic Press.

Dunton, K.H., E. Reimnitz and S. Schonberg. 1982. An Arctic kelp community in the Alaskan Beaufort Sea. Arctic 35:465–484.

Foster, M.S. 1975. Algal succession in a *Macrocystis pyrifera* forest. Mar. Biol. 32:313–329.

Jenkins, S.R., S.J. Hawkins and T.A. Norton. 1999. Interaction between a fucoid canopy and limpet grazing in structuring a low shore intertidal community. J. Exp. Mar. Biol. Ecol. 233:41–63.

Johnson M.P., M.T. Burrows, R.G. Hartnoll and S.J. Hawkins. 1997. Spatial structure on moderately exposed rocky shores: Patch scales and the interactions between limpets and algae. Mar. Ecol. Prog. Ser. 160:209–215.

Konar, B. 2000. Seasonal inhibitory effects of marine plants on sea urchins: Structuring communities the algal way. Oecologia 125:208–217.

Martin, L.R., and B.J. Gallaway. 1994. The effects of the Endicott Development Project on the Boulder Patch, an Arctic kelp community in Stefansson Sound, Alaska. Arctic 47:54–64.

Minerals Management Service [MMS]. 1996. Beaufort Sea planning area oil and gas lease sale 144. Final Environmental Impact Statement. MMS OCS EIS/EA MMS 96-0012. U.S. Dept. of Interior, MMS, Alaska Outer Continental Shelf Region, Anchorage.

Minerals Management Service [MMS]. 1998. Arctic Kelp Workshop Proceedings, Anchorage, Alaska. T.D. Newbury [ed.], OCS Study MMS 98-0038. U.S. Dept. of Interior, MMS, Alaska Outer Continental Shelf Region, Anchorage.

Morton, B. 1999. Competitive grazers and the predatory whelk *Lepsiella flindersi* (Gastropoda: Muricidae) structure a mussel bed (*Xenostrobus pulex*) on a southwest Australian shore. J. Mollus. Stud. 65:435–452.

Ojeda, F.P., and A.A. Muñoz. 1999. Feeding selectivity of the herbivorous fish *Scartichthys viridis*: effects on macroalgal community structure in a temperate rocky intertidal coastal zone. Mar. Ecol. Prog. Ser. 184:219–229.

Wilson, H.M. 1979. Beaufort Sea high bids top $1 billion. Oil Gas J. 77:26–29.

Wilson, W.G., C.W. Osenberg, R.J. Schmitt and R.M. Nisbet. 1999. Complementary foraging behaviors allow coexistence of two consumers. Ecology 80:2358–2372.

Worm, B., and A.R. Chapman. 1998. Relative effects of elevated gazing pressure and competition from a red algal turf on two post-settlement stages of *Fucus evanescens* C. Ag. J. Exp. Mar. Biol. Ecol. 220:247–268.

Water and Ice Dynamics in Cook Inlet, Alaska

Mark A. Johnson <johnson@ims.uaf.edu>
Stephen R. Okkonen <okkonen@alaska.net>

Institute of Marine Science
University of Alaska Fairbanks
Fairbanks, AK 99775–7220

Andrey Y. Proshutinsky <aproshutinsky@whoi.edu>

Physical Oceanography Department, MS #29
Woods Hole Oceanographic Institution
Woods Hole, MA 02543

Task Order 85308

Abstract

To better understand the circulation and dynamics of the water and ice in Cook Inlet, we use a high resolution numerical model forced by tides that is being validated using satellite-tracked drifting buoys and synthetic aperature radar (SAR) satellite imagery. The observational program using drogued, drifting buoys focuses on mapping the tide rips to understand their temporal and spatial variability. With more than 25 buoys now deployed, the complete position data set shows highest energy in the historical tide rip locations. We are now investigating the temporal variability of the rips. In the winter, satellite imagery allows us to track ice motion to further evaluate the rip locations.

Data Collection, Processing and Analyses

During the reporting period (October 2003–September 2004) we worked on data collection and tidal modeling. Data collection included a search for additional and more precise bathymetry information and particularly information about flooding/wetting areas or "mud flats", which in the existing digital bathymetry data archives are represented by a 0 m depth. This was not a trivial task because, as we now understand, the requested information does not exist in a digital form and we have digitized satellite images from Cold Regions Research and Engineering Laboratory report 76-25 [CRREL 1976] in order to improve our model bathymetry.

We have also collected river runoff data (major and small river locations, river discharge and its seasonal variability). This information has been used to simulated circulation of Cook Inlet driven by river runoff.

We are still working on the collection of wind fields and investigation of Cook Inlet wind-driven circulation and its seasonal variability. Our tidal modeling experiments and comparison of simulated buoy trajectories with observed trajectories allow us to conclude that wind-driven motion significantly influences dynamics of Cook Inlet waters and can dominate when the wind is strong enough (Figure 1).

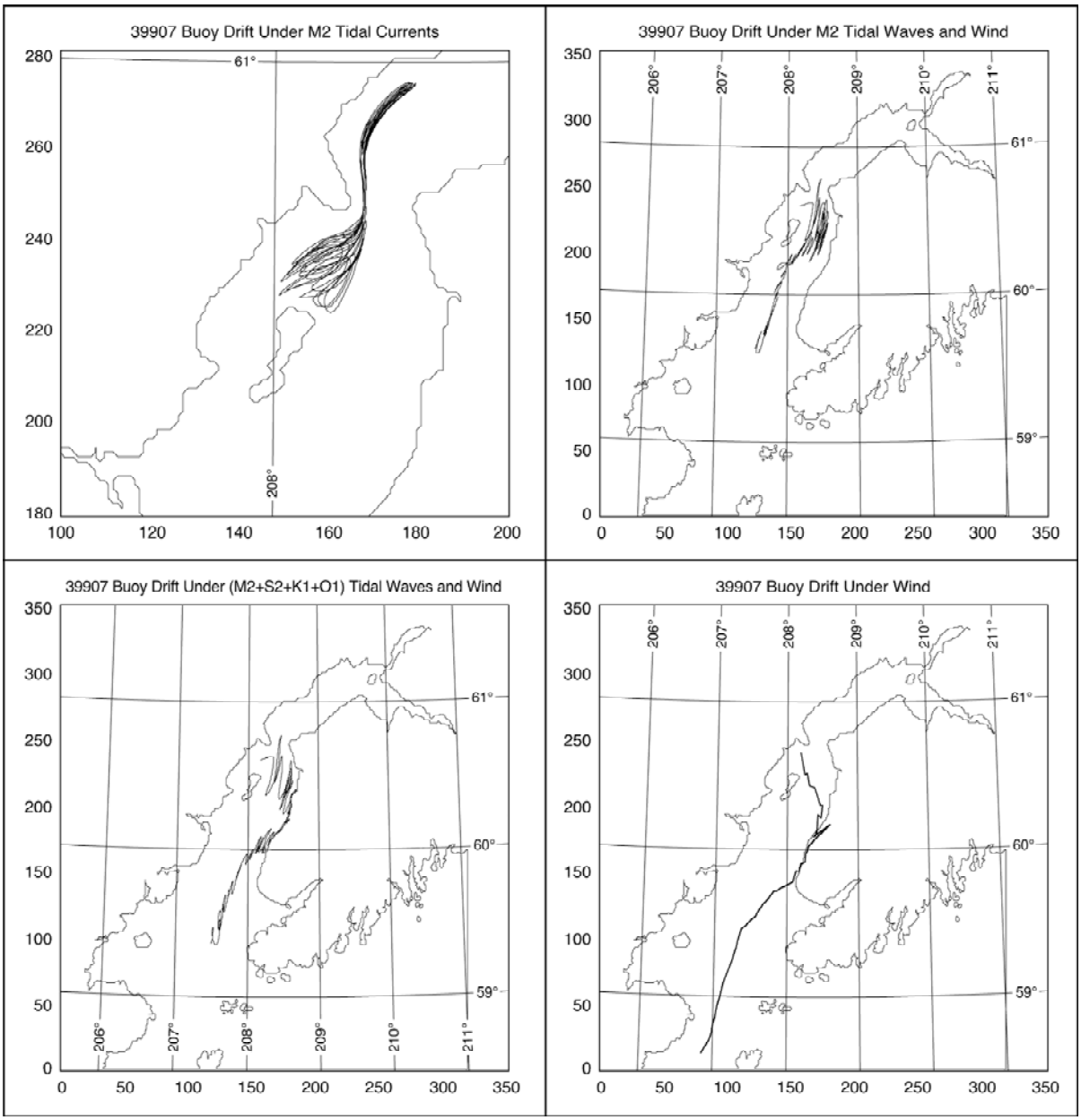

Figure 1. Trajectories of buoy 39907 simulated under various influences. Top left: M2 tidal currents only, top right: M2 tides and observed wind, bottom left: M2+S2+K1+O1 tides and observed wind, and bottom right: wind only for period 18–31 December 2003.

A substantial amount of time was dedicated to the collection of data for validation of our simulated tidal sea level and current constituents. Approximately 100 moorings deployed by the National Oceanic and Atmospheric Administration during a 1973–1975 circulatory survey of Cook Inlet were analyzed, digitized and used for model validation and calibration purposes.

Drifting buoy data were transferred in model coordinates in order to be compared with model results and used for model validation and calibration.

Modeling and Model Validation

We used our 2-D tidal model of Cook Inlet with a spatial resolution of 1 km to simulate eight major tidal waves in this region (five semidiurnal and three diurnal—these are waves for which we obtained boundary conditions from satellite-based archives of tidal constituents for the Gulf of Alaska and northern Pacific Ocean). Model results presenting tidal elevations and phases of four major waves are in Figures 2, 3, 4 and 5. Figures 6, 7, 8, 9, 10, 11, 12 and 13 show errors in tidal current (differences between observed and simulated data). In general, simulated current velocities are larger than the observed, but the direction of predicted currents coincides very well with observations. A similar conclusion could be drawn about observed and simulated constituents for sea level elevations (see Tables 1 and 2 where model validation results [observed/simulated] for semidiurnal and diurnal tidal sea level elevation constituents are shown.) Simulated tidal elevations are larger than those observed (except Anchorage), but the phase of wave propagation is in better agreement with observations.

Table 1. Observed/simulated amplitude and phase for semidiurnal constituents M2, S2, N2 and K2.

Station	M2 Tidal Wave		S2 Tidal Wave		N2 Tidal Wave		K2 Tidal Wave	
	Amplitude cm	Phase degree	Amplitude cm	Phase degree	Amplitude cm	Phase degree	Amplitude cm	Phase degree
Nikiski	251/292	030/039	087/105	062/072	049/050	359/017	025/017	054/076
Seldovia	223/265	324/339	082/088	359/007	047/042	297/304	023/019	353/349
Anchorage	353/287	108/109	100/148	150/150	060/098	082/085	027/048	142/151

Table 2. Observed/simulated amplitude and phase for diurnal constituents.

Station	O1 Tidal Wave		K1 Tidal Wave		Q1 Tidal Wave	
	Amplitude cm	Phase degree	Amplitude cm	Phase degree	Amplitude cm	Phase degree
Nikiski	069/089	307/291	039/039	291/255	006/009	290/249
Seldovia	056/065	279/270	034/028	263/246	006/007	258/242
Anchorage	069/112	341/299	039/047	322/268	006/010	331/257

In order to simulate 3-D tidal currents driven by tides, river runoff, and winds we are going to employ a 3-D finite volume model developed by Changsheng Chen from the University of Massachusetts Dartmouth [2003]. A new model grid is shown in Figure 14. This grid has a resolution of approximately 13 km along the southern and eastern boundaries of the model domain and approximately 162 m in the shallow coastal regions. We expect that this model will allow us to increase the accuracy of our simulations. We expect the first results by January 2005 and they will be presented in the 2005 quarterly report.

Figure 1 shows the results of simulation of drifting buoy 32097 motion under the influence of different forcing (tidal currents, winds, and a combination of tidal currents and winds). One sees that in many cases wind forcing leads to a significant change in buoy motion. Wind and tidal forcing results in numerous loops in buoy trajectories.

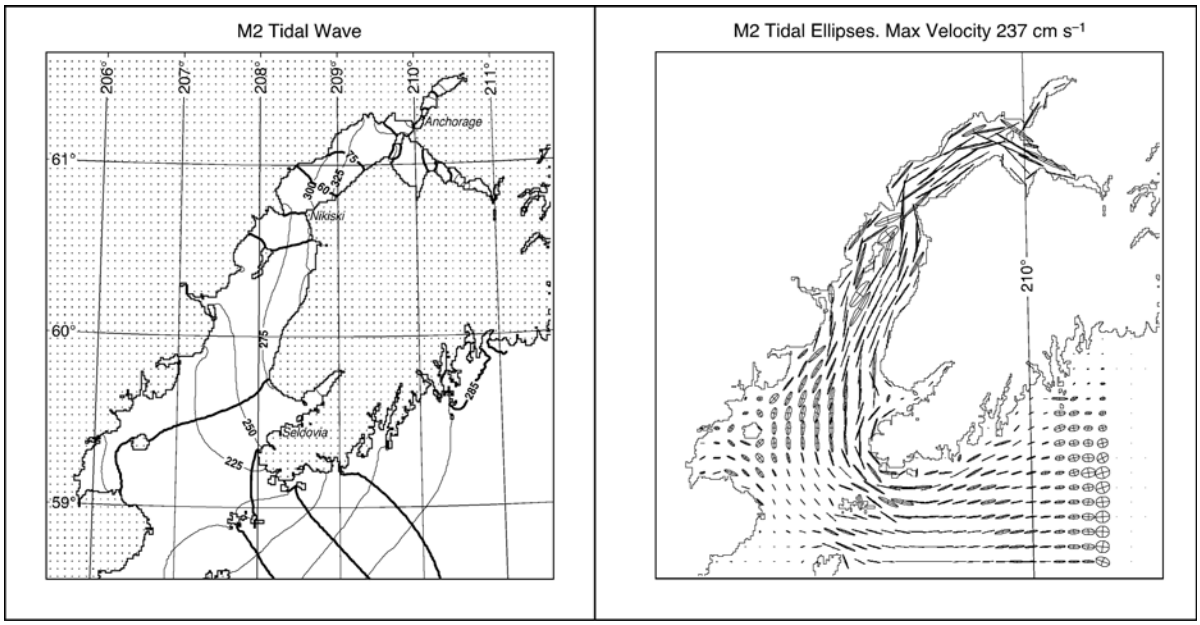

Figure 2. Left: Computed amplitude (in centimeters, thin lines) and phase (in degrees, thick lines) of surface elevation for the semidiurnal constituent M2. Right: Computed ellipses of the M2 tidal wave.

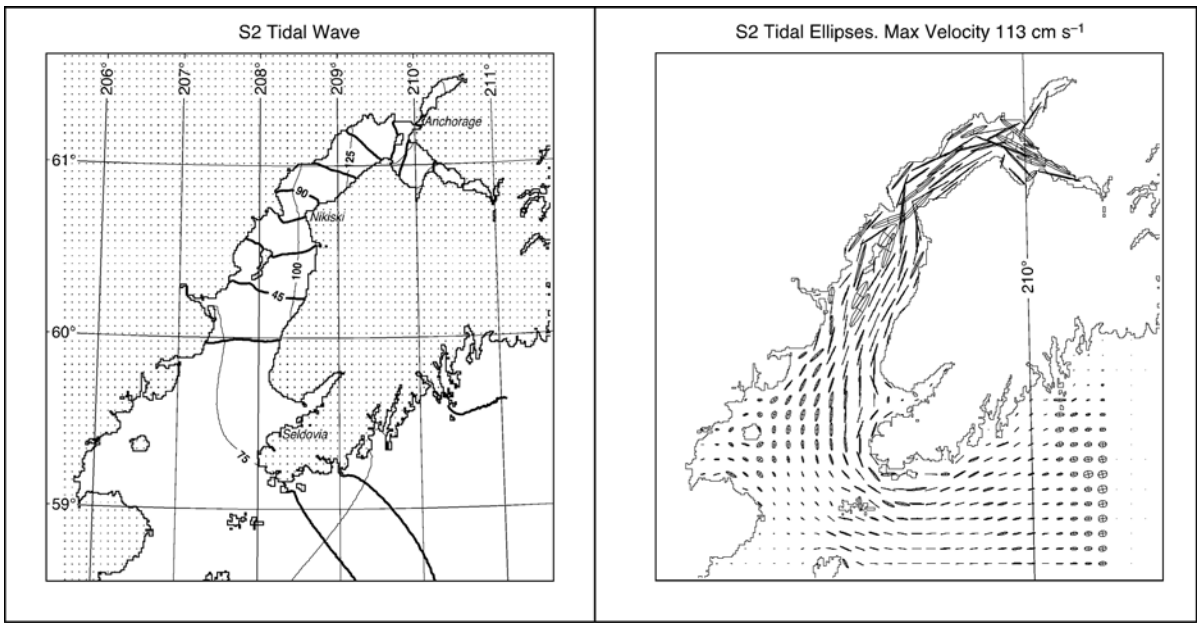

Figure 3. Left: Computed amplitude (in centimeters, thin lines) and phase (in degrees, thick lines) of surface elevation for the semidiurnal constituent S2. Right: Computed ellipses of the S2 tidal wave.

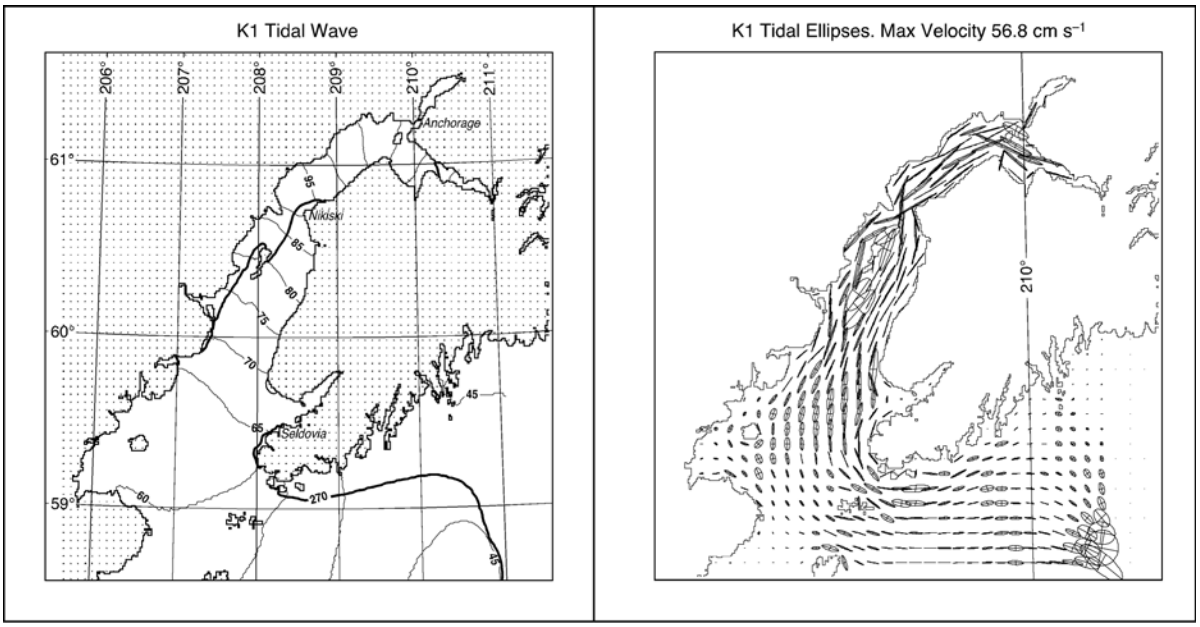

Figure 4. Left: Computed amplitude (in centimeters, thin lines) and phase (in degrees, thick lines) of surface elevation for the semidiurnal constituent K1. Right: Computed ellipses of the K1 tidal wave.

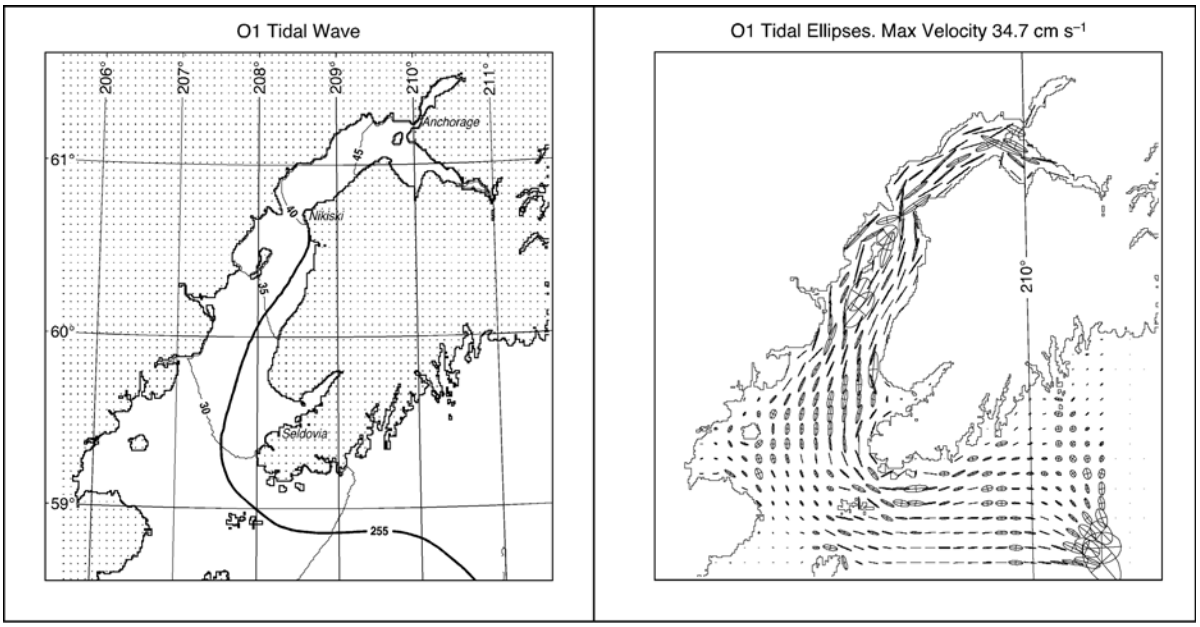

Figure 5. Computed amplitude (in centimeters, thin line) and phase (in degrees, thick line) of surface elevation for the diurnal constituent O1.

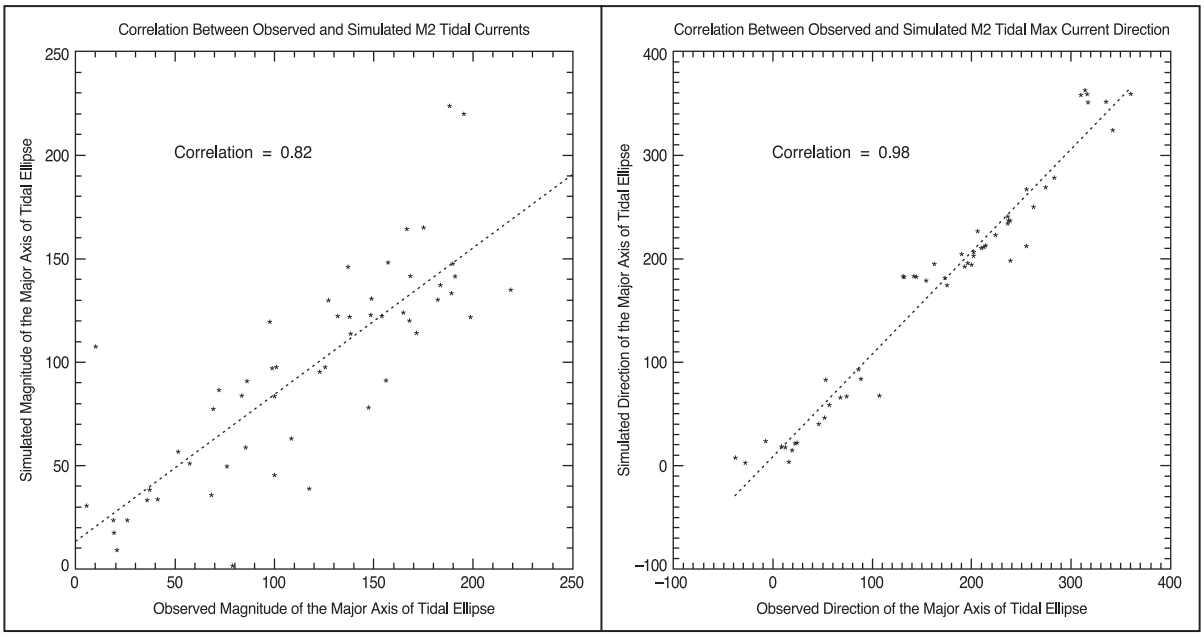

Figure 6. Left: Correlation between observed and computed M2 tidal velocities representing major axis of tidal ellipse (cm s^{-1}). Right: Correlation between observed and computed directions (degrees) of major axis of M2 tidal ellipses.

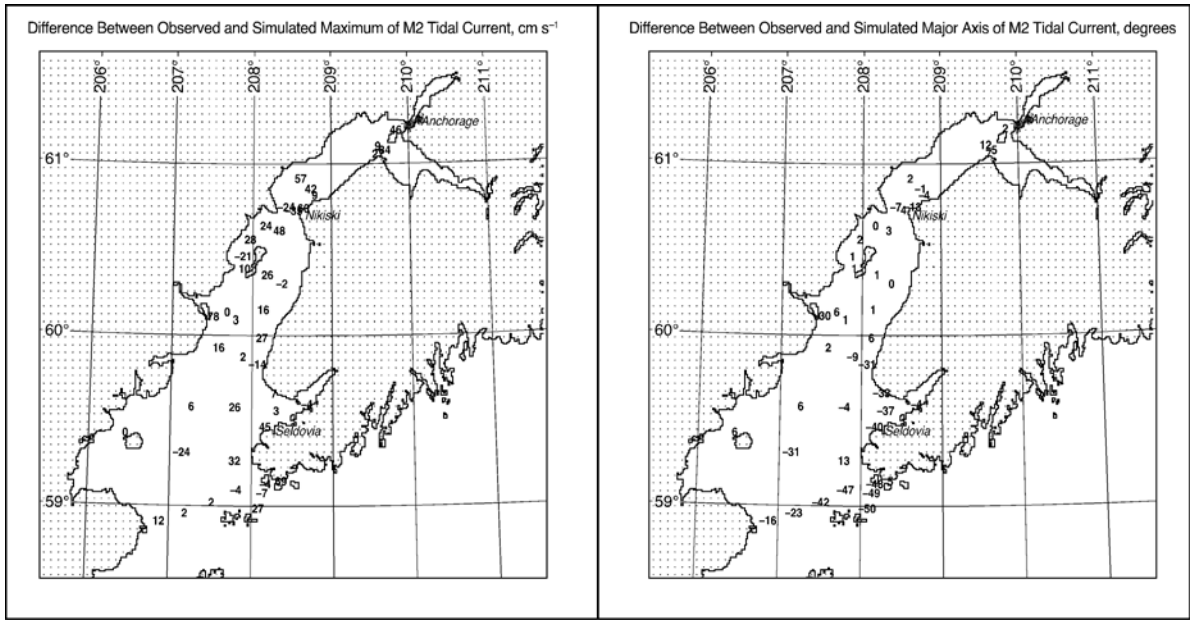

Figure 7. Left: Difference (cm s^{-1}) between observed and simulated M2 tidal velocities representing major axis of tidal ellipses. Right: Difference (degrees) between observed and simulated directions of major M2 tidal ellipses.

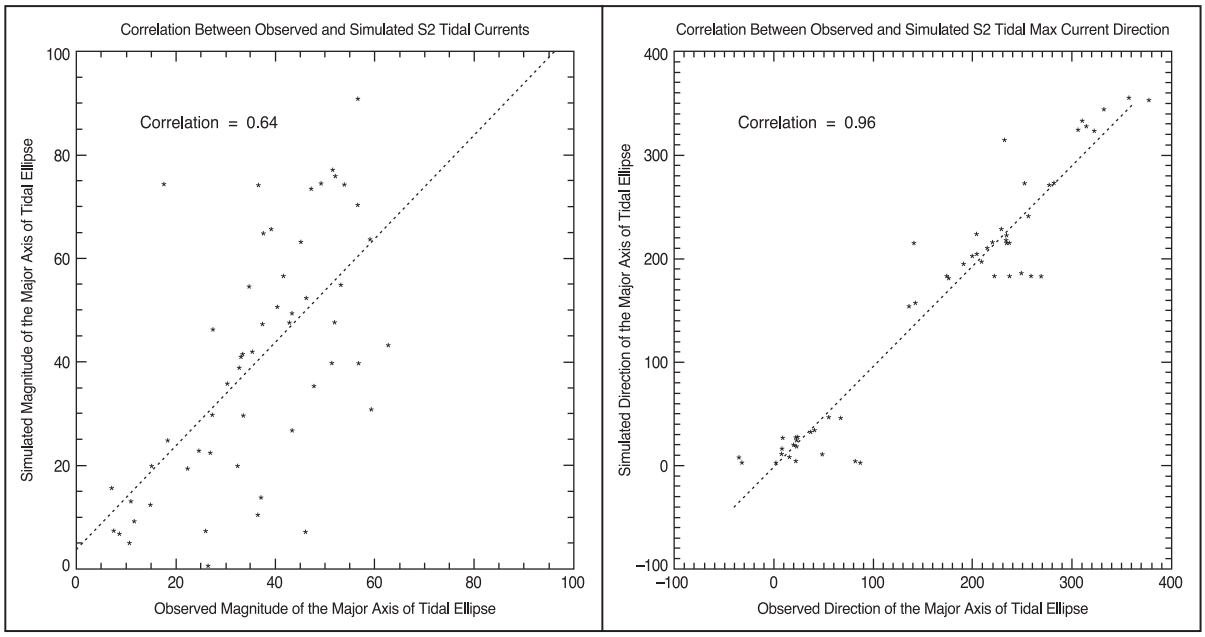

Figure 8. Left: Correlation between observed and computed S2 tidal velocities representing major axis of tidal ellipse (cm s^{-1}). Right: Correlation between observed and computed directions (degrees) of major axis of S2 tidal ellipses.

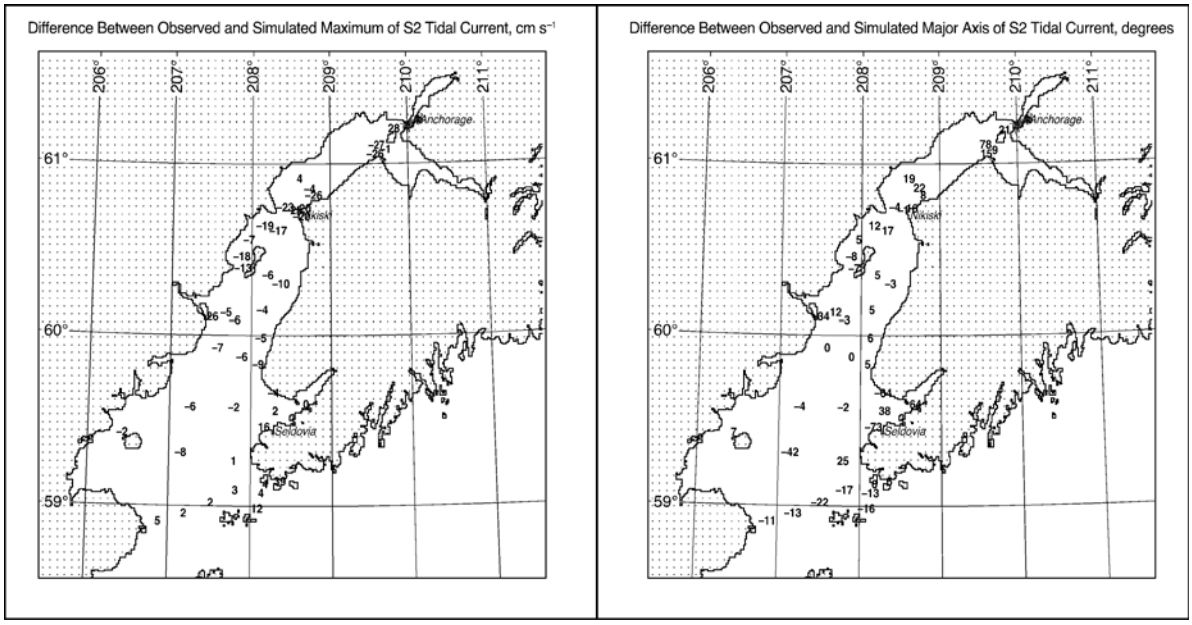

Figure 9. Left: Difference (cm s^{-1}) between observed and simulated S2 tidal velocities representing major axis of tidal ellipses. Right: Difference (degrees) between observed and simulated directions of major S2 tidal ellipses.

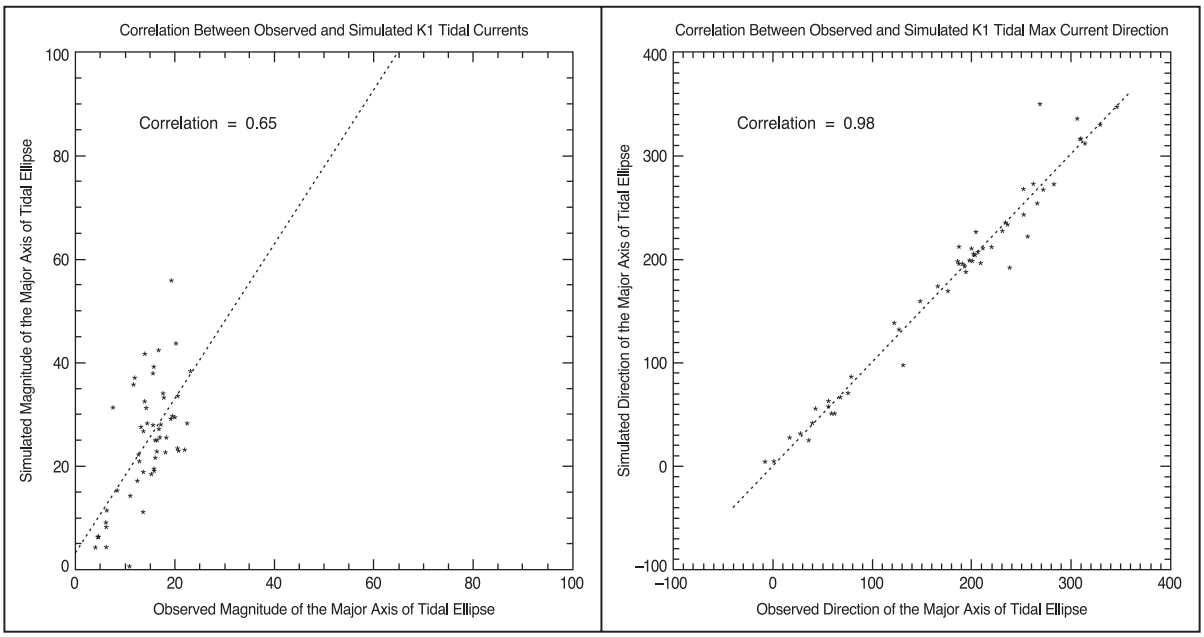

Figure 10. Left: Correlation between observed and computed K1 tidal velocities representing major axis of tidal ellipse (cm s^{-1}). Right: Correlation between observed and computed directions (degrees) of major axis of K1 tidal ellipses.

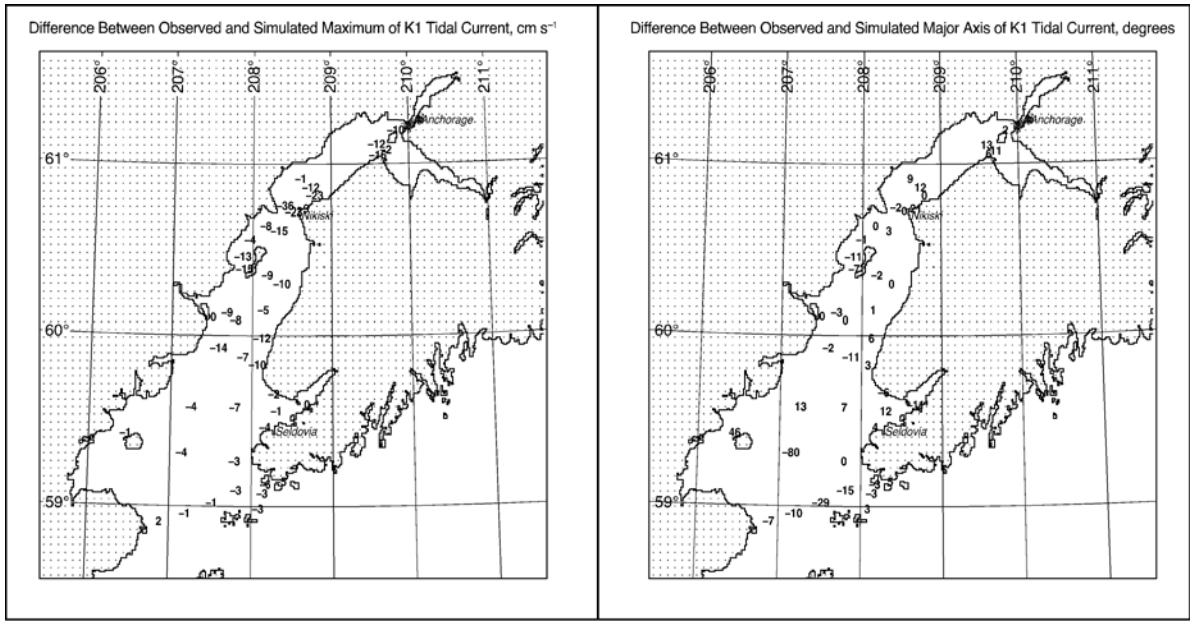

Figure 11. Left: Difference (cm s^{-1}) between observed and simulated K1 tidal velocities representing major axis of tidal ellipses. Right: Difference (degrees) between observed and simulated directions of major K1 tidal ellipses.

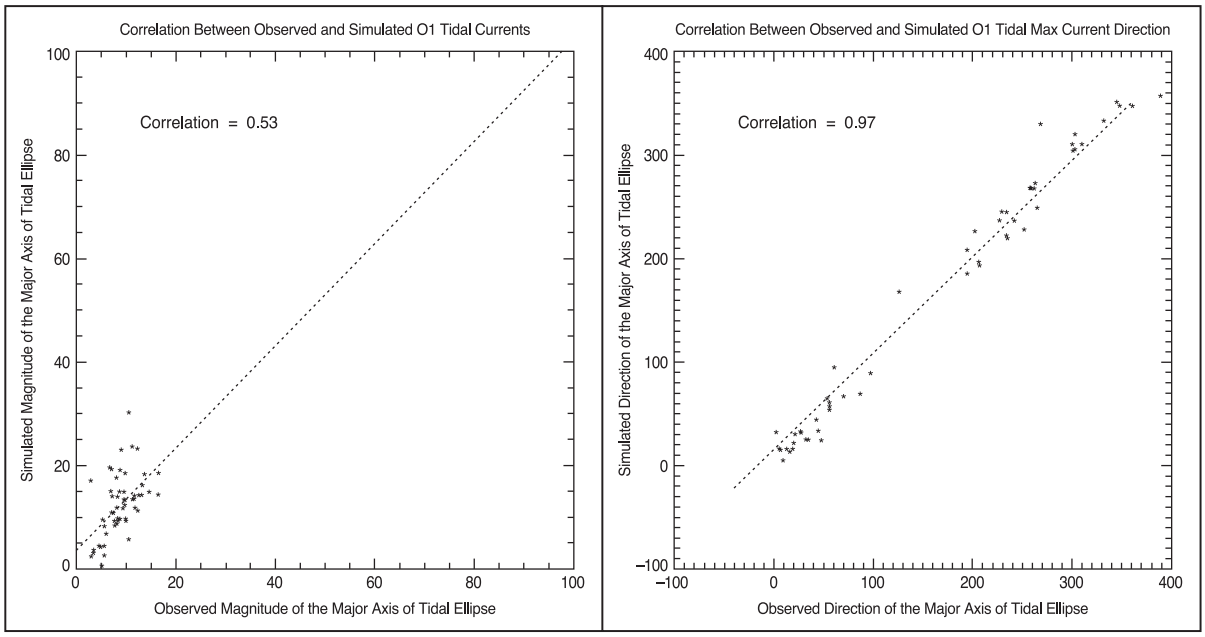

Figure 12. Left: Correlation between observed and computed O1 tidal velocities representing major axis of tidal ellipse (cm s^{-1}). Right: Correlation between observed and computed directions (degrees) of major axis of)1 tidal ellipses.

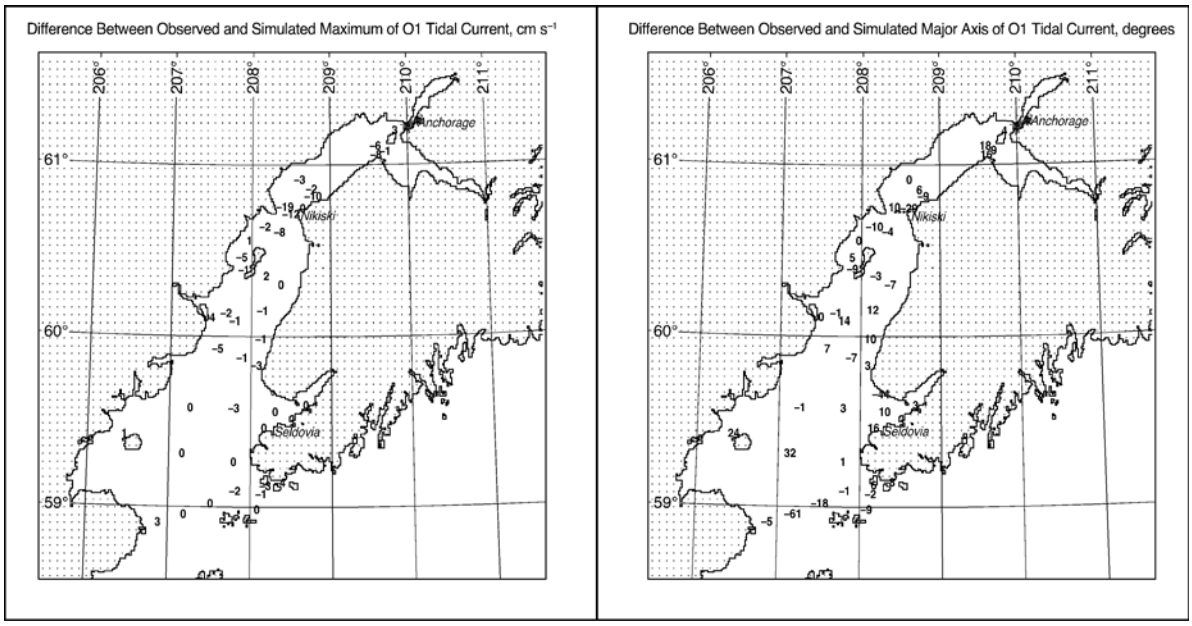

Figure 13. Left: Difference (cm s^{-1}) between observed and simulated O1 tidal velocities representing major axis of tidal ellipses. Right: Difference (degrees) between observed and simulated directions of major O1 tidal ellipses.

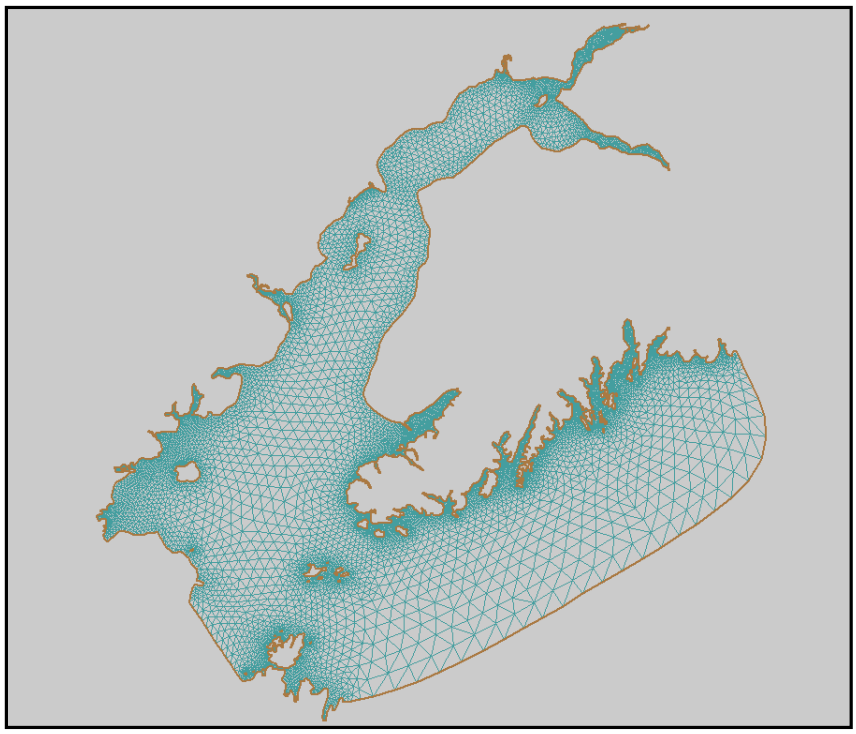

Figure 14. 3-D model grid covering Cook Inlet region with a spatial resolution from 13 km along open boundaries and up to 162 m in the shallow coastal regions.

Buoys

More than 20 drifting buoys have been deployed in Cook Inlet by CISPRI (Cook Inlet Spill Prevention and Response, Inc.) and other personnel since this project began. Position and time data are relayed to the Argos satellite and emailed to Mark Johnson on a daily basis. Data are converted to decimal data and velocities are computed using centered differences. Despite checksum error detection of data relayed via Argos, some still show position jumps that do not appear real. For obvious position changes outside of Cook Inlet and vicinity, those data are ignored. We are still looking at smaller data jumps to determine the cause. We speculate that such small jumps may be surprisingly large Cook Inlet velocities, or buoys that were snagged by local fisherman. The data discussed in this report include only those without any data jumps that have been fully quality checked for accuracy and trajectories that are visually “reasonable”.

Most buoys were deployed in the area south of the Forelands and northeast of Kalgin Island. All buoys in year one were equipped with a drogue tethered to follow the water at depths between 5 and 10 m. In year two, the drogue depth was made shallower to track water at depths between 3 and 5 m. No obvious differences between trajectories for different drogue depths have been noted. Within Cook Inlet, the area covered by buoy trajectories is excellent (Figure 15).

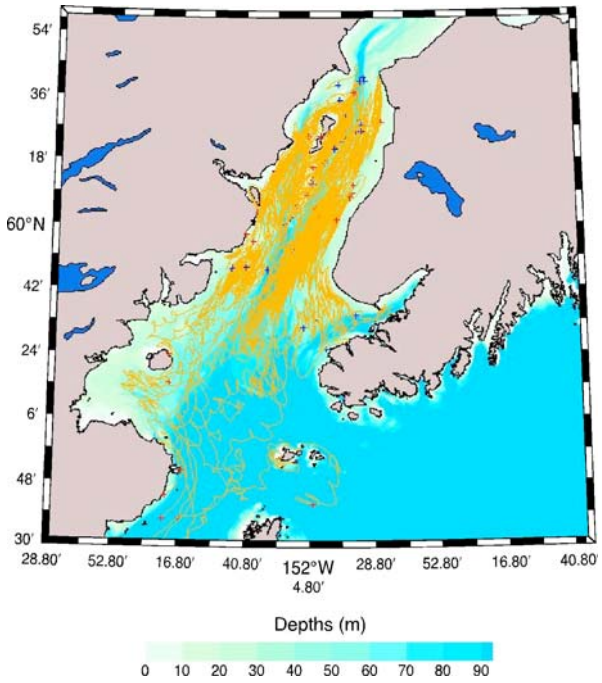

Figure 15. All buoy trajectories to date in lower Cook Inlet. First and last day of trajectory shown by the blue (start) and red (end) "plus" signs.

To date, only a single buoy failed completely upon deployment, and it was replaced at no cost to this project. All other buoys operated until grounding along the shore of Cook Inlet, or exiting to Shelikof Strait and into the northern Gulf of Alaska. Several grounded buoys have been recovered and redeployed by CISPRI and other personnel.

The "clean" velocity data were converted to kinetic energy (KE) and are characterized by a histogram (Figure 16). All data were then gridded into a lat–lon (latitude–longitude) grid and contours of the KE were made (Figures 17 and 18).

The highest KE values are east of Kalgin Island, along the middle rip. They appear to align along the steep bathymetric slope.

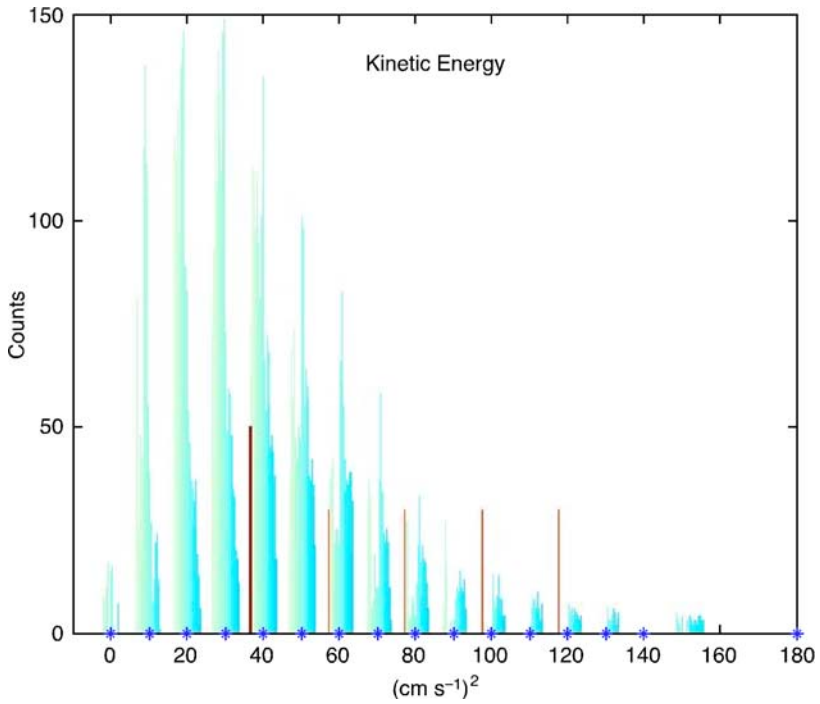

Figure 16. Histogram of the buoy KE. The mean falls at the heavy red line, and the thinner red lines mark standard deviation increments above the mean. The values above 100 cm s^{-1} are contoured in Figures 17 and 18.

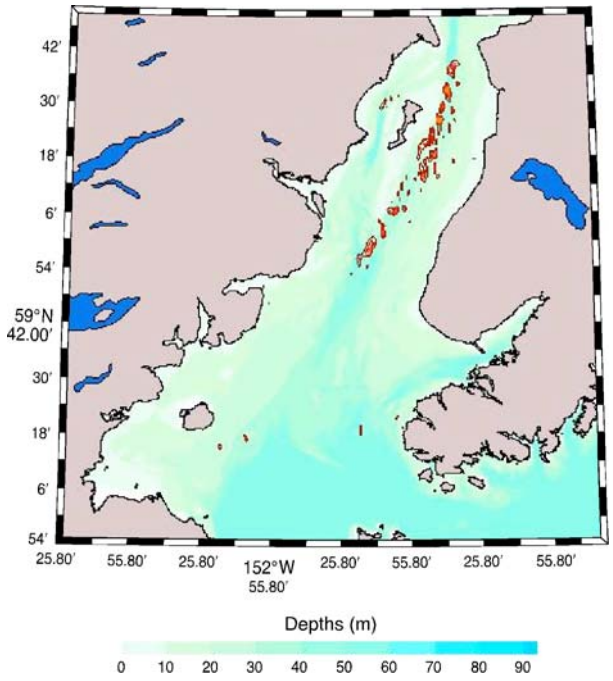

Figure 17. Kinetic energy contours. Only data valued above 100 cm s^{-1} have been contoured. The high values of KE align with the bathymetry.

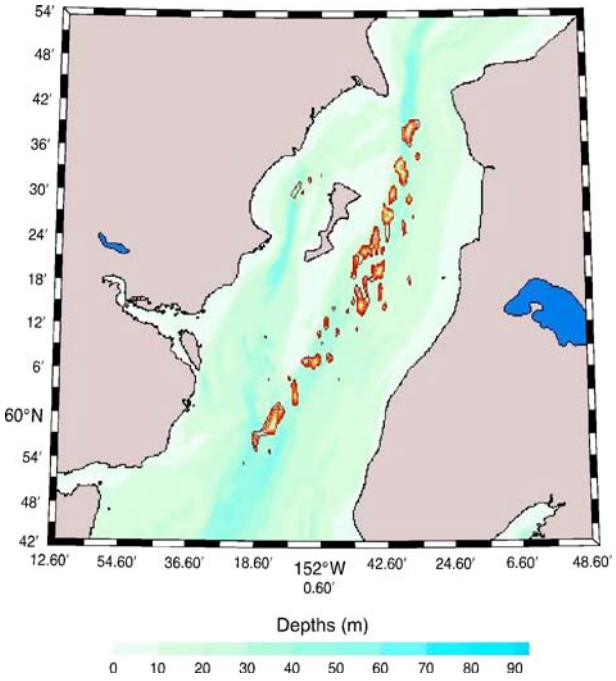

Figure 18. Kinetic energy as in Figure 16 showing close-up around Kalgin Island.

Satellite Imagery for Front Identification

Fronts are typically associated with convergence zones. In Cook Inlet, drifting sea ice tends to collect along tide rip fronts, thereby providing strong visual signatures for frontal locations. Radar backscatter (brightness) from sea ice is typically larger than from open water. As a consequence, the ice edge (frontal) location exhibits a relatively large spatial gradient in radar backscatter. Spatial brightness gradients are computed from SAR (synthetic aperature radar) imagery and the locations of the largest gradients (assumed to represent frontal locations) are written to file.

Preliminary Results

Figure 19 shows frontal locations identified from nine SAR images acquired in February 2002, December 2003, January 2004, and February 2004. The color coding corresponds to the difference between the image acquisition time and the time of high tide at the mouth of the Kenai River. The greatest number of frontal features occurs in a zone extending southwestward from near the West Foreland to along and beyond the eastern shore of Kalgin Island. This zone roughly corresponds to the location of what is locally known as the West Rip. Another somewhat less prominent assemblage of frontal features begins near the southwest end of Kalgin Island and extends southwestward along the western side of Cook Inlet. The area between these two frontal zones south of Kalgin Island is relatively shallow. The Middle Rip, which lies midway between Kalgin Island and the east side of Cook Inlet, is not well-defined in the plot.

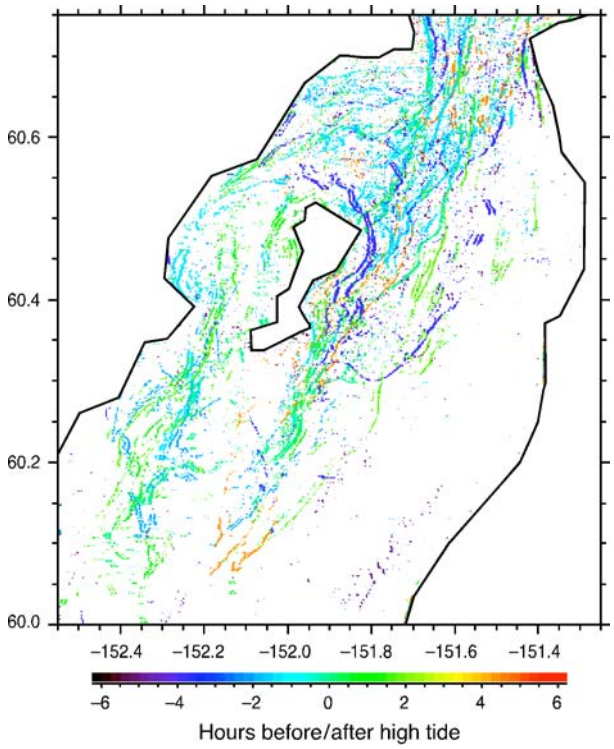

Figure 19. Front locations from SAR Imagery. Note differences with the locations of high KE from Figures 16 and 17.

Upcoming Work

In 2005, model results will be validated using buoy data. Another task for 2005 research is the seasonal variability of Cook Inlet dynamics under the influence of all possible external forcing (wind, river runoff, tides, and residual tidal circulation). Additional SAR images will be acquired and analyzed, statistical analyses of frontal locations will be undertaken, and SAR results will be integrated with buoy trajectory data.

References

Chen, C., H. Liu and R.C. Beardsley. 2003. An unstructured grid, finite-volume, three-dimensional, primitive equations ocean model: Application to coastal ocean and estuaries. J. Atmos. Ocean. Tech. 20(1):159–186.

CRREL (Cold Regions Research and Engineering Laboratory). 1976. Baseline data on the oceanography of Cook Inlet, Alaska, 1976. Report 76-25 CRREL, Hanover, New Hampshire,

Foraging Ecology of Common Ravens (*Corvus corax*) on Alaska's Coastal Plain

Abby N. Powell <ffanp@uaf.edu>
Stacia A. Backensto <ftsab@uaf.edu>

Institute of Arctic Biology
University of Alaska Fairbanks
Fairbanks, AK 99775–7000

Task Order 85294

Abstract

*Populations of common ravens (*Corvus corax*) on the North Slope of Alaska appear to be increasing where anthropogenic resources are available. The oil fields provide abundant anthropogenic resources in terms of infrastructure and food sources. Raven numbers are high in the oil fields compared to other areas of human habitation on the North Slope. Ravens use the infrastructure for nesting and foraging on human food. To assess the potential impact ravens may have as predators of tundra-nesting birds we captured 10 breeding adult ravens, attached VHF and satellite transmitters, and tracked their foraging movements during the breeding season. We collected pellet samples and prey remains from nest areas, as well as conducting nest observations to evaluate food items brought to the nest. We marked 28 fledglings to determine timing of dispersal and juvenile survival. To further investigate seasonal movements, dispersal, and anthropogenic resource use we engaged the community of oil field personnel in an observation program targeting marked birds. Our preliminary findings suggest that breeding adults maintain 1–2-km territories around facilities until late in the chick stage and gradually increase until fledge. Adults shift use of food sources based on availability throughout the breeding season. Juveniles remain with adults and siblings for a period of >4 weeks after fledge. We emphasize the preliminary nature of the results and further analyses will be necessary, as well as additional data collection for breeding adults and juveniles in the coming years, to fully understand the relationship between ravens and human activity on the North Slope.*

Introduction

Common raven (*Corvus corax*) populations have increased in many parts of their geographic range [Boarman and Heinrich 1999]. In some areas of the U.S. it is common for high numbers of ravens to be found in areas where anthropogenic resources (structures and food) are abundant. These subsidies are often localized and spatial patterns of hyper-predation and spill-over predation by ravens on local prey species assemblages can occur in these areas [Kristan and Boarman 2003]. In addition, anthropogenic subsidies influence raven demography [Restani et al. 2001; Roth et al. 2004; Webb et al. 2004]. In some areas outside of Alaska, breeding ravens establish core areas of space use around their nest sites near these food subsidies [Roth et al. 2004]. Juvenile survival is also enhanced by nest proximity to anthropogenic resources [Webb et al. 2004].

On the North Slope of Alaska where human activities are concentrated, such as the oil fields, raven numbers have increased over the last 30 years [National Audubon Society; Day 1998]. The role of the common raven as a scavenger and predator on the North Slope is not well understood. There is a great deal of speculation that where ravens occur on the slope they exert significant predation pressure on tundra-nesting birds. In the case of the oil fields, where it appears that ravens occur in higher numbers and densities than elsewhere, it is important and necessary to evaluate how they use the available anthropogenic resources in areas where human activity is high (e.g., Kuparuk and Prudhoe Bay oil fields), moderate (e.g., villages of Barrow and Nuiqsut) and low (National Petroleum Reserve–Alaska [NPR-A] Colville River Special Area).

In 2004 we established a marked population of ravens in the Kuparuk and Prudhoe Bay oil fields to investigate how anthropogenic resources are influencing raven demography and movements. We engaged the oil field community of personnel to participate in sharing information about marked ravens during the summer of 2004. This is the first of several years of field work for this study.

Methods

Study area

The oil fields of the North Slope of Alaska are flanked by two major rivers: the Colville River to the west and the Sagavanirktok to the east, and are characterized by extensive wetlands and tundra. Temperatures range between –90 °C and 25 °C, with an annual average precipitation of 13–18 cm. The ground remains frozen and snow covered for 8–9 months each year. Our work occurred throughout the two largest producing oil fields on the North Slope: Kuparuk (104,514 ha) operated by ConocoPhillips Alaska, Inc. and Prudhoe Bay (99,103 ha) operated by BP Exploration (Alaska) Inc. We worked across the entire field of Kuparuk and in both the Eastern and Western Operating Areas of Prudhoe Bay. Infrastructure consists primarily of gravel roads, pads, pipelines, production facilities, and camps where personnel are housed and fed.

Raven foraging movements

Adult ravens were captured near their nests primarily during incubation. One member from each breeding pair was captured. We trapped 10 adult breeding ravens from 21 April to 1 June 2004 using remote control bownets, drop-in traps, and leg-hold traps (under UAF Institutional Animal Care and Use Committee Protocol Number 02-59). Leg-hold traps were our most successful method, catching 8 of the 10 ravens. Nine adults were fit with 22-g, 1140 VHF transmitters (www.atstrack.com) and 1 adult was fit with a 24-g, bird-borne satellite transmitter (www.northstarts.com). Transmitters were attached with a permanent, Teflon ribbon backpack style harness and an aluminum j-clip fastener (pers. comm., Mark Pavelka, U.S. Fish and Wildlife Service [USFWS], Carlsbad, CA). After transmitter attachment a colored vinyl, patagial-wing tag with 2 alpha codes was fixed to the patagium area of the wing using a hog ear tag fastener (pers. comm., Mark Pavelka). All adults received a USFWS band on the left leg and a series of morphological measurements was collected (wing chord, culmen, tarsus length, tarsus width, bill depth). In some cases not all morphological measurements were obtained, depending on the length of handling time and apparent signs of stress. Blood samples were taken at the end of the handling period if the individual appeared to be in stable condition. Three to five drops of blood were drawn from the brachial vein, placed in buffer solution, and stored at 25 °C. Birds were released at the capture site and monitored twice within 12 h of capture to ensure that they would return to nests and normal flight behavior.

We began radio tracking these individuals from 3 June to 17 July 2004. Tracking sessions were conducted between 0600 and 2000 depending on the time each transmitter was on. We attempted to ensure that each bird had equal coverage during this time period. Tracking sessions consisted of locating the individual's signal first and then visually locating the bird. Once the bird was located we attempted to observe it without influencing its behavior for a period of 30 min, and recorded behavior during this interval. Behavioral observations were standardized for all observers and time spent displaying a particular behavior was noted for the start and end of each behavior category. We recorded GPS locations for foraging behaviors when possible, otherwise we estimated location with distance and bearing from a structure or GPS point on a road when necessary. Currently, locations are being entered into a geographic information system (ArcView 3.3) and will be analyzed with the Animal Movement analysis extension [Hooge and Eichenlaub 2000].

Diet composition

Pellets were collected from a 10-m radius around all nest sites ($n > 60$) and heavily used perch areas ($n > 30$) from 1 June to 17 July. Pellets were collected only after the area around the nest had been cleared of old pellets. New prey remains were also collected during this time at the nest area ($n > 40$). Nest observations were conducted for a period of 2 h in the morning and afternoon at a sub-sample of nests ($n = 8$) to identify what food items were brought back to the nest.

Productivity and nest success

From 21 April to 10 June we surveyed for raven nests using a combination of local knowledge and road surveys. The local knowledge assessment involved attending safety meetings (all supervisory field production personnel attend these meetings) for all of the production facilities at Kuparuk and most facilities at Prudhoe Bay. At these meetings production staff informed us where ravens had nested in the past, where there were active nests, and where areas of raven activity were. We subsequently investigated these areas to locate/confirm nest sites. Additionally we surveyed by road all of Kuparuk and Prudhoe Bay's Eastern and Western Operating Areas.

We described each nest's characteristics, such as height above ground, aspect, materials and substrate, as well as building features within the immediate area of the nest we thought might be important for site selection. We checked for the presence of eggs or chicks using a mirror and extension pole. Nests were then monitored every 5–7 d throughout the nest period until chicks fledged or nests failed. Not all nests could be accessed via mirror and pole. In these cases we assumed birds were on eggs until we observed chick-feeding behavior. In some situations facility personnel provided information as to when nest building and/or incubation began.

Juvenile survival/dispersal

We captured fledglings within 1–3 d of leaving the nest. Each individual chick received a USFWS band on the left leg and a white patagial tag with a 2-letter alpha code—on the left wing indicating a Prudhoe Bay origin and on the right wing for Kuparuk origin. Morphological measurements (same as the adults with the addition of the gape) and blood samples were also taken from these individuals. Fledglings were released near their nest and monitored twice within 12 h. Locations of juveniles were recorded during scheduled tracking sessions, and opportunistically while in the field from fledge date through 18 July. From 13 to 16 August, juvenile locations were recorded once again to determine if departure from the natal territory and adults had occurred. One additional juvenile dispersal assessment will occur at the end of September 2004.

Local knowledge investigation

Initial interaction with facility/production personnel occurred at the safety meetings (20 April–20 May). During these meetings Stacia Backensto gave a short informal presentation on the research project and solicited information about nesting sites. Shortly thereafter posters were distributed to all facilities summarizing the marking program and requesting sightings of marked birds from personnel in the field. Throughout the field season Stacia Backensto identified several key informants for future interviews focused on raven history, behavior, and perceptions. Most of the informants have been approached and expressed interest in participation.

Results

Raven movements

At Kuparuk, we tracked 3 (2 female, 1 male) individuals regularly, and at Prudhoe Bay we tracked 5 (2 female, 3 male) individuals regularly, using VHF telemetry in both locations (Table 1). Female "OE" was and continues to be tracked with a satellite transmitter. One individual, "OX", was tracked irregularly due to his lack of a breeding territory. Breeding ravens in the oil fields tended to stay close to the nest during incubation and brood rearing. Most of the locations for our VHF birds fall within 500 m–2 km of the nest site. Toward the end of brood rearing and during fledging this distance gradually increased. When fledglings were fully flight capable we located families >2 km from the nest site. Though the family groups are highly mobile at this time we found them returning to roost at the nest site facility or an adjacent facility. We will continue to analyze movement data in more detail over the next several months.

Table 1. Number of sites for 3 types of location input for each raven tracked at Kuparuk and Prudhoe Bay, 3 June–17 July 2004. GPS indicates latitude/longitude recordings; Estimated locations correspond to visual sightings with an estimated position from a known point; and Personnel Sightings refer to e-mail, phone, or direct notification of sightings.

Individual P-tag		Sex	GPS	Estimated	Personnel Sightings
AZ	Prudhoe	F	21	23	> 5
CZ	Prudhoe	M	2	28	> 2
EZ	Prudhoe	M	11	27	> 2
HZ	Prudhoe	F	5	26	> 7
JZ	Prudhoe	M	17	11	> 5
OZ	Kuparuk	F	9	28	> 5
JA	Kuparuk	M	17	20	> 4
EA	Kuparuk	F	13	21	> 4
OE	Kuparuk	F	>100	10	>10
OX	Kuparuk	?	2	10	> 2

Foraging observations

Anthropogenic food sources appear to be important to ravens when the tundra is snow covered in late spring/early summer. The birds were active scavengers at sites where human activity was high when obtaining this type of resource was likely. They also appeared to rely on cached food during this time. We found caches buried on the ground near nest sites and on the facility structures themselves. When the snow melted and tundra was exposed, before migrants returned and initiated nesting, we observed ravens hunting brown lemmings (*Lemmus trimuncronatus*) and collared lemmings (*Discrostonyx groenlandicus*). Ravens continued to hunt lemmings after geese, waterfowl, and shorebirds initiated nests in June; later we observed ravens carrying eggs. By the time we concluded our tracking season we observed ravens with various species of tundra-nesting bird chicks as well. Analyses of foraging observations and food items will continue during the coming months.

Diet contents

A thorough pellet analysis has not been completed at this time. Pellets and prey remains collected at the nest included egg shells, lemmings, bird remains, and anthropogenic food remains.

Productivity and nest success

Ravens in the oil fields layed 3–6 eggs in the early part of April and fledging occurred in mid- to late June (Table 2). Nests were attended by both parents; females appeared to do most of the incubating. Both parents were involved in brood rearing and they actively and aggressively defended their young when nests were approached. Nest characteristics have not been summarized at this time, but it appeared that most nests were 10 m above ground with 40–100% cover, and placed on human-made structures to minimize the effects of prevailing winds. Nests consisted primarily of industrial materials (welding rods, survey stakes, cable, electrical wire, pipe insulation fasteners, and various plastics).

Juvenile dispersal

Departure from the natal territory for juveniles began in early August (Table 3). Family groups maintained cohesion >4 weeks after fledge dates. In mid-August not all family groups had dissolved 8 weeks post-fledge. Juveniles learned to forage during this time. We observed family foraging arrays >2 km from nest sites during the end of our tracking period. In mid-August juveniles from 4 different nests at Prudhoe Bay were observed at the North Slope Borough landfill without parents or siblings. This suggests departure from natal territory may have occurred. Additionally, we have recently received sighting reports of juveniles having moved >40 km from natal territories.

Table 2. Final status of all nests found and actively monitored at Kuparuk and Prudhoe Bay in 2004. Nests are referenced by facility where they were located.

	Date Found	End Date	Chicks	Young Fledged
Kuparuk				
CPF1	21 Apr 04	19 Jun 04	4	4
CPF2	20 Apr 04	14 Jun 04	6	5
CPF3	20 Apr 04	21 May 04	0	0
2T	21 Apr 04	19 Jun 04	2	2
2P	1 May 04	13 Jul 04	2	2
Tarn Bridge	24 Apr 04	31 May04	failed	0
KCS	25 Apr 04	30 Apr 04	destroyed	0
Prudhoe Bay				
FS1	10 May 04	11 Jun 04	2	2
FS2	24 Apr 04	7 Jun 04	4	4
FS3	8 May 04	1 Jul 04	2	2
GC1	10 May 04	15 Jun 04	5	5
LPC	19 May 04	24 Jun 04	3	3
L5	20 May 04	22 Jun 04	4	4
M PAD	28 May 04	2 Jul 04	4	4
Deadhorse	1 Jun 04	21 Jun 04	4	4
DS16	8 May 04	21 Jun 04	5	5
Rig at North Star Logistics	10 Jun 04	14 Jun 04	6	6

Table 3. Number of tagged fledglings from monitored nests at Kuparuk and Prudhoe Bay for 2004. The last column represents how many young were found on the last tracking session, 16 August 2004.

	No. Fledged	No. Tagged	No. Resighted
Kuparuk			
CPF1	4	0	4
CPF2	5	4	3
2T	2	2	2
2P	2	2	2
Prudhoe Bay			
FS1	2	2	2
FS2	4	4	1
FS3	2	1	1
GC1	5	4	0
LPC	3	1	0
L5	4	3	0
M PAD	4	2	1
Deadhorse	4	1	1
DS16	5	2	1
Rig at North Star Logistics	6	6	1

Discussion

Demographic parameters and behaviors of ravens are necessary to understand their role as subsidized predators and to explain the apparent population increase in the arctic oil fields of Alaska. Our preliminary data reveal that the ravens are as opportunistic and highly adaptable in their environment as they are elsewhere in their geographic range. Their behavioral plasticity allows them to exploit the unique features of this industrial environment year round. Facility structures provide nesting substrates, heat, shelter, food caches, and the possibility of anthropogenic food subsidies.

Ravens established breeding territories approximately 1–2 km in size and actively defended these territories against intruding ravens [Boarman and Heinrich 1999; Roth et al. 2004]. Many of these territories include one major production facility and several smaller ones. In addition to acquiring anthropogenic food subsidies, ravens actively hunted small mammals, and removed eggs and chicks from waterfowl, geese, and shorebird nests. At this time we do not understand the degree to which they select one over the other, but we have observed them with all of these prey items. We suspect that within their breeding territories predation pressure exerted by ravens on other species is higher than outside of these territorial boundaries during egg laying, incubation, and the first 3–4 weeks of brood rearing. After this time, when chicks are fully feathered, foraging movements of adults increased in duration and distance. Shortly after fledging, the territories expanded and family foraging activities occured over a much wider area, >2 km. In 2004 we collected limited data on dispersal past two weeks of fledging, but believe this time period is important for understanding survival, recruitment and emigration from the local population.

Our field investigations, though valuable, can bridge only some of our knowledge gaps in how ravens began and continue to exploit the infrastructure of the oil fields. A wealth of information about their history and behavior resides in the community of people spending 50% of their lives living in and working at these facilities. A considerable body of literature is growing on how indigenous and rural people understand and relate to their landscape as well as how they identify and adapt to change in their environment [Krupnik and Jolly 2002; Fienup-Riordan 1990]. Cultural geographers discuss this type of understanding as “sense of place”. At Kuparuk and Prudhoe Bay many workers identify with the ecological surroundings and portray themselves to a certain extent as stewards of this area. These associations and meanings have often times been expressed through their feelings and thoughts about ravens. While working closely with many of these individuals during the 2004 field season we found they were keen observers and that a body of local knowledge of ravens exists. Though not typically identified as stakeholders in issues pertaining to resource management on the North Slope, oil field workers’ concerns about wildlife management and particularly raven management may illustrate how sense of place or land ethic applies in a large industrial setting. This presents a truly unique opportunity to further engage in an exchange of information with this group of people and document the relationship between industry personnel and ravens.

Future Field Plans

Breeding adult foraging movements

The 2005 field season will continue with tracking VHF adults from 2004 and trapping new breeding adults in the oil fields for satellite telemetry. Tracking methods for VHF birds will be slightly modified from 2004 based on preliminary data analysis to minimize potential tracking biases inherent in telemetry work. Additionally and most importantly we intend to cover a longer tracking period to further investigate resource use changes based on availability and season.

Analysis of 2004 telemetry data will include: home range estimation, activity pattern definition (foraging, caching, perching, etc.), prey characterization and quantification during foraging activities, and distance to multiple spatial and temporal levels of anthropogenic food resources. Additionally we hope to collaborate with the Wildlife Conservation Society where possible on predation patterns of tundra-nesting birds.

Breeding adult seasonal movements

In 2005 we plan to work with the Bureau of Land Management in NPR-A to capture adult breeding ravens in areas further away from concentrated human development and to fit them with satellite transmitters. The comparison with satellite data for breeding adults in the oil fields will enhance our understanding of how the use of anthropogenic resources varies between ravens that are closer to subsidies and ravens that are not.

Diet contents

In 2005 we will continue to collect pellets and prey remains from nest sites at Kuparuk and Prudhoe Bay, as well as within the NPR-A Colville River Special Area and the villages of Nuiqsut and Barrow.

Productivity and nest success

We will continue to locate and monitor all nests at Kuparuk and Prudhoe Bay in 2005.

Juvenile dispersal

We will continue to attempt to tag all juveniles from nest sites at Kuparuk and Prudhoe Bay in 2005. In addition, we will fit juveniles from a sub-sample of nests with VHF transmitters to monitor dispersal activities and events.

Local knowledge

Pending permission from ConocoPhillips Alaska, Inc. and BP Exploration (Alaska) Inc., we will conduct interviews with 10–15 willing oil field personnel on their knowledge of raven history, behavior, and perception of raven management in 2004/2005. Additionally, focus group meetings will be held at major facilities to document historical and current areas of raven use.

References

Boarman, W.I., and B. Heinrich. 1999. Common raven (*Corvus corax*), No. 476. *In* A. Poole and F. Gill [eds.], The Birds of North America, Volume 12. The Academy of Natural Sciences, Philadelphia and The American Ornithologists' Union, Washington, D.C., 32 p.

Day, Robert H. 1998. Predator populations and predation intensity on tundra-nesting birds in relation to human development. Unpub. rep. prepared for U.S. Fish and Wildlife Service, Fairbanks by ABR, Inc., Fairbanks, 106 p.

Fienup-Riordan, A. 1990. Original ecologists?: The relationship between Yup′ik Eskimos and animals, p. 167–191. *In* A. Fienup-Riordan [auth.], Eskimo Essays: Yup′ik Lives and How We See Them. Rutgers University Press, New Brunswick, NJ.

Hooge, P.N., and B. Eichenlaub. 2000. Animal Movement extension to ArcView, Version 2.0. Alaska Science Center–Biological Science Office, U.S. Geological Survey, Anchorage.

Kristan, W.B., and W.I. Boarman. 2003. Spatial pattern of risk of common raven predation on desert tortoises. Ecology 84(9):2432–2443.

Krupnik, I., and D. Jolly [eds.]. 2002. The Earth Is Faster Now: Indigenous Observations of Arctic Environmental Change. Arctic Research Consortium of the United States, Fairbanks, 384 p.

National Audubon Society. www.audubon.org/bird/cbc/103rdsummary.html

Restani, M., J.M. Marzluff and R.E. Yates. 2001. Effects of anthropogenic food sources on movements, survivorship, and sociality of common ravens in the Arctic. Condor 103(2):399–404.

Roth, J.E., J.P. Kelly, W.J. Sydeman and M.A. Colwell. 2004. Sex differences in space use of breeding common ravens in western Marin County, California. Condor 106(3):529–539.

Webb, W.C., W.I. Boarman and J.T. Rotenberry. 2004. Common raven juvenile survival in a human-augmented landscape. Condor 106(3):517–528.

High-Resolution Numerical Modeling of Near-Surface Weather Conditions over Alaska's Cook Inlet and Shelikof Strait

Peter Q. Olsson <olsson@aeff.uaa.alaska.edu>

Alaska State Climate Center
University of Alaska Anchorage
2811 Merrill Field Drive
Anchorage, AK 99501

Task Order 73070

Abstract

Along the north Gulf of Alaska coast, terrain plays an important role in determining local weather. The interaction of terrain with synoptic and mesoscale pressure gradients frequently produces ageostrophic gap and channel winds, often called low-level jets (LLJ) in places like Cook Inlet and Shelikof Strait. These winds may at times be quite strong, with gusts occasionally exceeding 50 m sec^{-1}.

This three year project was successfully and productively conducted for the first year period. Regional Atmospheric Modeling System (RAMS) parallel code was successfully migrated onto a new high performance computer cluster which consists of 15 Dell Poweredge dual Xeon 3 Ghz computers—15 nodes—with dual processors on each node. Domains with grid-spacing of 4 km, 16 km and 64 km were created, with domains being optimized through a series of sensitivity experiments.

Initially we had intended on focusing the study on Cook Inlet, with Shelikof Strait being the focus in later years. However, the acquisition of the computing cluster discussed above, under internal support from the University of Alaska Anchorage (UAA) to the Alaska Experimental Forecast Facility (AEFF), provided the additional computing power necessary to have the fine-mesh grid 3 cover both Cook Inlet and Shelikof Strait from the beginning of the project onwards. Since December 2003, we have been running the model on all three grids in real time as a forecast model, producing 36-hr forecasts with output every hour. A climatology of low-level wind jets in Cook Inlet and Shelikof Strait was also composed for the 2003 to 2004 winter.

Overview

The three year project, High-Resolution Numerical Modeling of Near-Surface Weather Conditions over Alaska's Cook Inlet and Shelikof Strait, has been successfully and productively conducted for the first year period. Regional Atmospheric Modeling System (RAMS) parallel code has been successfully migrated onto a new high performance computer cluster which consists of 15 Dell Poweredge dual Xeon 3 Ghz computers—15 nodes—with dual processors on each node.

Domains with grid-spacing of 4 km, 16 km and 64 km (grids 1, 2, and 3 respectively; see Figure 1) have been created, with domains being optimized through a series of sensitivity experiments. The coarsest grid (grid 1) covers all of Alaska and vicinity and much of the surrounding oceans. This grid is large enough to catch the synoptic weather patterns that force the smaller scale flows. The 16-km domain is required to scale down the simulations from the synoptic-scale grid 1. The finest domain, 4-km grid 3, covers Cook Inlet and Shelikof Strait, which enables detailed simulation of mesoscale phenomena such as low-level wind jets, orographic precipitation, mesoscale cyclones and fronts.

Initially we had intended on focusing the study on Cook Inlet, with Shelikof Strait being the focus in later years. However, the acquisition of the computing cluster discussed above, under internal support from the University of Alaska Anchorage (UAA) to the Alaska Experimental Forecast Facility (AEFF), provided the additional computing power necessary to have the fine-mesh grid 3 cover both Cook Inlet and Shelikof Strait (Figure 1) from the beginning of the project onwards. This required a realignment of the project to a certain extent to accommodate the larger data sets and extra analysis of the enlarged domain. However, from the scientific viewpoint, this has been advantageous and will allow for complete data sets for the full domain for the entire study period.

Since December 2003, we have been running the model on all three grids in real time as a forecast model, producing 36-hr forecasts with output every hour. We also ran simulations on all three grids retrospectively from 1 October until we started producing the routine forecasts in real time. This makes available finest-mesh simulations from the beginning of the project onwards. All simulation data sets are being archived at AEFF for future use and analysis by ourselves and other researchers. Results from the high-resolution real-time simulations are presented in hourly-resolution graphics, available to the public through the internet (aeff.uaa.alaska.edu/wx_brief.html) since December 2003.

A climatology of low-level wind jets in Cook Inlet and Shelikof Strait has been composed for the 2003 to 2004 winter. A manuscript about the low-level wind jet climatology over the study region has been composed and accepted for presentation in the Seventh International Marine Environmental Modeling Seminar (IMEMS 2004). The paper will hopefully be published in the international journal Environmental Modelling and Software after the peer review process.

Topography of Cook Inlet and Shelikof Strait

Figure 2a is a 2-dimensional image showing the location of mountain ranges, channels and water bodies of the Cook Inlet and Shelikof Strait region. Most of the mountain ranges are between 600 and 2000 m in height. Turnagain Arm, Tuxedni Bay, Iliamna Lake, Kaguyak and Puale Bay are marked with text. These places have nearby gaps with elevations under 600 m, much lower than the surrounding terrain. These gaps are the locations through which gap winds frequently blow. Cook Inlet is bounded on the west by the massive Aleutian Range and on the east by the Chugach and Kenai Ranges. Shelikof Strait has the Alaska Peninsula on the west and Kodiak Island on the east. During the winter storm season, strong atmospheric pressure gradients occur across this region as cyclones transit the north gulf. These pressure gradients are one of the main factors inducing strong wind events in this region. Figure 2b is a 3-dimensional perspective of the topography of the areas of interest. The perspective angle was chosen to emphasize the passes which produce major wind jets. Besides the channels, the gaps at Iliamna Lake and the Puale Bay vicinity are clearly visible.

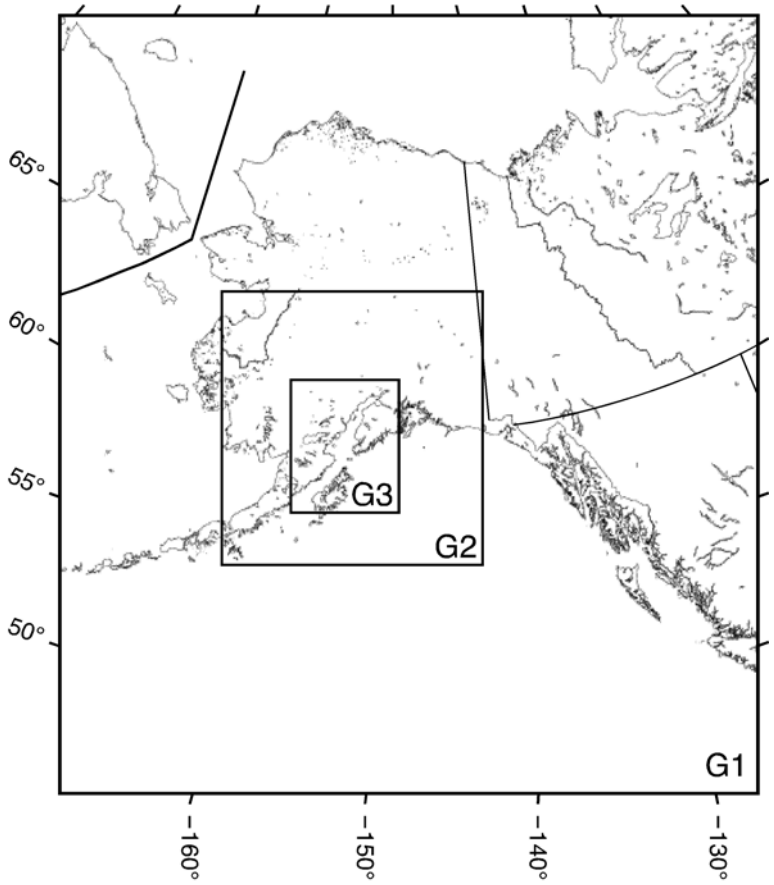

Figure 1. The RAMS domains for Cook Inlet and Shelikof Strait. G1 has a grid spacing of 64 km, G2 16 km and G3 4 km.

Low-Level Wind Jets Regimes

Through the examination of the simulated surface winds, ten frequently appearing wind regimes are recognized (Figure 3). These wind jets are classified into ten categories according to location and orientation: Turnagain Arm (TGA), Tuxedni Bay (TNB), Cook Inlet up channel (CIu), Cook Inlet down channel (CId), Iliamna (ILA), Iliamna reversed (ILAr), Kaguyak (KGY), Shelikof up channel (SKFu), Shelikof down channel (SKFd) and the Puale Bay (PUB) jet. They are further divided into four general groups according to their general wind direction: cross-channel westerly, easterly, and up and down inlet flows. The westerly includes ILA, KGY, PUB and TNB; the easterly includes ILAr and TGA; the down channel includes CId and SKFd; and the up channel includes CIu and SKFu. (The details of the climatology of these wind jets can be found in the conference manuscript.)

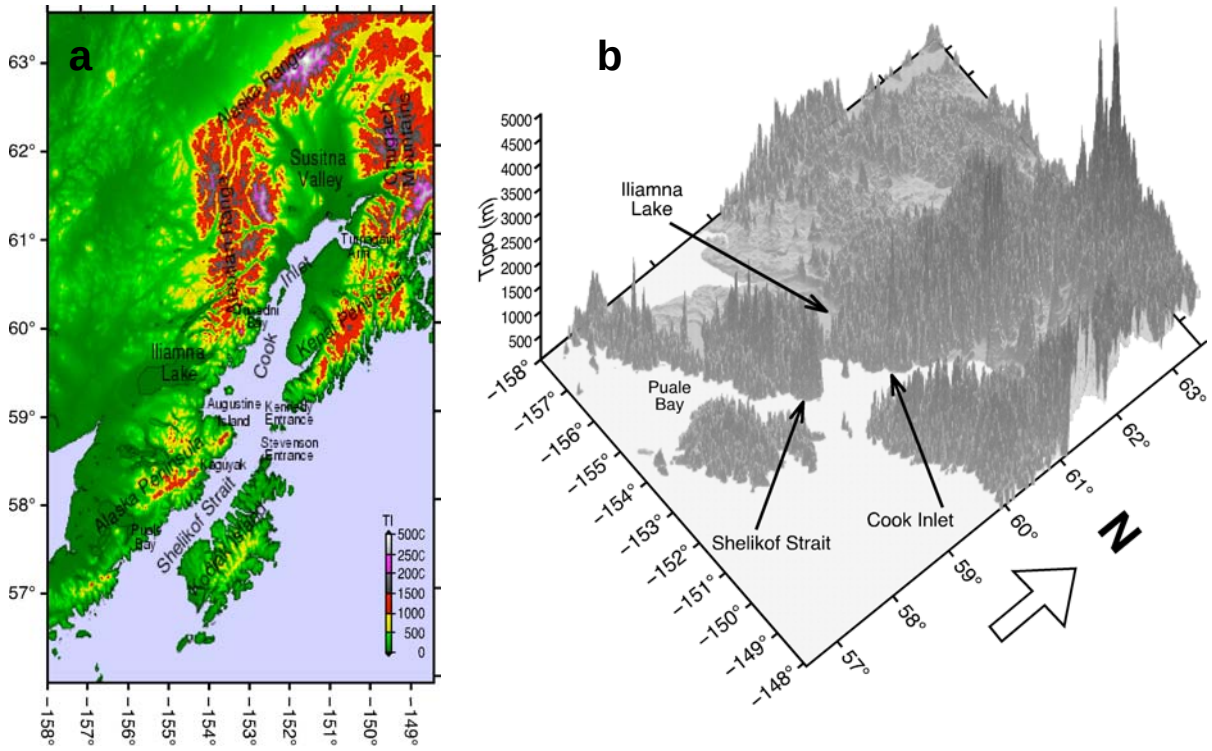

Figure 2. Topography of Cook Inlet and Shelikof Strait.

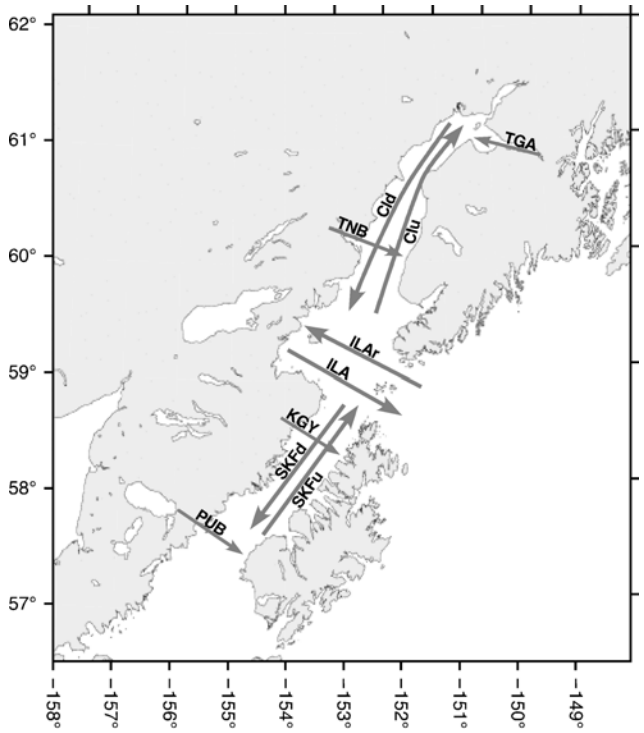

Figure 3. Schematic of the low-level wind jets in Cook Inlet and Shelikof Strait. The arrows indicate the locations and directions of the jets. A jet may occupy the whole channel where the arrow indicates.

Verification of RAMS Wind Forecasts in Cook Inlet and Shelikof Strait with Point Values

As part of this project, we need to verify simulation results. The study region has a paucity of observations, with the exception of the region around Anchorage and the northern Kenai Peninsula. (Indeed, a major rationale for this project is to produce low-level wind fields to ameliorate this situation). We have embarked on a program, largely focused on lower Cook Inlet and Shelikof Strait, to systematically compare our simulations with observed values, mostly NDBC (National Data Buoy Center) buoys and C-MAN (Coastal–Marine Automated Network) stations. We detail our approach here.

When the station observations are used, two verification approaches can be employed: grid-to-observation-point (G-P) and observation-point-to-grid (P-G). While less satisfactory than the P-G method, which requires a much greater density of observations than is available, G-P is the better method for data-sparse regions such as Alaska. There are only a few C-MAN and buoy stations in the Cook Inlet and Shelikof Strait region (see Figure 4) and several of these face instrument-sheltering issues for certain wind directions. Meteorological observations from these stations are being collected and a bi-linear algorithm is being used for grid-to-observation interpolation.

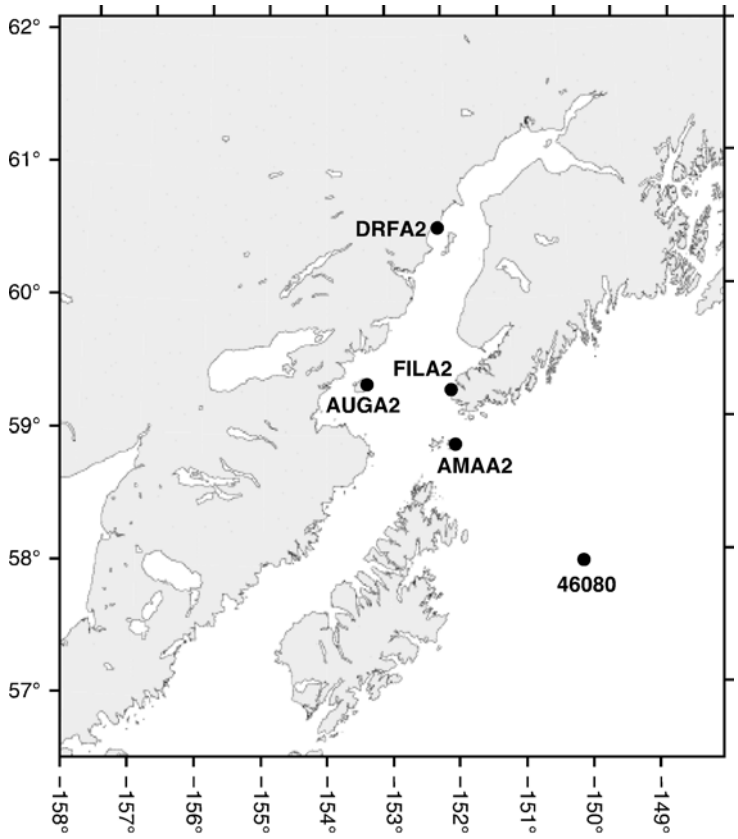

Figure 4. C-MAN and buoy stations in Cook Inlet and Shelikof Strait.

The statistical measures used to quantify model forecast errors are the bias (forecast-observation), root-mean-square (rms) error, and error standard deviation. For interpretation of results, it is helpful to recognize that the total model error includes contributions from both systematic and nonsystematic sources. Systematic errors (model biases) are usually caused by a consistent misrepresentation of such factors as orography, radiation, and convection. Nonsystematic errors are indicated by the error standard deviation and represent the random error component caused by initial condition uncertainty or inconsistent resolution of scales between the forecasts and observations. While it is possible to partially correct for known systematic errors by subtracting the bias, the nonsystematic errors are rather unpredictable in nature and may contribute to a degraded daily forecast product.

If Φ represents any of the parameters under consideration for a given time, then forecast error is defined as $\Phi' = \Phi_f - \Phi_o$, where the subscripts *f* and *o* denote forecast and observed quantities, respectively. Given *N* valid pairs of forecasts and observations, the bias is computed as

$$\bar{\Phi}' = \frac{1}{N}\sum_{i=1}^{N}\Phi'_i \qquad (1)$$

the rms error is computed as

$$rmse = [mse]^{1/2} = \left[\frac{1}{N}\sum_{i=1}^{N}\left(\Phi'_i\right)^2\right]^{1/2} \qquad (2)$$

the standard deviation (std) of the errors is computed as

$$\sigma' = \left[\frac{1}{N}\sum_{i=1}^{N}\left(\Phi'_i - \bar{\Phi}'\right)^2\right]^{1/2} \qquad (3)$$

The mean square error (mse) can be, at least theoretically, decomposed as follows:

$$mse = \bar{\Phi}'^2 + \sigma'^2 \qquad (4)$$

Therefore, the total model error consists of contributions from model biases $\bar{\Phi}'^2$ and random variations in the forecast and/or observed data. Note that if the model bias or systematic error is small, most of mse is due to random, nonsystematic type variability in the errors.

The surface wind bias, rms and std are calculated for each C-MAN and buoy station. The averages are calculated over 5 days, 10 days, 30 days and 60 days. Both wind direction and speed show reasonably good agreement with the observations. The longer the average period is, the better the result.

There is no doubt that grids 2 (16 km) and 3 (4 km) have more skill than grid 1 (64 km) in terms of objective and subjective verification. Grid 3 (4 km) has advantages over grid 2 because it has higher horizontal resolution and is able to resolve more details of the topography, which affects the weather. However, the finer grid (grid 3) may not show skills over the coarser (grid 2) in objective P-G verification, and the added value by the finer grid may not be evident from the P-G method. For an example, verification over the C-MAN station in Augustine Island (AUGA2, see Figure 5) shows that grid 2 is slightly better than grid 3. Unfortunately, AUGA2 is sheltered by the imposing upstream terrain in many wind events, giving smaller wind-speed values than would be observed in unsheltered areas, so we must use this station with some caution.

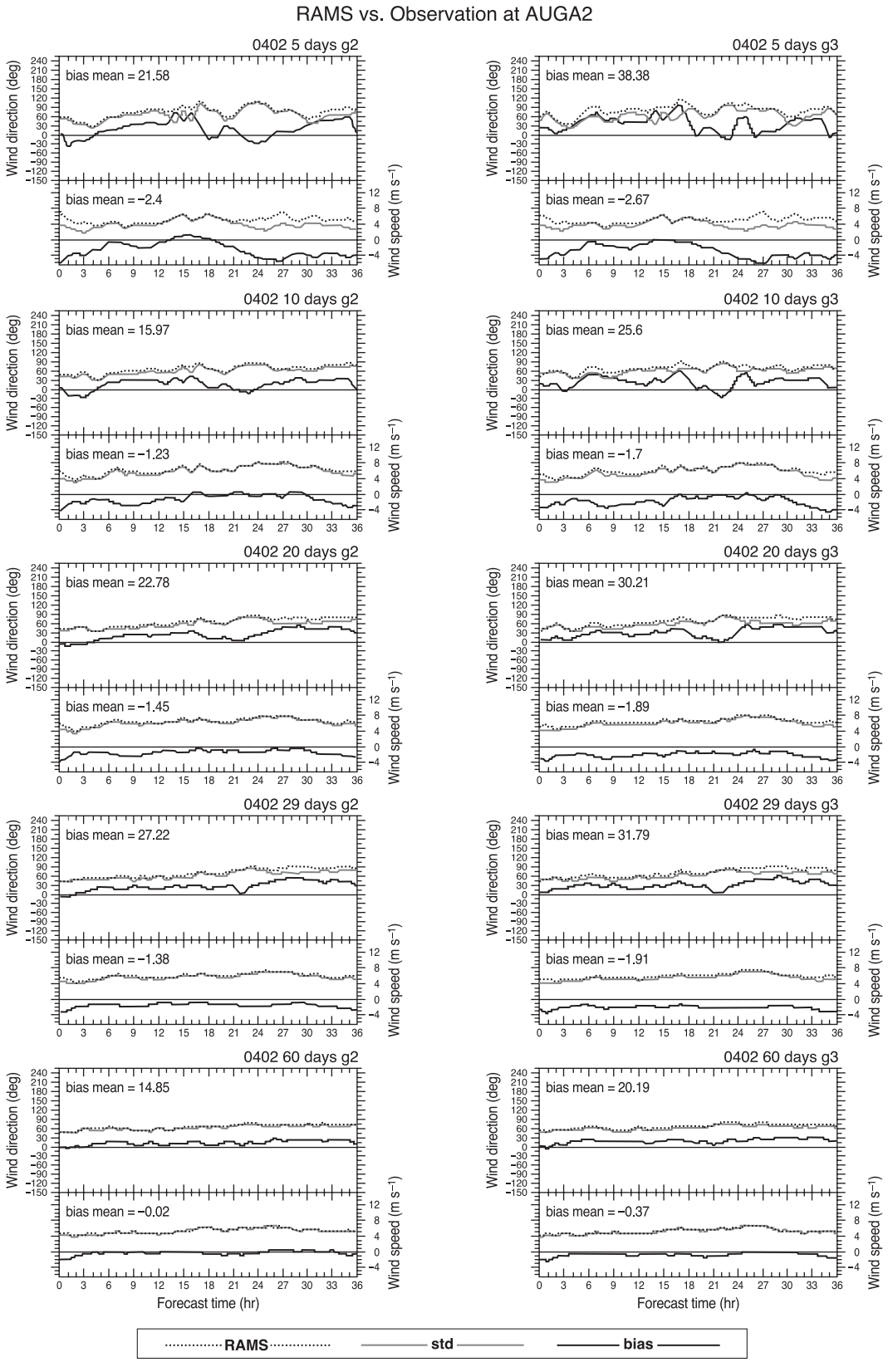

Figure 5. Comparison with the C-MAN station at Augustine Island for February and March 2004.

Subjectively, higher resolution (e.g., 4 km) appears to produce much more realistic structures when compared with qualitative observations such as synthetic aperture radar (SAR) wind retrieval images. We are investigating why the objective verification measures do not reflect this fact. Several issues are confounding factors with this verification method: 1) timing and position errors are more heavily penalized as resolution increases; and 2) as resolution increases, structures tighten and increase in amplitude. As a result, most traditional verification scores will find greater error for higher resolution simulations, even if the structures are more realistic. Timing errors (onset, duration and relaxation of low-level jets) almost always occur, so this is an ever-present issue.

Other verification approaches are being examined, such as pattern recognition and observation-based verification of phase and timing errors.

Case Simulations of Gap Wind in Lower Cook Inlet, Alaska

Another avenue of investigation for this project is the conducting of case studies to determine the internal structure of low-level gap and channel wind jets. Gap winds are strong low-level winds through a channel between two mountain ranges or a gap in a mountain barrier. Gap winds can be the result of interaction of large-scale flows with underlying topography. They can also be induced by thermal difference of the surfaces. Thermally induced gap winds, which are more moderate in speed, are also observed. The synoptic and mesoscale thermal effects can combine to contribute to the formation and enhancement of gap winds.

For a level channel, scale analysis shows that the momentum balances within gaps and their exit regions are highly dependent on the length and width, and long gaps favor a nearly geostrophic balance in the cross-gap direction, with the pressure gradient normal to the gap axis balancing the Coriolis force associated with the along-gap component of the winds. This geostrophic balance has been observed in high-latitude gaps such as Shelikof Strait. With the pressure gradient along the gap, theoretical analysis and observational studies, as well as results from hydraulic models and mesoscale models, have shown a three-way ageostrophic balance between acceleration, the pressure gradient force, and drag forces due to surface friction and entrainment at the top of the gap flow. Within a long gap, a point is usually reached where there is an approximate balance between the pressure gradient force and drag.

In the case of several of the cross-channel gap winds, the bed of a gap may not be level. In the case of presence of barriers in a gap, the flow in the gap may experience blocking and strength enhancement after crossing barriers, for example the Iliamna or Kamishak gap flows. The effect of upstream orography on offshore-directed winds depends on the characteristics of the incident flow. A nondimensional similarity parameter, the internal Froude number F_r, is related to the tendency for the flow to be constrained to horizontal planes.

If $F_r = \frac{U}{NH}$ (where U is the incident speed, N is the static stability, and H is the height of the obstacle) is small ($F_r < 1$) as defined with respect to the height of the obstacle, the low-level flow is largely blocked, except where it can flow around the obstacle or through gaps. When the cross-barrier pressure gradient is substantial, strong low-level wind shears occur at and downstream of the lateral boundaries of these obstacles. When $F_r \geq 1$, the flow has more of a tendency to cross the barriers and enhance in the lee of the topography.

An area of even more interest is the structure of the jet after it leaves the gap and emerges over open water, where a new balance of forces occurs. After leaving the gap and reaching the open water, the terrain-modulated flow accelerates due to the reduced surface drag over water and adjusts to open water configuration and approaches quasi-geostrophic balance at roughly a Rossby radius

$I_R = \frac{NH}{f}$ off the coast, where N and H are as above, and f is the Coriolis parameter. (Note that f is large in this high latitude setting). During conditions of flow characterized by a low Froude number the steady-state response to terrain is a coastal ridge—the phenomenon known as damming. The topographically induced pressure fields produce along-ridge pressure gradients that can result in barrier jets.

We intend to conduct a Froude number analysis in several case studies as an index for the likelihood of jet occurrence and intensity, as this is essentially a parameter diagnosable from model output.

As is the case in most realistic vs. idealized environments, the low-level wind jets in lower Cook Inlet (LCI) are very complicated, with several confounding factors acting together. They can result from composition of gap wind, cross barrier flow, and barrier jets as can be seen in a snapshot of a case study (Figure 6) of an ILA jet on 13 December 2003. The gap between the Alaska Range and the Alaska Peninsula is often a passageway of dense cold dry air from the Alaska continent to LCI. There is a barrier of about 600 m at the gap end towards the sea. The elevation of the area west to the barrier is less than 300 m. The blocking effect is clearly noticeable in the cross section of ILA (Figure 6b).

The wind maxima is close to the south side of the jet where a barrier (the Alaska Peninsula) extends. The shift of the wind maxima is caused by the blocking of the barrier to the south side part of the jet. Evidently a barrier jet takes place in this case in addition to the more generic gap flow.

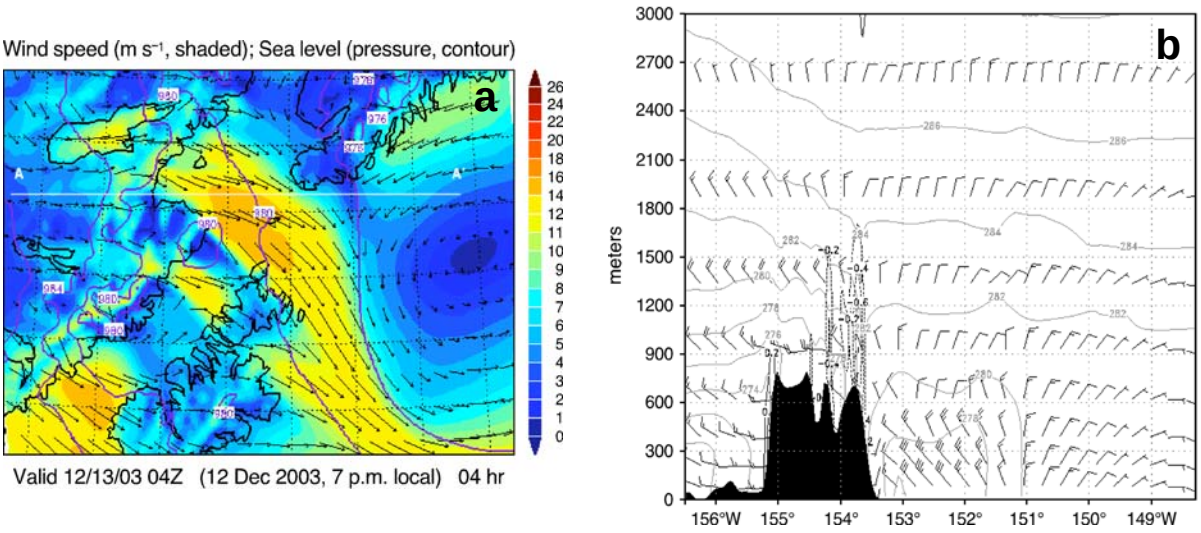

Figure 6. A jet on 13 December 2003. a: two surface winds and mean sea level pressure; b: cross section of the ILA corresponding to the line AA′ in a.

Conclusion

This project has progressed successfully for the first year. Graphics from the real-time high resolution forecasts are being published over the internet and benefit the community. The results of this project help and, in some ways, shape our understanding of the mesoscale weather phenomena over the Cook Inlet and Shelikof region. The results are encouraging and a more sound and thorough understanding of the severe weather situations in this region will be obtained through continuous study across the duration of the project.

Trace Metals and Hydrocarbons in Sediments of Beaufort Lagoon, Northeast Arctic Alaska

A. Sathy Naidu <ffsan@uaf.edu>
John J. Kelley <ffjjk@uaf.edu>

Institute of Marine Science
University of Alaska Fairbanks
Fairbanks, AK 99775-7220

Debasmita Misra <ffdm1@uaf.edu>

College of Engineering and Mines
University of Alaska Fairbanks
Fairbanks, AK 99775-5960

Task Order 74464

Abstract

There is a concern that anthropogenic contaminants discharged locally during petroleum-related activities can accumulate in Beaufort Lagoon sediments. In response to this concern we analyzed concentrations of 12 metals (Cu, Cr, Cd, Ni, V, Pb, Sn, Zn, As, Ba, Fe and Mn) in the mud fraction and total Hg and hydrocarbons (saturated compounds such as normal and isoprenoid alkanes, triterpanes, steranes, and polycyclic aromatic hydrocarbons) in gross sediments collected at 21 locations in the lagoon and in one natural oil seep.

*This report presents the concentrations of sediment trace metals and hydrocarbons, andalso discusses the sources of the hydrocarbons and provides a preliminary interpretation of the statistical analysis on the trace metal data. The concentration levels of the metals and hydrocarbons are generally similar to or below those reported for unpolluted nearshore regions. Comparison of time-series metal data on sandy mud and mud collected in 1977 and 2003, respectively, shows a significant decrease in V but an increase in Mn and Cu from 1977 to 2003. The differences are likely due to disparities in the granulometry of the two sample sets. Correlation coefficient analysis suggests that a large proportion of all the trace metals are adsorbed by clay or Fe oxyhydroxide. The analysis also suggests that some of the metals (Zn, Cd and Sn) occur as metal–organic complex*es in the sediments. *The hydrocarbon components in the sediments are biogenic with undetectable petroleum inputs. There is no evidence of a contribution of petroleum hydrocarbons to the lagoon sediments from oil seeps in the vicinity. The general composition of the hydrocarbon profiles is very similar to those found in our previous studies in the sediments from Elson Lagoon and the nearshore of the Colville Delta–Prudhoe Bay–Canning Delta region. We saw no impression of the natural oil seep and anthropogenic activities on the sediment chemistry. The metal and hydrocarbon data will serve as baselines, which will be critical for ecological risk management of the North Slope in context of contaminant inputs, and to better understand the inorganic and organic geochemistry of arctic sediments.*

Introduction

The North Slope of arctic Alaska and the contiguous nearshore zone are oil- and gas-bearing regions which have a high potential for commercial reserves. A number of onshore oil sites (Prudhoe, Alpine, Kuparuk, Milne) and a few offshore units (Northstar, Endecott) are now producing, while some offshore prospects (Liberty) are slated to be brought on line soon for drilling and production. As part of the forthcoming oil and gas development, the U.S. Department of Interior's Minerals Management Service (MMS) has proposed several offshore units (186, 195 and 202) for lease sales. The petroleum-related developmental activities (drilling operations laced with toxic metals and hydrocarbons, marine and onshore traffic, housing) and associated urbanization of the Native villages are bound to impact the nearshore environment, with a possible accumulation of anthropogenic contaminants in sediments [NORTEC 1981; Snyder-Conn et al.1990]. These contaminants can be transferred to benthic organisms and subsequently through the food chain to higher trophic levels. Environmental contamination is of particular concern in the Arctic where marine organisms which are lipid rich, with a relatively simple and short food chain and low biodiversity, are more vulnerable to bioaccumulation of toxic metals and hydrocarbons. In response to these concerns and our long-term interest in monitoring contaminants in the Alaskan Arctic nearshore we have investigated the time-series changes in trace metals and hydrocarbons in nearshore sediments from urbanized and industrial regions extending from Elson Lagoon adjacent to Pt. Barrow east to the Colville Delta–Prudhoe Bay–Canning Delta region of the North Slope [Naidu et al. 2001, 2003a, b and references therein]. Other investigations of a similar nature are those of Sweeney [1984] and Trefry et al. [2003] on trace metals and Steinhauer and Boehm [1992] on hydrocarbons. This report presents the progress of investigations on a two-year project (2003–2005) which has the major objective to measure the concentrations of a suite of trace metals and hydrocarbons in sediments of Beaufort Lagoon (Figure 1). This location is of particular interest for contaminant studies because it offers a range for comparing sediment chemistries between site-specific sectors which have been exposed to 1) a long-term natural oil seep, 2) past activities relating to a DEW Line military station on the lagoon shore, and 3) sites that presumably have remained relatively pristine. The results of this study will provide baselines of trace metals and hydrocarbons for monitoring contaminants in the nearshore environment off of the Arctic National Wildlife Refuge (ANWR), particularly off the refuge's 1.5-million acre coastal plain, which has potential petroleum reserves. The latter region is one of the most contentious areas for oil drilling and production because of the variety of wildlife habitats there [Douglas et al. 2002] and possible impact on them.

Hypothesis and Objectives

We hypothesize that the compositions and concentrations of trace metals and hydrocarbons in sediments of Beaufort Lagoon vary widely between the regions exposed to a long-term (prehistoric) natural oil seep (enriched in weathered crude), recent anthropogenic activities (with a possible input of refined petroleum products from activities at a former DEW Line site), and a pristine environment (no input from the oil seep or refined petroleum).

The primary objective of this proposal is to distinguish the concentrations of 12 metals (V, Cr, Cu, Ni, Zn, As, Cd, Pb, Sn, Ba, Fe and Mn) in the mud fraction (<63 μm size), and total Hg [THg] and hydrocarbons (polycyclic aromatics and saturated hydrocarbons such as normal and isoprenoid alkanes, triterpanes and steranes) in gross sediments between regions of Beaufort Lagoon that are exposed to long-term natural oil seep, anthropogenic activities with possible inputs of refined petroleum and military-related products, and pristine conditions. The objective is also to establish baselines on the above trace metals and hydrocarbons in the sediments of Beaufort Lagoon for contaminant monitoring.

Materials and Methods

Samples

In August 2003, van Veen grab sediment samples were collected from 22 stations spread over three arbitrarily defined location types in Beaufort Lagoon (Figure 1, Table 1). One suite of samples (BL03-5, -12, -13, -14 and -15 [hereafter samples and stations are referred to by number only]) was collected east of Angun Point adjacent to a known natural oil seep site (69.918° N and 142.395° W, pers. comm. Jim Clough, 31 July 2003; refer also to USGS [1999]) and one sample (4B) off of a seep site (OS) we discovered at the bank of a small stream located south of Nuvagapak Point (Figure 1, Table 1). OS itself was also a site for sample collection for hydrocarbon comparisons. We had intended to get closer to the shoreline at Angun Point to collect samples from that area, but it was not possible because of extensive shoals in the region, which made it impossible to navigate. A third suite of samples (4, 18, 19 and 20) was collected around Nuvagapak Point, a region that was impacted by anthropogenic activities connected with an abandoned DEW Line site and associated landing strip. A fourth suite of samples (1, 2, 3, 5B, 6B, 9, 9B, 10, 11A, 16 and 17) was obtained from areas east and up current of Nuvagapak Point, which are presumed pristine. The coordinates for the sample locations, fixed by GPS, are shown in Table 1. The surface oxidized 2–4-cm portion of each of the grab samples was taken and split into three sets of subsamples using a Teflon spatula. Each of the splits was transferred to three separate I-CAM glass jars, two of which were rinsed with acid and deionized distilled water (for trace metal, grain size and organic carbon analyses). The third jar was pre-baked and cap-lined with aluminum foil for hydrocarbon analysis. One set was sent to M.I. Venkatesan, subcontractor at the University of California, Los Angeles, for hydrocarbon analysis. A second set was sent to the subcontractor Frontier GeoSciences Inc. in Seattle for trace metal analysis. The third set was retained by the principal investigators for analysis of the grain size, organic carbon and nitrogen and their stable isotopes at the University of Alaska Fairbanks. All of these sediment samples were stored frozen until analysis.

Laboratory analysis of samples

The methods for the analyses of trace metals and hydrocarbons on sediments were the same as those adopted in our previous studies funded by CMI/MMS [Naidu et al. 2001, 2003b]. Brief descriptions of the methods follow: We analyzed 12 metals (V, Cu, Cr, Ni, Zn, As, Cd, Pb, Sn, Ba, Fe and Mn) in the mud fraction (<63 μm size) of the sediment samples and THg in total sediment. The rationale for choosing the mud fraction for the above 12 metals and gross sediments for THg has been discussed in our two previously CMI/MMS-funded studies on the North Slope lagoon sediments [Naidu et al. 2001, 2003b]. A 5-g split of each sediment sample was suspended in deionized distilled water and the resulting slurry was sieved through a 230-mesh nylon screen to obtain the mud fraction. The mud was freeze dried, pulverized using an agate mortar and pestle, and an aliquot of the powder was dissolved in a Teflon bomb by digesting in a HF–HNO_3 mixture in a microwave oven. After removing HF and diluting the digest to 100 ml, an aliquot of the acid solution was analyzed for the above 12 metals, using either a direct injection Zeeman graphite furnace atomic absorption spectrometer, an inductively coupled plasma/mass spectrometer (ICP/MS), or by Excaliber automated hydride generation atomic fluorescence spectrometry (for As, Environmental Protection Agency [EPA] method 1632). A split of the original gross sediment sample was taken for analysis of the total Hg. The split was digested in aqua regia, and after $SnCl_2$ reduction, pre-precipitation and dual gold amalgamation, Hg was analyzed by cold vapor atomic absorption spectrometry (CVAAS), following the method outlined in Bloom [1992] and Bloom et al. [1999]. The quality assurance/quality control (QA/QC) protocol prescribed by EPA for trace metal analysis was followed, which included analysis of spiked samples and reagent blanks, establishment of analytical precision through replicate runs, and checking analytical accuracy via analyses of the Certified Reference Materials (CRM), namely

National Institute of Standards and Testing (NIST) 2709 and International Atomic Energy Agency (IAEA) 405. Further, the analytical accuracy and precision of the trace metal analysis were checked by inter-laboratory comparison performance evaluation, which consisted of successful participation of our subcontractor (Frontier GeoSciences Inc., Seattle) in the1997 NIST/NOAA (National Oceanic and Atmospheric Administration) round-robin inter-laboratory exercise NOAA/11 that was conducted by the National Research Council of Canada (NRC). Frontier's rating was good to excellent.

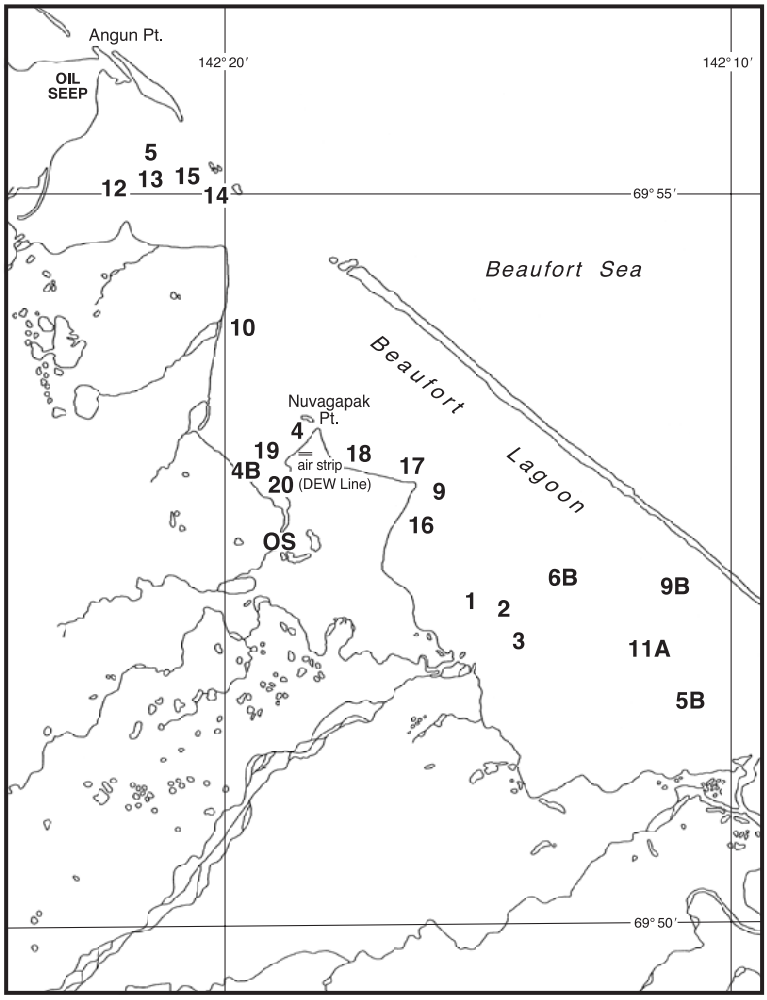

Figure 1. Study area showing locations of sediment samples in Beaufort Lagoon..

Table 1. Sample locations, grain sizes, organic carbon (OC), nitrogen (N), OC/N, and stable isotopes of OC ($\delta^{13}C$ ‰) and N ($\delta^{15}N$) of Beaufort Lagoon sediments.

Sample	Lat °N	Long °W	Solids %	Gravel %	Sand %	Silt %	Clay %	Mud %	OC %	N %	OC/N	$\delta^{13}C$	$\delta^{15}N$
BL03-1	69.87	142.23	53.4	0.00	6.43	77.39	16.18	93.57	2.39	0.22	10.86	–26.94	1.88
BL03-2	69.87	142.26	67.9	0.00	42.28	36.63	21.09	57.72	2.33	0.20	11.60	–26.89	2.02
BL03-3	69.89	142.33	51.9	0.00	18.11	51.87	30.02	81.89	2.17	0.20	10.85	–26.36	0.83
BL03-4	69.91	142.24	79.5	0.00	95.55	0.09	4.36	4.45	1.72	0.17	10.11	–24.98	2.90
BL03-4B	69.89	142.33	91.5	92.87	2.54	1.92	2.66	4.59	3.29	0.32	10.28	–26.99	3.09
BL03-5	69.93	142.36	99.10	NA	NA	NA	NA	NA	NA	NA	NA	NA	NA
BL03-5B	69.86	142.18	52.9	0.00	13.94	50.36	35.70	86.06	2.00	0.18	11.11	–26.24	1.60
BL03-6B	69.87	142.22	56.8	0.00	6.56	50.22	43.22	93.44	2.02	0.19	10.63	–26.49	2.05
BL03-9	69.88	142.27	61.2	0.28	33.60	42.13	23.98	66.12	3.96	0.36	11.00	–27.35	1.95
BL03-9B	69.87	142.19	65.0	0.00	27.86	48.44	23.69	72.14	2.27	0.19	11.94	–26.24	1.79
BL03-10	69.91	142.33	74.9	0.00	81.25	13.24	5.50	18.75	2.38	0.20	11.90	–27.14	3.41
BL03-11A	69.87	142.20	61.9	0.00	22.51	55.19	22.30	77.49	1.55	0.13	11.92	–27.26	1.07
BL03-12	69.92	142.37	61.4	0.00	19.01	58.97	22.02	80.99	2.04	0.17	12.00	–26.85	2.21
BL03-13	69.92	142.36	76.6	0.00	89.76	7.45	2.79	10.24	1.43	0.12	11.91	–26.85	2.07
BL03-14	69.92	142.34	67.0	0.00	77.97	9.18	12.85	22.03	1.66	0.15	11.07	–26.96	1.75
BL03-15	69.92	142.34	NA	0.00	83.42	3.15	13.42	16.58	1.76	0.17	10.35	–26.49	1.76
BL03-16	69.88	142.28	43.8	0.00	24.24	52.46	23.30	75.76	3.20	0.26	12.30	–27.53	1.80
BL03-17	69.87	142.28	79.6	0.12	97.88	0.05	1.95	1.99	2.57	0.30	8.56	–25.84	3.12
BL03-18	69.89	142.29	56.4	0.00	25.17	36.81	38.02	74.83	2.60	0.23	11.30	–26.85	2.83
BL03-19	69.89	142.31	89.8	28.60	63.62	1.34	6.45	7.78	4.05	0.38	10.66	–26.76	1.80
BL03-20	69.88	142.32	79.3	37.75	58.80	0.72	2.73	3.45	3.75	0.37	10.13	–27.21	2.23
OS	69.88	142.31	NA	NA	NA	NA	NA	NA	NA	NA	NA	NA	NA

Hydrocarbon analyses for *n*-alkanes, polycyclic aromatic hydrocarbons [PAHs,] triterpanes and steranes were performed on 19 gross sediment samples and according to well-established methods [Venkatesan et al. 1987; Venkatesan 1994]. After thawing the frozen sample the wet sediment was spiked with the following surrogates: deuterated *n*-alkanes (for *n*-alkanes) and hexamethylbenzene, dodecylbenzene and deuterated terphenyl (for PAHs). After solvent extraction and separation into individual compounds by gas chromatograph (GC) the alkanes were quantified using a flame ionization detector. Tricyclic di- and pentacyclic triterpenoids and PAHs were measured by GC/mass spectrometry. As in our last two CMI/MMS–funded investigations [Naidu et al. 2001, 2003b] 24 PAHs were analyzed as well as 6 additional PAHs, which are routinely analyzed by NIST/NOAA for its QA/QC program. Also, as in our previous studies [Naidu et al. 2001, 2003b], QA/QC measures were undertaken in the hydrocarbon analysis. In this context, our subcontractor, Dr. Venkatesan, participated successfully first in 1992 and then in 1999 in inter-laboratory round-robin exercises conducted by NIST/NOAA NS&T for its QA/QC program.

At the Institute of Marine Science/University of Alaska Fairbanks (IMS/UAF) laboratory, the sediment grain size distributions were analyzed by the sieve-pipette method [Folk 1968]. The purpose of this analysis is to gain understanding of the influence of granulometry on the concentrations of trace metals and hydrocarbons. The chemical data obtained in this study provide continuity for comparison with our previous database on lagoon sediments collected from several disjointed locations of the Beaufort Sea nearshore, because the analytical techniques were the same in all investigations. The contents of organic carbon (OC) and total nitrogen (N) and their stable isotopes ($\delta^{13}C$ and $\delta^{15}N$) were determined on carbonate-free muds, following the methods outlined in Naidu et al. [2000] and using a Thermo Finnigan Model Delta Plus XP isotope ratio mass spectrometer (IRMS). The values of $\delta^{13}C$ (‰) are referenced to the V-PDB standard and those of $\delta^{15}N$ to an air standard. The standard error of the isotope analysis is ± 0.2‰.

Statistical analysis

Statistical analysis to date has consisted of the following: Determination of the correlation coefficients between various sediment analytes, with an aim to understanding relationships between concentrations of metals, silt, clay and organic carbon in the mud fraction. The ultimate purpose of this analysis is to aid in the deduction of the geochemical partitioning of the metals. The time-series comparison was obtained between the concentrations of selected trace metals in sandy muds (>75% silt and clay collected in 1977 [after Naidu 1981; Naidu et al. 2003b]), and muds of this study (Table 2). Surface trend analysis was conducted using all data, to elucidate if there are any geographical gradient(s) in the individual analytes from point sources, such as the abandoned DEW Line site, or the oil seeps around Angun or Nuvagapak Point, respectively. Cluster analysis was undertaken to identify grouping, if any, of stations based on the trace metal compositions surrounding the above two point sources and the pristine lagoon. This was followed by stepwise multiple discriminant analysis of the chemical data to correlate station group separation by cluster analysis with sediment variables.

Table 2. Concentrations of metals in Beaufort Lagoon sediments. All are µg g^{-1}, except THg (ng g^{-1}) and Fe (%).

Sample	V µg g^{-1}	Cr	Mn	Ni	Cu	Zn	As	Cd	Sn	Ba	Pb µg g^{-1}	THg ng g^{-1}	Fe %
BL03-1	110	68.6	318	36.9	38.5	98.4	10.9	0.224	1.78	559	16.8	68.5	2.64
BL03-2	121	73.7	506	37.0	34.9	105	17.7	0.195	1.83	585	16.8	58.8	3.44
BL03-3	127	72.7	311	40.6	42.3	110	18.4	0.233	1.76	512	19.1	94.6	3.10
BL03-4	87.3	55.5	1222	27.2	19.9	60.2	10.0	0.196	1.53	355	11.0	11.7	2.21
BL03-4B	136	78.2	668	44.9	44.3	107	20.3	0.345	2.65	511	19.1	5.2	3.31
BL03-5	94.7	59.9	182	25.7	16.2	48.2	6.9	0.085	1.32	436	12.0	118	2.17
BL03-5B	121	71.4	407	41.8	44.0	107	15.8	0.286	1.73	583	18.5	113	3.27
BL03-6B	129	76.9	319	41.2	43.0	111	17.0	0.266	2.01	592	19.9	103	3.23
BL03-9	123	74.2	339	40.0	39.2	100	12.8	0.242	1.69	530	16.7	78.1	2.89
BL03-9B	131	83.8	370	45.0	44.7	107	12.5	0.287	1.83	649	18.6	77.1	3.31
BL03-10	106	71.1	457	32.7	28.5	80.4	11.7	0.246	1.60	473	13.1	22.8	2.82
BL03-11A	116	71.5	305	37.7	36.1	89.1	12.0	0.206	1.80	550	15.7	73.4	2.75
BL03-12	118	72.2	364	35.2	33.0	88.5	13.9	0.232	1.68	592	15.2	60.6	2.98
BL03-13	115	73.0	503	35.0	29.7	79.5	13.3	0.190	1.74	329	13.8	20.9	2.69
BL03-14	120	70.2	359	37.1	34.6	85.5	12.8	0.223	1.71	446	15.1	30.1	2.61
BL03-16	113	67.9	351	37.3	32.1	81.9	14.2	0.214	1.58	413	13.4	90.7	2.69
BL03-17	131	74.1	3132	54.3	55.2	93.3	16.4	0.341	4.86	430	28.7	13.4	3.24
BL03-18	136	81.7	346	42.2	37.9	104	16.8	0.207	1.88	572	18.3	62.0	3.52
BL03-19	125	82.2	868	43.0	41.2	107	16.4	0.623	3.99	479	23.1	7.89	3.56
BL03-20	136	81.3	829	50.8	40.8	111	15.0	0.454	4.13	496	20.3	21.5	3.07
A-Mean	120	73.0	608	39.0	37.0	94	14.0	0.265	2.00	505	17.0	57.0	2.98
Std AM	13	7.0	643	6.8	8.9	17	3.2	0.110	0.98	85	4.1	37.3	0.4004
G-Mean	119	73.0	472	39.0	36.0	92	14.0	0.246	2.00	497	17.0	41.0	2.95
Std GM	13	7.0	658	6.9	9.0	17	3.2	0.110	0.99	85	4.1	40.7	0.4014
% CV	11	9.7	139	17.7	25.2	19	23.2	46.400	49.40	17	24.3	99.9	14

A-Mean: Arithmetic mean
Std AM: Standard deviation of arithmetic mean
G-Mean: Geometric mean
Std GM: Standard deviation of geometric mean
% CV: Percent coefficient of variation

Results

The percents of solids, gravel, sand, silt, clay and mud in gross sediments, and organic carbon (OC) and nitrogen (N), OC/N ratios and stable isotopes of OC and N in the mud fraction of the individual samples are included in Table 1. In Table 2 are shown the concentrations (on a dry weight basis) of 12 metals (V, Cr, Mn, Ni, Cu, Zn, As, Cd, Sn, Ba, Pb and Fe) in the mud fraction and of total Hg in the gross sediments. Table 2 also provides the arithmetic and geometric means of the concentrations of the metals analyzed in the 21 samples and the standard deviations and coefficient of variation (CV) of the analysis relative to each of the metals analyzed.

The results of the QA/QC procedure for the trace metal analyses in reference to calibration verification, calibration blanks, spikes, replicate analyses (for precision determination), and assessment of the analytical accuracy based on Certified Reference Materials NIST 2709 and IAEA 405 are presented in Tables 3, 4, 5, 6, and 7, respectively. The concentrations of the *n*-alkanes, polycyclic aromatic hydrocarbons, triterpanes and steranes in gross sediments are shown in Tables 8, 9, 10, and 11, respectively.

The correlation coefficients (*r* values) determined between the concentrations of silt, clay, OC, N and the 12 metals in the mud fraction are shown in Table 12. These correlations were determined by assuming the total percentage of silt and clay in the mud fraction to be 100%, and then prorating (recalculating) the silt and clay percents based on their relative percents in the gross samples. Table 13 shows the time-series comparison for Beaufort Lagoon of the concentrations of selected trace metals in suites of sandy muds collected in 1977 [Naidu 1981; Naidu et al. 2003b] and muds sampled in 2003 (this study, Table 2).

Table 3. Results of the QA/QC analysis concerning calibration verification.

Analyte (unit)	Batch ID	ICV-TV	ICV-Obs	ICV-Rec	CCV1-TV	CCV1-Obs	CCV1-Rec	CCV2-TV	CCV2-Obs	CCV2-Rec
V (µg L^{-1})	A	50	45.3523091	90.7046182	10	10.10702359	101.0702359	10	9.869872351	98.69872351
Cr	A	50	46.96249819	93.92499637	10	10.42038436	104.2038436	10	10.31545133	103.1545133
Mn	A	50	45.61942801	91.23885601	10	10.47879367	104.7879367	10	10.2695745	102.695745
Fe	A	100	73.05313706	73.05313706	50.00000381	39.06361265	78.12721935	50.00000381	38.63918732	77.27836875
Ni	A	50	50.8867821	101.7735642	10	10.68007653	106.8007653	10	10.66856767	106.6856767
Cu	A	50	50.30532361	100.6106472	10	10.60041579	106.0041579	10	10.43874602	104.3874602
Zn	A	50	51.36481686	102.7296337	20	20.94026515	104.7013258	20	20.49771425	102.4885713
As	A	50	45.45553065	90.91106131	10	10.38048842	103.8048842	10	10.02663014	100.2663014
Cd	A	5	4.649514064	92.99028129	1	1.029401306	102.9401306	1	1.003388809	100.3388809
Sn	A	50	53.76962124	107.5392425		2.003951832			1.91100463	
Ba	A	100	97.20926536	97.20926536	10	9.892735523	98.92735523	10	9.796689174	97.96689174
Pb (µg L^{-1})	A	5	5.148574426	102.9714885	2	2.219005835	110.9502917	2	2.193373488	109.6686744
THg (ng L^{-1})	B	15	15.14149028	100.9432685	20	19.85846544	99.29232721	20	20.06355132	100.3177566
Analyte (unit)	**Batch ID**	**CCV3-TV**	**CCV3-Obs**	**CCV3-Rec**	**CCV4-TV**	**CCV4-Obs**	**CCV4-Rec**	**CCV5-TV**	**CCV5-Obs**	**CCV5-Rec**
V (µg L^{-1})	A	10	9.991375273	99.91375273	10	10.17824322	101.7824322	10	9.986948267	99.86948267
Cr	A	10	10.23747284	102.3747284	10	10.43125707	104.3125707	10	10.25176255	102.5176255
Mn	A	10	10.15512333	101.5512333	10	10.37120146	103.7120146	10	10.31078947	103.1078947
Fe	A	50.00000381	36.14374571	72.28748591	50.00000381	38.91393305	77.82786016	50.00000381	37.1038113	74.20761693
Ni	A	10	10.50028633	105.0028633	10	10.74240442	107.4240442	10	10.50248384	105.0248384
Cu	A	10	10.44103275	104.4103275	10	10.48291771	104.8291771	10	10.47122489	104.7122489
Zn	A	20	20.84492497	104.2246249	20	20.58320021	102.9160011	20	20.72900602	103.6450301
As	A	10	10.07112922	100.7112922	10	10.24800377	102.4800377	10	9.968211442	99.68211442
Cd	A	1	1.025773372	102.5773372	1	1.021258889	102.1258889	1	1.018553729	101.8553729
Sn	A		1.928422781			1.926497615			1.897775196	
Ba	A	10	9.859105991	98.59105991	10	9.892031641	98.92031641	10	9.648629084	96.48629084
Pb (µg L^{-1})	A	2	2.169817453	108.4908727	2	2.173315751	108.6657876	2	2.166242576	108.3121288
THg (ng L^{-1})	B	20	20.16609426	100.8304713	20	20.2686372	101.343186			
Analyte (unit)	**Batch ID**	**CCV6-TV**	**CCV6-Obs**	**CCV6-Rec**	**CCV7-TV**	**CCV7-Obs**	**CCV7-Rec**	**CCV8-TV**	**CCV8-Obs**	**CCV8-Rec**
V (µg L^{-1})	A	10	9.849617357	98.49617357	10	9.783745819	97.83745819	10	9.586111375	95.86111375
Cr	A	10	10.1783771	101.783771	10	10.02781438	100.2781438	10	9.836530337	98.36530337
Mn	A	10	10.09998875	100.9998875	10	10.10092558	101.0092558	10	9.867526868	98.67526868
Fe	A	50.00000381	38.19419485	76.38838388	50.00000381	36.77596348	73.55192136	50.00000381	37.05366884	74.10733202
Ni	A	10	10.36700825	103.6700825	10	10.13588373	101.3588373	10	9.880873234	98.80873234
Cu	A	10	10.31545979	103.1545979	10	10.4797927	104.797927	10	10.41173962	104.1173962
Zn	A	20	20.23273385	101.1636692	20	21.04050314	105.2025157	20	20.66332202	103.3166101
As	A	10	9.847302208	98.47302208	10	9.983570755	99.83570755	10	9.73225454	97.3225454
Cd	A	1	1.002141532	100.2141532	1	1.031852437	103.1852437	1	0.985930772	98.59307716
Sn	A		1.887518769			1.858317909			1.881666636	
Ba	A	10	9.763108636	97.63108636	10	9.730458986	97.30458986	10	9.69027078	96.9027078
Pb (µg L^{-1})	A	2	2.09613605	104.8068025	2	2.12493247	106.2466235	2	2.112768494	105.6384247
THg (ng L^{-1})	B									

Table 3. (continued)

Analyte (unit)	Batch ID	CCV9-TV	CCV9-Obs	CCV9-Rec	CCV10-TV	CCV10-Obs	CCV10-Rec	CCV11-TV	CCV11-Obs	CCV11-Rec
V (µg L^{-1})	A	10	9.650594968	96.50594968	10	9.30736503	93.0736503	10	9.423536979	94.23536979
Cr	A	10	9.76573373	97.6573373	10	9.544484373	95.44484373	10	9.628965848	96.28965848
Mn	A	10	9.827188222	98.27188222	10	9.458645312	94.58645312	10	9.694133285	96.94133285
Fe	A	50.00000381	39.53449401	79.06898199	50.00000381	42.37362985	84.74725323	50.00000381	47.00665316	94.01329915
Ni	A	10	9.932683621	99.32683621	10	9.576026001	95.76026001	10	9.668495115	96.68495115
Cu	A	10	10.2025627	102.025627	10	9.890386321	98.90386321	10	10.0324925	100.324925
Zn	A	20	20.3137235	101.5686175	20	19.52618759	97.63093797	20	19.51674111	97.58370555
As	A	10	9.585721832	95.85721832	10	9.299644052	92.99644052	10	9.489074512	94.89074512
Cd	A	1	0.989542451	98.9542451	1	0.947602132	94.76021317	1	0.971535371	97.15353708
Sn	A		1.918633807			1.824633062			1.902547083	
Ba	A	10	9.838818362	98.38818362	10	9.148799712	91.48799712	10	9.62317503	96.2317503
Pb (µg L^{-1})	A	2	2.12562117	106.2810585	2	2.025839268	101.2919634	2	2.117560977	105.8780489
THg (ng L^{-1})	B									

Analyte (unit)	Batch ID	CCV12-TV	CCV12-Obs	CCV12-Rec	CCV13-TV	CCV13-Obs	CCV13-Rec	CCV14-TV	CCV14-Obs	CCV14-Rec
V (µg L^{-1})	A	10	9.438779146	94.38779146	10	10.11357487	101.1357487	10	10.02901924	100.2901924
Cr	A	10	9.5126383	95.126383	10	10.31263132	103.1263132	10	10.23583896	102.3583896
Mn	A	10	9.651176105	96.51176105	10	10.29423463	102.9423463	10	10.19991661	101.9991661
Fe	A	50.00000381	53.94851826	107.8970283	50.00000381	43.16024445	86.32048232	50.00000381	38.81284795	77.62568998
Ni	A	10	9.577118118	95.77118118	10	10.4172239	104.172239	10	10.22561713	102.2561713
Cu	A	10	9.803673602	98.03673602	10	10.22385582	102.2385582	10	10.20193347	102.0193347
Zn	A	20	19.1865418	95.93270898	20	20.44292065	102.2146032	20	20.36064296	101.8032148
As	A	10	9.149850875	91.49850875	10	9.69797573	96.9797573	10	9.683501646	96.83501646
Cd	A	1	0.947509367	94.75093668	1	1.017795471	101.7795471	1	0.993801395	99.38013952
Sn	A		1.87476249			1.934516221			1.935159194	
Ba	A	10	9.423369849	94.23369849	10	9.725311342	97.25311342	10	9.599800774	95.99800774
Pb (µg L^{-1})	A	2	2.101084924	105.0542462	2	2.142351295	107.1175648	2	2.113897098	105.6948549
THg (ng L^{-1})	B									

Table 4. Results of the QA/QC analysis concerning calibration blanks.

Analyte (unit)	Batch ID	ICB	CCB1	CCB2	CCB3	CCB4	CCB5	CCB6	CCB7
V (µg L^{-1})	A	–0.019412662	–0.022915678	0.003640651	0.017759003	0.048708424	0.023439894	0.02438426	0.002141815
Cr	A	–0.002122966	0.003766614	0.010165725	–0.002818597	–0.009003925	–0.023367497	–0.030559529	–0.051678352
Mn	A	0.001514224	–0.000366763	0.001696906	0.000215278	0.001268211	–0.000454617	0.00102575	0.000273924
Fe	A	–1.281956901	2.199543674	2.977579904	2.51391155	1.110781557	0.8398272	0.879905186	–1.557955314
Ni	A	0.006692471	0.001049361	0.003343839	0.001642198	0.001944399	0.002645204	0.001884406	0.003968292
Cu	A	–0.002534501	–0.01197791	–0.016823747	–0.010802005	–0.007336244	–0.004534008	–0.005354424	–0.010948432
Zn	A	0.009717066	–0.007442436	0.000322795	0.006762036	–0.006444729	0.008655965	0.006723209	–0.002946931
As	A	0.03487219	0.023736137	0.056976428	0.045339725	0.040974748	0.03895845	0.078805291	0.045033425
Cd	A	0.001390389	0.00066378	*8.54564E–05*	0.000269234	–0.000194387	0.000389272	–0.000239253	*–9.69004E–05*
Sn	A	0.247473511	0.019964263	0.023887361	0.026699068	0.02564591	0.020272009	0.02815594	0.027853262
Ba	A	0.010189992	0.001502795	0.000655891	0.000560007	0.001351205	0.001324258	0.002003348	0.00180285
Pb (µg L^{-1})	A	0.000486244	0.000574009	0.000689952	0.000983047	0.000643604	0.000557415	0.000284386	*–9.19744E–05*
THg (ng L^{-1})	B	0.005127147	0.010254294	0.020508588	0.076907204	0.061525765			
Analyte (unit)	**Batch ID**		**CCB8**	**CCB9**	**CCB10**	**CCB11**	**CCB12**	**CCB13**	**CCB14**
V (µg L^{-1})	A		–0.010947072	–0.016725359	0.011709312	0.027295459	0.010289739	–0.013957262	–0.006775751
Cr	A		–0.056714697	–0.075768997	–0.066915037	–0.094584515	–0.116960163	–0.131259752	–0.112840693
Mn	A		–0.001074566	0.002161963	0.03136897	0.054314014	0.051490255	0.01542742	0.016643044
Fe	A		2.653762053	2.800329156	9.014763907	14.93157478	8.144938152	1.341967988	1.754123921
Ni	A		0.012223274	0.01125807	0.033918849	0.047015877	0.046362983	0.063122249	0.068449487
Cu	A		–0.008492945	–0.000696379	0.013466952	0.027762757	0.027535099	0.006185382	0.006529685
Zn	A		0.033953836	0.038064624	0.099442749	0.102272735	0.1616685	1.112588417	1.239113157
As	A		0.061924645	0.084226575	0.115874334	0.115621475	0.148838907	0.073167584	0.093352707
Cd	A		*–1.18679E–05*	0.000420587	0.002093238	0.003724701	0.004472952	0.000266891	0.001259444
Sn	A		0.020168967	0.01414789	0.033233545	0.026029557	0.025150975	0.013041776	0.013497487
Ba	A		0.000679496	0.001074303	0.025160283	0.044806803	0.045522298	0.011303463	0.011303808
Pb (µg L^{-1})	A		–0.000259981	–0.000394815	0.004911209	0.009329379	0.009550545	0.005268769	0.005122446
THg (ng L^{-1})	B								

Table 5. Results of the QA/QC analysis concerning spikes.

Analyte (unit)	Batch ID	Sample ID	Mean	Spike TV	Dup Spike TV	Obs Spike Value	Dup Obs Spike Value	Spike % Rec	Dup Spike % Rec	RPD
V (mg kg^{-1})	A	BL03-4	87.22	98.81	98.81	190.0	190.8	104.0	104.8	0.7
V	A	BL03-3	126.6	79.37	79.68	205.3	207.9	99.1	102.0	2.9
Cr	A	BL03-4	55.07	98.81	98.81	157.7	158.3	103.8	104.4	0.6
Cr	A	BL03-3	72.52	79.37	79.68	145.8	142.0	92.3	87.2	5.7
Mn	A	BL03-4	1215	98.81	98.81	1324	1324	110.4	109.6	0.8
Mn	A	BL03-3	312.4	79.37	79.68	385.4	394.4	92.1	102.9	11.1
Fe	A	BL03-3	30902	79.37	79.68	32448	30620	1949	–353.9	288.8
Fe	A	BL03-4	21899	494.1	494.1	22701	22647	162.3	151.4	6.9
Ni	A	BL03-3	40.88	79.37	79.68	124.0	126.3	104.8	107.2	2.3
Ni	A	BL03-4	27.48	123.5	123.5	154.7	156.6	103.0	104.5	1.4
Cu	A	BL03-4	20.40	123.5	123.5	148.1	146.4	103.4	102.0	1.4
Cu	A	BL03-3	42.67	79.37	79.68	127.3	128.1	106.7	107.2	0.5
Zn	A	BL03-3	111.6	79.37	79.68	187.8	188.3	96.1	96.3	0.2
Zn	A	BL03-4	60.59	247.0	247.0	311.7	313.3	101.6	102.3	0.6
As	A	BL03-3	18.48	79.37	79.68	91.56	92.81	92.1	93.3	1.3
As	A	BL03-4	9.84	98.81	98.81	113.1	111.9	104.5	103.3	1.1
Cd	A	BL03-3	0.229	79.37	79.68	76.35	76.99	95.9	96.3	0.4
Cd	A	BL03-4	0.196	9.881	9.881	10.47	10.27	103.9	101.9	2.0
Sn	A	BL03-3	1.774	79.37	79.68	80.55	79.81	99.3	97.9	1.3
Sn	A	BL03-4	1.523	24.70	24.70	27.54	26.69	105.3	101.9	3.3
Ba	A	BL03-3	497.2	79.37	79.68	596.7	521.8	125.4	30.9	120.9
Ba	A	BL03-4	357.1	197.6	197.6	578.6	576.8	112.1	111.2	0.8
Pb	A	BL03-3	19.08	79.37	79.68	98.77	98.35	100.4	99.5	0.9
Pb (mg kg^{-1})	A	BL03-4	11.04	24.70	24.70	35.68	35.48	99.7	99.0	0.8
THg (ng g^{-1})	B	BL03-4	12.62	48.75	50.20	59.84	61.63	96.9	97.6	0.8

Table 6. Results of the QA/QC analysis concerning replicates (precision determination).

Analyte (unit)	Batch ID	Sample ID	Sample	Duplicate	Mean	RPD
V (mg kg^{-1})	A	BL03-4	87.28	87.17	87.22	0.1
V	A	BL03-3	127.0	126.2	126.6	0.6
Cr	A	BL03-4	55.46	54.68	55.07	1.4
Cr	A	BL03-3	72.70	72.35	72.52	0.5
Mn	A	BL03-4	1222	1209	1215	1.1
Mn	A	BL03-3	310.5	314.3	312.4	1.2
Fe	A	BL03-3	30998	30805	30902	0.6
Fe	A	BL03-4	22087	21711	21899	1.7
Ni	A	BL03-3	40.63	41.13	40.88	1.2
Ni	A	BL03-4	27.23	27.74	27.48	1.8
Cu	A	BL03-4	19.87	20.94	20.40	5.3
Cu	A	BL03-3	42.27	43.07	42.67	1.9
Zn	A	BL03-3	110.4	112.8	111.6	2.1
Zn	A	BL03-4	60.21	60.96	60.59	1.2
As	A	BL03-3	18.36	18.60	18.48	1.3
As	A	BL03-4	9.97	9.71	9.84	2.6
Cd	A	BL03-3	0.233	0.225	0.229	3.4
Cd	A	BL03-4	0.196	0.196	0.196	0.2
Sn	A	BL03-3	1.76	1.79	1.77	1.6
Sn	A	BL03-4	1.53	1.51	1.52	1.1
Ba	A	BL03-3	511.6	482.8	497.2	5.8
Ba	A	BL03-4	355.0	359.2	357.1	1.2
Pb	A	BL03-3	19.10	19.05	19.08	0.2
Pb (mg kg^{-1})	A	BL03-4	11.03	11.05	11.04	0.2
THg (ng g^{-1})	B	BL03-4	11.68	13.56	12.62	14.9
% Total Solids	C	BL03-4	79.5	78.9	79.2	0.8
% Total Solids	C	BL03-17	79.6	79.5	79.6	0.1

Table 7. Results of the QA/QC analysis concerning analytical accuracy using certified reference materials, NIST 2709 and IAEA 405.

Analyte (unit)	Batch ID	CRM Identity	Cert Value	Obs Value	% Rec
V (mg kg^{-1})	A	NIST 2709	112.00	97.12	86.7
V	A	BlankSpike	80.00	85.78	107.2
V	A	IAEA 405	95.00	90.21	95.0
Cr	A	IAEA 405	84.00	67.42	80.3
Cr	A	BlankSpike	80.00	86.14	107.7
Cr	A	NIST 2709	130.00	93.28	71.8
Mn	A	NIST 2709	538.00	420.18	78.1
Mn	A	IAEA 405	495.00	384.99	77.8
Mn	A	BlankSpike	80.00	87.95	109.9
Fe	A	BlankSpike	80.00	58.29	72.9
Fe	A	NIST 2709	35000.00	28463.83	81.3
Fe	A	IAEA 405	37400.00	29885.25	79.9
Ni	A	IAEA 405	32.50	32.42	99.8
Ni	A	BlankSpike	80.00	93.66	117.1
Ni	A	NIST 2709	88.00	76.19	86.6
Cu	A	BlankSpike	80.00	89.09	111.4
Cu	A	NIST 2709	34.60	37.34	107.9
Cu	A	IAEA 405	47.70	54.28	113.8
Zn	A	IAEA 405	279.00	281.40	100.9
Zn	A	NIST 2709	106.00	106.90	100.8
Zn	A	BlankSpike	80.00	83.51	104.4
As	A	NIST 2709	17.70	16.84	95.1
As	A	IAEA 405	23.60	23.47	99.5
As	A	BlankSpike	80.00	75.32	94.2
Cd	A	BlankSpike	80.00	78.38	98.0
Cd	A	NIST 2709	0.38	0.65	172.1
Cd	A	IAEA 405	0.73	0.74	101.8
Sn	A	IAEA 405	7.60	9.54	125.5
Sn	A	BlankSpike	80.00	79.93	99.9
Ba	A	NIST 2709	968.00	845.36	87.3
Ba	A	BlankSpike	80.00	97.11	121.4
Pb	A	NIST 2709	18.90	19.29	102.1
Pb	A	IAEA 405	74.80	77.83	104.0
Pb (mg kg^{-1})	A	BlankSpike	80.00	78.63	98.3
THg (ng g^{-1})	B	IAEA 405	810.00	765.78	94.5

Table 8. Distribution (ng g^{-1} dry wt) of *n*-alkanes in gross sediments of Beaufort Lagoon. All sample numbers have the prefix BL03.

Sample ID – UCLA No.	**1**	**2**	**3**	**3D***	**4**	**4R***	**5B**	**6B**	**9**	**9B**	**9BD***	**10**	**11A**	**12**
Surrogate Recovery (%)														
Deu C14	nd[$]	52	52	53	56	57	53	55	52	62	62	52	55	53
Deu C24	nd[$]	66	67	69	69	64	70	63	65	76	76	76	66	67
Deu C36	nd[$]	67	78	75	61	66	72	65	66	66	79	66	65	67
***n*-alkane (ng g^{-1} dry wt)**														
n-C10	nd	nd	nd	nd	nd	nd	nd	nd	nd	nd	nd	nd	nd	nd
n-C11	nd	nd	nd	nd	nd	nd	62.9	217.6	nd	nd	nd	nd	nd	nd
n-C12	nd	nd	nd	nd	nd	nd	nd	nd	nd	nd	nd	nd	nd	nd
n-C13	nd	nd	nd	nd	nd	nd	nd	nd	nd	nd	nd	nd	nd	38.9
n-C14	nd	nd	nd	nd	nd	nd	nd	nd	nd	nd	nd	nd	nd	46.9
n-C15	67.1	34.4	60.7	52.6	nd	nd	38.7	72.3	45.5	41.1	30.7	0.0	55.1	70.9
n-C16	96.2	26.0	56.6	41.9	nd	nd	32.8	62.5	56.9	50.9	40.5	0.0	58.9	77.4
n-C17	184.3	70.9	192.5	172.5	3.2	3.8	117.0	198.8	192.8	98.5	76.0	51.6	137.6	163.6
pr	nd	nd	nd	nd	nd	nd	nd	nd	nd	nd	nd	nd	nd	51.6
n-C18	89.6	38.2	108.7	98.0	1.8	2.2	63.5	110.4	102.0	54.3	46.2	29.4	76.8	95.0
ph	nd	nd	nd	nd	nd	nd	nd	nd	nd	nd	nd	nd	nd	nd
n-C19	280.1	99.8	317.3	287.4	3.8	4.6	181.5	307.2	321.8	162.1	140.2	73.9	215.4	231.6
n-C20	166.5	65.2	198.8	180.4	2.8	3.4	116.9	202.4	191.1	110.5	96.5	52.3	148.5	167.6
n-C21	579.0	204.2	630.6	584.7	7.3	7.5	382.1	627.9	623.2	360.7	316.3	162.5	496.3	501.2
n-C22	312.8	116.1	323.6	311.7	5.1	5.7	196.5	332.7	330.7	196.8	180.1	91.0	285.4	292.6
n-C23	990.9	354.0	1056.6	974.1	13.2	14.9	672.8	1068.7	995.0	676.7	605.0	302.1	943.3	948.8
n-C24	268.7	105.7	287.0	294.6	5.6	6.0	186.8	318.7	305.5	188.1	184.1	86.3	277.8	279.1
n-C25	826.3	341.2	839.9	814.5	14.9	14.6	573.5	951.2	819.1	735.8	661.7	318.9	1403.9	1126.0
n-C26	126.6	58.2	153.8	146.9	3.9	3.6	103.0	178.8	146.2	112.4	109.5	48.8	155.5	162.3
n-C27	1015.9	472.0	1483.4	1450.0	18.1	18.5	867.3	1239.8	1738.7	1496.4	1370.4	460.7	1817.5	1985.2
n-C28	73.3	34.5	94.5	176.6	3.5	3.4	70.0	120.0	80.1	81.0	144.5	33.3	110.7	108.0
n-C29	886.5	376.5	1217.9	1346.5	17.9	18.6	933.4	1323.9	1054.3	1160.3	1450.2	414.2	1342.7	1413.3
n-C30	83.2	29.9	128.9	141.1	3.6	2.8	79.0	129.8	35.0	100.8	116.7	38.8	126.0	128.2
n-C31	749.0	308.8	1190.4	1330.8	18.4	18.4	889.2	1312.5	938.5	988.7	1152.2	378.4	1201.3	1269.8
n-C32	146.2	46.7	82.0	39.4	1.8	2.0	49.0	86.0	41.5	68.5	39.2	39.9	85.4	41.5
n-C33	210.3	90.1	378.7	444.7	7.1	7.1	274.4	424.7	264.6	300.5	375.4	119.7	377.4	407.1
n-C34	nd	26.7	58.2	63.3	2.4	2.0	nd	67.6	80.1	nd	47.9	nd	nd	71.0
n-C35	nd	nd	nd	44.7	2.0	2.6	nd	nd	nd	nd	nd	nd	nd	nd
n-C36	nd	nd	nd	nd	nd	nd	nd	nd	nd	nd	nd	nd	nd	nd
Total *n*-alkanes (ng g^{-1} dry wt)	7152.4	2899.1	8860.1	8996.4	136.5	142.0	5890.2	9353.3	8362.6	6984.2	7183.3	2701.9	9315.4	9625.9
Σ C12–C19 (ng g^{-1} dry wt)	717.3	269.4	735.9	652.3	8.8	10.7	433.5	751.2	719.0	407.0	333.5	155.0	543.7	724.4
Σ C20–C33 (ng g^{-1} dry wt)	6435.1	2603.0	8066.0	8236.0	123.2	126.7	5393.8	8316.9	7563.5	6577.3	6801.8	2546.9	8771.7	8830.5
Pr/Ph	nd	nd	nd	nd	nd	nd	nd	nd	nd	nd	nd	nd	nd	nd
Odd/Even**	4.2	4.3	4.9	5.0	3.5	3.5	5.5	4.7	5.1	6.3	6.1	5.4	6.0	5.7

Table 8. (continued)

Sample ID – UCLA No.	13	14	15	16	17	18	19	20	OS[#]	Pr. Blk	XSPIKE 1 % Recovery	XSPIKE 2 % Recovery	XSPIKE % Rec Avg
Surrogate Recovery (%)													
Deu C14	57	55	58	nd[$]	53	58	60	54	nd[$]	51	52	52	52
Deu C24	76	64	61	nd[$]	65	68	61	66	nd[$]	57	64	66	65
Deu C36	80	65	58	nd[$]	92	70	65	68	nd[$]	66	74	72	73
***n*-alkane (ng g^{-1} dry wt)**									**µg g^{-1} dry wt**				
n-C10	nd	nd	nd	nd	nd	nd	25.4	nd	499.6	nd	18	19	19
n-C11	nd	nd	nd	nd	nd	nd	34.2	nd	3761.2	nd	28	22	25
n-C12	nd	nd	nd	nd	nd	nd	17.3	nd	489.6	nd	33	35	34
n-C13	nd	32.2	nd	nd	nd	nd	nd	nd	253.8	nd	40	41	41
n-C14	nd	27.2	nd	nd	nd	nd	nd	nd	148.3	nd	50	50	50
n-C15	74.2	66.1	nd	nd	2.7	31.7	14.9	17.0	65.0	nd	57	58	57
n-C16	55.7	53.9	nd	223.8	2.0	31.4	15.2	9.6	nd	nd	66	64	65
n-C17	170.8	144.6	75.4	754.9	5.7	103.6	66.4	37.1	nd	nd	65	68	67
pr	nd	38.7	nd	nd	nd	13.1	7.7	nd	nd	nd	67	68	67
n-C18	94.4	80.1	41.0	339.8	3.9	58.9	37.5	19.1	nd	nd	69	69	69
ph	nd	18.4	nd	nd	nd	nd	nd	nd	nd	nd	69	69	69
n-C19	36.0	208.0	103.7	1141.0	1.9	174.1	122.4	62.6	nd	nd	70	70	70
n-C20	146.1	147.8	73.7	680.8	5.3	112.2	76.4	36.1	58.1	1.51	72	72	72
n-C21	421.2	464.0	227.0	2275.8	13.9	364.2	246.9	109.3	86.9	nd	72	72	72
n-C22	36.9	260.3	138.3	1238.2	7.5	199.6	127.8	61.3	53.2	nd	76	72	74
n-C23	831.6	834.4	444.2	4079.3	20.6	630.8	400.8	167.0	67.6	nd	69	66	68
n-C24	35.0	250.1	142.8	1116.4	6.9	186.7	112.7	51.3	71.8	nd	60	63	62
n-C25	911.3	888.6	491.9	3918.1	19.4	556.5	349.5	136.0	218.4	nd	65	69	67
n-C26	191.3	124.6	86.3	574.5	4.2	100.5	52.0	27.0	87.9	nd	70	69	70
n-C27	1608.1	1718.1	863.0	5131.4	20.6	1085.1	369.4	146.4	179.1	nd	69	70	69
n-C28	159.2	97.3	65.5	328.6	3.1	64.3	26.1	15.5	60.2	nd	66	70	68
n-C29	1628.0	1538.0	682.9	4763.2	25.7	855.6	325.2	143.7	138.0	nd	66	67	67
n-C30	149.4	98.4	60.2	334.1	2.2	93.1	41.0	20.4	230.1	nd	66	65	66
n-C31	1621.1	1150.4	600.7	4488.1	25.2	861.2	339.9	156.5	171.2	nd	67	64	66
n-C32	68.6	32.3	0.0	784.7	0.0	26.2	15.1	11.8	169.6	nd	64	69	66
n-C33	564.4	354.9	195.2	1339.2	8.3	271.3	110.5	51.0	nd	nd	66	63	64
n-C34	49.4	52.6	nd	330.4	nd	45.8	29.9	13.5	nd	nd	64	62	63
n-C35	75.2	30.2	nd	nd	nd	24.4	10.9	nd	nd	nd	60	63	62
n-C36	nd	nd	nd	nd	nd	nd	nd	nd	nd	nd	69	69	69
Total *n*-alkanes (ng g^{-1} dry wt)	8927.9	8654.2	4291.7	33842.3	179.2	5877.3	2967.7	1292.1	6819.4				
Σ C12–C19 (ng g^{-1} dry wt)	431.1	612.2	220.1	2459.5	16.1	399.7	273.8	145.3	956.6				
Σ C20–C33 (ng g^{-1} dry wt)	8372.3	7959.2	4071.7	31052.4	163.1	5407.4	2593.5	1133.3	1602.1				
Pr/Ph	nd	2.1	nd	nd	nd	na[†]	na[†]	nd	nd				
Odd/Even**	8.1	6.2	6.1	4.7	4.1	5.4	4.4	3.9	1.3				

* Duplicate (D) or replicate (R) analysis
** Summed *n*-C15–*n*-C36
[#] OS = oil spill sample; note change in units of concentration
nd[$] = dilution too great to measure surrogates
nd = not detected
na[†] = not applicable, phytane not detected

Table 9. Distribution (ng g^{-1} dry wt) of PAHs in gross sediments of Beaufort Lagoon. All lagoon sample numbers have the prefix BL03.

Sample ID – UCLA No.	1	2	3	3D*	4	5B	6B
Surrogate Recovery (%)							
hexamethylbenzene	62	53	50	50	38	41	44
n-dodecylbenzene	57	58	62	64	59	59	60
4-terphenyl-D14	64	60	75	68	68	65	57
PAH (ng g^{-1} dry wt)							
naphthalene	7.7	7.4	13.0	16.7	nd	7.3	6.7
C1-naphthalenes	18.9	21.3	26.3	27.2	nd	15.4	21.4
2-methylnaphthalene	10.0	10.7	14.8	14.9	nd	6.4	12.1
1-methylnaphthalene	8.9	10.6	11.6	12.4	nd	9.0	9.4
C2-naphthalenes	27.1	33.3	41.6	48.2	0.4	28.9	50.0
2,6-dimethylnaphthalene	8.0	8.5	6.9	7.5	nd	5.6	16.0
C3-naphthalenes	14.7	26.8	34.1	37.8	0.5	13.8	39.6
2,3,5-trimethylnaphthalene	nd	4.4	6.1	7.0	nd	2.4	3.8
C4-naphthalenes	1.7	12.0	17.9	19.8	nd	7.0	18.9
biphenyl	5.6	4.3	9.2	9.9	nd	4.9	7.1
acenaphthylene	nd	nd	nd	nd	nd	nd	nd
acenaphthene	nd	0.6	0.9	1.1	nd	nd	nd
fluorene	nd	2.9	4.9	5.1	nd	2.7	5.4
2-methylfluorene	nd	2.7	4.3	5.1	nd	nd	nd
C1-fluorenes	3.2	3.8	6.4	nd	tr	2.8	5.8
C2-fluorenes	4.9	6.7	13.3	nd	tr	6.4	18.6
C3-fluorenes	tr	tr	nd	nd	nd	tr	tr
phenanthrene	19.5	15.2	27.8	32.0	1.1	17.9	33.4
1-methylphenanthrene	4.4	4.9	6.7	7.5	nd	3.4	8.8
anthracene	1.6	nd	1.3	1.3	nd	nd	nd
C1-phenanthrenes/anthracenes	47.9	51.3	72.5	77.1	20.8	34.6	123.2
C2-phenanthrenes/anthracenes	12.8	26.7	32.6	35.7	1.8	19.4	57.5
3,6-dimethylphenanthrene	nd	1.2	3.7	4.2	nd	nd	1.8
C3-phenanthrenes/anthracenes	18.0	23.7	43.7	46.6	4.7	22.2	58.3
C4-phenanthrenes/anthracenes	5.2	10.9	17.0	17.5	1.0	9.5	28.0
2,3-benzofluorene	nd	1.6	2.5	3.2	nd	1.3	2.9
1,1´-binaphthalene	nd	nd	nd	nd	nd	nd	nd
dibenzothiophene**	nd	3.4	5.4	7.6	0.2	3.4	6.7
C1-dibenzothiophenes**	2.5	3.5	3.5	3.8	0.3	2.1	6.3
C2-dibenzothiophenes**	2.6	4.6	6.1	6.6	nd	2.9	12.0
C3-dibenzothiophenes**	5.9	23.7	6.5	6.8	nd	1.8	6.8
C4-dibenzothiophenes**	nd	tr	1.8	1.9	nd	nd	nd
fluoranthene	3.8	2.7	4.1	4.3	nd	2.5	5.6
pyrene	5.7	4.9	7.6	8.6	0.6	4.4	9.6
C1-fluoranthenes/pyrenes	3.8	4.2	6.8	7.1	tr	4.3	10.8
C2-fluoranthenes/pyrenes	7.5	7.2	7.9	8.1	tr	7.2	12.8

	1	2	3	3D*	4	5B	6B
PAH (ng g^{-1} dry wt) (cont.)							
C3-fluoranthenes/pyrenes	4.9	2.6	2.2	2.3	nd	1.3	5.2
C4-fluoranthenes/pyrenes	nd	1.7	3.3	3.6	nd	tr	6.3
benz(a)anthracene	4.0	1.4	2.7	3.7	0.5	1.3	3.9
chrysene/triphenylene	12.0	8.0	14.8	15.3	0.8	9.5	19.4
C1-chrysenes/triphenylenes	7.9	9.2	12.5	13.0	tr	7.6	18.9
C2-chrysenes/triphenylenes	2.6	4.3	6.0	6.4	nd	1.0	8.1
C3-chrysenes/triphenylenes	tr	tr	nd	nd	nd	nd	nd
C4-chrysenes/triphenylenes	nd	nd	nd	nd	nd	nd	nd
benzo(k)fluoranthene	3.8	1.0	1.0	1.1	0.3	0.5	1.8
benzo(b)fluoranthene	7.6	4.5	8.0	8.5	0.5	6.8	13.3
benzo(e)pyrene	9.2	5.6	8.1	8.8	0.5	5.4	12.0
benzo(a)pyrene	3.8	1.6	1.6	1.9	0.2	1.5	1.7
9,10-diphenylanthracene	nd	nd	nd	nd	nd	nd	nd
perylene	30.3	35.9	42.5	43.1	2.6	22.1	53.4
indeno(1,2,3-cd)pyrene	nd	nd	nd	nd	nd	nd	nd
dibenz(a,h)anthracene	nd	nd	nd	nd	nd	nd	nd
picene	nd	nd	nd	nd	nd	nd	nd
benzo(ghi)perylene	nd	3.6	4.6	5.0	nd	nd	nd
anthanthrene	nd	nd	nd	nd	nd	nd	nd
coronene	nd	nd	nd	nd	nd	nd	nd
1,2,4,5-dibenzopyrene	nd	nd	nd	nd	nd	nd	nd
C1-C20H12 aromatics	9.5	5.1	6.9	7.2	nd	5.5	15.3
C2-C20H12 aromatics	tr	1.7	2.6	2.7	nd	1.0	2.9
C3-C20H12 aromatics	nd	tr	nd	nd	nd	nd	nd
C4-C20H12 aromatics	nd	tr	nd	nd	nd	nd	nd
sum-naphthalenes(N)	70.1	100.9	132.9	149.6	0.9	72.3	136.7
sum-fluorenes(F)	8.1	13.4	24.6	5.1	nd	11.9	29.8
sum-phenanthrenes/anthracenes(PA)	105.1	127.9	194.8	210.2	29.3	103.6	300.5
sum-dibenzothiophenes(D)	11.0	35.2	23.3	26.7	0.6	10.2	31.8
sum-fluoranthenes/pyrenes(FP)	25.8	23.2	31.8	33.9	0.6	19.7	50.3
sum-chrysenes(C)	22.5	21.5	33.3	34.7	0.8	18.2	46.4
sum-C20H12 aromatics(C20)	64.2	55.2	70.6	73.4	4.1	42.9	100.3
sum- 4,5 PAH (4,5 PAH)	107.0	94.6	128.9	135.8	6.0	75.4	182.7
sum-PAH(t-PAH)	316.4	388.8	531.3	556.7	36.7	286.3	709.7
N/PA	0.67	0.79	0.68	0.71	0.03	0.70	0.46
N/perylene	2.31	2.81	3.13	3.47	0.34	3.26	2.56
F/perylene	0.27	0.37	0.58	0.12	nd	0.54	0.56
PA/perylene	3.47	3.56	4.59	4.88	11.16	4.68	5.62
FP/perylene	0.85	0.65	0.75	0.79	0.22	0.89	0.94
t-PAH/perylene	10.45	10.83	12.51	12.92	13.99	12.93	13.29

Table 9. (continued)

Sample ID – UCLA No.	9	9B	10	11A	12	13	14
Surrogate Recovery (%)							
hexamethylbenzene	46	43	39	44	40	40	45
n-dodecylbenzene	66	50	59	62	56	56	59
4-terphenyl-D14	72	63	72	63	69	69	71
PAH (ng g^{-1} dry wt)							
naphthalene	8.3	7.6	1.7	8.9	3.3	1.0	9.7
C1-naphthalenes	19.2	12.4	4.4	26.4	18.2	4.6	25.9
2-methylnaphthalene	9.7	7.0	2.5	13.8	9.3	2.7	14.8
1-methylnaphthalene	9.5	5.5	2.0	12.7	8.9	1.9	11.2
C2-naphthalenes	23.3	19.5	7.8	42.7	46.9	9.4	46.7
2,6-dimethylnaphthalene	7.3	6.2	2.0	14.4	12.9	2.5	12.1
C3-naphthalenes	16.5	13.6	7.7	33.0	40.1	7.4	34.0
2,3,5-trimethylnaphthalene	3.0	nd	nd	3.1	4.2	0.9	4.1
C4-naphthalenes	7.0	6.5	2.6	13.1	16.1	4.6	18.4
biphenyl	4.5	4.8	1.3	7.2	4.7	1.5	5.9
acenaphthylene	nd	nd	nd	nd	nd	nd	nd
acenaphthene	nd	nd	nd	nd	nd	nd	nd
fluorene	2.5	2.6	nd	4.3	4.0	1.1	4.0
2-methylfluorene	nd	nd	nd	nd	3.1	0.8	3.0
C1-fluorenes	3.5	3.1	1.2	5.3	5.5	1.2	6.3
C2-fluorenes	6.0	5.6	2.6	15.0	13.1	1.9	13.1
C3-fluorenes	tr	tr	tr	tr	tr	tr	tr
phenanthrene	14.9	17.3	5.3	24.0	25.1	6.4	21.3
1-methylphenanthrene	3.1	5.1	1.6	6.7	8.0	1.9	6.5
anthracene	nd	nd	nd	nd	nd	nd	nd
C1-phenanthrenes/anthracenes	25.9	37.2	41.5	112.8	138.0	56.6	193.7
C2-phenanthrenes/anthracenes	15.9	18.1	10.0	36.0	52.7	11.9	47.3
3,6-dimethylphenanthrene	1.2	1.2	0.4	1.8	1.8	0.4	1.9
C3-phenanthrenes/anthracenes	15.0	14.1	17.2	63.7	82.7	21.4	100.4
C4-phenanthrenes/anthracenes	6.3	7.8	5.4	20.3	18.6	6.4	22.9
2,3-benzofluorene	1.1	nd	0.3	2.1	2.6	nd	2.1
1,1′-binaphthalene	nd	nd	nd	nd	nd	nd	nd
dibenzothiophene**	3.5	3.3	1.0	5.0	nd	1.4	3.7
C1-dibenzothiophenes**	2.1	1.8	1.5	4.4	6.5	1.5	6.0
C2-dibenzothiophenes**	3.1	1.2	1.2	6.3	8.5	nd	4.1
C3-dibenzothiophenes**	8.0	nd	0.7	4.2	8.4	nd	3.1
C4-dibenzothiophenes**	tr	nd	nd	nd	tr	nd	nd
fluoranthene	3.2	2.4	0.9	4.1	5.1	1.2	3.7
pyrene	4.6	4.8	1.5	6.5	8.5	2.1	7.6
C1-fluoranthenes/pyrenes	3.0	3.4	1.7	6.7	8.0	2.3	7.6
C2-fluoranthenes/pyrenes	3.1	7.8	2.6	7.7	11.4	2.5	8.8

	9	9B	10	11A	12	13	14
PAH (ng g^{-1} dry wt) (cont.)							
C3-fluoranthenes/pyrenes	1.6	2.9	1.3	2.0	3.7	1.0	3.6
C4-fluoranthenes/pyrenes	nd	3.2	1.1	nd	tr	nd	1.9
benz(a)anthracene	1.8	1.7	0.6	1.6	2.0	0.9	2.1
chrysene/triphenylene	9.3	8.9	3.3	12.3	15.6	3.9	12.8
C1-chrysenes/triphenylenes	6.7	6.8	2.4	12.4	18.5	3.2	14.6
C2-chrysenes/triphenylenes	1.9	2.4	0.9	4.8	12.4	tr	6.0
C3-chrysenes/triphenylenes	nd	nd	nd	3.8	tr	nd	nd
C4-chrysenes/triphenylenes	nd	nd	nd	nd	tr	nd	nd
benzo(k)fluoranthene	nd	0.6	0.3	1.1	1.3	0.4	1.2
benzo(b)fluoranthene	4.7	5.3	2.1	7.0	8.5	2.2	9.6
benzo(e)pyrene	4.1	4.8	2.0	5.9	9.6	2.5	7.5
benzo(a)pyrene	nd	nd	0.4	nd	nd	nd	nd
9,10-diphenylanthracene	nd	nd	nd	nd	nd	nd	nd
perylene	15.6	79.8	13.7	32.5	44.8	16.5	20.3
indeno(1,2,3-cd)pyrene	nd	nd	nd	nd	nd	nd	nd
dibenz(a,h)anthracene	nd	nd	nd	nd	nd	nd	nd
picene	nd	nd	nd	nd	nd	nd	nd
benzo(ghi)perylene	nd	nd	nd	4.8	7.6	nd	nd
anthanthrene	nd	nd	nd	nd	nd	nd	nd
coronene	nd	nd	nd	nd	nd	nd	nd
1,2,4,5-dibenzopyrene	nd	nd	nd	nd	nd	nd	nd
C1-C20H12 aromatics	2.7	4.4	3.1	4.6	2.2	3.1	4.3
C2-C20H12 aromatics	nd	3.7	0.7	tr	tr	nd	2.2
C3-C20H12 aromatics	nd	nd	nd	tr	nd	nd	nd
C4-C20H12 aromatics	nd	nd	nd	nd	nd	nd	nd
sum-naphthalenes(N)	74.3	59.5	24.2	124.0	124.7	26.9	134.7
sum-fluorenes(F)	12.0	11.3	3.8	24.6	22.6	25.6	23.4
sum-phenanthrenes/anthracenes(PA)	81.5	94.5	79.4	256.8	317.1	102.7	385.6
sum-dibenzothiophenes(D)	16.8	6.3	4.4	19.9	23.5	2.9	17.0
sum-fluoranthenes/pyrenes(FP)	15.5	24.6	9.1	27.1	36.7	9.2	33.2
sum-chrysenes(C)	17.8	18.1	6.6	33.3	46.5	7.1	33.4
sum-C20H12 aromatics(C20)	27.1	98.6	22.3	51.1	66.4	24.7	45.2
sum- 4,5 PAH (4,5 PAH)	59.6	134.8	34.8	108.4	149.4	38.7	107.3
sum-PAH(t-PAH)	252.6	319.4	152.0	552.5	654.5	201.4	682.6
N/PA	0.91	0.63	0.30	0.48	0.39	0.26	0.35
N/perylene	4.78	0.75	1.77	3.82	2.79	1.63	6.64
F/perylene	0.77	0.14	0.28	0.76	0.51	1.55	1.15
PA/perylene	5.24	1.18	5.80	7.90	7.09	6.23	19.00
FP/perylene	1.00	0.31	0.66	0.83	0.82	0.56	1.64
t-PAH/perylene	16.24	4.00	11.11	17.00	14.62	12.23	33.63

Table 9. (continued)

Sample ID – UCLA No.	15	16	17	18	19	20	OS#
Surrogate Recovery (%)							µg g^{-1} dry wt
hexamethylbenzene	44	46	43.0	47	40	51	50
n-dodecylbenzene	63	59	50.0	58	59	56	61
4-terphenyl-D14	70	68	69.0	63	68	69	70
PAH (ng g^{-1} dry wt)							
naphthalene	nd	9.1	nd	9.6	1.3	0.5	2.9
C1-naphthalenes	nd	11.9	0.1	24.2	2.7	1.0	nd
2-methylnaphthalene	nd	8.7	0.1	12.1	1.5	0.5	nd
1-methylnaphthalene	nd	3.3	nd	12.0	1.2	0.5	4.8
C2-naphthalenes	nd	20.9	0.3	34.6	4.5	1.9	83.0
2,6-dimethylnaphthalene	nd	7.5	nd	10.0	1.4	0.4	31.0
C3-naphthalenes	4.9	7.7	0.3	26.2	4.3	1.4	44.2
2,3,5-trimethylnaphthalene	nd	nd	nd	4.5	0.8	nd	7.4
C4-naphthalenes	5.9	nd	nd	13.2	2.1	0.6	15.0
biphenyl	nd	4.8	0.1	5.4	0.8	0.3	nd
acenaphthylene	nd	nd	nd	nd	nd	nd	nd
acenaphthene	nd	nd	nd	nd	nd	nd	0.5
fluorene	nd	nd	nd	3.3	0.7	nd	1.5
2-methylfluorene	nd	nd	nd	2.7	0.4	nd	2.2
C1-fluorenes	2.7	nd	0.3	3.9	0.9	0.8	2.0
C2-fluorenes	8.5	nd	0.4	10.6	3.7	1.6	2.1
C3-fluorenes	tr	nd	tr	nd	tr	tr	nd
phenanthrene	10.3	17.1	1.0	18.3	3.6	1.9	2.3
1-methylphenanthrene	nd	3.7	nd	4.8	0.9	nd	1.1
anthracene	nd	nd	nd	nd	nd	nd	0.7
C1-phenanthrenes/anthracenes	86.7	25.3	15.0	124.1	24.2	109.3	3.8
C2-phenanthrenes/anthracenes	25.8	13.6	1.4	36.5	6.5	10.6	4.4
3,6-dimethylphenanthrene	nd	nd	nd	1.8	0.2	nd	0.3
C3-phenanthrenes/anthracenes	64.0	6.8	7.2	61.9	21.9	57.4	5.7
C4-phenanthrenes/anthracenes	13.5	nd	1.4	24.3	5.9	6.2	2.1
2,3-benzofluorene	1.4	nd	nd	1.3	nd	nd	nd
1,1´-binaphthalene	nd	nd	nd	nd	nd	nd	nd
dibenzothiophene**	2.2	nd	0.2	2.8	0.5	0.3	nd
C1-dibenzothiophenes**	3.2	nd	0.3	3.5	0.7	0.6	0.4
C2-dibenzothiophenes**	3.2	nd	0.1	2.8	0.8	0.4	0.3
C3-dibenzothiophenes**	4.3	nd	tr	2.1	0.9	1.4	0.5
C4-dibenzothiophenes**	nd	nd	nd	nd	tr	nd	0.5
fluoranthene	2.4	2.6	0.2	3.2	1.8	0.7	2.5
pyrene	4.3	4.5	0.3	4.9	2.0	0.8	2.0
C1-fluoranthenes/pyrenes	4.5	0.9	0.1	5.6	1.0	0.7	0.9
C2-fluoranthenes/pyrenes	3.7	nd	0.3	5.2	0.8	1.2	1.1

	15	16	17	18	19	20	OS#
PAH (ng g^{-1} dry wt) (cont.)							µg g^{-1} dry wt
C3-fluoranthenes/pyrenes	1.5	nd	tr	2.4	0.6	0.3	1.1
C4-fluoranthenes/pyrenes	2.0	nd	nd	tr	0.7	0.2	1.4
benz(a)anthracene	0.8	4.8	0.1	1.6	0.4	nd	2.5
chrysene/triphenylene	6.8	10.2	0.3	9.9	3.7	1.3	2.8
C1-chrysenes/triphenylenes	6.1	6.6	0.1	10.5	4.3	0.7	1.6
C2-chrysenes/triphenylenes	2.5	nd	nd	2.0	5.3	0.4	2.4
C3-chrysenes/triphenylenes	nd	nd	nd	nd	1.1	nd	2.6
C4-chrysenes/triphenylenes	nd	nd	nd	nd	tr	nd	2.1
benzo(k)fluoranthene	0.8	nd	nd	0.7	0.4	nd	nd
benzo(b)fluoranthene	3.8	5.9	0.2	5.7	1.1	nd	nd
benzo(e)pyrene	4.5	nd	0.2	6.1	1.5	nd	nd
benzo(a)pyrene	nd	nd	nd	nd	nd	nd	nd
9,10-diphenylanthracene	nd	nd	nd	nd	nd	nd	nd
perylene	19.2	29.2	nd	18.8	4.8	1.1	nd
indeno(1,2,3-cd)pyrene	nd	nd	nd	nd	nd	nd	nd
dibenz(a,h)anthracene	nd	nd	nd	nd	nd	nd	nd
picene	nd	nd	nd	nd	nd	nd	nd
benzo(ghi)perylene	nd	nd	nd	5.3	nd	nd	nd
anthanthrene	nd	nd	nd	nd	nd	nd	nd
coronene	nd	nd	nd	nd	nd	nd	nd
1,2,4,5-dibenzopyrene	nd	nd	nd	nd	nd	nd	nd
C1-C20H12 aromatics	4.2	tr	0.3	2.9	0.7	1.9	7.5
C2-C20H12 aromatics	nd	tr	nd	nd	tr	0.8	4.1
C3-C20H12 aromatics	nd	nd	nd	nd	nd	nd	1.7
C4-C20H12 aromatics	nd	nd	nd	nd	nd	nd	nd
sum-naphthalenes(N)	10.9	49.6	0.7	107.8	14.8	5.3	145.0
sum-fluorenes(F)	11.2	nd	0.7	17.8	5.4	2.4	5.5
sum-phenanthrenes/anthracenes(PA)	200.3	62.8	26.0	265.0	62.2	185.5	19.0
sum-dibenzothiophenes(D)	12.8	nd	0.6	11.3	2.8	2.6	1.7
sum-fluoranthenes/pyrenes(FP)	18.5	8.0	0.9	21.3	6.9	3.9	8.9
sum-chrysenes(C)	15.4	16.8	0.4	22.3	14.4	2.3	11.4
sum-C20H12 aromatics(C20)	32.5	35.2	0.7	34.1	8.5	3.8	13.3
sum- 4,5 PAH (4,5 PAH)	62.9	64.7	1.9	76.4	29.5	7.4	22.8
sum-PAH(t-PAH)	303.7	181.9	30.3	493.2	116.3	206.1	207.9
N/PA	0.05	0.79	0.03	0.41	0.24	0.03	7.62
N/perylene	0.57	1.70	na	5.75	3.06	4.80	na
F/perylene	0.58	nd	na	0.95	1.11	2.14	na
PA/perylene	10.45	2.15	na	14.13	12.85	167.36	na
FP/perylene	0.96	0.27	na	1.13	1.43	3.54	na
t-PAH/perylene	15.84	6.22	na	26.30	24.01	185.96	na

Table 9. (continued)

Sample ID – UCLA No.	Pr. Blk	X-SPIKE 1	X-SPIKE 2	X-SPIKE Avg	Ref Sed SRM 1941†	NIST Values†
Surrogate Recovery (%)						
hexamethylbenzene	40	55	55	55	43	
n-dodecylbenzene	65	71	61	66	64	
4-terphenyl-D14	75	83	93	88	67	
PAH (ng g^{-1} dry wt)						
naphthalene	nd	34	30	32	1230	1322±14
C1-naphthalenes	nd			43		
2-methylnaphthalene	nd	44	40	42	336	406±36
1-methylnaphthalene	nd	43	45	44	214	229±19
C2-naphthalenes	nd			49		
2,6-dimethylnaphthalene	nd	50	48	49	237	198±23
C3-naphthalenes	nd			57		
2,3,5-trimethylnaphthalene	nd	59	55	57	87	96.3
C4-naphthalenes	nd			57		
biphenyl	nd	57	65	61	104	115±15
acenaphthylene	nd	58	60	59	106	115±10
acenaphthene	nd	57	53	55	46	52±2
fluorene	nd	57	59	58	88	104±5
2-methylfluorene	nd	80	76	78	61	73.7
C1-fluorenes	nd			78		
C2-fluorenes	nd			75		
C3-fluorenes	nd			75		
phenanthrene	nd	81	79	77	551	577±59
1-methylphenanthrene	nd	80	76	78	92	109±6
anthracene	nd	78	78	78	171	202±42
C1-phenanthrenes/anthracenes	nd			78		
C2-phenanthrenes/anthracenes	nd			75		
3,6-dimethylphenanthrene	nd	79	71	75	56	78.0
C3-phenanthrenes/anthracenes	nd			75		
C4-phenanthrenes/anthracenes	nd			75		
2,3-benzofluorene	nd	76	84	80	139	124.8
1,1´-binaphthalene	nd	70	82	76	98	117.0
dibenzothiophene**	nd	35	41	38	163	209.8
C1-dibenzothiophenes**	nd			78		
C2-dibenzothiophenes**	nd			75		
C3-dibenzothiophenes**	nd			75		
C4-dibenzothiophenes**	nd			75		
fluoranthene	nd	80	88	84	1132	1220±240

Sample ID – UCLA No.	Pr. Blk	X-SPIKE 1	X-SPIKE 2	X-SPIKE Avg	Ref Sed SRM 1941†	NIST Values†
PAH (ng g^{-1} dry wt) (cont.)						
pyrene	nd	78	86	82	976	1080±200
C1-fluoranthenes/pyrenes	nd			78		
C2-fluoranthenes/pyrenes	nd			75		
C3-fluoranthenes/pyrenes	nd			75		
C4-fluoranthenes/pyrenes	nd			75		
benz(a)anthracene	nd	59	63	61	449	550±79
chrysene/triphenylene	nd	88	84	86	622	641.0
C1-chrysenes/triphenylenes	nd			78		
C2-chrysenes/triphenylenes	nd			75		
C3-chrysenes/triphenylenes	nd			75		
C4-chrysenes/triphenylenes	nd			75		
benzo(k)fluoranthene	nd	61	67	64	386	444±49
benzo(b)fluoranthene	nd	74	74	74	712	780±19
benzo(e)pyrene	nd	68	60	64	534	573.0
benzo(a)pyrene	nd	56	62	59	561	670±130
9,10-diphenylanthracene	nd	77	74	76		
perylene	nd	68	62	65	397	422±33
indeno(1,2,3-cd)pyrene	nd	63	64	63	466	569±40
dibenz(a,h)anthracene	nd	62	60	61		
picene	nd	69	71	70		
benzo(ghi)perylene	nd	62	66	64	438	516±83
anthanthrene	nd	52	56	54		
coronene	nd	70	70	70		
1,2,4,5-dibenzopyrene	nd	58	66	62		
C1-C20H12 aromatics	nd			78		
C2-C20H12 aromatics	nd			75		
C3-C20H12 aromatics	nd			75		
C4-C20H12 aromatics	nd			75		

* Duplicate analysis
** Very low recovery due to activated copper treatment for sulfur removal
# OS = oil spill sample; note change in units of concentration

nd = not detected, below MDL
tr = trace amounts, not quantifiable
na = not applicable

% recovery of some methylated homologs assumed to be the same as that of methylated phenanthrenes

Table 10. Distribution (ng g^{-1} dry wt) of triterpenoids in gross sediments of Beaufort Lagoon. All sample numbers have the prefix BL03. O. is the oil spill sample.

SAMPLE ID – UCLA No. Triterpanes (ng g^{-1} dry wt)*	**1**	**2**	**3**	**4**	**5B**	**6B**	**9**	**9B**	**10**	**11A**
18α(H),21β(H)-22,29,30-trisnorhopane	tr[#]	tr	tr	tr	tr	2	1	1	1	1
17 α(H),21 β(H)-22,29,30-trisnorhopane	9	tr	6	tr	tr	6	4	3	1	3
17 β(H),21 β(H)-22,29,30-trisnorhopane	54	20	51	1	24	51	55	25	14	27
17 α(H),18α(H),21 β(H)-28,30-bisnorhopane	nd[##]	nd	nd	nd	nd	nd	nd	nd	nd	nd
17 α(H),21 β(H)-30-norhopane	16	10	20	1	11	22	18	11	2	13
17 β(H),21α(H)-30-norhopane	32	12	30	1	15	32	28	15	8	17
17 β(H),21 β(H)-30-norhopane**	138	37	111	2	61	125	128	39	33	39
18 α(H)-oleanane	nd	nd	nd	nd	nd	nd	nd	nd	nd	nd
17 α(H),21 β(H)-hopane	8	5	11	1	5	13	7	5	3	7
17 β(H),21α(H)-hopane	tr	9	nd	tr	16	tr	tr	27	tr	nd
17 β(H),21 β(H)-hopane	14	6	14	nd	7	14	12	6	3	8
22S-17 α(H),21 β(H)-30-homohopane	nd	nd	nd	nd	nd	nd	nd	nd	nd	nd
22R-17 α(H),21 β(H)-30-homohopane	tr	tr	tr	nd	nd	15	tr	nd	nd	nd
17 β(H),21 β(H)-30-homohopane	10	3	13	tr	6	13	8	6	2	5
22S-17 α(H),21 β(H)-30,31-bishomohopane	nd	nd	nd	nd	nd	nd	nd	nd	nd	nd
22R-17 α(H),21 β(H)-30,31-bishomohopane	nd	nd	tr	nd	nd	nd	nd	nd	nd	nd
22S-17 α(H),21 β(H)-30,31-trishomohopane	nd	nd	nd	nd	nd	nd	nd	nd	nd	nd
22R-17 α(H),21 β(H)-30,31-trishomohopane	nd	nd	nd	nd	nd	nd	nd	nd	nd	nd
22S-17 α(H),21 β(H)-30,31-tetrahomohopane	nd	nd	nd	nd	nd	nd	nd	nd	nd	nd
22R-17 α(H),21 β(H)-30,31-tetrahomohopane	nd	nd	nd	nd	nd	nd	nd	nd	nd	nd
hop-13(18)-ene	32	13	25	1	14	26	40	27	8	4
hop-21(22)-ene	nd	nd	nd	nd	nd	nd	nd	nd	nd	nd
diploptene	260	112	182	3	148	254	181	173	93	116

SAMPLE ID – UCLA No. Triterpanes (ng g^{-1} dry wt)*	**12**	**13**	**14**	**15**	**16**	**17**	**18**	**19**	**20**	**OS µg g^{-1} dry wt**
18α(H),21β(H)-22,29,30-trisnorhopane	1	3	1	3	nd	nd	1	1	nd	56
17 α(H),21 β(H)-22,29,30-trisnorhopane	6	8	5	4	13	nd	5	2	1	57
17 β(H),21 β(H)-22,29,30-trisnorhopane	44	32	36	16	202	nd	46	18	7	nd
17 α(H),18α(H),21 β(H)-28,30-bisnorhopane	nd	nd	nd	nd	nd	nd	nd	nd	nd	nd
17 α(H),21 β(H)-30-norhopane	24	23	23	15	57	1	19	8	2	315
17 β(H),21α(H)-30-norhopane	24	17	18	11	118	1	26	11	5	30
17 β(H),21 β(H)-30-norhopane**	87	70	83	29	398	1	107	45	13	56
18 α(H)-oleanane	nd	nd	nd	nd	nd	nd	nd	nd	nd	nd
17 α(H),21 β(H)-hopane	11	16	9	9	18	nd	8	3	1	263
17 β(H),21α(H)-hopane	tr	nd	nd	12	nd	nd	nd	nd	nd	nd
17 β(H),21 β(H)-hopane	13	11	10	2	44	nd	13	4	2	nd
22S-17 α(H),21 β(H)-30-homohopane	nd	nd	nd	nd	nd	nd	nd	nd	nd	103
22R-17 α(H),21 β(H)-30-homohopane	nd	6	nd	nd	nd	nd	nd	1	nd	68
17 β(H),21 β(H)-30-homohopane	11	6	9	3	11	nd	11	3	2	nd
22S-17 α(H),21 β(H)-30,31-bishomohopane	nd	nd	nd	nd	nd	nd	nd	nd	nd	44
22R-17 α(H),21 β(H)-30,31-bishomohopane	nd	nd	nd	nd	nd	nd	nd	nd	nd	31
22S-17 α(H),21 β(H)-30,31-trishomohopane	nd	nd	nd	nd	nd	nd	nd	nd	nd	27
22R-17 α(H),21 β(H)-30,31-trishomohopane	nd	nd	nd	nd	nd	nd	nd	nd	nd	7
22S-17 α(H),21 β(H)-30,31-tetrahomohopane	nd	nd	nd	nd	nd	nd	nd	nd	nd	7
22R-17 α(H),21 β(H)-30,31-tetrahomohopane	nd	nd	nd	nd	nd	nd	nd	nd	nd	Tr
hop-13(18)-ene	32	30	18	15	53	nd	21	9	2	?
hop-21(22)-ene	nd	nd	nd	nd	nd	nd	nd	nd	nd	nd
diploptene	352	211	314	143	903	1	184	64	28	nd

* Quantification based on m/z 191; also note change in the units for OS sample
** May be coeluting with C30 βα hopane in some samples
[#] Trace amounts, not quantifiable [##] Not detected, below detection limits

Table 11. Distribution (ng g^{-1} dry wt) of steroids in gross sediments of Beaufort Lagoon. All sample numbers have the prefix BL03. OS is the oil spill sample.

SAMPLE ID – UCLA No. Steranes (ng g^{-1} dry wt)*		1	2	3	4	5B	6B	9	9B	10	11A
5α(H)androstane		nd[##]	nd	nd	nd	nd	nd	nd	nd	nd	nd
5α(H)pregnane		nd	nd	1.4	0.1	nd	nd	nd	nd	nd	nd
5β(H)pregnane		nd	0.7	1.6	0.1	0.7	2.8	1.1	nd	nd	nd
20-methyl-5α(H)pregnane		nd	nd	nd	0.2	0.4	1.0	nd	nd	nd	nd
20S-13β(H),17α(H)-diacholestane**	S1[#]	nd	nd	nd	0.3	0.8	3.7	1.0	0.9	nd	1.3
20R-13β(H),17α(H)-diacholestane	S2	nd	nd	nd	0.2	0.7	2.3	0.7	0.9	nd	nd
20S-5α(H),14α(H),17α(H)-cholestane	S3	nd	nd	nd	0.2	0.8	2.6	1.1	1.0	nd	1.2
20R-5α(H),14α(H),17α(H)-cholestane	S6	nd	nd	nd	0.2	0.8	2.6	0.8	nd	nd	nd
20R-5α(H),14β(H),17β(H)-cholestane	S4	nd	nd	nd	0.4	2.8	6.7	1.8	nd	nd	nd
20S-5α(H),14β(H),17β(H)-cholestane	S5	nd	nd	nd	0.2	1.5	5.2	nd	nd	nd	3.3
20R-24-ethyl-13β(H),17α(H)-diacholestane	S7	nd	nd	nd	0.2	1.2	3.2	1.8	nd	nd	nd
20S-5α(H),14α(H),17α(H)-ergostane	S8	nd	nd	nd	nd	nd	nd	nd	nd	1.3	nd
20R-5α(H),14α(H),17α(H)-ergostane	S11	nd	nd	nd	0.2	nd	nd	2.5	nd	nd	nd
20R-5α(H),14β(H),17β(H)-ergostane	S9	nd	nd	nd	nd	nd	nd	nd	nd	nd	nd
20S-5α(H),14β(H),17β(H)-ergostane	S10	nd	nd	nd	0.2	nd	nd	nd	nd	nd	nd
20S-5α(H),14α(H),17α(H)-stigmastane	S12	nd	nd	nd	0.2	nd	nd	nd	nd	nd	nd
20R-5α(H),14α(H),17α(H)-stigmastane	S15	7.5	6.9	5.4	0.1	3.1	3.2	1.6	1.4	2.0	1.1
20R-5α(H),14β(H),17β(H)-stigmastane	S13	nd	nd	nd	0.3	0.8	2.3	1.5	nd	1.1	nd
20S-5α(H),14β(H),17β(H)-stigmastane	S14	nd	nd	nd	nd	nd	nd	nd	nd	nd	nd

SAMPLE ID – UCLA No. Steranes (ng g^{-1} dry wt)*		12	13	14	15	16	17	18	19	20	OS μg g^{-1} dry wt
5α(H)androstane		nd	nd	nd	nd	nd	nd	nd	nd	nd	8
5α(H)pregnane		nd	1.5	0.8	nd	nd	nd	nd	nd	nd	8
5β(H)pregnane		1.4	4.2	1.9	2.1	nd	0.1	nd	0.7	nd	11
20-methyl-5α(H)pregnane		0.9	1.7	1.4	nd	nd	0.1	0.8	nd	nd	4
20S-13β(H),17α(H)-diacholestane**	S1[#]	1.7	4.4	2.0	3.1	nd	0.1	1.7	0.9	0.5	116
20R-13β(H),17α(H)-diacholestane	S2	1.8	2.6	1.3	1.8	nd	nd	1.0	0.6	0.2	92
20S-5α(H),14α(H),17α(H)-cholestane	S3	1.3	1.9	2.4	2.3	nd	0.1	1.5	0.8	nd	64
20R-5α(H),14α(H),17α(H)-cholestane	S6	1.7	2.9	1.7	nd	nd	nd	0.9	0.5	0.2	55
20R-5α(H),14β(H),17β(H)-cholestane	S4	4.2	6.6	3.4	nd	nd	nd	2.1	1.1	0.6	215
20S-5α(H),14β(H),17β(H)-cholestane	S5	2.3	3.9	1.8	nd	nd	nd	2.3	1.3	0.3	125
20R-24-ethyl-13β(H),17α(H)-diacholestane	S7	1.0	5.0	1.5	nd	nd	nd	1.1	0.5	0.2	170
20S-5α(H),14α(H),17α(H)-ergostane	S8	nd	5.2	nd	nd	nd	nd	nd	nd	nd	37
20R-5α(H),14α(H),17α(H)-ergostane	S11	nd	7.5	1.3	nd	nd	nd	2.3	nd	nd	126
20R-5α(H),14β(H),17β(H)-ergostane	S9	5.5	4.3	nd	nd	nd	nd	1.9	nd	nd	217
20S-5α(H),14β(H),17β(H)-ergostane	S10	nd	7.2	5.5	nd	nd	nd	nd	nd	nd	63
20S-5α(H),14α(H),17α(H)-stigmastane	S12	nd	1.0	1.5	nd	nd	nd	nd	nd	nd	69
20R-5α(H),14α(H),17α(H)-stigmastane	S15	3.7	5.4	13.0	8.7	38.2	0.1	2.1	1.4	1.2	26
20R-5α(H),14β(H),17β(H)-stigmastane	S13	3.2	3.0	2.4	nd	nd	nd	2.0	0.7	nd	141
20S-5α(H),14β(H),17β(H)-stigmastane	S14	nd	nd	nd	nd	nd	nd	nd	nd	nd	55

* Note change in units for OS sample

** Steranes of similar configuration assumed to have the same RF as in the standard compounds mixture

[#] Notation to be used in figures [##] Not detected, below detection limits

Table 12. Correlation coefficients (*r*) for chemical and physical parameters of muds from Beaufort Lagoon (N = 19; significant correlations [p <0.05] are shown in bold and insignificant correlations are in gray).

	V	Cr	Mn	Ni	Cu	Zn	As	Cd	Sn	Ba	Pb	Fe	OC %	Silt %	Clay %
V	**1.00**														
Cr	**0.89**	**1.00**													
Mn	0.07	–0.07	**1.00**												
Ni	**0.85**	**0.71**	**0.48**	**1.00**											
Cu	**0.80**	**0.64**	0.39	**0.91**	**1.00**										
Zn	**0.84**	**0.78**	–0.16	**0.69**	**0.76**	**1.00**									
As	**0.72**	**0.52**	0.12	**0.55**	**0.58**	**0.68**	**1.00**								
Cd	0.41	**0.54**	0.30	**0.57**	0.45	0.45	0.31	**1.00**							
Sn	**0.48**	0.43	**0.74**	**0.78**	**0.61**	0.35	0.40	**0.78**	**1.00**						
Ba	**0.53**	**0.57**	–0.38	0.31	**0.47**	**0.70**	0.26	0.08	–0.12	**1.00**					
Pb	**0.70**	**0.50**	**0.80**	**0.89**	**0.92**	**0.58**	**0.68**	**0.63**	**0.86**	0.10	**1.00**				
Fe	**0.73**	**0.85**	0.28	**0.58**	**0.62**	**0.77**	**0.71**	**0.59**	**0.50**	**0.48**	**0.70**	**1.00**			
OC %	0.37	0.40	0.12	0.42	0.31	**0.62**	0.44	**0.66**	**0.46**	0.07	0.38	0.44	**1.00**		
Silt %	**–0.63**	–0.40	**–0.75**	**–0.81**	**–0.73**	**–0.51**	**–0.72**	**–0.73**	**–0.93**	0.19	**–0.88**	**–0.52**	–0.44	**1.00**	
Clay %	**0.64**	0.40	**0.74**	**0.82**	**0.75**	**0.55**	**0.72**	**0.72**	**0.93**	–0.17	**0.88**	**0.52**	**0.58**	**–1.00**	**1.00**

Table 13. Time-series changes in the mean concentrations (μg g^{-1} dry wt) of trace metals in sediments of Beaufort Lagoon.[a]

Year	V	Cr	Mn	Ni	Cu	Zn
1977[b]						
N = 5						
$\overline{X}$	**139**	69	**359**	48	**22**	81
SD	17	12	69	6	4	11
CV%	12	17	19	13	18	14
2003[c]						
N = 21						
$\overline{X}$	**119**	73	**472**	39	**36**	92
SD	13	7	659	7	9	17
CV%	11	10	139	18	25	19

[a]Significant differences ($p < 0.05$) in bold
[b]Naidu [1981, 2003a]
[c]This study (Table 2)

Discussion

Sediment grain size, and organic carbon and nitrogen and their isotope composition

Beaufort Lagoon has a mosaic of sediment types consisting of sandy muds to muddy sands with rare gravel (Table 1). The exceptions are sediments 4B, 19 and 20, which have significant or predominant amounts of gravel (Table 1). The mud fractions of sediments, which were sampled for trace metal, OC, N and isotope analysis, generally contain relatively higher contents of silt than clay particles. In the gross sediments, which were collected for THg analysis, there are wide differences in the content of sand relative to mud. We discuss later the possible control of granulometry on the concentrations of 12 metals in the mud fraction and THg in the gross sediments.

The contents of organic carbon and nitrogen (N) in the mud fraction of Beaufort Lagoon sediments in this study (Table 1) are generally higher by a factor of 1.7 compared to the gross sediments from the Simpson Lagoon–Prudhoe Bay region and by a factor of 2.9 compared to gross sediments collected from Beaufort Lagoon in 1977 [Naidu 1981]. The higher content of OC in mud than in gross sediments is not surprising, because OC (tied with organic grains) invariably is co-deposited with hydraulically similar finer silt and clay (mud) particles; also, clays concentrated in mud have a greater ability to adsorb organics. Coarser particles such as sand in gross sediments are generally not associated with organic particles of similar size and, therefore, their presence in gross sediments tends to dilute the OC contents.

The OC/N ratios and compositions of the stable isotopes of carbon ($\delta^{13}C$) and nitrogen ($\delta^{15}N$) in Beaufort Lagoon sediments (Table 1) indicate that all of the samples consist predominantly of OC/organic matter derived from terrestrial C_3 plant sources, with minor input from marine or macrophyte sources. This interpretation is based on conclusions from very exhaustive investigations relating to the isotopic and OC/N signatures of the end-member sources of OC/organic matter (terrestrial, marine phytoplankton, sea ice algae and marine macrophytes, kelp) in the coastal region of the Alaskan and Canadian Beaufort Sea [Naidu et al. 2000; Macdonald et al. 2004]. Results of our

studies on the sources of OC/organic matter in Beaufort Lagoon sediments are consistent with those reported for the above areas and, as discussed later, with conclusions on the sources of organics in the lagoon sediments based on the hydrocarbon composition. It is suggested that the high input of terrestrial OC/organic matter to Beaufort Lagoon, as well as lagoons of the contiguous coastal region, is due to the large supply of sediments derived from the peat-rich shoreline, which has one of the world's highest coastal erosion rates, 2–10 m y^{-1}, [Naidu et al. 2000; Macdonald et al. 2004 and references therein].

Trace metal studies

QA/QC

The results of the calibration verification procedure (Table 3) include, for each metal, the known initial calibration verification (true value, ICV-TV), the ICV-observed value (ICV-Obs), and the ICV recovery value (ICV-Rec). ICV-Obs indicated that the percentage ICV-Rec for all metals except Fe was at an acceptable level (close to 100%). Likewise, the blank analysis (Table 4), based on an initial calibration blank (ICB) and the continuation calibration blank (CCB), indicates, for several runs, very low contamination from the chemicals used throughout the analysis. Further, with reference to the use of spikes (Table 5) run in duplicates, and based on the values of the mean concentration of an individual metal via replicate analyses of a sample (Mean), spike true value (Spike TV), and the observed spike value (Obs Spike Value), we show that the spike percent recovery is close to 100% for all metals except Fe and Ba. The reason for the consistent poor showing for Fe and Ba is unknown, but perhaps reflects the inherent limitation of the use of the ICP/MS technique. The analytical precision (Table 6), as suggested by the relative percent difference (RPD) on duplicate analytical runs of two sediment samples, would seem to be excellent for all metals except THg, in which case it is very good and at acceptable level (<25%). Likewise, the analytical accuracy (Table 7), determined via the certified values (Cert Value), and analyzed or observed values (Obs Value) of two certified reference materials (CRM – NIST 2709 and IAEA 405) are again at accepted levels for all metals with reference to both the standards, except for Cr and Cd for NIST 2709 and Fe and Sn for both of the CRMs. The above discussion indicates that the QA/QC for the trace metal analysis is generally very good to excellent and our data are of high quality.

Statistical analysis on the trace metal is in progress. Here we report the preliminary results of the analysis. The high % CV about the mean for all the 13 metals (Table 2) obviously indicates that there are wide inter-sample variations in the concentrations of all the metals, with relatively low variability, though, for V, Cr and Fe. The reason for the high inter-sample variability in the THg content may be ascribed to the wide differences in sand content in the gross sediments; the silt and clay content within the mud fraction may account for variability in the rest of the metals. The other possible reason could be the differences in the contents of organic carbon (a measure of organic matter) between sediments. Yet another reason could be the differences in the Mn and Fe content between the sediments analyzed. It is to be expected that the greater the amount of clay size particles, Mn and Fe content, and/or larger content of organic carbon (and by implication organic matter) in the mud fraction or gross sediments there will be relatively greater concentrations of metals. This concentration could result from several likely processes, such as adsorption of metals on clays, formation of organic–metal complexes by ligand bonding, and/or co-precipitation of metals with Fe and Mn oxyhydroxides. That such a granulometric control on metal content is present in the case of Beaufort Lagoon muds is demonstrated by the significant ($p < .05$) positive correlations between all of trace metals, except Cr and Ba, and the clay content. The positive significant correlations observed between all the trace metals and Fe, suggests that Fe, as an oxyhydroxide, has an important role in scavenging and accumulating metals in the mud of Beaufort Lagoon. In this context, it is to be noted that all of the 2–5-cm surficial sediments (portions analyzed for trace metals) showed at the time of

collection a brownish ochre coloration distinct from the underlying gray layers—an indication that Fe in the mud analyzed is most likely present in a highly oxidized state. Additional detailed investigations on metal partitioning in sediments from Simpson Lagoon (located east of the Colville Delta) and Beaufort Lagoon, based on sequential extraction techniques, further substantiate the role of Fe oxyhydroxides in sequestering metals in the north Alaskan arctic sediments [Sweeney 1984; Sweeney and Naidu 1989]. Likewise, organic carbon and Mn in the muds (Table 12) to some extent bond a selected few metals (Zn, Cd, As and Sn by OC, and Ni, Sn and Pb by Mn).This interpretation is consistent with our earlier conclusions on partitioning of trace metals on lagoon sediments from a wide region off of the North Slope coast, namely from the Colville–Canning Delta area [Naidu et al. 2001 and references therein] and also from Beaufort Lagoon [Naidu et al. 2003a].

Results of further exploratory statistical analysis of trace metal concentrations in Beaufort Lagoon consisted of the following: We examined dot plots of metal concentrations by station and identified two (4 and 5) with unusually low concentrations of a number of metals, including V, Zn, Fe, Ni, As, Cr, and Cu. In contrast, station 17 was characterized by unusually high concentrations of Sn, Mn, Ni, Pb and Cu. Histograms, box-and-whisker plots, and normal probability plots suggested that most metal concentrations were approximately normally distributed but that several extreme outliers were present, including high concentrations of Mn, Sn, and Pb at station 17, as well as high concentrations of Sn at 19 and 20. Other outliers included the low concentration of Cr at stations 4 and 5. Because of the presence of a number of outliers, we supplemented the above mentioned correlation coefficient analysis (Table 12) with rank-based correlations (Spearman's rank correlation, r) to examine relationships among various metals in the Beaufort Lagoon samples. The Spearman's rank correlation analysis showed very strong positive correlations among most metals (r = 0.58 to 0.91, $p < 0.01$). However, concentrations of Mn and Ba were only weakly correlated with each other and with any of the other metals, except for a relatively strong correlation between Ba and Zn (r = 0.604, p = 0.005). These results are generally consistent with those shown in the initial correlation coefficient analysis (Table 12).

Multivariate analyses of metal concentrations in mud across all locations, including a cluster analysis and a principal components (PC) analysis, confirmed that metal concentrations at stations 4, 5, and 17 were most different from each other and from any of the other stations. A cluster analysis showed that the remaining stations form three relatively distinct groups (Figure 2), but these groups did not correspond to geographically distinct regions. Because of the strong correlations among metal concentrations, 80% of the variability in these correlations can be summarized by only two principal components. A plot of the stations in the space of the first two components also shows the unusual characteristics of stations 4, 5, and 17 (Figure 3). The first PC had positive loadings for all metals, implying a general increase in metal concentrations along the x-axis in Figure 2. This PC was negatively correlated with latitude (r = –0.531, p = 0.023). This implies that the trend of metal concentrations decreases from south to north across the sampling area. It seems clear, therefore, that there are no definite distributional patterns in the concentrations of trace metals in the mud of Beaufort Lagoon, especially in context of the hypothesis that we had enunciated at the start of the project: We had hypothesized that there will be significant differences in the metal concentrations between the regions exposed to natural oil seeps, anthropogenic activities such as those related to the now abandoned DEW Line station, and pristine environment portions of the lagoon. It is suggested that any input of the 13 metals investigated which might have been introduced into the lagoon from the oil seeps and/or past military activities are dispersed so widely and diluted that the affect of the point sources of the natural and anthropogenic contaminants are not decipherable in the lagoon mud. In summary, there is no significant difference between mud collected from possible impacted areas and the pristine portion of the lagoon, suggesting that the lagoon has remained uncontaminated as far as the trace metals analyzed in this study.

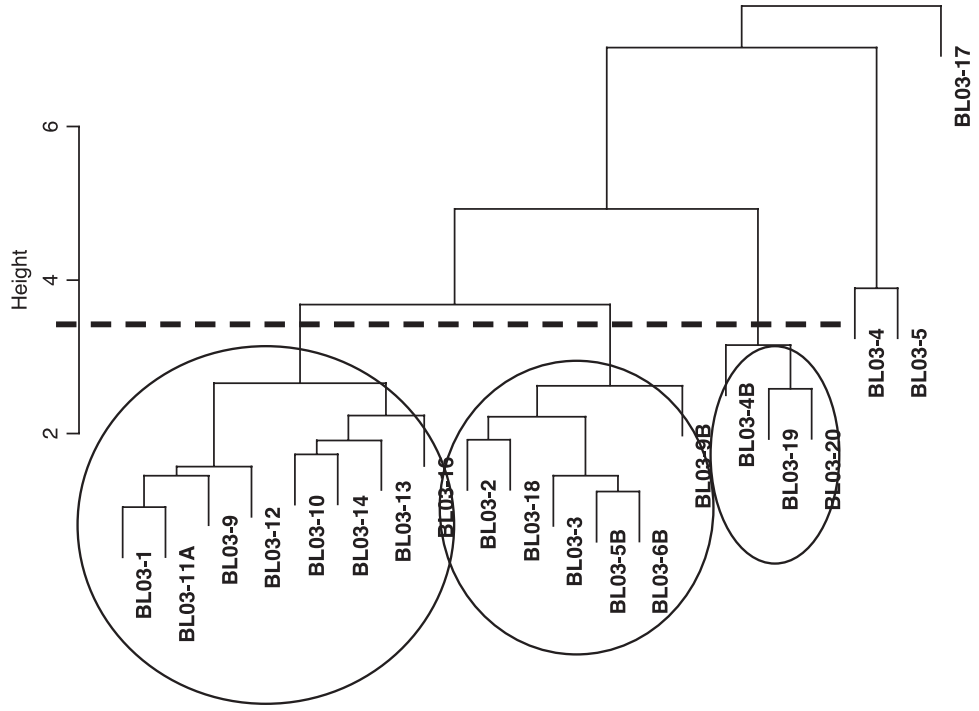

Figure 2. Dendrogram based on Ward's linkage clustering (Euclidean distances) and on concentrations of 13 metals measured at each station.

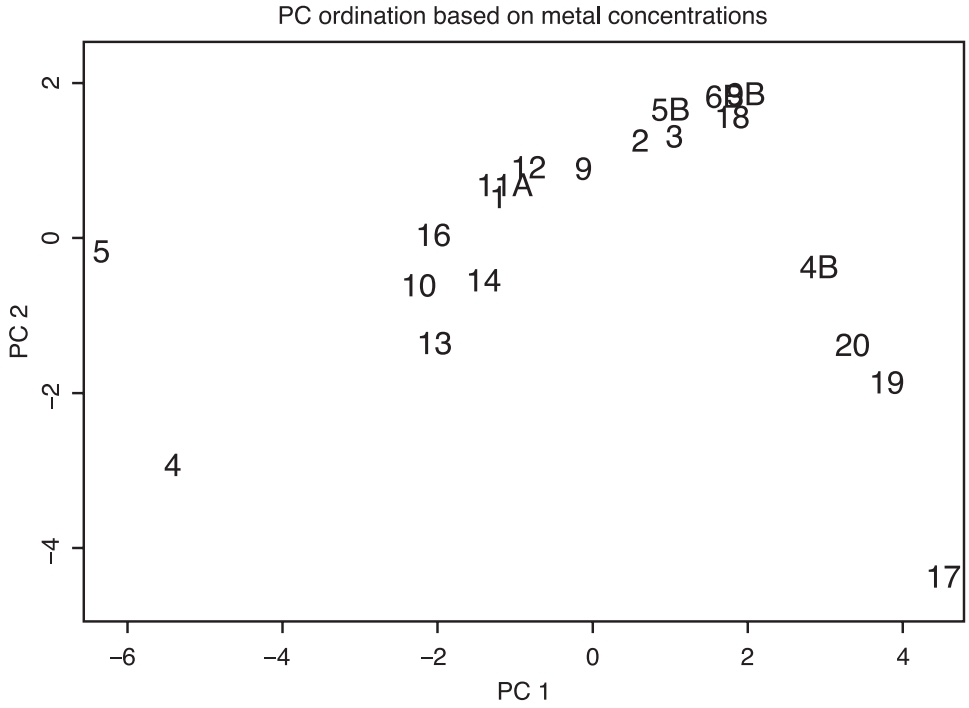

Figure 3. Beaufort Lagoon stations in the space of the first two principal components (PC).

Tentative examination of the data suggests that the mean concentrations of all trace metals, except THg, in the muds of Beaufort Lagoon are generally at the same level as those we reported from the Colville Delta–Prudhoe Bay–Canning Delta region. The significantly higher THg values in Beaufort Lagoon mud (mean = 57 ng g^{-1}) than in the above region (mean = 19 ng g^{-1}) are probably due to differences in the natural input of the metal from the hinterland source, a proposition that remains to be further investigated.

Time-series comparison of the mean concentrations of metals

Table 13 shows a comparison of the mean concentrations of six selected metals between 5 sandy mud (>75% silt plus clay) and 21 mud samples which were collected from Beaufort Lagoon in 1977 and for this study. A significant ($p < .05$) decrease in V and an increase in Mn and Cu are noted from 1977 to 2003, whereas no differences in the time-series mean concentrations in Cr, Ni and Zn are identified. The differences may be artifacts of the variations in the granulometry and organic carbon contents between the two sets of samples rather than metal pollution, as alluded to previously. It is to be noted that we have minimized the affect of granulometry by restricting the comparison to mean metal values on sandy mud samples from 1977 and mud samples in this study. The fact that there is no wholesale increase in the mean concentrations of all or most of the metals concerned is consistent with our earlier inference that Beaufort Lagoon has remained generally a clean environment over the 26-year period (1977–2003), despite its having been subjected to past anthropogenic activities from the operation of the Dew Line station.

Hydrocarbon studies

The discussions on the hydrocarbon studies are focused on two aspects: one to elucidate the sources of the hydrocarbons, and the second to assess whether the types and concentrations of hydrocarbons in Beaufort Lagoon sediments are any way different than those in nearshore sediments collected elsewhere in the North Slope region.

Criteria to infer hydrocarbon sources

We assessed the relative abundance of the various sources of hydrocarbons (natural oil seep, refined petroleum, fresh crude and natural terrestrial and marine biogenic origin) in each of the sediments analyzed by using, for example, the following guidelines.

Natural crude seepage: Weathered petroleum; alkane gas chromatogram with a hump (unresolved complex mixture of branched and cyclic components) [Farrington and Tripp 1977; Simoneit and Kaplan 1980; Venkatesan et al. 1980].

Fresh petroleum: Unweathered petroleum; characterized by *n*-alkane distribution with no odd/even carbon preference throughout the carbon number envelope [Philp 1985); alkylcyclohexanes and alkylbenzenes are found at significant levels, pristine and phytane are usually more dominant than C_{17} and C_{18} *n*-alkanes [Zafiriou et al. 1972], triterpenoids are of high thermal maturity characterized by the presence of predominantly the 17α-hopanes and moretanes (17$\alpha\beta$-hopanes) [Dastillung and Albrecht 1976]. Alkylated PAHs are more dominant than the parent PAHs [Youngblood and Blumer 1975].

Biogenic hydrocarbons: Alkane gas chromatogram normally has baseline resolved peaks and does not have a hump [Venkatesan and Kaplan 1982]; C_{15}, C_{17} dominant *n*-alkanes from marine plankton, whereas dominance of C_{25} to C_{31} *n*-alkanes indicates terrestrial plant wax, with C_{25}, C_{27}, C_{29}, C_{31} and C_{33} more dominant than the even carbon *n*-alkanes (resulting in high odd/even ratio) and with maximum at C_{29} or C_{31} *n*-alkane [Simoneit and Kaplan 1980; Venkatesan et al. 1980]; presence of a significant level of alkanes from marine biota [Blumer et al. 1971]; triterpenoids are of low thermal

maturity characterized by the presence of predominantly the 17α-hopanes and hopanes [Dastillung and Albrecht 1976]; not many alkylated PAHs.

Characteristics of hydrocarbons and their sources

Alkanes: The alkane gas chromatogram exhibits baseline separation of the components and is generally bimodal with the major maximum at *n*-C_{27} in 14 of the 20 samples analyzed and at *n*-C_{29} or *n*-C_{31} in the remaining sediments (Table 8). Normal alkanes > C_{25} predominate in all of the sediment samples with an odd/even carbon alkane ratio in the range from 3.5 to 8.1. These alkanes are derived from higher plants. The secondary maximum at n-C_{17} is characteristic of aquatic algae. The C_{20} and C_{21} olefins found are derived from plankton and bacteria. Although the total *n*-alkane level varies from 0.1 to 34 μg g^{-1} similar to the Elson Lagoon sediments, Beaufort Lagoon sediments, in general, seem to exhibit relatively greater vascular inputs than those of Elson Lagoon.

In contrast, the oil seep (OS) sample contains a 100- to 1000-fold concentration of *n*-alkanes compared to the sediments (i.e., μg g^{-1} vs. ng g^{-1} as found in sediments, Table 8). Very high amounts of *n*-C_{10} through *n*-C_{15} and significant levels of alkanes from *n*-C_{20} to *n*-C_{32} over a pronounced unresolved hump (unresolved complex mixture spanning *n*-C_{21}–*n*-C_{34}) are found in this sample. The most dominant alkane is *n*-C_{11}. There is practically no single dominant *n*-alkane at the high molecular weight end where the odd/even ratio is at 1.3, typical of petroleum input. From the overall profile of the *n*-alkanes, it appears that OS may be degraded petroleum.

In addition, the L/H ratio (ΣC_{12}–$C_{19}/\Sigma C_{20}$–C_{33} alkanes) of OS is 0.6 which is much higher than in sediments (0.05–0.13) as computed from Table 10. Only one sample (14) has measurable pristane and phytane and OS has neither of the two. The C_{20} and C_{21} planktonic olefins, which are found in all of the sediments, are absent in the OS sample. Therefore, the *n*-alkane distribution in the sediment samples is markedly different from that in the OS sample, implying that the lagoon sediment is relatively pristine with no measurable petroleum contribution.

Polycyclic aromatic hydrocarbons: The levels of total PAH in the Beaufort Lagoon sediments range from 30 to 710 ng g^{-1} (Table 9) and are comparable to sediments from the Colville Delta –Prudhoe Bay–Canning Delta region (2001), Elson Lagoon [Naidu et al. 2003b] and other nearshore regions of the Beaufort Sea. The PAH composition is dominated by the homologous series of phenanthrenes. The sum of parent PAHs and their methyl homolog distribution follows generally in the order: phenanthrenes > naphthalenes ≥ chrysenes/triphenylenes > fluoranthenes/pyrenes. C_2-naphthalene and C_1-phenanthrene in all of the samples and C_1-chrysene in four samples are the most dominant PAH homologs. The general dominance of parent and monomethylated PAHs over higher methylated homologs in the lagoon sediment samples suggests the absence of significant petroleum input in the sediments. Compared to the lower molecular weight PAHs, 4- and 5-ring PAHs are relatively less and perylene is the most dominant parent PAH in all of the samples except for 17, which has the least PAH content and contains no perylene. The dominance of perylene in the sediments is consistent with its origin in Alaskan peats similar to that found in coastal and other lagoon sediments of north arctic Alaska [Naidu et al. 2001, 2003b and references therein]. This interpretation is consistent with the very light (negative) values of carbon isotope ratios ($\delta^{13}C‰$, Table 1) of all sediments, which point to a predominantly terrestrial (C_3) plant source of OC/organic matter in Beaufort Lagoon.

The OS sample contains 208 μg g^{-1} of total PAHs, about 1000-fold greater than the Beaufort Lagoon sediments (Table 9), which is also consistent with the trend in *n*-alkane content. Unlike the sediments, naphthalenes are the most dominant PAHs in OS, and similar to the dominance of low molecular weight C_{10}–C_{15} *n*-alkanes over high molecular weight analogs. Further, an anomalously high value of

the naphthalene/phenanthrene ratio in OS is observed (7.62) in contrast to the very low range in the sediments (0.03–0.91). C_2-naphthalenes, C_2-phenanthrenes and C_3-chrysene/triphenylenes are the most dominant methyl homologs, characteristic of petroleum. Neither any PAHs beyond C_4-chrysene/ triphenylenes nor perylene are detected in the oil seep. The sum of parent PAH and methyl homologs follow the order: naphthalenes>>>phenanthrenes~chrysenes/triphenylenes>fluoranthenes/pyrenes.

The overall molecular composition of PAHs in Beaufort Lagoon sediments and a comparison to that of the OS sample imply absence of petroleum in the Beaufort Lagoon sediments, which is consistent with that noted above from the alkane profiles. The hydrocarbon composition of the sediments from Beaufort Lagoon is comparable to those from Elson Lagoon and most of the Beaufort Sea sediments we investigated in previous CMI/MMS studies.

Triterpenoids: Triterpanes are mostly biogenic in the sediments as reflected by the presence of 5 major components, i.e., 27(17β)-, 29ββ-, 29βα-, 30ββ-hopanes and diploptene (Table 10). The most dominant hopanoid is diploptene and 29ββ-hopane is the second most dominant. Thermally mature 29αβ- and 30αβ-hopanes are present in much smaller/trace amounts relative to biogenic hopanes. Extended hopanes with $\geq C_{31}$ are either not detected or present only in trace quantities and only the R isomer is detected.

Similar to *n*-alkanes, total triterpanes are at the μg g^{-1} level and about 1000-fold greater in the OS sample than in the lagoon sediment samples where they occur at the level of ng g^{-1} (Table 10). Further, OS contains a whole suite of thermally mature αβ-hopanes and none of the biogenic ββ- and βα-hopanes or the hopenes. Both S and R diastereomers of the extended hopanes (i.e., $\geq C_{31}$-hopanes) are present. This hopane distribution in OS is typical of petroleum/thermally mature sediments.

The trace amounts of isolated thermally mature (αβ and/or βα-hopane) biomarkers detected in the sediments most probably derive from peat and/or coal. The overall fingerprint of the triterpanes in sediments of Beaufort Lagoon do not support any contribution from the oil seep.

Steranes: Steranes are generally absent in Beaufort Lagoon sediment samples. If present, they are only in small/trace amounts, usually about 10 times lower than triterpanes (Table 11). Sediment samples 12, 13 and 14 contain almost a complete suite of target steranes and at relatively higher levels than the other sediments. This probably implies minimal petroleum input. However, this observation is not supported by triterpane or *n*-alkane profiles. Also, considering the extremely low levels of steranes in these samples, the possible input from petroleum may not be warranted. The other samples which contain smaller amounts of a few steranes are 6B, 18 and 19.

All of the target steranes are present in the OS sample and it is about 1000-fold greater than in the lagoon sediments. The sterane profile of OS clearly indicates petroleum characteristics.

In summary, normal and cyclic alkane distribution is characteristic of biogenic origin in all of the sediment samples and is different from that of the OS sample, thus indicating very little or no petroleum input to Beaufort Lagoon sediments. The overall profile of alkanes in the Beaufort Lagoon sediments is similar to that of nearshore sediments from the Beaufort Sea which we analyzed in previous CMI/MMS projects [Naidu et al. 2001, 2003b]. The alkane distribution of the OS sample, in contrast, clearly reflects that of petroleum. The overall profiles of its hydrocarbons indicate a significant derivation from terrestrial plants, which is corroborated by the OC/N and stable carbon isotope ratios. In fact, terrestrial organic material pervades (50%) the organic matter of sediments throughout the Alaskan–Canadian nearshore, which is substantiated by more extensive investigations on OC/N, $\delta^{13}C$ and *n*-alkanes of.sediments of the region [Naidu et al. 2000; Macdonald et al. 2004].

Study Products

Naidu, A.S., J.J. Kelley and J.J. Goering. 2003. Three decades of investigations on heavy metals in coastal sediments, North Arctic Alaska: A synthesis. J. Phys. IV France 107:913–916.

Kelley, J.J., A.S. Naidu and J.J. Goering. 2004. Trace metals in sediments of Elson Lagoon (Northwest Arctic Alaska) as related to the Prudhoe Bay industrial region, p. 175–179 (abstract). *In* Proc. 19th Int. Symp. on Okhotsk Sea and Sea Ice, Mombetsu, Hokkaido, Japan. Oral presentation by J.J. Kelley.

Naidu, A.S. and J.J. Kelley and D. Misra. 2004. Heavy metal monitoring in sediments of the North Alaskan Arctic. Asia Oceania Geosciences Society (AOGS) First Annual Meeting, Singapore, July, 2004. Abstract 57-OOA-A447. Oral presentation (invited) by A.S. Naidu.

Naidu, A.S., J.J. Kelley, D. Misra and M.I. Venkatesan. 2004. Trace Metals and Hydrocarbons in Sediments of Beaufort Lagoon, Northeast Arctic Alaska, Exposed to Long-term Natural Oil Seepage, Recent Anthropogenic Activities and Pristine Conditions. Oral Presentation by A.S. Naidu at the University of Alaska Coastal Marine Institute Annual Research Review, February 2003, Fairbanks.

Naidu, A.S., J.J. Kelley, D. Misra and J.J. Goering. 2004. Responsible industrial development in the North Slope nearshore: sediment trace metal history. Luncheon talk given by A. S. Naidu at the Alaska Miners Association, Fairbanks.

Naidu, A.S., J.J. Kelley and J.J. Goering. 2005. Heavy Metals, p. 851–852. *In* Mark Nuttall [ed.], Encyclopedia of the Arctic, Volume 2. Routledge, New York.

References

Bloom, N.S. 1992. On the chemical form of mercury in edible fish and marine invertebrate tissue. Can. J. Aquatic Sci. 49:1010–1017.

Bloom, N.S., G.A. Gill, S. Cappellino, C. Dobbs, L. McShea, C. Driscoll, R. Mason and J. Rudd. 1999. Speciation and cycling of mercury in Lavaca Bay, Texas, sediments. Environ. Sci. Technol. 33(1):7–13.

Blumer, M., R.R.L. Guillard and T. Chase. 1971. Hydrocarbons of marine phytoplankton. Mar. Biol. 8:183–189.

Brown, R.E. 1987. Emergency/Survival Handbook, 4th ed. American Outdoor Safety League. Mountaineers Books, Seattle, WA, 45 p.

Dastillung, M., and P. Albrecht. 1976. Molecular test for oil pollution in surface sediments. Mar. Poll. Bull. 7(1):13–15.

Douglas, D.C., P.E. Reynolds and E.B. Rhode [eds.]. 2002. Arctic Refuge Coastal Plain Terrestrial Wildlife Research Summaries. Biological Science Report, USGS/BRD/BSR-2002-0001, U.S. Geol. Survey, Reston, VA, 75 p.

Farrington, J.W., and B.W. Tripp. 1977. Hydrocarbons in western North Atlantic surface sediments. Geochim. Cosmochim. Acta 41(11):1627–1641.

Folk, R. 1968. Petrology of Sedimentary Rocks. Hemphill Publishing Co., Austin, Texas, 70 p.

Macdonald, R.W., A.S. Naidu, M.B. Yunker and C. Gobeil. 2004. The Beaufort Sea: Distribution, sources, fluxes, and burial rates of organic carbon, p. 177–192. *In* R. Stein and R.W. Macdonald [eds.], The Organic Carbon Cycle in the Arctic Ocean. Springer, Berlin/New York.

Naidu, A.S. 1981. Sources, Transport Pathways, Depositional Sites and Dynamics of Sediments in the Lagoon and Adjacent Shallow Marine Region, Northern Arctic Alaska. Annual Report to NOAA–OCSEAP Office, Boulder, Colorado, 39 p.

Naidu, A.S. 1985. Organic carbon, nitrogen, and C/N ratios of deltaic sediments, North Arctic Alaska, p. 311–321. *In* SCOPE/UNEP Sonderband Heft 58, Mitt. Geol-Paläont. Inst., Univ. Hamburg, Germany.

Naidu, A.S., L.W. Cooper, B.P. Finney, R.W. Macdonald, C. Alexander and I.P. Semiletov. 2000. Organic carbon isotope ratios ($\delta^{13}C$) of Arctic Amerasian continental shelf sediments, p. 522–532. *In* R. Stein [ed.], Circum-Arctic River Discharge and Its Geological Record, Int. J. Earth Sci., Spec. Issue, Vol. 89.

Naidu, A.S., J.J. Goering, J.J. Kelley and M.I. Venkatesan. 2001. Historical Changes in Trace Metals and Hydrocarbons in the Inner Shelf, Beaufort Sea: Prior and Subsequent to Petroleum-Related Industrial Developments. Final Report. OCS Study MMS 2001-061, University of Alaska Coastal Marine Institute, University of Alaska Fairbanks and USDOI, MMS, Alaska OCS Region, 80 p.

Naidu, A.S., J.J. Kelley and J.J. Goering. 2003a. Three decades of investigations on heavy metals in coastal sediments, North Arctic Alaska: A synthesis. J. Phys. IV France 107:913–916.

Naidu, A.S., J.J. Kelley, J.J. Goering and M.I. Venkatesan. 2003b. Trace Metals and Hydrocarbons in Sediments of Elson Lagoon (Barrow, Northwest Arctic Alaska) as Related to the Prudhoe Bay Industrial Region. Final Report. OCS Study MMS 2003-057, University of Alaska Coastal Marine Institute, University of Alaska Fairbanks and USDOI, MMS, Alaska OCS Region, 33 p.

NORTECH (Northern Technical Services). 1981. Beaufort Sea Drilling Effluent Disposal Study. Report for SOHIO Alaska Petroleum Co., Anchorage, 329 p.

Philp, R.P. 1985. Fossil Fuel Biomarkers: Applications and Spectra. Methods in Geochemistry and Geophysics, 23. Elsevier, New York, 294 p.

Simoneit, B.R.T., and I.R. Kaplan. 1980. Triterpenoids as molecular indicators of paleoseepage in recent sediments of the Southern California Bight. Mar. Environ. Res. 3(2):113–128.

Snyder-Conn, E., D. Densmore, C. Moitoret and J. Stroebele. 1990. Persistence of trace metals in shallow arctic marine sediments contaminated by drilling effluents. Oil & Chem. Pollut. 7:225–247.

Steinhauer, M.S., and P.D. Boehm. 1992. The composition and distribution of saturated and aromatic hydrocarbons in nearshore sediments, river sediments, and coastal peat of the Alaskan Beaufort Sea: Implications for detecting anthropogenic hydrocarbon inputs. Mar. Environ. Res. 33:223–253.

Sweeney, M.D. 1984. Heavy Metals in the Sediments of an Arctic Lagoon, Northern Alaska. M.S. Thesis, Univ. of Alaska Fairbanks, 256 p.

Sweeney, M.D., and A.S. Naidu. 1989. Heavy metals in the sediments of the inner shelf of the Beaufort Sea, northern arctic Alaska. Mar. Pollut. Bull. 20:140–143.

Trefry, J.H., R.D. Rember, R.P. Trocine and J.S. Brown. 2003. Trace metals in sediments near offshore oil exploration and production sites in the Alaskan Arctic. Environmental Geol. 45(2):149–160. DOI: 10.1007/s00254-003-0882-2

USGS (U.S. Geological Survey) ANWR Assessment Team. 1999. The Oil and Gas Resource Potential of the Arctic National Wildlife Refuge 1002 Area, Alaska. U.S. Geolological Survey Open File Report 98-34. http://energy.cr.usgs.gov/OF98-34

Venkatesan, M.I. 1994. Historical Trends in the Deposition of Organic Pollutants in the Southern California Bight. UCLA, Final report to NOAA, 35 p.

Venkatesan, M.I., S. Brenner, E. Ruth, J. Bonilla and I.R. Kaplan. 1980. Hydrocarbons in age-dated sediment cores from two basins in the Southern California Bight. Geochim. Cosmochim. Acta 44(6):789–802.

Venkatesan, M.I., and I.R. Kaplan. 1982. Distribution and transport of hydrocarbons in surface sediments of the Alaskan outer continental shelf. Geochim. Cosmochim. Acta 46:2135–2149.

Venkatesan, M.I., E. Ruth, S. Steinberg and I.R. Kaplan. 1987. Organic geochemistry of sediments from the continental margin off southern New England, U.S.A. – Part II. Lipids. Mar. Chem. 21:267–299.

Youngblood, W.W., and M. Blumer. 1975. Polycyclic aromatic hydrocarbons in the environment: Homologous series in soils and recent marine sediments. Geochim. Cosmochim. Acta 39(9):1303–1314.

Zafiriou, O.C., M. Blumer and J. Myers. 1972. Correlation of oils and oil products by gas chromatography. Woods Hole Oceanographic Institution Tech. Rep. 72-55, 110 p.

New Projects

Six new projects are being funded this federal fiscal year along with the ongoing projects reported above. Preliminary reports (Quakenbush & Small [TO 35248] and Powell [TO 35269]) and abstracts (Wang & Jin [TO 35262, TO 35407], Foster, Lees & Saupe [TO 37357] and Okkonen, Pegau and Saupe [TO 37628]) are presented here to show the full range of work being supported by the University of Alaska Coastal Marine Institute.

Satellite Tracking of Bowhead Whales: The Planning Process

Lori T. Quakenbush <lori_quakenbush@fishgame.state.ak.us>

Institute of Marine Science
University of Alaska Fairbanks
Fairbanks, AK 99775–7220

Robert J. Small <bob_small@fishgame.state.ak.us>

Marine Mammal Program
Alaska Department of Fish and Game
Division of Wildlife Conservation
P.O. Box 25526
Juneau, AK 99802-5526

Task Order 35248

Abstract

*Bowhead whales (*Balaena mysticetus*) are an important subsistence and cultural resource for coastal people of northern Alaska. They migrate through the Beaufort Sea twice annually: during their eastward, spring migration and their westward, fall migration. Oil and gas leasing, exploration, development, and production are ongoing in the Alaskan Beaufort Sea and an understanding of bowhead migration and feeding behavior in this area is important for the conservation and management of the species. Satellite transmitters placed on bowhead whales near Kaktovik in fall and near Barrow in spring would provide information on migration routes, migration timing, swim speed, diving behavior, residence times in portions of their range, and incidental exposure to industry activity. The objectives of this phase of the project are to accomplish the preliminary work necessary to determine whether the whaling captains and commissioners of the Alaska Eskimo Whaling Commission are supportive of a satellite tagging study and if they are interested in participating in the study design and tag deployment. If so, we will work cooperatively with the whaling captains of Barrow and Kaktovik, the commissioners of the Alaska Eskimo Whaling Commission, the North Slope Borough, the National Marine Fisheries Service, the Minerals Management Service, the oil and gas industry, and the Alaska Department of Fish and Game to determine the best available tag, tag deployment method, and study design, and pursue the funding to subsequently deploy the tags and conduct the study. The study will be designed in a way that does not interfere with subsistence whaling activities.*

Introduction

Bowhead whales are the most important species for the subsistence communities along the Beaufort Sea coast both for the amount of nutrition and for their cultural importance. Subsistence whaling communities are concerned that offshore and nearshore oil and gas activities (e.g., marine seismic

projects, offshore oil drilling from ships and islands) may deflect whales away from shore, making hunting more difficult and dangerous and possibly displacing whales from feeding areas during the short open water season. Oil spills during whale migrations are also of concern.

The importance of the Beaufort Sea as feeding habitat to bowhead whales is unclear. An analysis of stable isotope ratios in the baleen of adult bowhead whales showed little change in their isotope ratios seasonally, indicating that the major signal came from feeding in the Bering and Chukchi seas in winter [Schell et al. 1989; Hobson and Schell 1998; Schell and Saupe 1993], not from feeding in the Beaufort Sea in summer/fall. Baleen from subadult bowheads, however, showed strong seasonal changes between summer (Beaufort) and winter (Bering) feeding, indicating significant feeding in both places. A more recent study [Hoekstra et al. 2002] analyzed isotope ratios in bowhead muscle instead of baleen and found seasonal fluctuation in $\delta^{13}C$ for all age classes, suggesting that the Bering and Beaufort seas are both important for feeding.

Within the Beaufort Sea, the eastern Canadian Beaufort Sea and Amundsen Gulf regions are thought to be used as summer feeding areas for bowhead whales [Fraker and Bockstoce 1980; Würsig et al. 1985], and although feeding has been observed in the Alaskan Beaufort Sea [Ljungblad et al. 1983, 1986; Lowry and Frost 1984; Moore et al. 1989] there is less agreement regarding its relative importance. Richardson [1987] concluded that the bowhead population obtained <1% and <1.4% of its annual energy needs in the Alaskan Beaufort Sea between Kaktovik and Canada in 1985 and 1986, respectively. Another feeding study conducted in 1998–2000 [Richardson and Thomson 2001] concluded that although bowheads in the Alaskan Beaufort Sea spent an average of 47% of their time feeding, they did not obtain more than 5% of their annual energy needs there. Aerial photography and resightings of identifiable individuals was the primary method used to determine residence time for whales in the study area, but this method may have underestimated the amount of time and/or the number of whales feeding there. A significant amount of feeding may also be occurring during behavior that has been recorded as migration [Ljungblad et al. 1986].

Over 75% of 132 bowhead whales harvested for subsistence at Barrow and Kaktovik (1976–2000) were feeding prior to their death [Lowry and Sheffield 2002]. Subadult bowheads harvested in fall are heavier and have blubber with higher lipid content than in the spring [Thomson 2002]. Stable isotopes, behavioral observations, stomach contents, and lipid levels indicate bowhead whales are feeding in the eastern and western areas of the Beaufort Sea, but further investigation is needed to determine the importance of the region to their annual energy requirements.

Satellite telemetry is a powerful tool that can be used to address questions regarding marine mammal habitat use [Boyd et al. 2002; Baumgartner and Mate 2001a, b; Lowry et al. 2000]. Detailed movements of individual whales can determine residence time in potential feeding areas. Satellite transmitters can collect and transmit diving information to provide behavior-at-location data that can be correlated with feeding. Some satellite telemetry work has been done with bowhead whales [Mate et al. 2000; Heide-Jørgensen et al. 2003] and the existing satellite transmitter technology is well suited for use with bowheads, but consistency in deployment and retention time of transmitters have been less than ideal [Mate et al. 2000] until recently. Two of the issues include: 1) positioning the transmitter on the whale so that the transmitter comes out of the water frequently to maximize transmissions to the satellite for good location data, and 2) retention of the tag on the whale due to the design of the attachment and the physiological processes of healing in the whale.

Our objectives during the planning phase are to: 1) seek approval for this study from the whaling community; 2) determine the level at which the whalers would like to be involved in the study; 3) provide a forum for collaboration with whaling captains, the Alaska Eskimo Whaling Commission (AEWC), the North Slope Borough (NSB), National Marine Fisheries Service (NMFS), Minerals

Management Service (MMS), Alaska Department of Fish and Game (ADF&G) and the oil and gas industry; 4) design a satellite telemetry study; and 5) identify funding for the study. Because of the importance of bowhead whales for subsistence, their endangered species status, and the interest in their summer habitat for oil and gas exploration and development, coordination with the whalers, the agencies involved in marine mammal management, and the oil and gas industry will be necessary for a successful project.

Results

Lori Quakenbush coordinated with NSB staff Craig George and Harry Brower, and NSB director Charles Brower and AEWC executive director Maggie Ahmaogak, for an opportunity to present the satellite tagging study idea to a meeting of the AEWC commissioners in Barrow 24 June 2004. Many of the commissioners were present in Barrow, others attended via telephone, and some were absent. The presentation occurred at the end of a long meeting and there were numerous questions. It was suggested that a presentation and discussion be placed on the agenda of the next quarterly AEWC meeting so that all of the commissioners could participate in person in a discussion. This meeting will occur on 27 October 2004 in Anchorage.

If the meeting in October concludes with approval to conduct the study, we discussed the best time and place for a workshop on its design. Maggie Ahmoagak felt that having a workshop in conjunction with their annual AEWC mini-convention in Anchorage in February 2005 would be best. The commissioners would be there for the AEWC meeting, and representatives from the agencies and oil industry could easily attend.

We are researching the existing tags, deployment methods, retention times, and health effects on the whales in order to choose the tag and method that will accomplish the study objectives with the least impact to the whales. We have collected relevant literature, contacted scientists actively tagging large whales and continue to monitor the progress of tagged whales. Several researchers have made advances recently but have not published their results. For example, recent tags placed on blue whales (*Balaenoptera musculus*) and sperm whales (*Physeter macrocephalus*) have lasted more than 300 days (B. Mate, unpubl. data). Tags were placed on two Pacific right whales for the first time this summer, and while both are working only one is providing locations (P. Wade, pers. comm.). Because of the need for better deployment and attachment systems, NMFS has announced their interest in holding a workshop for researchers involved in tagging large whales to discuss problems and recent developments. No suitable date for the workshop has been identified.

Discussion

Although our original plan was to have meetings in Kaktovik to talk with the whaling captains, the meetings in Barrow and Anchorage will allow collaboration with all of the AEWC commissioners from all of the whaling villages. A workshop in Anchorage with all of the AEWC commissioners will also be ideal for participation of all interested parties.

Acknowledgements

The University of Alaska Coastal Marine Institute (Minerals Management Service) funded this project with support provided by the North Slope Borough, Department of Wildlife Management.

Charlie Brower, Craig George, Harry Brower, and Robert Suydam of the North Slope Borough have provided helpful comments and ideas. We thank Maggie Ahmoagak of the AEWC for her ideas, assistance, and the opportunities to address the commissioners.

References

Baumgartner, M.F., and B.R. Mate. 2001a. Understanding the relationship between North Atlantic right whale movements and habitat characteristics from satellite-monitored radio tag data: A novel approach. 14th Biennial Conference on the Biology of Marine Mammals. Vancouver, Canada, 28 November–3 December 2001 (Abstract).

Baumgartner, M.F., and B.R. Mate. 2001b. Summer feeding season movements and fall migration of North Atlantic right whales from satellite-monitored radio tags. 14th Biennial Conference on the Biology of Marine Mammals. Vancouver, Canada, 28 November–3 December 2001 (Abstract).

Boyd, I.L., I.J. Staniland and A.R. Martin. 2002. Distribution of foraging by female Antarctic fur seals. Mar. Ecol. Progr. Ser. 242:285–294.

Fraker, M.A., and J.R. Bockstoce. 1980. Summer distribution of bowhead whales in the eastern Beaufort Sea. Mar. Fish. Rev. 42(9–10):57–64.

Heide-Jørgensen, M.P., K.L. Laidre, Ø. Wiig, M.V. Jensen, L. Dueck, L.D. Maiers, H.C. Schmidt and R.C. Hobbs. 2003. From Greenland to Canada in ten days: Tracks of bowhead whales, *Balaena mysticetus*, across Baffin Bay. Arctic 56(1):21–31.

Hobson, K.A., and D.M. Schell. 1998. Stable carbon and nitrogen isotope patterns in baleen from eastern Arctic bowhead whales (*Balaena mysticetus*). Can. J. Fish. Aquat. Sci. 55:2601–2607.

Hoekstra, P.F., L.A. Dehn, J.C. George, K.R. Solomon, D.C.G. Muir and T.M. O'Hara. 2002. Trophic ecology of bowhead whales (*Balaena mysticetus*) compared with that of other arctic marine biota as interpreted from carbon-, nitrogen-, and sulfur-isotope signatures. Can. J. Zool. 80:223–231.

Ljungblad, D.K., S.E., Moore and J.T. Clarke. 1986. Assessment of bowhead whale (*Balaena mysticetus*) feeding patterns in the Alaskan Beaufort and northeastern Chukchi seas via aerial surveys, fall 1979–1984. Report of the International Whaling Commission 336:265–272.

Ljungblad, D.K., S.E., Moore and D. R. Van Schoik. 1983. Aerial surveys of endangered whales in the Beaufort, eastern Chukchi and northern Bering seas, 1982. NOSC Technical Document 605. Report from Naval Ocean Systems Center, San Diego for U.S. Minerals Management Service, Anchorage, NTIS AD-A134 772/3, 382 p.

Lowry, L.F., V.N. Burkanov, K.J. Frost, M.A. Simpkins, R. Davis, D.P. DeMaster, R. Suydam and A. Springer. 2000. Habitat use and habitat selection by spotted seals (*Phoca largha*) in the Bering Sea. Can. J. Zool. 78(11):1959–1971.

Lowry, L.F., and K.J. Frost. 1984. Foods and feeding of bowhead whales in western and northern Alaska. Scientific Reports of the Whales Research Institute, Tokyo 35:1–16.

Lowry, L.F., and G. Sheffield. 2002. Stomach contents of bowhead whales harvested in the Alaskan Beaufort Sea. Chapter 18. *In* W.J. Richardson and D.H. Thomson [eds.], Bowhead Whale Feeding in the Eastern Alaskan Beaufort Sea: Update of Scientific and Traditional Information, Vol. 2. OCS Study MMS 2002-012. LGL Report TA2196-7. Report from LGL Ltd., King City, Ontario Canada to U.S. Minerals Management Service Anchorage.

Mate, B.R., G.K, Krutzikowsky and M.H. Winsor. 2000. Satellite-monitored movements of radio-tagged bowhead whales in the Beaufort and Chukchi seas during the late-summer feeding season and fall migration. Can. J. Zool. 78(7):1168–1181.

Moore, S.E., J.T. Clarke and D.K. Ljungblad. 1989. Bowhead whale (*Balaena mysticetus*) spatial and temporal distribution in the central Beaufort Sea during late summer and early fall 1979–86. Report to the International Whaling Commission 39:283–290.

Richardson, W.J. [ed.]. 1987. Importance of the eastern Alaskan Beaufort Sea to feeding bowhead whales, 1985–1986. Report by LGL Ecological Research Associates Inc. to U.S. Minerals Management Service, NTIS No. PB 88 150271/AS, 131 p.

Richardson, W.J., and D.H. Thomson [eds.]. 2001. Bowhead whale feeding in the eastern Alaskan Beaufort Sea: Update of scientific and traditional information. 2 Vols. Draft final report by LGL Limited, Environmental Research Associates and LGL Ecological Research Associates Inc. to U.S. Minerals Management Service MMS# 1435-01-97-/CT-30842.

Schell, D.M., and S.M. Saupe. 1993. Feeding and growth as indicated by stable isotopes, p. 491–509. *In* J.J. Burns, J.J. Montague and C.J. Cowles [eds.], The Bowhead Whale. Special Publication No. 2, The Society for Marine Mammalogy, Lawrence, KS.

Schell, D.M., S.M. Saupe and N. Haubenstock. 1989. Bowhead whale (*Balaena mysticetus*) growth and feeding as estimated by $\delta^{13}C$ techniques. Mar. Biol. (Berl.) 103:433–443.

Thomson, D.H. 2002. Energetics of bowhead whales. Chapter 22. *In* W.J. Richardson and D.H. Thomson [eds.], Bowhead Whale Feeding in the Eastern Alaskan Beaufort Sea: Update of Scientific and Traditional Information, Vol. 2. OCS Study MMS 2002-012. LGL Report TA2196-7. Report from LGL Ltd., King City, Ontario Canada to U.S. Minerals Management Service Anchorage.

Würsig, B., E.M. Dorsey, M.A. Fraker, R.S. Payne and W.J. Richardson. 1985. Behavior of bowhead whales, *Balaena mysticetus*, summering in the Beaufort Sea: A description. Fish. Bull. 83:357–377.

Workshop on Hydrological Modeling for Freshwater Discharge from the Alaska Arctic Coast

Jia Wang <jwang@iarc.uaf.edu>
Meibing Jin <ffjm@uaf.edu>

International Arctic Research Center–Frontier Research System for Global Change
University of Alaska Fairbanks
Fairbanks, AK 99775-7340

Task Order 35262

Abstract

Although there have been digital elevation data collected with 1-km or finer spatial resolution from the North Slope and six hydrological gauges north of the Brooks Range, there has not yet been a high resolution digital elevation model (DEM)-based hydrological model constructed for the region to calculate the freshwater discharge into the Arctic Ocean from the Alaskan Arctic coast. Freshwater discharge is important locally because it controls breakup of nearshore landfast ice and the release of spilled oil from landfast ice, and defines the water mass properties and the density-driven current of the nearshore shelf. Furthermore, we do not know what portion of the the discharge goes ungauged because it is due to snow melt, small creeks, streams and ungauged rivers.

We propose to hold a workshop on hydrological modeling of freshwater runoff in the North Slope region. The workshop will focus on precedents in data processing, hydrological modeling, and field observations, including needs, scientific and economic issues, and possible solutions in the region. The workshop will be designed to include scientists from the University of Alaska Fairbanks (UAF), the University of Washington (UW), the University of New Hampshire (UNH), the U.S. Geological Survey (USGS), the State of Alaska, the North Slope Borough, and the Alaska Native communities.

Pre-Migratory Movements and Physiology of Shorebirds Staging on Alaska's North Slope

Abby N. Powell <ffanp@uaf.edu>
Audrey R. Taylor <ftart@uaf.edu>

Institute of Arctic Biology
University of Alaska Fairbanks
Fairbanks, AK 99775–7000

Richard B. Lanctot <richard_lanctot@fws.gov>

U.S. Fish and Wildlife Service
Migratory Bird Management
1011 East Tudor Road, MS 201
Anchorage, AK 99503

Task Order 35269

Abstract

Preliminary work conducted in the 1970s in Barrow, Alaska, indicated that arctic littoral habitats were of critical importance for most arctic-breeding shorebirds during the staging period (prior to southbound migration to wintering areas). However, no information exists to quantify pre-migratory shorebird use of Alaska's North Slope or what factors may influence site use. This information is critical given increased levels of human activity and development across the arctic plain. This project was initiated to gain a better understanding of the basic biology of post-breeding shorebirds during the staging period, and to aid in assessing how future industrial and human activity across the North Slope may affect shorebird populations. Our proposal to the Coastal Marine Institute involved studying staging shorebird populations on the slope using a two-level approach, which includes:

- *An intensive analysis of staging behavior characteristics and factors influencing shorebird choice of staging sites in Barrow, Alaska, from 2004 to 2006.*
- *An extensive aerial survey in 2005 to determine how pre-migratory shorebirds are distributed across selected staging areas on the North Slope.*

Research during the summer of 2004 investigated the location of staging sites within the Barrow vicinity, the phenology of staging among different shorebird species using the Barrow area prior to fall migration, and the residency time of individual birds captured during the staging period. We also collected data on shorebird density along historical transects last surveyed for staging shorebirds during the Outer Continental Shelf Environmental Assessment Program in the late 1970s. We found that numbers of birds at prominent staging locations and on the historical transects varied widely throughout the staging period. Adult shorebirds were recorded in the study area through July and the first few days of August; thereafter all birds seen in Barrow were juveniles (with the exception of adult dunlin). Staging shorebirds generally used areas of saline tundra, the shores of small brackish ponds and lagoons, and the Barrow sewage lagoon as foraging habitats. We captured 204 birds during August 2004 and recorded 182 resightings of banded or painted birds within the study area. The longest residency time recorded for a painted bird was 17 days (red phalarope); one radio-

*tagged dunlin was recorded in the Barrow area for 13 days. In addition, individuals from four species of shorebirds (red phalaropes [*Phalaropus fulicaria*], semipalmated sandpipers [*Calidris pusilla*], western sandpipers [*Calidris mauri*], and dunlin [*Calidris alpina*]) captured during the staging period were blood-sampled to compare fattening rates and stress levels among species and staging sites around Barrow.*

Introduction

The possible impacts of current and future energy development and climate change around the North Slope are of concern to scientists, managers, and many citizens of the United States. Pre-migratory staging shorebirds may be particularly susceptible to the effects of these environmental changes because they are concentrated in coastal areas during a critical period in their life cycles. For example, a study of shorebirds staging at the Colville River Delta on the North Slope estimated that 41,000 individuals might use the delta prior to and during the fall migration [Andres 1994]. Insufficient information exists to determine how habitat alterations and disturbance may affect shorebird populations across much of Alaska [Brown et al. 2001]. In particular, little is known about shorebird use of littoral zones along the North Slope during the pre-migratory staging period. It is likely that staging shorebirds depend on food resources found in coastal areas to acquire fat necessary for southward migration. As pressure for energy development and potential for accelerated climate change increase along the North Slope, so does the need for understanding the importance of coastal areas in preparing shorebirds for southbound migration. If shorebirds are concentrated in and depend on littoral zones at this critical period in their life cycle, the potential for climate change or disturbance and contamination from development to impact a large segment of a species' population is considerable. Shoreline oiling from offshore spills could directly affect staging shorebirds by oiling their plumages, or indirectly by contaminating or killing invertebrate food sources [Andres 1994]. In addition, construction and maintenance of industrial development could negatively impact shorebirds by causing them to flee from noise or human presence, or may eliminate important staging habitats entirely. Of all waterbirds at Jamaica Bay National Wildlife Refuge in New York, shorebirds appeared most susceptible to human-induced disturbance [Burger 1981]. Based on this evidence, it seems plausible that the effects of energy development and associated human disturbance on staging shorebirds could be detrimental to populations that already appear to be in decline [Brown et al. 2001]. Accelerated climate change may add to the effects of development and disturbance by changing the spatial or temporal availability of littoral habitats suitable for staging shorebirds. A mechanistic understanding of shorebird distribution and habitat use will help to pinpoint where and when these impacts may have the largest effect and allow proactive rather than reactive management.

This study will help determine how pre-migratory shorebirds are distributed in littoral zones in Barrow and around the North Slope, what habitats are particularly valuable during this period, and how species composition and abundance at various staging sites may have changed between the 1970s and the present. It will also lend insight into what role physiological factors play in staging site choice. This research is warranted because many North American species of shorebirds appear to be declining in abundance [Brown et al. 2001]. This research will supply basic knowledge regarding staging requirements and habitat for several species of arctic-breeding shorebirds in order to facilitate an evaluation of the potential effects of development along the Arctic Coastal Plain.

Objectives

The specific objectives of this research are to:

1. Assess the abundance, species composition, and distribution of shorebirds staging along selected North Slope coastlines prior to the fall migration.
2. Quantify habitat use characteristics of staging shorebirds, timing of arrival after breeding, and residency times at staging sites.
3. Compare current densities of staging shorebirds with those reported in Connors et al. [1979, 1984] to determine if shorebird use of coastal habitats near Barrow has changed between the 1970s and the present.
4. Examine physiological factors influencing shorebird use of staging areas. Are there quantifiable differences in local site quality (in terms of fattening rates and physiological stress levels) that may affect how and when shorebirds use staging areas? Such knowledge will allow an assessment of the relative importance of different staging areas in preparing shorebirds for migration south from Alaska.

Study Area

During 2004, our studies were conducted at Barrow, Alaska, and the surrounding coastal vicinity (71.290°N, 156.788°W). Barrow is bordered by the Chukchi Sea on the western side and the Beaufort Sea and Elson Lagoon on the northern and eastern sides. This area is characterized by continuous tundra inland and gravel beaches along most shorelines. Also present are many brackish water ponds and lagoons with mud or sand shorelines that are heavily utilized by staging shorebirds. The Barrow human population numbers near 5000, and many people use coastal areas near the village for hunting, fishing, and other recreational activities.

Methods

To address Objectives 1–3, we conducted shorebird surveys along historical transects and at prominent staging locations within the Barrow vicinity in 2004. The historical transects were last surveyed in the 1970s by Peter Connors and colleagues during the OCSEAP (Outer Continental Shelf Environmental Assessment) Program. Ten of Connors' 1-km long transects were reestablished this summer and surveyed once every three days from 21 July to 5 September (Figure 1). Surveys were conducted by walking the transect line from start to finish, and recording the following for each bird or group of birds present: number of birds in the group, species, age, perpendicular distance from the transect line, and location along the transect line. In addition, several prominent staging locations (i.e., areas with large and reliable numbers of birds) were surveyed daily for species and numbers of shorebirds present.

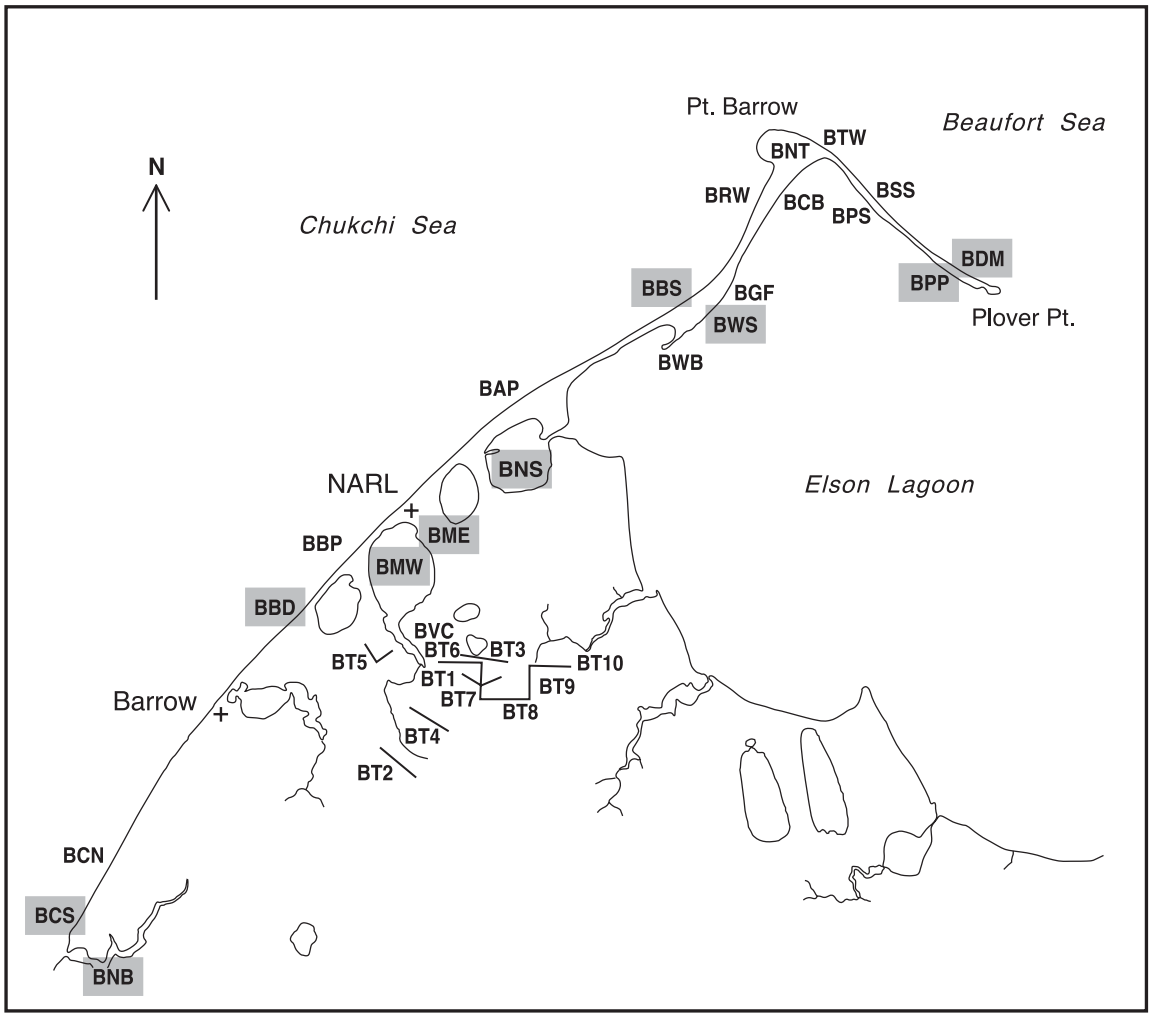

Figure 1. Map of historical shorebird abundance transects run in 1970s during the OCSEAP program. Shaded transect names indicate those surveyed during 2004. Modified from Connors et al. [1984].

To understand how long shorebirds stage in the Barrow area before either migrating south or moving to other areas on the North Slope to stage (residency time; Objective 2), we captured staging shorebirds between 4–29 August at various locations around Barrow using walk-in traps and mist nets, and subsequently resighted them. Captured birds were banded and their heads or necks marked with a unique color combination of non-toxic enamel paint according to the date they were captured (Table 1). Resightings of painted or banded birds on transects or at prominent staging locations were recorded daily; paint and color band combinations allowed us to determine the minimum time the bird had stayed in Barrow. In addition, we placed 1.2-g radio transmitters (Holohil Systems Ltd.) on 15 birds (Table 2) and monitored their locations daily within the Barrow vicinity using an ATS radio receiver and an H-antenna mounted to the front of an ATV. All radio frequencies were monitored until the birds had not been heard within the study area for at least four days.

Table 1. Paint/band combinations and number of individuals captured by date in Barrow during the staging period in 2004.

Date	Paint	Band Combination	Number Captured
4 Aug	Red on head	No color bands; metal only	4
5 Aug	Yellow on head	Yellow lower right	7
6 Aug	Blue on head	Dark blue lower right	27
7 Aug	Green on head	Dark green lower right	15
9 Aug	Red + yellow on head	Red, yellow lower right	8
11 Aug	Red + green on head	Red, dark green lower right	16
14 Aug	Green + yellow on head	Dark green, yellow lower right	5
15 Aug	Blue + yellow on head	Dark blue, yellow lower right	4
17 Aug	Blue + red on head	Dark blue, red lower right	22
19 Aug	Blue + green on head	Dark blue, dark green lower right	22
21 Aug	Purple on head or neck	Light green lower right	17
22 Aug	Red around neck	Red lower left	11
23 Aug	Yellow around neck	Yellow lower left	8
25 Aug	Green around neck	Dark green lower left	16
27 Aug	Red + yellow around neck	Red, yellow lower left	11
30 Aug	Blue around neck	Dark blue lower left	11

Table 2. VHF radio frequencies, species, date tagged, and date last heard for 15 birds radio tagged in Barrow in 2004. REPH – red phalarope. SEPH – semipalmated sandpiper, WESA – western sandpiper, DUNL – dunlin

Frequency	Species	Date Tagged	Last Detected in Barrow	Days Present Post-Capture
165.004	REPH	11 Aug 04	11 Aug 04	<1
165.058	SESA	11 Aug 04	14 Aug 04	3
165.094	WESA	14 Aug 04	23 Aug 04	9
165.134	WESA	14 Aug 04	18 Aug 04	4
165.172	REPH	15 Aug 04	15 Aug 04	<1
165.206	REPH	15 Aug 04	17 Aug 04	2*
165.246	WESA	17 Aug 04	28 Aug 04	11
165.285	DUNL	17 Aug 04	29 Aug 04	12
165.322	DUNL	21 Aug 04	3 Sep 04	13
165.358	WESA	19 Aug 04	23 Aug 04	4
165.396	DUNL	21 Aug 04	21 Aug 04	<1
165.433	SESA	23 Aug 04	24 Aug 04	1
165.470	WESA	25 Aug 04	4 Sep 04	10
165.508	DUNL	25 Aug 04	31 Aug 04	6
165.543	DUNL	25 Aug 04	26 Aug 04	1

*Questionable detection on 17 Aug for this bird; otherwise was not detected after tagging

To address Objective 4, we collected up to 300 µL of blood from each individual captured during the staging period. To obtain a blood sample, we swabbed the brachial vein of each bird with isopropyl alcohol to clear the feathers and then punctured the vein with a sterile 26-gauge needle. Blood was collected in 75-µL heparinized capillary tubes and blown into heparinized 1.6-mL microcentrofuge tubes. After bleeding we held a small piece of cotton over the puncture site on the vein such that bleeding ceased rapidly. The blood was subsequently centrifuged for 15 min and separated into plasma samples for fat metabolite and stress hormone analysis. Plasma samples were frozen immediately after separation. The bird handling and bleeding procedures were approved by the Institutional Animal Care and Use Committee at the University of Alaska Fairbanks (Protocol Number 04-31).

Results

Each of the historical transects was surveyed 16 times throughout the staging period. Shorebirds were seen regularly on each transect but many transects did not support large numbers of birds. The transect data will be compared to that collected in the 1970s and analyzed using the program Distance to obtain the best estimate of shorebird abundance for each transect over time. Repeated surveys of staging locations with regular concentrations of birds indicated shorebird numbers fluctuated dramatically throughout the staging period (see example: Figure 2). Shorebird species present in the largest numbers around Barrow included red and red-necked phalaropes (*Phalaropus lobatus*), semipalmated sandpipers, western sandpipers, dunlin, and long-billed dowitchers (*Limnodromus scolopaceus*). We collected data to determine when species were first observed at Barrow staging areas and which habitats each used; these data will be collated later in tabular form. Generally, adult shorebirds were found on the staging areas through the end of July; by early August only juveniles were left in the Barrow vicinity. Staging habitats used by shorebirds in Barrow included saline tundra interspersed with brackish water ponds, small ponds and lagoons regularly inundated with salt water, and the Barrow sewage treatment lagoon. Gravel lagoon and ocean beaches were rarely used by staging shorebirds. To assess whether bird movements are correlated with local wind speed and direction, we will relate shorebird abundance on our surveys with daily weather and wind data for Barrow.

We captured 204 individuals of eight species at five different locations between 4 August and 29 August 2004. Species captured included red and red-necked phalaropes, semipalmated sandpipers, western sandpipers, dunlin, long-billed dowitchers, ruddy turnstones (*Arenaria interpres*), and semipalmated plovers (*Charadrius semipalmatus*). We recorded 182 resightings of painted or banded birds, including several adult dunlin that had been previously banded on the adjacent tundra area during the breeding season by either the U.S. Fish and Wildlife Service (2003 or 2004) or by Japanese researchers (2001 or 2003). The longest interval between banding and subsequent resighting was 17 days (red phalarope). The longest residency time of a radioed bird was 13 days (dunlin) and the shortest residency times were <1 day (three radio-tagged red phalaropes were never heard after they were banded and the radios attached). As phalaropes tend to be pelagic species, radios may have been difficult to detect due to signal attenuation in salt water. We also recorded the location of each resighting (for both paint/band resightings and radio-tagged birds) with a handheld GPS unit so that movements away from the banding locations and within the Barrow study area can be determined. Preliminary examination of the movement data indicates that marked or radio-tagged birds moved widely around the study area on a daily basis. Additional analyses on site tenure and movements are underway.

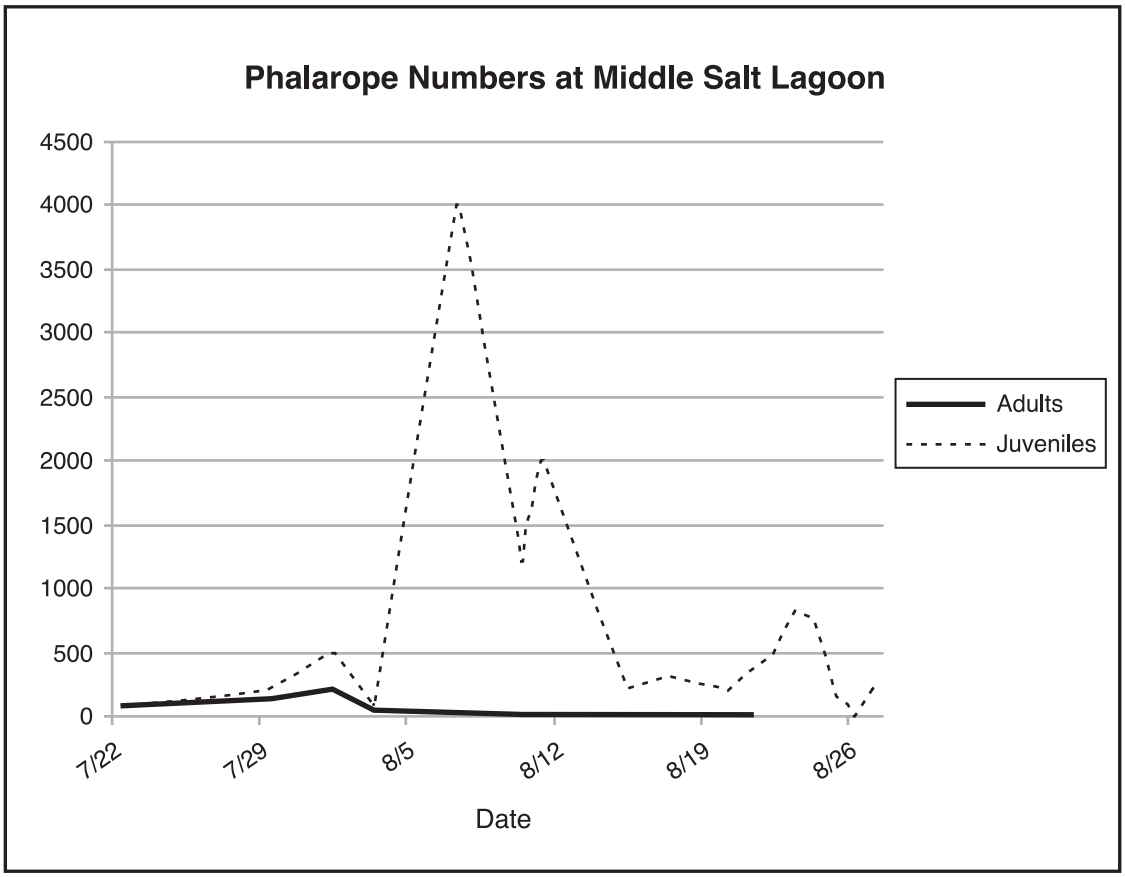

Figure 2. Red and red-necked phalarope numbers on Middle Salt Lagoon (Barrow sewage treatment lagoon) during August 2004. This lagoon was one of the prominent staging locations surveyed daily for shorebird abundance and species composition.

Blood was collected for stress hormone and fat metabolite analysis from individuals of four species (sample size in parentheses): red phalaropes (n = 84), semipalmated sandpipers (n = 23), western sandpipers (n = 40), and dunlin (n = 26). Audrey Taylor will run the fat metabolite analysis at Simon Fraser University and the stress hormone analysis at UAF during the fall semester 2004.

Discussion

It is clear from the 2004 field season that a number of shorebirds use the Barrow area as staging habitat prior to fall migration. However, use of the area by adult birds was limited, resulting in primarily juvenile birds being present throughout August and September. This pattern differs from that documented by Peter Connors in the 1970s in which he found adults present on the littoral transects through mid-August [Connors and Risebrough 1977]. Further data collection is needed to determine whether the staging of adults during early July is due to high predation on shorebird nests during the 2004 breeding season (resulting in adult migration out of Barrow being early and protracted as failed breeders trickled out of the area) or whether this is the contemporary pattern of

staging in our study area. If typical, this may mean that Barrow is a more important staging area for juveniles than for adults of most shorebird species.

The amount of time that individuals staged within the study area varied widely, with resightings of painted birds occurring anywhere from <1 to 17 days post-capture, and radioed birds remaining in the area from 0 to 13 days post-capture. Residency time did not appear to be different for different species, although further examination of the data is needed. One notable exception may be adult dunlin: some uniquely color-banded individuals remained at Barrow staging areas for up to four weeks at a time, well past the date when adults of other species appeared to have left the area. This may be due to the timing of prebasic flight feather molt in adult dunlin, which begins with regrowth of primaries on the breeding grounds and is completed prior to migration [Warnock and Gill 1996]. Dunlin undergoing the highly energetic molt process may be unable to gain enough mass to successfully migrate, and may therefore choose to stay in Barrow to complete molt and fatten prior to southbound migration.

Preliminary examination of the movement data indicates that marked or radio-tagged birds moved regularly from banding locations to other nearby areas, suggesting that Barrow itself can be viewed as one large staging area rather than as multiple small staging sites. Analysis of blood plasma fat metabolites and stress hormone levels from birds at different banding locations should lend further insight into movement of birds within the Barrow area.

Future Plans

We will continue to analyze and interpret data from the 2004 field season; this information will be used to refine existing and suggest new objectives. Audrey Taylor will attend the International Wader Study Group annual conference in November 2004, during which she will participate in a workshop on estimating residency times for staging and migrating shorebirds. Logistical planning for the 2005 field season will begin this fall and continue into the spring of 2005. Current plans for 2005 include aerial surveys across the North Slope from Kasegaluk Lagoon to Demarcation Bay to determine where staging shorebirds are concentrated, and in what numbers and species composition. We also plan to have four ground camps across the slope (in addition to the Barrow camp) in which personnel will conduct ground counts to provide a species composition “correction factor” for the aerial surveys, and to capture, bleed, and band shorebirds using the methods developed in Barrow in 2004. These data should provide a broader perspective of where and when shorebirds stage, their movements, and how physiology affects where and for how long shorebirds use staging areas across the North Slope.

Acknowledgements

This project would not be possible without financial support from the UA Coastal Marine Institute and Minerals Management Service. We would also like to thank the staff of the Barrow Arctic Science Consortium and the North Slope Borough Department of Wildlife Management (especially Robert Suydam) for logistical support. Sigma Xi and the Arctic Audubon Society provided funding for radio transmitters. Data collection was accomplished with much help from our field technicians (Juliette Juillerat, Greg Norwood, Jennifer Selvidge, and Bob Wilkerson). We also gratefully acknowledge Audrey Taylor’s graduate advisory committee at UAF (Tony Williams, Sasha Kitaysky, and Falk Huettmann).

References

Andres, B.A. 1994. Coastal zone use by postbreeding shorebirds in northern Alaska. J. Wildlife Manage. 58(2):206–213.

Brown, S., C. Hickey, B. Harrington and R. Gill [eds.]. 2001. United States Shorebird Conservation Plan, Second Edition. Manomet Center for Conservation Sciences, Manomet, Massachusetts, 61 p.

Burger, J. 1981. The effect of human activity on birds at a coastal bay. Biological Conserv. 21(3):231–241.

Connors, P.G., C.S. Connors and K.G. Smith. 1984. Shorebird littoral zone ecology of the Alaskan Beaufort Coast, p. 295–396. *In* Outer Continental Shelf Environmental Assessment Program. Final Reports of Principal Investigators, Volume 23. NOAA, National Ocean Service, Office of Ocean and Marine Assessment, Ocean Asessments Division, Alaska Office, Anchorage.

Connors, P.G., J.P. Myers and F.A. Pitelka. 1979. Seasonal habitat use by arctic Alaskan shorebirds, p. 101–111. *In* F.A. Pitelka [ed.], Shorebirds in Marine Environments. Studies in Avian Biology – Number 2. Cooper Ornithological Society.

Connors, P., and R.W. Risebrough. 1977. Shorebird dependence on arctic littoral habitats. Report R.U. 172, p. 402–524. *In* Environmental Assessment of the Alaskan Continental Shelf, Annual Reports of Principal Investigators for the year ending March 1977, Volume II: Receptors – Birds. Outer Continental Shelf Environmental Assessment Program, NOAA, Boulder, Colorado.

Warnock, N.D., and R.E. Gill, Jr. 1996. Dunlin (*Calidris alpina*), No. 203. *In* A. Poole and F. Gill [eds.], The Birds of North America, Volume 6. The Academy of Natural Sciences, Philadelphia and The American Ornithologists' Union, Washington, D.C., 24 p.

Sea Ice–Ocean–Oil Spill Modeling System (SIOMS) for the Nearshore Beaufort and Chukchi Seas: Improvement and Parameterization (Phase II)

Jia Wang <jwang@iarc.uaf.edu>
Meibing Jin <ffjm@uaf.edu>

International Arctic Research Center–Frontier Research System for Global Change
University of Alaska Fairbanks
Fairbanks, AK 99775-7340

Task Order 35407

Abstract

We established a nested, fine-resolution (3.4 km) coupled ice–ocean–oil spill modeling system during 2000–2003 (phase I) in the Beaufort and Chukchi Seas titled, "A Nowcast/Forcast Model for the Beaufort Sea Ice–Ocean–Oil Spill System (NFM-BSIOS)". This modeling system can capture some important thermodynamical and dynamical features of both sea ice and the ocean which have been validated by available observations. Furthermore, we have developed an oil spill model with ice under the forcing of observed wind at the MET-stations sponsored by MMS [Wang et al. 2002, 2003]. Nevertheless, it cannot resolve the landfast ice as observed. Because the model minimum depth is 10 m, the landfast ice formation, extent, breakup anchoring and ridging cannot be studied. The barrier islands are not included due to the 3.4-km resolution and 10-m depth cutoff. Sea ice categories are not yet parameterized. Ocean tides are not included. Problems exist in the conjunction boundary between the coarse- and fine-resolution models.

To further improve this coupled ice–ocean–oil spill modeling system, we propose to improve the Sea Ice–Ocean–Oil Spill Modeling System *(SIOMS) for the nearshore Beaufort and Chukchi Seas by increasing the resolution to 1–3 km and the minimum depth to 5 m to include: 1) geographically—the barrier islands, inlets, river mouths up to 5-m depth using the fine resolution bathymetry data (ETOP30); 2) physically—landfast ice parameterization for seasonal variations including breakup, freezing, extent, and anchoring; 3) for such a small-scale sea ice model (1–3 km), we first need to implement the viscous–plastic (VP) or elastic–viscous–plastic (EVP rheology) sea ice model [Hunke and Dukowicz 1997] to the ocean model in the same region; 4) then we need to parameterize the sea ice thickness not only into several categories [Wang et al. 2002], but also to represent thin ice, new ice, level ice, lead ice, rafted ice, rubble ice, and ridged ice [Haapala 2000]; 5) stretched grids will be used to replace the nested grids to avoid a conjuntion boundary effect; and 6) furthermore, ocean tides will be included in this SIOMS. Whether we add the anisotropic property into the model will depend upon our simulation results compared to the observations and the availability of such a model delivered by the MMS/NASA interagency project.*

The goal is to establish the stand-alone SIOMS by adding these new features into the existing modeling system, which was sponsored by MMS during 2000–2003, to better assess and predict ice–ocean conditions and possible nearshore oil spill impacts on the surrounding environment.

Evaluating a Potential Relict Arctic Invertebrate and Algal Community on the West Side of Cook Inlet

Nora R. Foster <swamprat@mosquitonet.com>

University of Alaska Museum of the North
University of Alaska Fairbanks
Fairbanks, AK 99775–6960

Dennis C. Lees <dennislees@earthlink.net>

Littoral Ecological & Environmental Services
1075 Urania Avenue
Leucadia, CA 92024

Susan M. Saupe <saupe@circac.org>

Cook Inlet Regional Citizens Advisory Council
910 Highland Avenue
Kenai, AK 99611-8033

Task Order 37357

Abstract

We propose to conduct an analysis of archived samples and specimens collected during intertidal and subtidal surveys in Cook Inlet to evaluate whether they are relict arctic species. The proposed study is based on previous work conducted on the lower west side of Cook Inlet when taxonomic identifications of epifaunal invertebrates collected in the 1970s for the Outer Continental Shelf Environmental Assessment Program bore a striking resemblance to species reported for the Alaskan Arctic. Additional information provided by other historical invertebrate collections in the area indicate that these west side species and assemblages more closely matched arctic species and assemblages than those on Cook Inlet's east side or in other areas of the Gulf of Alaska and this study will further evaluate these historical specimens. Appropriate international taxonomic experts for each group of species will be contracted to provide the level of detail required to assess the potential for a relict arctic flora and fauna assemblage on Cook Inlet's west side.

Seasonality of Boundary Conditions for Cook Inlet, Alaska

Stephen R. Okkonen <okkonen@alaska.net>

Institute of Marine Science
University of Alaska Fairbanks
Fairbanks, AK 99775–7220

W. Scott Pegau <scott_pegau@fishgame.state.ak.us>

Kachemak Bay Research Reserve
Alaska Department of Fish and Game
95 Sterling Highway, Suite 2
Homer, AK 99603

Susan M. Saupe <saupe@circac.org>

Cook Inlet Regional Citizens Advisory Council
910 Highland Avenue
Kenai, AK 99611-8033

Task Order 37628

Abstract

In order to improve our understanding of the physical environment of lower Cook Inlet, Alaska and to augment recent MMS-funded observational and modeling efforts we propose to conduct an oceanographic monitoring program to measure the seasonal changes in volume and property fluxes at the inflow and outflow boundaries in lower Cook Inlet and the northern Gulf of Alaska and to investigate the mechanism(s) influencing these fluxes. The proposed program will acquire hydrographic and velocity measurements along transect lines crossing: 1) Kennedy Entrance and Stevenson Entrance from Port Chatham to Shuyak Island (80 km), 2) Shelikof Strait from Shuyak Island to Cape Douglas (65 km), 3) Cook Inlet from Red River to Anchor Point (55 km), 4) Kachemak Bay from Barbara Point to Bluff Point (19 km), and 5) the Forelands from East Foreland to West Foreland (16 km). These lines correspond to convenient geographical boundaries and encompass the current OCS lease region. Each transect will consist of vertical casts at 4-km intervals to profile the water column using a caged array of instruments to measure temperature, conductivity, and light transmission. A towed ADCP will acquire absolute water column velocities along transects. Each transect will be measured monthly from May through October and in March and December starting in March 2004 and ending in October 2005.

Funding Summary

Student Support

The cooperative agreement that formed the University of Alaska Coastal Marine Institute stressed the need to support education as well as research. The following student support information is summarized from proposals and may not accurately reflect actual expenditures:

		Funds from MMS	Matching Funds
Fiscal Year 94			
1 Ph.D. student		22,558	9,220
6 M.S. students		65,107	37,411
1 undergrad		4,270	0
	Source Total	$ 91,935	$ 46,631
Fiscal Year 95			
4 Ph.D. students		53,061	9,523
8 M.S. students		90,367	64,380
5 undergrads		4,297	13,933
	Source Total	$147,725	$ 87,836
Fiscal Year 96			
5 Ph.D. students		75,499	8,499
5 M.S. students		80,245	18,661
2 undergrads		4,644	0
	Source Total	$160,388	$ 27,160
Fiscal Year 97			
2 Ph.D. students		37,714	0
2 M.S. students		22,798	0
2 undergrads		2,610	0
	Source Total	$ 63,122	$ 0
Fiscal Year 98			
2 Ph.D. students		17,109	17,109
2 M.S. students		26,012	7,200
2 undergrads		0	2,548
	Source Total	$ 43,121	$ 26,857
Fiscal Year 99			
6 Ph.D. students		66,750	38,073
4 M.S. students		31,650	8,730
4 undergrads		0	10,704
	Source Total	$ 98,400	$ 57,507
Fiscal Year 00			
6 Ph.D. students		61,383	30,551
2 M.S. students		5,868	10,135
7 undergrads		0	21,299
	Source Total	$ 67,251	$ 61,985
Fiscal Year 01			
2 Ph.D. students		19,159	22,019
1 M.S. student		0	5,800
3 undergrads		10,983	5,761
	Source Total	$ 30,142	$ 33,580
Fiscal Year 02			
3 Ph.D. students		48,476	0
5 M.S. students		66,676	7,500
	Source Total	$115,152	$ 7,500
Fiscal Year 03			
3 Ph.D. students		45,032	12,000
5 M.S. students		79,448	7,500
1 undergrad		1,349	0
	Source Total	$115,152	$ 19,500
Fiscal Year 04			
4 Ph.D. students		55,365	15,000
2 M.S. students		34,715	0
	Source Total	$90,080	$ 15,000
	Total to Date	**$1,033,145**	**$383,556**

Total CMI Funding

The total MMS funding committed to CMI projects through federal fiscal year 2003 is approximately $11 million. Since all CMI-funded projects require a one-to-one match with non-federal monies, total CMI project commitments through fiscal year 2003 have totaled approximately $22 million.

Sources of Matching Funds

Matching for CMI-funded projects has come from a wide variety of sources. Identifying and verifying match remains a major administrative challenge in the development of CMI proposals. In general, match has been available to those investigators who expend the necessary extra effort to locate and secure the support. The following partial list of fund matching participants demonstrates the breadth of support for CMI-funded programs:

Afognak Native Corporation

Alaska Beluga Whale Committee

Alaska Department of Environmental Conservation (ADEC)

Alaska Department of Fish and Game (ADF&G)

ADF&G – Kachemak Bay Research Reserve

Alaska Department of Transportation and Public Facilities

Alaska Science and Technology Foundation

Alyeska Pipeline Service Company

Ben A. Thomas Logging Camp

BP Amoco

BP Exploration (Alaska) Inc.

Canadian Wildlife Service

CODAR Ocean Sensors

Cominco Alaska, Inc.

ConocoPhillips Alaska, Inc.

Cook Inlet Regional Citizens Advisory Council

Cook Inlet Spill Prevention & Response, Inc.

Department of Fisheries and Oceans Canada

Exxon Valdez Oil Spill Trustee Council

Frontier Geosciences, Inc.

Golden Plover Guiding Co.

Littoral Ecological & Environmental Services

Japanese Marine Science and Technology Center (JAMSTEC)

Kodiak Island Borough

North Slope Borough

Oil Spill Recovery Institute

Phillips Alaska, Inc.

Prince William Sound Aquaculture Corporation

Simon Fraser University

University of Alaska Anchorage

University of Alaska Fairbanks
- College of Science, Engineering and Mathematics
- Frontier Research System for Global Change, IARC
- Institute of Arctic Biology
- Institute of Marine Science
- International Arctic Research Center (IARC)
- School of Agriculture and Land Resources Management
- School of Fisheries and Ocean Sciences
- School of Management
- School of Mineral Engineering
- University of Alaska Museum
- Wadati Fund
- Water Research Center

University of Alaska Natural Resources Fund

University of Alaska Southeast

University of California, Los Angeles

University of Northern Iowa

University of Texas

Woods Hole Oceanographic Institution

Some of the CMI-funded projects are closely related to other federally-funded projects which cannot be considered as match but nevertheless augment and expand the value of a CMI project. Related or joint projects have been funded by the National Science Foundation, the Office of Naval Research, the National Aeronautics and Space Administration, the U.S. Geological Survey, the National Oceanographic and Atmospheric Administration including the National Marine Fisheries Service, and the Alaska Sea Grant College Program.

A positive relationship has been fostered between MMS, the University of Alaska, and the State of Alaska since the formation of CMI. Residents of Alaska, as well as the parties to the agreement, benefit from the cooperative research that has been and continues to be funded through CMI.

University of Alaska CMI Publications

These publications may be obtained from CMI until supplies are exhausted. Reports marked with an asterisk are no longer available in hard copy from CMI.

Contact information

e-mail: cmi@sfos.uaf.edu
phone: 907.474.1811
fax: 907.474.1188
postal: Coastal Marine Institute
School of Fisheries and Ocean Sciences
University of Alaska Fairbanks
Fairbanks, AK 99775-7220

ALEXANDER, V. (Director). 1995. University of Alaska Coastal Marine Institute **Annual Report No. 1**. University of Alaska Fairbanks and USDOI, MMS, Alaska OCS Region, 16 p.

ALEXANDER, V. (Director). 1996. University of Alaska Coastal Marine Institute **Annual Report No. 2**. OCS Study MMS 95-0057, University of Alaska Fairbanks and USDOI, MMS, Alaska OCS Region, 122 p.

ALEXANDER, V. (Director). 1997. University of Alaska Coastal Marine Institute **Annual Report No. 3**. OCS Study MMS 97-0001, University of Alaska Fairbanks and USDOI, MMS, Alaska OCS Region, 191 p.

ALEXANDER, V. (Director). 1998. University of Alaska Coastal Marine Institute **Annual Report No. 4**. OCS Study MMS 98-0005, University of Alaska Fairbanks and USDOI, MMS, Alaska OCS Region, 81 p.

ALEXANDER, V. (Director). 1998. University of Alaska Coastal Marine Institute **Annual Report No. 5**. OCS Study MMS 98-0062, University of Alaska Fairbanks and USDOI, MMS, Alaska OCS Region, 72 p.

ALEXANDER, V. (Director). 2000. University of Alaska Coastal Marine Institute **Annual Report No. 6**. OCS Study MMS 2000-046, University of Alaska Fairbanks and USDOI, MMS, Alaska OCS Region, 86 p.

ALEXANDER, V. (Director). 2000. University of Alaska Coastal Marine Institute **Annual Report No. 7**. OCS Study MMS 2000-070, University of Alaska Fairbanks and USDOI, MMS, Alaska OCS Region, 92 p.

ALEXANDER, V. (Director). 2002. University of Alaska Coastal Marine Institute **Annual Report No. 8**. OCS Study MMS 2002-001, University of Alaska Fairbanks and USDOI, MMS, Alaska OCS Region, 109 p.

ALEXANDER, V. (Director). 2003. University of Alaska Coastal Marine Institute **Annual Report No. 9**. OCS Study MMS 2003-003, University of Alaska Fairbanks and USDOI, MMS, Alaska OCS Region, 108 p.

ALEXANDER, V. (Director). 2004. University of Alaska Coastal Marine Institute **Annual Report No. 10**. OCS Study MMS 2004-002, University of Alaska Fairbanks and USDOI, MMS, Alaska OCS Region, 119 p.

ALEXANDER, V. (Director). 2005. University of Alaska Coastal Marine Institute **Annual Report No. 11**. OCS Study MMS 2005-055, University of Alaska Fairbanks and USDOI, MMS, Alaska OCS Region, 157 p.

BRADDOCK, J.F., and Z. RICHTER 1998. **Microbial Degradation of Aromatic Hydrocarbons in Marine Sediments**. Final Report. OCS Study MMS 97-0041, University of Alaska Coastal Marine Institute, University of Alaska Fairbanks and USDOI, MMS, Alaska OCS Region, 82 p.

BRADDOCK, J.F., K.A. GANNON and B.T. RASLEY. 2004. **Petroleum hydrocarbon–degrading microbial communities in Beaufort–Chukchi Sea sediments**. Final Report. OCS Study MMS 2004-061, University of Alaska Coastal Marine Institute, University of Alaska Fairbanks and USDOI, MMS, Alaska OCS Region, 38 p.

COOK, J.A., and G.H. JARRELL. 2002. **The Alaska Frozen Tissue Collection: A Resource for Marine Biotechnology, Phase II**. Final Report. OCS Study MMS 2002-027, University of Alaska Coastal Marine Institute, University of Alaska Fairbanks and USDOI, MMS, Alaska OCS Region, 23 p.

COOK, J.A., G.H. JARRELL, A.M. RUNCK and J.R. DEMBOSKI. 1999. **The Alaska Frozen Tissue Collection and Associated Electronic Database: A Resource for Marine Biotechnology**. Final Report. OCS Study MMS 99-0008, University of Alaska Coastal Marine Institute, University of Alaska Fairbanks and USDOI, MMS, Alaska OCS Region, 23 p.

DUESTERLOH, S., and T.C. SHIRLEY. 2004. **The Role of Copepods in the Distribution of Hydrocarbons: An Experimental Approach**. Final Report. OCS Study MMS 2004-034, University of Alaska Coastal Marine Institute, University of Alaska Fairbanks and USDOI, MMS, Alaska OCS Region, 53 p.

DUFFY, L.K., R.T. BOWYER, D.D. ROBY and J.B. FARO. 1998. **Intertidal Effects of Pollution: Assessment of Top Trophic Level Predators as Bioindicators**. Final Report. OCS Study MMS 97-0008, University of Alaska Coastal Marine Institute, University of Alaska Fairbanks and USDOI, MMS, Alaska OCS Region, 62 p.

HENRICHS, S.M., M. LUOMA and S. SMITH. 1997. **A Study of the Adsorption of Aromatic Hydrocarbons by Marine Sediments**. Final Report. OCS Study MMS 97-0002, University of Alaska Coastal Marine Institute, University of Alaska Fairbanks and USDOI, MMS, Alaska OCS Region, 47 p.

HERRMANN, M., S.T. LEE, C. HAMEL, K.R. CRIDDLE, H.T. GEIER, J.A. GREENBERG and C.E. LEWIS. 2001. **An Economic Assessment of the Sport Fisheries for Halibut, Chinook and Coho Salmon in Lower and Central Cook Inlet**. Final Report. OCS Study MMS 2000-061, University of Alaska Coastal Marine Institute, University of Alaska Fairbanks and USDOI, MMS, Alaska OCS Region, 135 p.

HIGHSMITH, R.C., S.M. SAUPE and A.L. BLANCHARD. 2001. **Kachemak Bay Experimental and Monitoring Studies: Recruitment, Succession, and Recovery in Seasonally Disturbed Rocky-Intertidal Habitat**. Final Report. OCS Study MMS 2001-053, University of Alaska Coastal Marine Institute, University of Alaska Fairbanks and USDOI, MMS, Alaska OCS Region, 66 p.

HOLLADAY, B.A., B.L. NORCROSS and A. BLANCHARD. 1999. **A Limited Investigation into the Relationship of Diet to the Habitat Preferences of Juvenile Flathead Sole**. Final Report. OCS Study MMS 99-0025, University of Alaska Coastal Marine Institute, University of Alaska Fairbanks and USDOI, MMS, Alaska OCS Region, 27 p.

JOHNSON, M.A., and S.R. OKKONEN [eds.]. 2000. **Proceedings Cook Inlet Oceanography Workshop**. November 1999, Kenai, AK. Final Report. OCS Study MMS 2000-043, University of Alaska Coastal Marine Institute, University of Alaska Fairbanks and USDOI, MMS, Alaska OCS Region, 118 p.

KLINE, T.C., JR., and J.J. GOERING. 1998. **North Slope Amphidromy Assessment**. Final Report. OCS Study MMS 98-0006, University of Alaska Coastal Marine Institute, University of Alaska Fairbanks and USDOI, MMS, Alaska OCS Region, 25 p.

NAIDU, A.S., J.J. GOERING, J.J. KELLEY and M.I. VENKATESAN. 2001. **Historical Changes in Trace Metals and Hydrocarbons in the Inner Shelf Sediments, Beaufort Sea: Prior and Subsequent to Petroleum-Related Industrial Developments**. Final Report. OCS Study MMS 2001-061, University of Alaska Coastal Marine Institute, University of Alaska Fairbanks and USDOI, MMS, Alaska OCS Region, 80 p.

NAIDU, A.S., J.J. KELLEY, J.J. GOERING and M.I. VENKATESAN. 2003. **Trace Metals and Hydrocarbons in Sediments of Elson Lagoon (Barrow, Northwest Arctic Alaska) as Related to the Prudhoe Bay Industrial Region**. Final Report. OCS Study MMS 2003-057, University of Alaska Coastal Marine Institute, University of Alaska Fairbanks and USDOI, MMS, Alaska OCS Region, 33 p.

NIEBAUER, H.J. 2000. **Physical–Biological Numerical Modeling on Alaskan Arctic Shelves**. Final Report. OCS Study MMS 2000-041, University of Alaska Coastal Marine Institute, University of Alaska Fairbanks and USDOI, MMS, Alaska OCS Region, 84 p.

*NORCROSS, B.L. 1996. **Recruitment of Juvenile Flatfishes in Alaska: Habitat Preference near Kodiak Island, Vol. I**. Final Report. OCS Study MMS 96-0003, University of Alaska Coastal Marine Institute, University of Alaska Fairbanks and USDOI, MMS, Alaska OCS Region, 118 p.

*NORCROSS, B.L. 1996. **Recruitment of Juvenile Flatfishes in Alaska: Habitat Preference near Kodiak Island, Vol. II**. Final Report, Appendices. OCS Study MMS 96-0003, University of Alaska Coastal Marine Institute, University of Alaska Fairbanks and USDOI, MMS, Alaska OCS Region, 118 p.

NORCROSS, B.L., B.A. HOLLADAY, A.A. ABOOKIRE and S.C. DRESSEL. 1998. **Defining Habitats for Juvenile Groundfishes in Southcentral Alaska, Vol. I**. Final Report. OCS Study MMS 97-0046, University of Alaska Coastal Marine Institute, University of Alaska Fairbanks and USDOI, MMS, Alaska OCS Region, 131 p.

NORCROSS, B.L., B.A. HOLLADAY, A.A. ABOOKIRE and S.C. DRESSEL. 1998. **Defining Habitats for Juvenile Groundfishes in Southcentral Alaska, Vol. II**. Final Report, Appendices. OCS Study MMS 97-0046, University of Alaska Coastal Marine Institute, University of Alaska Fairbanks and USDOI, MMS, Alaska OCS Region, 127 p.

OKKONEN, S.R., and S.S. HOWELL. 2003. **Measurements of Temperature, Salinity and Circulation in Cook Inlet, Alaska**. Final Report. OCS Study MMS 2003-036, University of Alaska Coastal Marine Institute, University of Alaska Fairbanks and USDOI, MMS, Alaska OCS Region, 28 p.

PROSHUTINSKY, A.Y. 2000. **Wind Field Representations and Their Effect on Shelf Circulation Models: A Case Study in the Chukchi Sea**. Final Report. OCS Study MMS 2000-011, University of Alaska Coastal Marine Institute, University of Alaska Fairbanks and USDOI, MMS, Alaska OCS Region, 136 p.

PROSHUTINSKY, A.Y., M.A. JOHNSON, T.O. PROSHUTINSKY and J.A. MASLANIK. 2003. **Beaufort and Chukchi Sea Seasonal Variability for Two Arctic Climate States**. Final Report. OCS Study MMS 2003-024, University of Alaska Coastal Marine Institute, University of Alaska Fairbanks and USDOI, MMS, Alaska OCS Region, 197 p.

SHAW, D.G., and J. TERSCHAK. 1998. **Interaction Between Marine Humic Matter and Polycyclic Aromatic Hydrocarbons in Lower Cook Inlet and Port Valdez, Alaska**. Final Report. OCS Study MMS 98-0033, University of Alaska Coastal Marine Institute, University of Alaska Fairbanks and USDOI, MMS, Alaska OCS Region, 27 p.

SCHELL, D.M. 1998. **Testing Conceptual Models of Marine Mammal Trophic Dynamics Using Carbon and Nitrogen Stable Isotope Ratios**. Final Report. OCS Study MMS 98-0031, University of Alaska Coastal Marine Institute, University of Alaska Fairbanks and USDOI, MMS, Alaska OCS Region, 137 p.

TERSCHAK, J.A., S.M. HENRICHS and D.G. SHAW. 2004. **Phenanthrene Adsorption and Desorption by Melanoidins and Marine Sediment Humic Acids**. Final Report. OCS Study MMS 2004-001, University of Alaska Coastal Marine Institute, University of Alaska Fairbanks and USDOI, MMS, Alaska OCS Region. 65 p.

TYLER, A.V., C.O. SWANTON and B.C. MCINTOSH. 2001. **Feeding Ecology of Maturing Sockeye Salmon (*Oncorhynchus nerka*) in Nearshore Waters of the Kodiak Archipelago**. Final Report. OCS Study MMS 2001-059, University of Alaska Coastal Marine Institute, University of Alaska Fairbanks and USDOI, MMS, Alaska OCS Region, 34 p.

WANG, J. 2003. **Proceedings of a Workshop on Small-Scale Sea-Ice and Ocean Modeling (SIOM) in the Nearshore Beaufort and Chukchi Seas**. Final Report. OCS Study MMS 2003-043, University of Alaska Coastal Marine Institute, University of Alaska Fairbanks and USDOI, MMS, Alaska OCS Region, 56 p.

WEINGARTNER, T.J. 1998. **Circulation on the North Central Chukchi Sea Shelf**. Final Report. OCS Study MMS 98-0026, University of Alaska Coastal Marine Institute, University of Alaska Fairbanks and USDOI, MMS, Alaska OCS Region, 39 p.

WEINGARTNER, T.J., and S.R. OKKONEN. 2001. **Beaufort Sea Nearshore Under-Ice Currents: Science, Analysis and Logistics**. Final Report. OCS Study MMS 2001-068, University of Alaska Coastal Marine Institute, University of Alaska Fairbanks and USDOI, MMS, Alaska OCS Region, 22 p.

WEINGARTNER, T.J., and T. PROSHUTINSKY. 1998. **Modeling the Circulation on the Chukchi Sea Shelf**. Final Report. OCS Study MMS 98-0017, University of Alaska Coastal Marine Institute, University of Alaska Fairbanks and USDOI, MMS, Alaska OCS Region, 75 p.

WINKER, K., and D.A. ROCQUE. 2004. **Seabird Samples as Resources for Marine Environmental Assessment**. Final Report. OCS Study MMS 2004-035, University of Alaska Coastal Marine Institute, University of Alaska Fairbanks and USDOI, MMS, Alaska OCS Region, 26 p.